

**BIOSYNTHESIS OF CHIRAL POLY-HYDROXYACYL  
ESTERS AND THEIR ENZYMATIC FUNCTIONALIZATION  
AS GLYCOPOLYMERS**

**AHMAD MOHAMMED GUMEL**

**THESIS SUBMITTED IN FULFILLMENT OF THE  
REQUIREMENTS FOR THE DEGREE OF  
DOCTOR OF PHILOSOPHY**

**INSTITUTE OF BIOLOGICAL SCIENCES  
FACULTY OF SCIENCE  
UNIVERSITY OF MALAYA  
KUALA LUMPUR**

2013

**Abstract:**

The use of biodegradable polymers such as polyhydroxyalkanoates (PHAs) over their non-degradable petro-chemical based counterparts is among the measures taken towards environmental friendliness and sophistication in industrial and biomedical applications. Issues such as rate of degradability and the increasing demand in specialty applications for these biopolymers, particularly in biomedical field e.g in controlling the precise target delivery of a therapeutic drug, as well as the capability of the polymeric drug carrier to release a drug at an independent time scale warrant an intense research in the processes for biopolymer production, functionalization and modification. Although several approaches in devising simpler and cost effective means to improve the desirable traits (e.g. degradability, molecular weight, crystallinity etc) of these biodegradable polymers have been reported, which include chemical synthesis and blending, wider options need to be explored.

In this research, a mild and environmental-friendly process for the biosynthetic preparation of PHA was investigated. In the *in vitro* enzymatic PHA biosynthesis, a sonication process enhanced the rate of polymer propagation by more than two-fold, while the enzymatic turnover number increases by 3 times. In addition, the polymer properties *viz* molecular weight, crystallinity and polydispersity were improved under sonication as compared to the non-sonicated process. The *in vivo* PHA production by bacterial fermentation utilizes renewable carbon substrates. The process was observed to be growth associated, resulting in PHA accumulation of about 50 to 77% (w/w) and PHA yields ranging from 10. g L<sup>-1</sup> to 15.5 g L<sup>-1</sup>, respectively. The type and composition of accumulated PHA depend on the type of carbon source fed and the bacterial species. For example, feeding fatty acids from octanoic acid (C<sub>8:0</sub>) to oleic acid (C<sub>18:1</sub>) as sole carbon and energy source in the newly isolated strain of *Pseudomonas putida* Bet001, as much as 50 to 69% of the microbial dry mass PHA accumulation with a molecular weight ranging from 56 to 78 kDa was observed. On the other

hand, another new bacterial isolate *Delftia tsuruhatensis* Bet002, failed to use medium-chain-length fatty acids i.e. C<sub>8</sub> to C<sub>10</sub> for growth and PHA accumulation. When the bacterium was fed with C<sub>14:0</sub> to C<sub>18:0</sub> fatty acids, a homopolymer of poly-3-hydroxybutyrate (PHB) accumulation was observed. When the bacterium was supplied with unsaturated oleic acid (C<sub>18:1</sub>), a copolymer containing C<sub>4</sub> to C<sub>10</sub> acids with both even and odd carbon atom monomers is accumulated. As in *P. putida* Bet001, PHA accumulation for *D. tsuruhatensis* Bet002 is also growth associated with PHA yield of about 45 to 77% on cell dry weight basis and a molecular weight ranging from 131 to 199 kDa. Independent of the species, the type of carbon source influences both the thermal stability and crystallinity of the PHA.

With the aim to improve the degradability of these important polymers and possibly expanding their niche applications, the PHA was conjugated with sugar moieties *via* enzyme catalysis. Besides showing better compostability, the biodegradability of the functionalized glycopolymers increase by factor of 1.5 compared to the non-functionalized materials. They showed an improved thermal stability with highest melting and thermal degradation temperatures of 150°C and above 300°C, respectively. The functionalization reaction afforded a glycopolymer with an average molecular weight ( $M_w$ ) of 1.7 to 16.8 ( $\pm 0.2$ ) kDa depending on the solvent polarity. As such, controlling the binary solvent mixtures as reaction media, enables to influence and/or manipulate the rate of product formation and reaction stability resulting in higher efficiency and yield. The polymer functionalization with sugar moieties was carried out *via* a simple, single-step enzymatic catalysis, which is specific, viable and environmental-friendly.

## Abstrak

Penggunaan polimer terurai seperti *polyhydroxyalkanoates* (PHA) berbanding polimer yang menggunakan asas petro-kimia yang tidak terurai telah menjadi salah satu langkah untuk memastikan bahan industri yang mesra alam serta memberi impak baharu terhadap aplikasi biomedikal. Kadar penguraian dan peningkatan permintaan terhadap aplikasi khusus pada polimer ini, terutamanya di bidang biomedikal (cth: mengawal perembesan bahan kimia kepada sel khusus serta keupayaan untuk menjadi pembawa bahan kimia yang tidak dipengaruhi oleh masa) telah menyebabkan peningkatan dalam penyelidikan untuk menghasilkan biopolimer, mengubah tahap keaktifan biopolimer serta strukturnya. Walaupun beberapa pendekatan penyelidikan yang murah dan jimat telah digunakan dalam penambahbaikan terhadap ciri-ciri biopolimer yang merangkumi proses kimia serta bercampur telah dilaporkan, lebih banyak pilihan proses perlu diadakan.

Kajian ini adalah berfokuskan kepada perangkaan proses penghasilan PHA yang lebih mudah dan mesra alam. Proses biosintesis PHA secara *in vitro* secara sonikasi telah meningkatkan tahap pemanjangan polimer sebanyak dua kali ganda, manakala bilangan perolehan enzim meningkat sebanyak 3 kali ganda. Ciri-ciri PHA seperti berat molekul, kristaliniti serta penyebarannya juga telah ditambahbaik melalui proses penghasilan dengan menggunakan sonikasi. Proses penghasilan PHA secara *in vivo* melalui proses penapaian dengan menggunakan karbon sebagai substrat didapati adalah berhubungkait dengan tahap perkembangan bakteria. Proses penapaian telah berjaya menghasilkan 50 sehingga 70% PHA dalam kepekatan 10. g L<sup>-1</sup> sehingga 15.5 g L<sup>-1</sup>. Jenis dan komposisi PHA juga didapati adalah bergantung kepada jenis karbon



yang digunakan oleh bakteri. Penggunaan asid lemak tepu yang mempunyai 8 karbon (asid oktanoik) sehingga 18 karbon asid lemak tak tepu (asid oleik) sebagai sumber karbon dan tenaga terhadap *Pseudomonas putida* Bet001, sebanyak 50-69% berat kering PHA telah berjaya dihasilkan. PHA tersebut mempunyai berat molekul daripada 56 sehingga 78 kDa. Bakteria *Delftia tsuruhatensis* Bet002 telah didapati gagal untuk menggunakan asid lemak yang mempunyai 8 karbon sehingga 10 karbon sebagai tenaga untuk perkembangannya seterusnya untuk menghasilkan PHA. Apabila asid lemak yang mempunyai bilangan karbon antara 14 sehingga 18 karbon digunakan sebagai sumber karbon, didapati polimer yang mempunyai ulangan monomer yang sama (*poly-3-hydroxybutyrate*) (PHB) terhasil. Penghasilan polimer yang mempunyai monomer campuran didapati terhasil apabila *D. tsuruhatensis* menggunakan asid lemak tak tepu asid oleik. Pengumpulan PHA oleh *D. tsuruhatensis* Bet002 juga didapati adalah berhubungkait dengan tahap perkembangannya. PHA yang terhasil adalah dalam lingkungan 45-77% daripada berat kering sel dan mempunyai berat molekul antara 131 hingga 199 kDa. Tahap ketahanan terhadap suhu tinggi dan tahap kristaliniti PHA yang terhasil adalah bergantung kepada jenis karbon yang digunakan untuk kesemua spesis bakteria yang digunakan.

Konjugasi PHA dengan pelbagai jenis karbohidrat melalui tindakan enzim telah dijalankan untuk menambahbaik tahap penguraian polimer serta memperluaskan lagi penggunaan polimer tersebut. Proses konjugasi telah menghasilkan produk yang mempunyai tahap penguraian yang lebih baik yang mana tahapnya meningkat sebanyak 1.5 kali ganda berbanding polimer biasa. Polimer terubahsuai juga mempunyai tahap ketahanan terhadap suhu tinggi yang lebih baik iaitu suhu takat lebur

adalah pada 150°C dan suhu pemecahan molekul adalah lebih daripada 300°C. Berat molekular polimer yang terubahsuai telah dicatatkan antara 1.7 to 16.8 ( $\pm 0.2$ ) kDa dan ini bergantung kepada polariti medium. Maka, penggunaan larutan bercampur sebagai medium penghasilan produk dapat mempengaruhi/menambahbaikkkan kadar sintesis produk, tahap keberkesanan proses sintesis serta bilangan produk yang terhasil. Proses penghasilan polimer yang terubahsuai dengan karbohidrat telah dijalankan melalui proses biosintesis dengan menggunakan enzim dan ianya hanya memerlukan satu peringkat proses dan proses yang digunakan adalah mesra alam.

## **Acknowledgement**

The realization of this Doctoral research would not have been possible without the constant support and academic assistance not only on technical aspects but also by providing scientific and academic advise as well as encouragement from numerous people throughout the research period. For this I want to express my sincere gratitude and appreciation to the following:

I am indebted to acknowledge my distinguished academic supervisors in persons of Associate Professor Dr. Mohamad Suffian Mohamad Annuar and Associate Professor Dr. Thorsten Heidelberg; for trusting me with this work and for always being by my side, attend to my problems whenever I need them throughout this work. I would like to express my humble appreciation to Professor Dr. Yusuf Chisti (Biochemical Engineering Chair, Massey University, New Zealand) for his academic advice and editing in some of the published scientific papers.

I would like to express my sincere gratitude to all the members of Integrative Bioprocess Technology research group for their support during the research work, without which this study would have been impossible. I acknowledge my beloved parents and my friends, especially Sani Bashari (Yayo), for their moral guidance throughout my life. I am eternally indebted to you for that.

Last but not the least the University of Malaya is acknowledged for funding this work through the research grants PV036/2012A , UM.C/625/1/HIR/MOHE/05 and RG165/ 11AFR respectively.

## List of Publications and Conferences

### Publications

1. **Gumel, A.M.**, Annuar, M.S.M., Heidelberg, T. (2013) Current application of controlled degradation processes in polymer modification and functionalization. *Journal of Applied Polymer Science* 129(6):3079-3088 (*ISI-Cited Publication*)
2. **Ahmad M. Gumel**, Suffian M. Annuar, Thorsten Heidelberg (2013) Single-step lipase-catalyzed functionalization of medium-chain-length polyhydroxyalkanoates. *Journal of Chemical Technology and Biotechnology* 88(7):1328-1335 (*ISI-Cited Publication*)
3. **A.M. Gumel**, M.S.M. Annuar, T. Heidelberg (2013) Enzymatic synthesis of 6-O-glucosyl-poly(3-hydroxyalkanoate) in organic solvents and their binary mixture. *International Journal of Biological Macromolecules* 55:127-136 (*ISI-Cited Publication*)
4. **A.M. Gumel**, M.S.M. Annuar, Y. Chisti (2013) Recent advances in the production, recovery and applications of polyhydroxyalkanoates. *Journal of Polymers and the Environment*. 21(2): 580-605 (*ISI-Cited Publication*)
5. **Ahmad Mohammed Gumel**, Mohamad Suffian Mohamad Annuar, Thorsten Heidelberg, (2012) Biosynthesis and characterization of polyhydroxyalkanoates copolymers produced by *Pseudomonas putida* Bet001 isolated from palm oil mill effluent. *PLoS ONE* 7(9): e45214 (*ISI-Cited Publication*)
6. **A.M. Gumel**, M.S.M. Annuar, T. Heidelberg (2012) Effects of carbon substrates on biodegradable polymer composition and stability produced by *Delftia tsuruhatensis* Bet002 isolated from palm oil mill effluent. *Polymer Degradation and Stability* 97:1227-1231 (*ISI-Cited Publication*)
7. **A.M. Gumel**, M.S.M. Annuar, Y. Chisti (2013) Lipase catalyzed ultrasonic synthesis of poly-4-hydroxybutyrate-co-6-hydroxyhexanoate. *Ultrasonics Sonochemistry* 20(3):937-947 (*ISI-Cited Publication*)
8. **A.M. Gumel**, M.S.M. Annuar, Y. Chisti, T. Heidelberg (2012) Ultrasound assisted lipase catalyzed synthesis of poly-6-hydroxyhexanoate in 1-ethyl-3-methyl-imidazolium tetrafluoroborate [Emim][BF<sub>4</sub>]. *Ultrasonics Sonochemistry* 19:659–667 (*ISI-Cited Publication*)
9. **A.M. Gumel**, M.S.M. Annuar, T. Heidelberg, Y. Chisti (2011) Lipase mediated synthesis of sugar fatty acid esters. *Process Biochemistry* 46:2079-2090 (*ISI-Cited Publication*)

10. **Gumel, A.M.**, Annuar, M.S.M., Heidelberg, T., Chisti, Y. (2011) Thermo-kinetics of lipase-catalyzed synthesis of 6-O-glucosyldecanoate *Bioresource Technology* 102(19):8727-8732. (ISI-Cited Publication)
11. **Gumel, A.M.**, Annuar, M.S.M., Heidelberg, T., Chisti, Y. Kinetics of chain propagation rate and polymer properties in the enzymatic synthesis of poly-ε-caprolactone in ultrasound assisted process. *Applied Biochemistry and Biotechnology* (In peer review process)
12. **Gumel, A.M.**, Annuar, M.S.M., Heidelberg, T., Growth kinetics, effects of carbon substrates chain length on poly-3-hydroxyalkanoates physico-chemical structures synthesized by *Pseudomonas putida* Bet001 isolated from palm oil mill effluents. *Brazilian Journal of Microbiology* (In peer review process)
13. **Gumel, A.M.**, Annuar, M.S.M., PHA-PEGMA copolymers for pH responsive and shape memory hydrogel. *AIChE* (In peer review process)

## CONFERENCES

1. **Gumel, A.M.**, Annuar, M.S.M., Heidelberg, T., *Candida antarctica* lipase catalyzed functionalization of medium-chain-length polyhydroxyalkanoates isolated from *Delftia tsuruhatensis* Bet002, International Symposium of Biotechnology and Conservation of Species from Arid region, 10<sup>th</sup>-13<sup>th</sup> February, 2013, Sultan Qaboos University, Muscat, Oman (International)
2. **Gumel, A.M.**, Annuar, M.S.M., Heidelberg, T., *Candida antarctica* lipase B catalyzed regio-selective synthesis of poly(6-O-glucosyl-3-hydroxyalkanoates), 17th Biological Sciences Graduate Congress, 8 Dec 2012 to 9th Dec 2012, Chulalongkorn University, Thailand (International)
3. **Gumel, A.M.**, Annuar, M.S.M., Heidelberg, T., Application of sonochemistry in enzymatic synthesis of biodegradable poly-6-hydroxyhexanoate, University of Malaya Researchers' Conference 2012, 23 Apr 2012 to 24 Apr 2012, University of Malaya, (University)



**Massey University**

**PROFESSOR YUSUF CHISTI**

School of Engineering PN456  
Massey University, Private Bag 11 222  
Palmerston North  
New Zealand 4447

TEL: +64-6-350-5934

FAX: +64-6-350-5604

EMAIL: Y.Chisti@massey.ac.nz

28 December 2012

**Re: PhD (Biotechnology) thesis of Mr Ahmad Mohammed Gumel**

This confirms that I have co-authored the following research papers with Mr Ahmad Mohammed Gumel:

1. Gumel, A.M., Annuar, M.S.M., Heidelberg, T., Chisti, Y., *Process Biochemistry*, 46, 2079-2090 (2011). Lipase mediated synthesis of sugar fatty acid esters. Doi: 10.1016/j.procbio.2011.07.021
2. Gumel, A.M., Annuar, M.S.M., Heidelberg, T., Chisti, Y., *Bioresource Technology*, 102, 8727-8732 (2011). Thermo-kinetics of lipase-catalyzed synthesis of 6-O-glucosyldecanoate. Doi: 10.1016/j.biortech.2011.07.024
3. Gumel, A.M., Annuar, M.S.M., Chisti, Y., Heidelberg, T., *Ultrasonics Sonochemistry*, 19, 659-667 (2012). Ultrasound assisted lipase catalyzed synthesis of poly-6-hydroxyhexanoate. Doi: 10.1016/j.ultsonch.2011.10.016
4. Gumel, A.M., Annuar, M.S.M., Chisti, Y., Lipase catalyzed ultrasonic synthesis of poly-4-hydroxybutyrate-co-6-hydroxyhexanoate. *Ultrasonics Sonochemistry*, in press. <http://dx.doi.org/10.1016/j.ultsonch.2012.09.015>
5. Gumel, A.M., Annuar, M.S.M., Chisti, Y., Recent advances in the production, recovery and applications of polyhydroxyalkanoates. *Journal of Polymers and the Environment*, in press. Doi: 10.1007/s10924-012-0527-1
6. Gumel, A.M., Annuar, M.S.M., Chisti, Y., Heidelberg, T., Sonication improves chain propagation rate and polymer properties in enzymatic synthesis of poly-6-hydroxyhexanoate from  $\epsilon$ -caprolactone. Manuscript ABAB-D-12-05533 being reviewed for possible publication in *Applied Biochemistry and Biotechnology*.

I agreed to co-author the above referenced papers with Mr Gumel and give him permission to include these papers in his PhD thesis. The work described in the above cited papers is Mr Gumel's original work. I participated in the papers in an advisory capacity.

Yusuf Chisti, PhD, Dr hc  
Professor of Biochemical Engineering

## Contents

| Title  | Page      |
|--|-----------|
| Title page   | i         |
| Original literary work declaration   | ii        |
| Abstract   | iii       |
| Acknowledgement  | viii      |
| List of publications   | ix        |
| Conferences  | x         |
| Evidence of permissions  | xi        |
| <b>CHAPTER 1 Introduction</b>  | <b>1</b>  |
| 1.1 Research Background  | 1         |
| 1.2 Research Objectives  | 9         |
| 1.3 Research Approach  | 10        |
| 1.3.1 Biosynthesis of the biodegradable polymer  | 11        |
| 1.3.2 PHA esterification and functionalization   | 13        |
| 1.4 Thesis organization and linkage of scientific papers   | 14        |
| <b>CHAPTER 2 Recent advances in the production, recovery and applications of polyhydroxyalkanoates</b>   | <b>21</b> |
| Statement of contributions of joint authorship   | 21        |
| Published paper  | 22-47     |
| <b>CHAPTER 3 Lipase mediated synthesis of sugar fatty acid esters</b>  | <b>48</b> |
| Statement of contributions of joint authorship   | 48        |
| Published paper  | 49-60     |
| <b>CHAPTER 4 Current application of controlled degradation processes in polymer modification and functionalization</b>   | <b>61</b> |
| Statement of contributions of joint authorship   | 61        |
| Published paper  | 62-71     |
| <b>CHAPTER 5 Ultrasound assisted lipase catalyzed synthesis of poly-6-hydroxyhexanoate</b>   | <b>72</b> |
| Statement of contributions of joint authorship   | 72        |
| Published paper  | 73-81     |
| <b>CHAPTER 6 Lipase catalyzed ultrasonic synthesis of poly-4-hydroxybutyrate-co-6-hydroxyhexanoate</b>   | <b>82</b> |
| Statement of contributions of joint authorship   | 82        |
| Published paper  | 83-93     |
| <b>CHAPTER 7 Biosynthesis and characterization of polyhydroxyalkanoates copolymers produced by <i>Pseudomonas putida</i> Bet001 isolated from palm oil mill effluent</b> | <b>94</b> |

|   |         |
|---|---------|
| Statement of contributions of joint authorship  | 94      |
| Published paper   | 95-102  |
| <b>CHAPTER 8 Effects of carbon substrates on biodegradable polymer composition and stability produced by <i>Delftia tsuruhatensis</i> Bet002 isolated from palm oil mill effluent</b> | 103     |
| Statement of contributions of joint authorship  | 103     |
| Published paper   | 104-111 |
| <b>CHAPTER 9 Single-step lipase-catalyzed functionalization of medium-chain-length polyhydroxyalkanoates</b>  | 112     |
| Statement of contributions of joint authorship  | 112     |
| Published paper   | 113-120 |
| <b>CHAPTER 10 Enzymatic synthesis of 6-O-glucosyl-poly(3-hydroxyalkanoate) in organic solvents and their binary mixture</b>   | 121     |
| Statement of contributions of joint authorship  | 121     |
| Published paper   | 122-131 |
| <b>CHAPTER 11 Conclusions</b>   | 132     |
| 11.1 Principal findings   | 132     |
| <b>References</b>   | 134     |



# CHAPTER 1.0

## Introduction

---

### 1.1 Research Background

Rapid advancement in science and technology in the last century, particularly in the current era of advanced industrialization had led to a surge in demand and production of polymeric materials. Most are based on petro-chemical origins, leading to a variety of synthetic polymers, fibers, plastics, and rubbers. They are utilized in several fields, including transportation, construction, packaging, electronic devices, aeronautics, and medical appliances. It is reported that about 140 million tons of these plastics are produced and consumed annually all over the world, requiring 150 million tons of fossil fuel for production (Okada, 2002; Suriyamongkol et al., 2007). In 2011 alone nearly 280 million tons of petrochemical-based polymers were produced and the market is expected to further increase with 4% annual growth up to 2016 (Bauwens, 2011). The production of synthetic polymers is anticipated to increase to around 810 million tons by 2050 (Piet, 2010). Unfortunately, the high demand for polymeric materials results in increased oil consumption all over the globe. More importantly, most of these polymers are non-degradable; hence contribute significantly to environmental pollution. Moreover, the current waste disposal of polymers causes health and environmental risks due to greenhouse gasses emission, toxic wastes and aquatic plastic-soup accumulation.

Concurrently, these effects have led to the interests in the replacement of petrochemical-derived plastics by biodegradable polymers. Among the biopolymers of

interest are aliphatic polymers such as polyhydroxyalkanoates (PHAs) e.g. poly-3-hydroxyalkanoates and poly-6-hydroxyhexanoate (poly- $\epsilon$ -caprolactone). These high molecular weight biodegradable polymers share the physical and mechanical properties similar to petroleum derived thermoplastics such as polypropylene (PP) and polyethylene (PET), with the advantage of biodegradability (Zakaria et al., 2010) and biocompatibility (Suriyamongkol et al., 2007). In fact, these biodegradable polymers are now seen as possible replacement for polyolefins in medical applications e.g. for drug delivery systems, suture threads, resorbable implants, tissue engineering scaffolds and inter-positional spacers in osteoarthritis (Kobayashi, 2010; Nair & Laurencin, 2007; Nobes et al., 1996; Woodruff & Hutmacher, 2010).

However, the industrial production of these biopolymers such as polyesters by conventional chemical catalysis relies on the use of organometallic catalysts, high energy consumption and complex chemical processing steps, like hydroxyl protection and de-protection, as well as the use of toxic chemicals. This makes the overall process non-attractive, particularly in biomedical applications which require complete removal of metallic catalysts.

One of the strategies to solve these difficulties is through the use of a biocatalytic processes. Advances in microbial genetic engineering and non-aqueous enzymology pave the way for a greener synthetic process of biodegradable polymers using enzymes such as hydrolases and esterases. For example, lipases function as hydrolases in aqueous media to hydrolyze ester bonds (Sharma et al., 2001); however, in microaqueous media, lipases can catalyze the formation of ester bonds.

Recently, *in vitro* enzymatic polymerization has received much attention as an environmental friendly process for polymer synthesis (Gumel et al., 2012a; Gumel et al., 2012b; He et al., 2005; Kobayashi, 2010; Zinck, 2009). Through this process, biodegradable polyesters can be synthesized either by polycondensation (step growth polymerization) or by ring opening polymerization (chain growth polymerization) of substrates like lactones (Kobayashi, 2010). A specific functionality can be introduced through these polymerizations by applying either functionalized monomers or functionalized initiators (Loh et al., 2009). The products of enzyme mediated biocatalytic ring opening polymerization have little or no potential for adverse health impact. Moreover, enzymatic biocatalysis offers excellent enantiomeric selectivity and specificity, thus avoiding contaminations and the catalysis can be achieved under mild reaction conditions.

Among the various enzymatic polymerization methods employed, ring-opening polymerization (ROP) is considered as an important alternative route for the biosynthesis of these polymers, due to the lack of leaving group generation during polymerization, which limits monomer conversion and reduce the degree of polymerization (He et al., 2005). In addition, enzyme catalyzed ROP can make use of a myriad of substrates particularly lactones. Cutinase of the soft-rot fungus *Humicola insolens* has been used to catalyze polycondensations and ring-opening polymerizations of lactones (Hunsen et al., 2008). Immobilized lipase B of *Candida antarctica* proved to be especially effective in production of PHAs *via* ring opening polymerization of cyclic lactones (Arumugasamy & Ahmad, 2011; Gumel et al., 2012b; Kadokawa & Kobayashi, 2010). However, lipases and cutinases are not the only

enzymes capable of polymerizing substrates *in vitro*. Purified PHA synthase has been shown to polymerize substrates *in vitro* (Sato et al., 2010). For example, PHA synthase (PhaC<sub>1Pp</sub>) class II from *Pseudomonas putida* and class III PHA synthase (PhaEC<sub>Av</sub>) from *Allochromatium vinosum*, were used on a hydrophobic support of highly oriented pyrolytic graphite (HOPG) to synthesize PHA of few nanometer thickness (Sato et al., 2010).

Alternatively, *in vivo* biosynthesis of these biodegradable polyesters in microbial cells has been reported. For instance, several bacterial species, such as *Pseudomonas* spp., *Enterobacter* spp., *Necator* spp., *Escherichia coli*, *Rhodobacter* spp., *Cupriavidus* spp. were found to accumulate either homopolymer or copolymer of PHA *in vivo* in the presence of an excess of a carbon source under deprived nutrient condition e.g. nitrogen source (Annur et al., 2008; Rai et al., 2011b; Tian et al., 2010). In addition, mixed microbial cultures have been successfully used in producing PHAs (Albuquerque et al., 2010; Albuquerque et al., 2011). Random copolymers of PHA have been successfully produced in monoculture fermentations by controlling the type of carbon feed and composition (Gumel et al., 2012c). This has been shown to be possible using both native and recombinant bacteria (Li et al., 2010). Accumulation of PHA homopolymer containing solely poly-3-hydroxyoctanoate (PHO) has been recently shown to occur in a wild-type *Pseudomonas mendocina* (Rai et al., 2011a). Changing the fermentation temperature could influence the type of PHA and/or other metabolites to be accumulated or produced. For example, using *Pseudomonas aeruginosa* IFO3924 both medium-chain-length PHA (mcl-PHA) and rhamnolipids were produced

simultaneously (Hori et al., 2011). Production of rhamnolipids was favored by changing the fermentation temperature from 30 °C to 28 °C (Hori et al., 2011).

Many metabolizable carbon sources including carbohydrates, fatty acids, and industrial wastes can be used as energy source substrate for the production of PHAs. Methane has been used as a carbon source for producing PHAs using consortia of methanotrophic bacteria as well as single strains. In one such study, *Methylobacterium organophilum* pure culture was used to accumulate PHA in a two-phase partitioning reactor (Zúñiga et al., 2011). An increase in fermentation medium salinity could also influence the PHA accumulation. For example a two fold increase in NaCl concentration in the culture medium was observed to enhance the PHA accumulation in *Spirulina subsalsa* (Shrivastav et al., 2010). The cost of the carbon source is a substantial contributor to the production cost of PHAs by microbial processes (Reemmer, 2009). Furthermore, recovering the microbial biomass from the fermentation broth and further processing to extract the PHA in a large scale process is expensive. A current and future trend for the potentially cheaper production option is to use atmospheric carbon dioxide and sunlight to produce PHAs in genetically modified plants (Ariffin et al., 2011; Bohmert-Tatarev et al., 2011b; Snell, 2010). Plants are easily harvested and a large amount of water does not need to be removed from plant biomass for extracting PHAs. Plant platforms for producing PHA have been extensively reviewed (Börnke & Broer, 2010; Poirier & Brumbley, 2010; Reemmer, 2009). Production of PHB in genetically modified tobacco plant (*Nicotiana tabacum*) has been reported (Bohmert-Tatarev et al., 2011a). The plant had been transformed with a plasmid construct containing genes from *Acinetobacter* sp. and *Bacillus megaterium* to code the enzymes required for PHA

synthesis. The modified tobacco produced between 17% and 19% (w/w) PHB in leaf tissue and nearly 9% in the total plant biomass. However, high level of PHB expression in plants cause chlorosis, a condition characterized by a reduced chlorophyll production, consequently reduced production of carbohydrate and reduced plant growth (Reemmer, 2009). This problem may be alleviated by either delaying the synthesis of PHB until the photosynthetic tissues of the plant are well developed. This may be achieved, for example, by using a chemically induced gene-switch (Kourtz et al., 2010), or by inducing the PHA accumulation within the plant peroxisomes (Tilbrook et al., 2011).

As mentioned earlier, PHAs have attracted much attention as materials for biodegradable implants in biomedical and tissue engineering applications. Specifically, PHB has been reported to be biocompatible with various kinds of cells (Puppi et al., 2010). Use of PHAs as drug delivery systems for prolonged release of therapeutics into systemic circulation is currently receiving huge attention (Bansal et al., 2011). Polyhydroxyesters such as block copolymer of PEG-*b*-PCL in the form of micelles and nanoparticles have been used for parenteral delivery of taxanes (Gaucher et al., 2010). A matrix of nanoparticles of poly-3-hydroxybutyrate-co-3-hydroxyhexanoate (PHBHHx) has been used to deliver antineoplastic agents to cancer cells (Kiliçay et al., 2011). PHB nanoparticles functionalized with a tumor-specific ligand have been examined for specifically targeting certain breast cancer cells (Lee et al., 2011). The non-steroidal anti-inflammatory drug, ibuprofen has been conjugated to nontoxic oligo(3-hydroxybutyrate), in an attempt to improve drug delivery but this novel formulation remains to be thoroughly assessed (Zawidlak-Wegrzynska et al., 2010).

Furthermore, poly-3-hydroxybutyrate microsphere has been tested *in vitro* for releasing the antibiotics gentamycin and tetracycline (Francis, 2011). Multifunctional PHB/45S5 bioglass composite system has been discussed as drug delivery agents and for use in certain bone tissue engineering applications (Francis, 2011).

Polycaprolactone (PCL) tends to be highly permeable attributing an attractive feature to this polymer especially in some drug delivery applications. Despite the mentioned advantages of these polymeric materials, they exhibit a poor bio-resorbability *in vivo*. Polycaprolactone in tissue for example is reported to take about 3-4 years and lacks of total elimination of the degraded monomers out of the organism (Woodruff & Hutmacher, 2010). In addition, the enzymatic synthesis of PHAs in microaqueous media is conventionally carried out in potentially hazardous volatile organic solvents, such as tetrahydrofuran (Gorke et al., 2010). The reaction process is commonly characterized by poor enzyme stability, slow rate of reaction, and low molecular weight of the polymeric product. This necessitates the use of large amounts of enzymes to ensure that the desired extent of polymerization occurs within a stipulated time scale (Henderson et al., 1996; Kumar & Gross, 2000).

Furthermore, most of the synthesized biopolymers lack biological stimulus found in either intra or extra cellular matrix. Thus, specialized biopolymers are needed to be applied for this purpose. Recent advances in biopolymer engineering resulted in significant efforts towards the synthesis of biopolymers with specific functional groups capable of coupling bioactive ligands. It is not surprising that these biopolymers have attracted much attention recently due to their ability to respond to specific changes in

basic environmental stimuli such as temperature (Xu et al., 2011), pH (Bawa et al., 2009; Meng et al., 2009; Stuart et al., 2010), photo (Cui et al., 2008) and eletro (Barinov et al., 2006) stimuli while others were reported to respond to multiple stimuli (Costa et al., 2011). For example, stimuli responsive biopolymers having an ability to mimic the cellular response process were synthesized (Jocić et al., 2010; Motornov et al., 2010; Tian et al., 2012). Recently, a thermo-sensitive triblock of PLA-*b*-PNIPAAm-*b*-PLA having a lower critical solution temperature (LSCT) of 31.15 to 32.62°C has been reported (Xu et al., 2011). It has been reported that the thermal stimuli of these polymers to have arisen as a result of the hydrophobic interactions among PNIPAAm molecular chains, the intermolecular hydrogen bonding between the PNIPAAm chains, water molecules, and the intramolecular hydrogen bonding between the -CONH<sub>2</sub> groups (Tian et al., 2012).

PHB macro initiator was used in atom transfer radical polymerization (ATRP) to initiate the synthesis of a novel thermo sensitive amphiphilic triblock hydrophobic PHB flanks by hydrophilic PNIPAAm (Loh et al., 2009). Zhu et al. (2007) reported the synthesis of polycaprolactone based temperature sensitive polymer (PNIPAM-*b*-(HEMA-PCL)) using PNIPAAm as the macroinitiator in reversible addition fragmentation chain transfer (RAFT) polymerization process. Bawa et al. (2009) reported the general blood and tissue pH to be about 7.4 while in carcinogenic cells the pH was found to be about 1.0. Hence, differences in cellular pH have been utilized in designing novel drug delivery devices. Sugars such as galactose and mannose were reported to be specific ligands to the asialoglycoprotein receptor (ASGPR) receptor, which is overexpressed in hepatocellular carcinoma (Ross et al., 1994). Jiang et al. (2011) observed the



solution behavior of PCL functionalized hydroxyethyl cellulose (HEC). Previously, Lu et al. (2002) reported the synthesis of poly(1'-O-vinyladipoyl-sucrose) in chemo-enzymatic process resulting in polymer with molecular weight as high as 53 kDa having improved solvation properties that can be explored as promising biomaterial.

In general, polymer functionalization has resulted in recent increasing demand of biodegradable polymers in diverse industrial applications. Functionalization of polymer has opened a new avenue for the production of novel polymers with specific applications that were not possible earlier.

In this research project, factors like PHA production yield and its physico-chemical properties, such as thermal stability, structural composition, hydrophilicity and biodegradability, are hypothesized to be improved through rational biosynthesis of the polymer and subsequent enzymatic functionalization to incorporate biologically relevant functional groups like sugars into the polymeric backbone.

## **1.2 Research Objectives:**

This research is aimed to study the biosynthesis of biodegradable polyhydroxyalkanoates and its subsequent transesterification with acyl acceptor moieties (e.g carbohydrates), as well as to study the kinetic behavior of the production and esterification through solvents/substrate engineering for possible process optimization.

In summary:

1. The research will investigate the process of PHAs biosynthesis focusing on the effects of reaction parameters, media engineering on the structural characterization of the produced polymer;
2. The research will further observe the problems of low polymer propagation, and explore ways to improve polymerization degree, the molecular weight as well as the process yield. This will be achieved through solvent/substrate engineering and culture manipulation techniques;
3. The research will also address the issue of enhancing the biodegradability, and other physical properties of the synthesized polymers, such as hydrophilicity, by esterification of the synthesized polymer with carbohydrates. It is anticipated that a PHA-sugar ester as surfactant improves the hydrophilic properties of the polymeric material and, thus, increases its solubility, while retaining its strength, biodegradability and compatibility to be used e.g. as a tissue scaffold or drug delivery device.

### **1.3 Research Approach**

The research approach was implemented in such a way that it encompasses the research aims and objectives of the project. In general, the research methodology adopted for this project on the biosynthesis and functionalization of polyhydroxyalkanoates is based on a two (2) step process:

1. Biopolymer synthesis by (a) *in vitro* enzymatic catalysis and (b) *in vivo* microbial fermentation, followed by characterization of the synthesized biopolymer;

2. Enzymatic catalyzed esterification/functionalization of the biopolymer, followed by subsequent characterization and analyses of the functionalized polymer.

### 1.3.1 Biosynthesis of the biodegradable polymer

#### **(a) *In vitro* enzymatic catalysis**

The *in vitro* biopolymer synthesis was observed using enzymatic catalysis based on ring opening polymerization of cyclic lactone in the presence of different lipases such as *Candida antarctica* lipase A, immobilized *C. antarctica* lipase B, *C. rugosa* lipase and phospholipase A<sub>1</sub> (Lecitase Ultra). The lactone substrates ( $\epsilon$ -caprolactone and/or  $\gamma$ -butyrolactone) were used in either organic solvents or ionic liquids with known water content and water activities. In reaction vials, a specified volume of solvent/ ionic liquids was mixed with different substrate concentrations. The reaction was initiated by the addition of a specified enzyme load (10 mg to 12 mg ml<sup>-1</sup>) unless otherwise stated and incubated at different temperature ranging from 30 to 90°C. At regular time intervals, the synthesized PHA was extracted out of the filtered reaction mixture. This was done by concentrating the filtrate to about 1/5<sup>th</sup> by volume of the reaction mixture at 60°C in a rotary evaporator under reduced pressure. Cold methanol was then added to precipitate the product and the solids were filtered. The crude white precipitate of the polymer was re-dissolved in 1:5 weight per volume of chloroform, concentrated as above, precipitated again with methanol and recovered. This process was repeated for three times to purify the product. The recovered product was dried overnight under vacuum and subsequently subjected to characterization analyses.

### **(b) *In vivo* microbial biosynthesis**

The *in vivo* PHA biosynthesis was carried out using a batch fermentation process in a shake flask system (Figure 1.1).

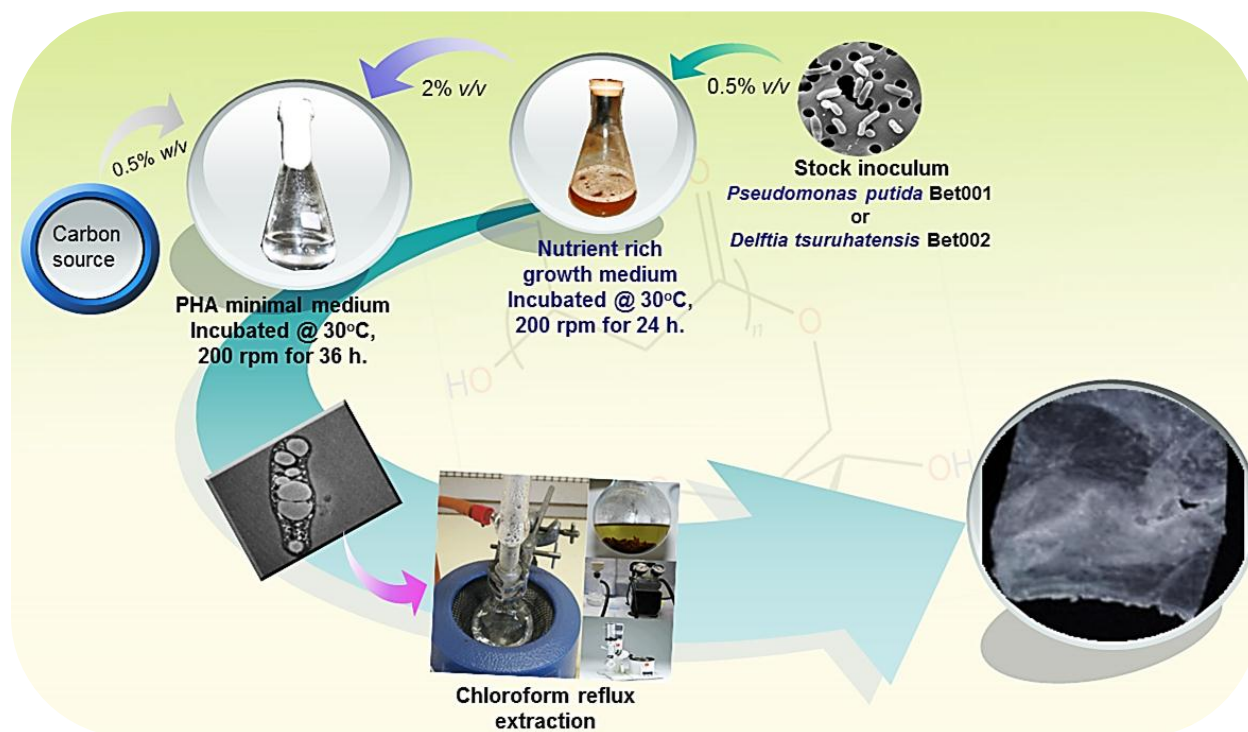


Figure 1.1 PHA biosynthesis by microbial shake-flask fermentation process

Bacterial isolates were obtained from an extended aerobic pond for the treatment of palm oil mill effluent at SIME Darby plantation palm oil industry Sdn. Bhd., Nilai, Malaysia. The isolates were identified based on biochemical and molecular 16S RNA analyses as *P. putida* Bet001 and *D. tsuruhatinensis* Bet002 respectively, were used as a microbial fermentation agent for the accumulation of the PHA. Different carbon sources like glucose, and fatty acids were evaluated as a potential carbon source for the fermentation process. A continuous solvent extraction method was applied to

isolate the synthesized polymer from the microbial biomass after the fermentation process was stopped. The recovered polymer was subjected to analytical processes such as gas chromatography (GC), gel permeation chromatography (GPC), thermal analyses, NMR and Raman FT-IR spectroscopy.

### 1.3.2 PHA esterification and functionalization

The functionalization of the synthesized biopolymers was carried out *via* an enzyme catalyzed esterification process, as illustrated in Figure 1.2. Hydrolases, such as Novozym 435 (EC 3.1.1.3) were used as catalyst. The carbohydrate such as glucose or sucrose was employed as acyl acceptor substrates, while the previously synthesized polymers from section 1.3.1 were used as acyl donor substrates.

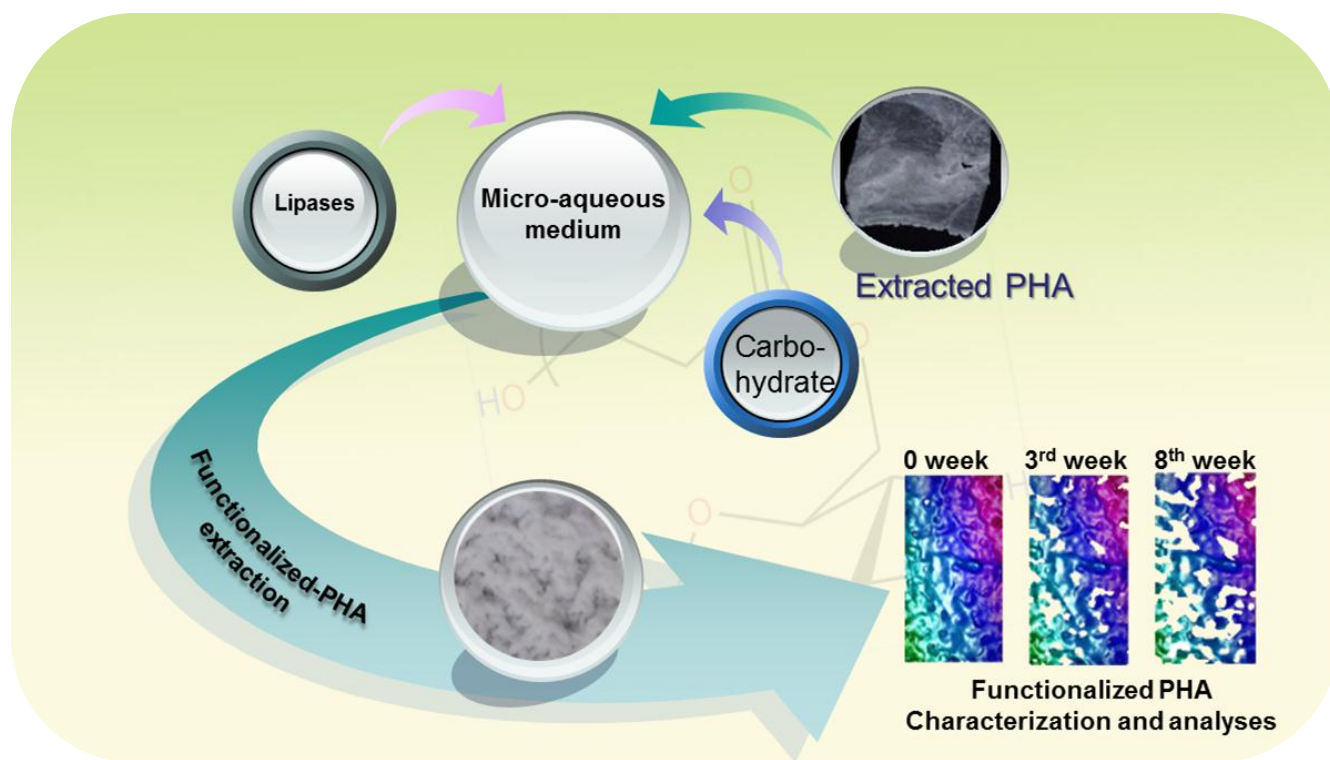


Figure 1.2 Enzymatic *in vitro* esterification of sugar-based PHA

The reaction was conducted in a batch process. Aliquot reaction samples were taken at regular time intervals and analyzed for residual sugar as well as for water content. At the end of the reaction, the mixture was filtered to remove the immobilized enzyme. The functionalized PHA was extracted by solvent extraction. The solution was concentrated in vacuum, and the PHA subsequently precipitated with either cold methanol or cold acetone. The extracted products were subjected for gravimetric analysis, NMR, GPC, GC and thermal analyses (TGA and DSC), biodegradability, biotoxicity and other structural analyses.

#### **1.4 Thesis organization and linkage of scientific papers**

The thesis is organized based on a thematic linking of scientific papers published throughout the course of the research.

The literature on the of polyhydroxyalkanoates biosynthesis, applications and functionalization as well as degradation were extensively reviewed in Chapters Two through Four. **Chapter 2** (*Recent advances in the production, recovery and applications of polyhydroxyalkanoates*) presents an extensive review of PHA production, use of media and metabolic engineering to enhance the PHA accumulation in both microbial and plant cells, as well as the recovery and applications of these biodegradable polymers. **Chapter 3** (*Lipase mediated synthesis of sugar fatty acid esters*) is a review on the esterification of sugar and carboxylic acid esters catalyzed by lipases. The paper reviewed the current utilization of enzymes and their modification as well as reactants, reaction media and reaction parameters in sugar ester synthesis and process optimization.

The demand for functionalized polymers in specialty applications has promoted intensive research on different controlled degradation processes and their applications. However, the production of these functionalized or modified polymers by conventional synthetic routes is expensive and time consuming. The advancement in degradation technology is becoming an enabling factor in the production of modified polymers and their functionalization. **Chapter 4** (*Current application of controlled degradation processes in polymer modification and functionalization*) presents a concise review on the application of high energy radiation (gamma rays), ozonization, ultrasound irradiation, ultraviolet light, and enzymatic hydrolysis for controlled degradation or modification of polymeric materials.

Early studies of the *in vitro* lipase mediated synthesis of PHA by ring opening polymerization (ROP) were characterized by poor enzyme stability, a slow reaction rate and a low polymer weight. These problems continue to limit large-scale commercial use of lipase mediated polymer synthesis. The literature reported various attempts to improve the performance of lipase mediated ROP through the use of microwave irradiation, supercritical fluids, and ionic liquids. The use of ultrasound holds substantial potential for enhancing the performance of biocatalytic processes, but sonication has not been evaluated for lipase mediated ROP. **Chapter 5** (*Ultrasound assisted lipase catalyzed synthesis of poly-6-hydroxyhexanoate*) reports the use of high dissipating energy and extreme shear forces produced by the cavitation bubbles collapse in ultrasound irradiation process to overcome the previously mentioned limitations. In addition, detailed characterization of the synthesized homopolymer was also reported in the paper.

In **Chapter 6** (*Lipase catalyzed ultrasonic synthesis of poly-4-hydroxybutyrate-co-6-hydroxyhexanoate*), the studies is extended on utilizing the same ultrasound irradiation advantages to synthesize a copolymeric PHA. In this study, four lipases were compared for the synthesis of a biodegradable and biocompatible biomaterial i.e. poly-4-hydroxybutyrate-co-6-hydroxyhexanoate. From the results obtained, it was found that ultrasound improved the rate of polymerization catalyzed by the enzymes as compared to controls. The effective sonication regime, however, depended on the enzyme used. The use of the lipase preparation Lecitase Ultra<sup>TM</sup> for the copolymerization of PHA is reported for the first time, and was found to be effective for the synthesis of the biopolymer under ultrasonication. The most widely used lipase, i.e. Novozym 435, still proved to be the best catalyst for the reaction studied. In addition, kinetics of the polymerization and the most suitable model for its description were outlined. The effects of sonication power, time and temperature on the rate of copolymerization were also investigated. The results also indicated the effects of the sonication variables on the catalyst system used.

Biodegradable polymers combine attractive physical properties with microbial degradability. Medium-chain-length poly (3-hydroxyalkanoates) (mcl-PHA) is an example of such a biopolymer. A new approach for its bioproduction is described in **Chapter 7** (*Biosynthesis and characterization of polyhydroxyalkanoates copolymers produced by *Pseudomonas putida* Bet001 isolated from palm oil mill effluent*). This study reports on isolation, biochemical characterization and post PCR analyses of a new bacterial strain from palm oil mill effluent (POME), a high strength agro-industrial waste; and the examination of its growth and mcl-PHA production characteristics and



characterization of the copolymer produced. We found that the intracellular accumulation of mcl-PHA in the new bacterium isolate, identified as *Pseudomonas putida* Bet001, followed a growth associated trend, which is uncommon for Pseudomonads species. Usually the PHA accumulation in the Pseudomonads starts when the nutrient(s) become limited and growth is no longer possible.

Furthermore, the newly isolated strain also exhibited an unusual nature of mcl-PHA composition when fed with a particular fatty acid. For example, when fed with long chain unsaturated fatty acid, such as oleic acid, the strain produced a copolymer consisting of short chain even numbered carbon monomers and odd numbered carbon chain monomer simultaneously with other monomers normally produced by Pseudomonads. This phenomenon was not observed when medium chain or short chain fatty acids substrates were used. Depending on the substrates fed, the incorporation of longer monomers into the accumulated mcl-PHA improved the polymer thermal stability. In addition, no unsaturated monomers were detected in the PHA, even when oleic acid was fed as sole carbon and energy source, unlike reported in other studies employing similar conditions. This is unusual, since the mechanistic action of beta-oxidation cycle is well known. This observation may open up further research, especially related to the beta oxidation pathway in these isolates.

Further study on the effect of carbon source on the polymer composition and stability was reported using another isolate of PHA accumulating bacterium in **Chapter 8** (*Effects of carbon substrates on biodegradable polymer composition and stability produced by Delftia tsuruhatensis Bet002 isolated from palm oil mill effluent*). The paper reports the growth-associated accumulation of PHA with 76.7% polymer content based

on cell dried weight and molecular weight ranging from 131 to 199 kDa. In addition, the molar concentration ratio of carbon to nitrogen source was found to have little effect on the PHA composition, but affected the biomass, PHA yield and polymer degradation stability. In general, the polymer comprised of even and odd carbon chain length ( $C_4$  to  $C_{10}$ ). The PHA produced a semi-crystalline polymer with good thermal stability, thermal degradation temperature ( $T_d$ ) 270 to 392°C, melting temperature ( $T_m$ ) 164 to 177°C, glass transition temperature ( $T_g$ ) -1 to 4°C and apparent melting enthalpy of fusion ( $\Delta H_f$ ) of 53 to 211 J g<sup>-1</sup>.

In regards to functionalization of polymers, a wide range of biodegradable functionalized polymers has been produced using enzymatic catalysis. Most of the reported polymer functionalization was based on polyvinyl, polyacrylate and polycaprolactone esters. In addition, most of the synthetic processes are not solely enzymatic but a hybrid system (chemo-enzymatic), where enzymatic transesterification of the vinyl or acrylic ester with the sugar moiety is followed by chemical radical polymerization. In most cases, the functionalized polymer obtained through this approach, has toxic chemical impurities, which make it less attractive for biomedical applications. Secondly, the pendant carbohydrate moiety is attached to the main polymeric chain by a di-carboxylic acid spacer arm, which could probably increase the hydrophobicity of the polymer rather than improving the hydrophilicity. Literature reporting bacterial PHA functionalization is very scarce, particularly reports on the single-step enzymatic functionalization of medium chain length PHA (mcl-PHA).

In **Chapter 9** (*Single-step lipase-catalyzed functionalization of medium-chain-length polyhydroxyalkanoates*), The paper reports for the first time a *Candida antarctica*

lipase B (EC 3.1.1.3) catalyzed functionalization of bacterial mcl-PHA with sucrose in the absence of the spacer arm to yield poly(1'-O-3-hydroxyacyl-sucrose). Effects of reaction variables, such as temperature, enzyme loading, reactant ratio and reaction time in relation to enzymatic reaction rate,  $v^{app}$ , as well as and reactant conversion were studied. Using  $H_2O_2$  as micro initiator, the enzyme-mediated synthesis led to a reaction rate,  $v^{app}$  of  $0.076 \times 10^{-5} \text{ mol L}^{-1} \text{ s}^{-1}$ . In addition, the research provided a detailed physico-chemical characterization of the functionalized polymer and biodegradability analyses using 3D optical surface texture analyzer. In this study, the biodegradability of the functionalized polymer is found to increase by 1.5 fold compared to the non-functionalized material apart from showing better compostability.

**Chapter 10** (*Enzymatic synthesis of 6-O-glucosyl-poly(3-hydroxyalkanoates) in organic solvents and their binary mixture*) reports further on the effect of reaction parameters on enzyme catalyzed PHA-glucosyl functionalization based on reaction media engineering. The paper reports for the first time the use of Lecitase™ Ultra in the functionalization of bacterial medium-chain-length PHA (mcl-PHA). The study reports the effect of mono-phasic organic solvents and their binary mixtures in improving the enzymatic functionalization of mcl-PHA, which is a novel subject in itself. It was found that binary mixture of organic solvent provides a better medium for the functionalization. For example, an equal volume binary mixture of DMSO and chloroform with moderate polarity was more favorable for the rate of enzyme-catalyzed synthesis of the carbohydrate polymer and reactant conversion compared to mono-phasic and other binary solvents. The apparent reaction rate constant as function of the water activity ( $a_w$ ) of the medium increased with increasing solvent polarity, with optimum  $a_w$  of 0.2,

0.4 and 0.7 ( $\pm 0.1$ ) observed in hydrophilic DMSO, binary mixtures DMSO:isooctane and hydrophobic isooctane, respectively. Control of  $a_w$  can be achieved by optimum molecular sieve loading. In this study, a reaction temperature between 40 to 50°C was found to be optimal, and the functionalized PHA polymer was observed to possess good physico-chemical characteristics and biodegradability.

## CHAPTER 2

### Recent advances in the production, recovery and applications of polyhydroxyalkanoates

---

**A. M. Gumel,<sup>1</sup> M. S. M. Annuar,<sup>1\*</sup> Y. Chisti<sup>2</sup>**

<sup>1</sup> *Institute of Biological Sciences, Faculty of Science, University of Malaya, 50603 Kuala Lumpur, Malaysia*

<sup>2</sup> *School of Engineering, PN 456, Massey University, Private Bag 11 222, Palmerston North, New Zealand*

**Published:** *Journal of the Polymer and the Environment* (2013) 21(2): 580-605.  
(DOI 10.1007/s10924-012-0527-1) (ISI cited publication)

#### Statement of contributions of joint Authorship

**Gumel, A.M:** (Candidate)

Writing and compilation of the review literature. Main author of the manuscript

**Annuar, M.S.M:** (Principal Supervisor)

Supervised and assisted with manuscript compilation, editing and co-author of the manuscript.

**Chisti, Y:** (Research collaborator)

Editing and co-author of manuscript

# Recent Advances in the Production, Recovery and Applications of Polyhydroxyalkanoates

A. M. Gumel · M. S. M. Annuar · Y. Chisti

Published online: 18 September 2012  
© Springer Science+Business Media, LLC 2012

**Abstract** Polyhydroxyalkanoates (PHAs) are biodegradable and biocompatible polyesters that can potentially replace certain plastics derived from petroleum. PHAs can be produced using a combination of renewable feedstocks and biological methods. Native and recombinant microorganisms have been generally used for making PHAs via fermentation processes. As much as 90 % of the microbial dry mass may accumulate as PHAs. A range of PHAs has been produced using fermentation methods, including copolymers and block copolymers. Alternative production schemes based on genetically modified plants are becoming established and may become the preferred route for producing certain PHAs. Production in plants is likely to be inexpensive compared to production by fermentation, but it does not appear to be as versatile as microbial synthesis in terms of the range of products that may be generated. Cell-free enzymatic production of PHAs in vitro is receiving increasing attention and may become the preferred route to some specialty products. This review discusses the recent advances in production of polyhydroxyalkanoates by the various methods. Methods of recovering the polymer from microbial biomass are reviewed. Established and emerging applications of PHAs are discussed.

**Keywords** Biopolymers · Bioplastics · Polyhydroxyalkanoates · Polymerization · Applications

## Abbreviations

|                  |   |
|------------------|---|
| ATRP             | Atom transfer radical polymerization              |
| CALB             | <i>Candida antarctica</i> lipase B                |
| CSTR             | Continuous stirred tank reactor                   |
| DO               | Dissolved oxygen                                  |
| DNA              | Deoxyribonucleic acid                             |
| DW               | Dry weight  |
| cPHB             | Complexed poly-(R)-3-hydroxybutyrate              |
| EDTA             | Ethylenediaminetetraacetic acid                   |
| FNL              | <i>Fervidobacterium nodosum</i> lipase (FNL)      |
| HACoA            | HydroxyalkanoylCoA                                |
| HB               | Hydroxybutyrate                                   |
| 3HB              | 3-Hydroxybutyrate, or 3-hydroxybutyric acid       |
| 4-HB             | 4-Hydroxybutyrate                                 |
| HEC              | Hydroxyethyl cellulose                            |
| HEMA             | 2-Hydroxyethyl methacrylate                       |
| HHx              | Hydroxyhexanoate                                  |
| HOPG             | Highly oriented pyrolytic graphite                |
| HV               | Hydroxyvelarate                                   |
| mcl-PHA          | Medium-chain-length PHA                           |
| NAD <sup>+</sup> | Nicotinamide adenine dinucleotide                 |
| NADH             | Reduced form of nicotinamide adenine dinucleotide |
| P3HB3HV          | Poly(3-hydroxybutyrate-co-3-hydroxyvalerate)      |
| PANi             | Polyalanine                                       |
| PCL              | $\epsilon$ -Caprolactone, or polycaprolactone     |
| PDH              | Pyruvate dehydrogenase                            |
| PDL              | $\omega$ -Pentadecalactone                        |
| PEG              | Polyethylene glycol                               |
| PEO              | Polyethylene oxide                                |
| PHA              | Polyhydroxyalkanoates                             |
| PHB              | Polyhydroxybutyric acid                           |
| PHBHHx           | Poly-3-hydroxybutyrate-co-3-hydroxyhexanoate      |

A. M. Gumel · M. S. M. Annuar (✉)  
Faculty of Science, Institute of Biological Sciences,  
University of Malaya, 50603 Kuala Lumpur, Malaysia  
e-mail: suffian\_annuar@um.edu.my

Y. Chisti  
School of Engineering, PN 456, Massey University,  
Private Bag 11 222, Palmerston North, New Zealand

|                    |   |
|--------------------|---|
| PHBV               | Polyhydroxybutyrate- <i>co</i> -valerate  |
| PHBVHHx            | Poly-3-hydroxybutyrate- <i>b</i> -3-hydroxyvalerate- <i>b</i> -3-hydroxyhexanoate |
| PHF                | Polyhistidine   |
| PHO                | Poly-3-hydroxyoctanoate   |
| PLA                | Polylactide   |
| PNIPAAm            | Poly(N-isopropyl acrylamide)  |
| RAFT               | Reversible addition fragmentation chain transfer                                  |
| ( <i>R</i> )-LATP  | Thiophenyl ( <i>R</i> )-lactate   |
| ( <i>R</i> )-3HBTP | Thiophenyl ( <i>R</i> )-3-hydroxybutyrate   |
| scCO <sub>2</sub>  | Supercritical carbon dioxide  |
| SDS                | Sodium dodecylsulfate   |
| TMC                | Trimethylene carbonate  |

## Introduction

In 2011, nearly 280 million tons of petrochemicals-based polymers were produced with expected increased in 4 % per annum to 2016 [1]. Production of synthetic polymers is expected to increase to around 810 million tons by 2050 [2]. A strong interest exists in attempting to replace petrochemicals-derived plastics with biologically produced alternatives. Here we review the production, recovery and applications of polyhydroxyalkanoate (PHA) biopolymers.

PHAs are a class of biopolymers with useful physicochemical properties for diverse industrial and biomedical applications. PHAs are biocompatible and biodegradable. PHAs can be produced sustainably using renewable resources and biological methods. Accumulation of PHAs in the bacterium *Bacillus megaterium* was first reported in 1926 [3]. Since then, many microorganisms have been shown to accumulate PHAs as intracellular granules [4–6] or secrete the polymer extracellularly [3, 7, 8]. Good yields of PHAs have been reported from certain genetically engineered plants [9–12].

Synthetically produced polymers are generally inexpensive, but their persistence in the environment poses a significant problem. Furthermore, production of fossil-based polymers has a significant environmental impact [13] as a net contributor to the level of atmospheric carbon dioxide. Processes for making synthetic polymers often use hazardous materials. In contrast to most petropolymers, biologically produced polymers are generally biodegradable, biocompatible [14, 15] and may be produced sustainably using processes with a reduced environmental impact. Technology for producing various biopolymers is developing rapidly, but because of their relatively high cost, they are used mostly in specialty applications. By 2018, the production of biopolymers is expected to grow by

nearly 35 % and around \$5 billion worth of biopolymers are expected to be produced [16, 17].

Continuing advances in genetic engineering, metabolic engineering and enzymology are improving accessibility of an increasing number of biopolymers. In addition to production in microorganisms and plants, in vitro enzymatic production of biopolymers is attracting much attention [18–23]. PHAs are commercially produced and are perhaps the best studied of the biopolymers [24, 25]. Nevertheless, they are still relatively expensive and this hinders their wider commercial use.

## PHA Production

### Production by Microbial Fermentation

In bacteria, PHAs accumulate in the presence of an excess of a carbon source coupled to a deprivation of nutrients such as nitrogen [26]. All metabolizable carbon sources can be used for the production of PHAs, including fatty acids and carbohydrates. PHA polymers accumulate as intracellular inclusions in bacteria of the genera such as *Alcaligenes*, *Pseudomonas*, *Enterobacter*, *Necator*, *Rhodobacter*, *Ralstonia* and *Cupriavidus* [27–32]. Literature on PHA production in bacteria is extensive [24, 25, 33, 34]. Some of the most recent studies are summarized in Table 1. Certain cyanobacteria also accumulate PHAs under suitable environmental conditions [35, 36] and so do some halophiles [33].

Random copolymers of PHA have been successfully produced in monoculture fermentations by controlling the type of carbon feed and composition [37]. This has been shown to be possible using both native and recombinant bacteria [38]. Using *Cupriavidus necator* in fed-batch fermentations to produce the copolymer poly-3-hydroxybutyrate-*co*-4-hydroxybutyrate, Chanprateep et al. [27] attained a polymer level of 77 % (w/w) in the biomass. This was achieved with a C:N mole ratio of 200:1 with fructose as the precursor for 3-hydroxybutyrate (3HB) and 1,4-butanediol as the precursor for 4-hydroxybutyrate (4HB). Ammonium sulfate was the nitrogen source. The composition of the copolymer, i.e., the ratio of 3HB to 4HB in it, was affected by the molar ratio of the two carbon substrates in the culture medium. For example, if the carbon source contained 25 % (w/w) 1,4-butanediol, a copolymer with a 30 % mole fraction of 4HB was produced, but this could be increased to 80 % by increasing the 1,4-butanediol level to 75 % (w/w). Another commonly used precursor for 4HB is the sodium salt of  $\gamma$ -hydroxybutyrate, but this is more expensive than 1,4-butanediol. Although using too high a concentration of 1,4-butanediol has been found to be toxic to cells [27]. In the production of poly(3-hydroxybutyrate-*co*-3-hydroxyvalerate)

**Table 1** PHA fermentation processes

| Fermentation conditions  | Microorganism   | Carbon source                                    | Product | PHA yield (%) | References |
|--|---|--|---------|---------------|------------|
| Fed batch: 30 °C, 200 rpm, DO 20 %, 72 h                                 | <i>Cupriavidus</i> sp. USMAA2-4                                   | Oleic acid (0.82 % v/v), 1-pentanol (0.11 % v/v) |         | 29            | [31]       |
| Continuous: 30 °C, 500 rpm, pH 7, air flow 2.5 mL min <sup>-1</sup>      | <i>Cupriavidus necator</i> A-04                                   | Brown sugar, rock sugar, toddy palm sugar, etc.  |         | 77            | [27]       |
| Two-stage CSTR: 30 °C, pH 6, 400 rpm                                     | Mixed culture   | Molasses   |         | 77            | [42]       |
| SBR: 30 °C, pH 6, 500 rpm  | Mixed culture   | Volatile fatty acids                             |         | 77            | [43]       |
| Fed batch: 30 °C, 400 rpm, pH 6.8, DO 50 %                               | <i>Ralstonia eutropha</i> DSM428, ATCC 17699, NCIB 10442          | Fructose   |         | 45            | [28]       |
| Two-stage continuous fed-batch: 30 °C, 200 rpm, 48 h, pH 6.5, DO 30 %    | <i>Pseudomonas putida</i> KTOY06ΔC ( <i>phaPC<sub>lac</sub></i> ) | Mixed fatty acids                                |         | –             | [51]       |
| Batch shake flask: 30 °C, 200 rpm, pH 7                                  | <i>P. mendocina</i> CH50  | Sodium octanoate                                 |         | 31            | [38]       |
| Two-phase partition reactor: air flow 0.42 L min <sup>-1</sup> , 500 rpm | <i>Methylobacterium organophilum</i> CZ-2                         | Methane  |         | 57            | [45]       |

Abbreviations CSTR continuously stirred tank reactor, SBR sequencing batch reactor, DO dissolved oxygen



(P3HB3HV) by a *Cupriavidus* sp. changes in culture pH were reported to affect the composition of the copolymer produced [31].

Accumulation of poly-3-hydroxyoctanoate (PHO) homopolymer has been recently shown to occur in a wild-type *Pseudomonas mendocina* [39]. Up to 31 % of the cell dry weight consisted of PHO, but the biomass concentration in this preliminary study was relatively low [39]. A two-stage approach was proposed for accumulating the polymer. This consisted of a first stage tailored to achieving a high concentration of the biomass, followed by a second stage tailored to accumulation of the polymer within the cells [39]. Using a controlled feeding strategy based on a metabolic flux balance analysis, Ramalingam et al. [40] achieved a PHA content in the biomass of 35.6 % (w/w) with a PHA concentration in the fermentation broth of  $1.14 \text{ g L}^{-1}$  in a continuous fermentation involving *Pseudomonas putida* MTCC 102 (Type B). Linoleic acid was used as the carbon source.

In some cases at least, the culture temperature can alter whether PHA or some other metabolite is produced preferentially. For example, using *Pseudomonas aeruginosa* IFO3924 both medium-chain-length PHA (mcl-PHA) and rhamnolipids were produced simultaneously [41]. Production of rhamnolipids was favored by changing the temperature from 30 to 28 °C [41]. *P. aeruginosa* IFO3924 fed with fatty acids having an even-number of carbons led to the production of 3-hydroxyalkanoates containing only an even-number of carbons in the in the polymer. In contrast, feeding of fatty acids with an odd-number of carbons resulted in 3-hydroxyalkanoates containing both odd- and even-numbered carbon chains. Of the different fatty acids fed, C11 and C12 fatty acids proved to be the best carbon sources for this microorganism [41]. The feeding of C11 substrate resulted in  $504 \text{ mg L}^{-1}$  PHA.

Recombinant *Escherichia coli* harboring *phaABC* and *phaP* of *Azotobacter* sp. has been reported to accumulate PHB (polyhydroxybutyrate) when fed with glycerol [42], a relatively inexpensive carbon source. Accumulation of PHB decreased with an improved supply of oxygen. Changing the carbon source to glucose also led to PHB accumulation, but in this case accumulation was enhanced by an improved supply of oxygen. Presumably, therefore, differences in the oxidation state of the cells differently affect PHB accumulation from carbon sources with different oxidation state [42]. Glycerol has a lower oxidation state of  $-2$  compared to glucose ( $0$ ). Depending on the oxidation state, catabolism of a carbon source would produce different ratios of  $\text{NADH/NAD}^+$  and this will determine how much of the carbon flows to the synthesis of a more reduced product [42].

The utilization of complex low cost carbon substrates and the elimination of sterilization energy cost made mixed

microbial culture (MMC) to be a cost-effective PHA production process [43]. In fact, it has been suggested that based on life cycle analysis (LCA), PHA production by MMC could be more favorable compared to using pure cultures in both economic and environmental perspectives [44]. MMC have been successfully used in producing PHAs [43]. In such an operation with a 2-stage stirred tank reactor, the use of molasses as the carbon source provided a PHA content in the biomass of 61 % (w/w) [43]. In similar studies with continuous stirred tank reactors and sequencing batch reactors, the fermentation conditions were found to greatly influence the accumulation of PHA in the microbial cells growing on volatile fatty acids [44]. For example, a feast–famine operational regimen affected PHA content in the biomass [44]. The composition of the biopolymer formed in the mixed culture could be manipulated by changing the composition of the carbon source and by whether it was fed pulse-wise or continuously [44]. Such changes could be used to alter the ratio of hydroxybutyrate (HB) and hydroxyvalerate (HV) in the PHA copolymer to change its average molecular weight, degree of crystallinity and other physical properties [44].

The production economics of PHAs depend very much on the cost of the carbon feedstock and whether aseptic (monoculture) or open mixed culture production methods are used. In some applications, the use of mixed carbon sources and microbial cultures as found in municipal wastewaters, for example, may be acceptable for making PHAs. Use of palm oil for producing PHAs has been discussed [34].

In attempts to use a cheap feedstock for producing PHA, ruthenium (Ru) was used for catalytic hydrolysis of inexpensive cellulose to glucose [45]. The hydrolysis occurred at 220 °C and converted 15–20 % of cellulose to glucose and other products. The crude hydrolysate was then used to culture a recombinant *E. coli*. The bacterium accumulated 42 % (w/w) of its biomass as PHB in a 72 h fermentation at 30 °C, but the concentration of biomass was low because of Ru toxicity. The polymer produced had a number averaged molecular weight of  $3.1 \times 10^5 \text{ Da}$ . For otherwise the same fermentation conditions, the use of pure analytical grade glucose as the feed yielded a polymer with a somewhat higher number averaged molecular weight of  $4.3 \times 10^5 \text{ Da}$ .

Methane has been used as a carbon source for producing PHAs using consortia of methanotrophic bacteria as well as single strains. In one such study, *Methylobacterium organophilum* pure culture was used in a two-phase partitioning reactor [46]. The specific methane consumption rate of the isolate was  $100 \text{ mg CH}_4 \text{ g}^{-1} \text{ h}^{-1}$  compared to much lower rates reported for consortia of methanotrophic bacteria. The isolate accumulated nearly 57 % (w/w) PHB in the biomass under nitrogen limiting conditions.

Exposure of the activated sludge bacteria to a 7 mT static magnetic field has been claimed to enhance PHB accumulation by the cells under conditions of elevated concentrations of acetate [47]. This effect is said to be a consequence of a reduced uptake of acetate which is toxic to cells in high concentration [47]. The imposed magnetic field alters acetate uptake by modifying the net-charge on the surface of the cell membrane [47].

Certain photosynthesizing microorganisms are known to accumulate PHAs [35, 36]. In cyanobacteria such as *Spirulina subsalsa* [48], accumulation of PHA has been shown to be influenced by the salinity of the culture medium. A two-fold increase in NaCl concentration enhanced PHA accumulation relative to control, although the PHA yield was relatively low. The mechanism of this ionic strength effect is not entirely clear. PHAs accumulate also in certain halophilic bacteria as reviewed elsewhere [33].

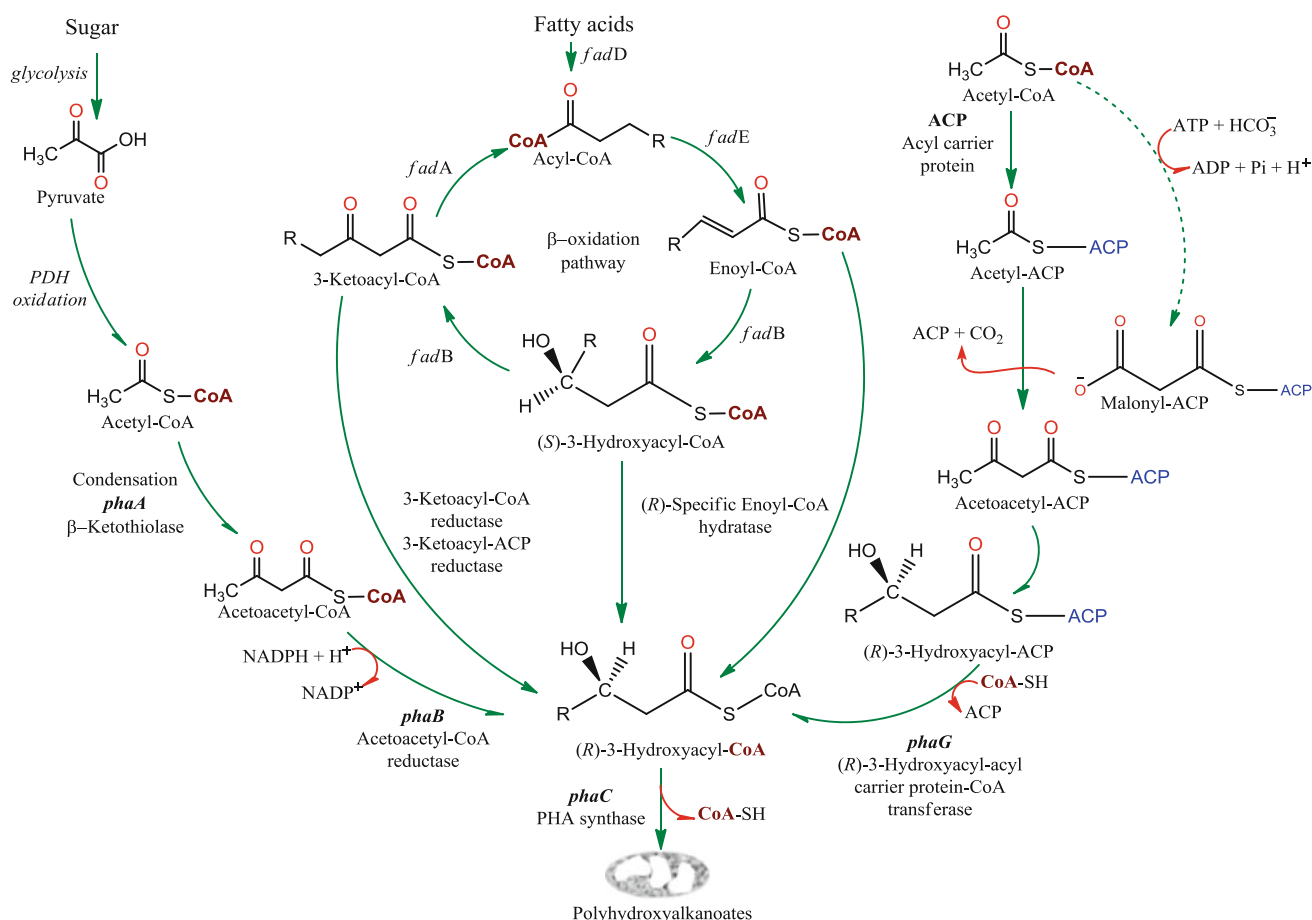
### Metabolic Engineering

In bacteria, the synthesis of polyhydroxyalkanoates from sugars normally begins with glycolysis of the sugar to

pyruvate. The latter is converted to acetyl-CoA via the pyruvate dehydrogenase (PDH) oxidation pathway. Two molecules of acetyl-CoA are then condensed to form acetoacetyl-CoA through the action of  $\beta$ -ketothiolase, an enzyme encoded by the *phaA* gene. Acetoacetyl-CoA is reduced by acetoacetyl-CoA reductase (*phaB*) to form the monomer of (*R*)-3-hydroxyacyl-CoA, the building block of PHAs. PHA synthase (*phaC*) finally polymerizes the monomers to PHA (Fig. 1).

Metabolic engineering of PHA biosynthesis pathways (Fig. 1) has been used to produce PHAs of different types and properties in various bacterial species. For example, *Escherichia coli* strains have been metabolically engineered to regulate the expression of short chain fatty acid catabolism operon to significantly enhance the expression of short chain complexed poly-(*R*)-3-hydroxybutyrate (cPHB) [49, 50]. Theodorou et al. [50] reported a 1.7-fold increase in accumulation of cPHB in a mutant *E. coli* compared to the wild-type.

Acetoacetate induction was used to regulate expression of the product [49–51]. Reducing the production of acetic acid capability is reported to improve carbon channeling to



**Fig. 1** General scheme of PHA biosynthesis from sugar catabolism, fatty acid  $\beta$ -oxidation and intermediary pathways

polymer biosynthesis. Recently, Jian et al. [52] reported a 2-fold increase in production of biomass and 3.5-fold increase in production of PHA in an *E. coli* mutant that had been engineered to reduce the excretion of acetate, lactate, ethanol and formate. The excretion of acetate by the mutant was 90 % lower compared to the parent strain [52]. Simultaneous production of succinate and PHA in a metabolically engineered *Escherichia coli* has also been reported [53, 54]. This was achieved by deleting *ptsG*, *sdhA* and *pta* genes and overexpressing the *phaC1* gene of *Pseudomonas aeruginosa*. The engineered *E. coli* produced nearly 21 g L<sup>-1</sup> succinate and 0.54 g L<sup>-1</sup> PHA, equivalent to a polymer content of nearly 6 % in the biomass. The feed used was a mixture of glycerol and fatty acids. The PHA produced consisted of 3-hydroxyoctanoate (58.7 % by mol) and 3-hydroxydecanoate (41.3 % by mol).

Liu et al. [55] reported the use of  $\beta$ -oxidation inhibition to produce mcl-PHA homopolymer in a mutant *Pseudomonas putida* (KTQQ20) fed with the relevant fatty acid. Six genes of the  $\beta$ -oxidation pathway were knocked out to significantly reduce the fatty acid  $\beta$ -oxidation activity. Feeding dodecanoic acid to the mutant strain resulted in mcl-PHA accumulation at a 10 % (w/w) level in the biomass. The PHA homo-copolymer contained 3-hydroxydecanoate monomer (16 % by mol) and 3-hydroxydodecanoate monomer (84 % by mol). Changing the feed carbon source to decanoic acid resulted in a total PHA accumulation of about 5 % (w/w) in the biomass. The accumulated PHA was a pure homopolymer of 3-hydroxydecanoate. If the feed was changed to tetradecanoic acid, the PHA content of the biomass was higher at 78 % (w/w) and the product was a pure homopolymer of 3-hydroxytetradecanoate. The polymers produced in the  $\beta$ -oxidation inhibited mutant had improved mechanical properties compared to the polymers produced in the native bacterium [55].

Similar observations have been reported in relation to the effect of inhibition of  $\beta$ -oxidation on production of PHA (Fig. 1) in a mutant *Pseudomonas entomophila* [56]. The  $\beta$ -oxidation inhibited mutant produced by knocking out some of the genes of the relevant pathway, accumulated PHA at the level of >90 % (w/w) in the biomass [56]. The product consisted of mainly (99 % by mol) 3-hydroxydodecanoates. The number averaged molecular weight of the polymer formed was as high as 39,000 Da and it had a polydispersity index of 2.1.

In the biosynthesis of PHA copolymers when the focus is on increasing the mole fraction of a particular monomer in the copolymer, the use of a high concentration of the precursor of the preferentially desired monomer is required in the culture medium. However, a high concentration of certain precursors can be quite toxic to cells. One possible way of overcoming this toxicity is to use a PHA synthase gene that has a high affinity for polymerizing the toxic

co-monomer [57]. For example, if a copolymer with a high content of 3HV is wanted, the culture medium would need to be rich in a 3HV precursor such as valeric acid which may be toxic. The producing microorganism may be engineered to contain the PHA synthase gene such as *phaC* of *Chromobacterium* sp. USM2, which is reported to have a high affinity towards valeric acid. This strategy was used to accumulate poly(3HB-co-3HV-co-3HHx) (HHx = hydroxyhexanoate) to the level of 86 % (w/w) in the biomass of an engineered *Cupriavidus necator* [57]. The 3HV monomer content in the terpolymer was nearly 91 % (by mol) and the polymer had mechanical properties comparable to those of the common low density polyethylene [57].

An *Aeromonas hydrophila* mutant with two genes of the acetic acid metabolic pathway deleted, accumulated poly(3HB-co-3HHx) at the level of 47 % (w/w) in the dry biomass, corresponding to a polymer concentration of around 3 g L<sup>-1</sup> in the broth [55]. This level of production was nearly 45 % greater compared to the native strain [55]. Further transformation of the already engineered bacterium to harbor genes relating to fatty acids biosynthesis increased production of PHBHHx by 63 % compared to the strain with only the genes of the acetic acid metabolism deleted.

Yeasts generally have a larger cell size than bacteria and consequently are comparatively easier to recover from the fermentation broth by processes such as centrifugation and filtration. Compared to bacteria, yeast cells are also easier to break for recovering intracellular products [58]. For these reasons, there is an interest in using yeasts to produce PHAs. PHA production by different metabolically engineered yeasts has been reported [7, 8, 59, 60]. For example, Buelhamd et al. [59] produced PHAs in a transgenic *Saccharomyces pombe*. The yeast was engineered to produce PHB by transfection with the plasmid pBHR68 harboring the PHB synthesis genes encoding  $\beta$ -ketothiolase (*phbA<sub>Re</sub>*), acetoacetyl-CoA reductase (*phbB<sub>Re</sub>*) and PHB synthase (*phbC<sub>Re</sub>*) of *Ralstonia eutropha*. Under optimized conditions, the yeast accumulated PHB at the level of nearly 9 % (w/w) in the biomass.

Properties of the PHA synthesized in engineered *Saccharomyces pombe* and *Saccharomyces cerevisiae* have been discussed in detail [59]. PHA produced in these yeasts was found to have a melting temperature in the range of 153–171 °C. The degree of crystallinity of the product ranged from 27 to 32 % during heating and 36 to 50 % during cooling [7].

A metabolically engineered yeast of the genus *Kloeckera* accumulated PHA within the cells and secreted a water-soluble bioflocculant polymer in the extracellular medium [7]. The mutant accumulated PHA to the level of about 7 % (w/w) in the biomass. This yeast had been made

by transfection with *R. eutropha*'s *phaABC* operon harboring genes encoding *phaA*, *phaB* and *phaC* [59].

PHAs accumulate as intracellular inclusions; therefore, their recovery from the cells is inherently expensive. The overall cost of producing PHAs would reduce greatly if the cells could be coaxed into secreting the polymer into the extracellular broth. Extracellular production may be made possible through genetic engineering of the producing cells. This approach is attracting attention. Extracellular secretion of PHA in an *Alcanivorax borkumensis* mutant specifically engineered for this purpose was observed when the microorganism was fed on either pyruvate or octadecane as the sole carbon source [61].

### Recovery of PHAs

Scalable processes are needed for inexpensively recovering the intracellular PHAs from microorganisms. Examples of the recently published recovery methods are provided in Table 2. Although other recovery methods have been published [62], extraction of the polymer with organic solvents appears to be a commonly used approach and has been reported to have an undoubted advantages over the other PHA extraction methods [63]. Its simplicity and rapidity is reported to incur its frequent use in laboratory scale PHA extractions. Solvents extract the polymer without degrading it by improving the cellular membrane

permeability and subsequent solubilization of the PHA [63]. Solvent extraction process was also reported to effectively prevent Gram-negative bacterial endotoxin contamination of the polymer, therefore improving the polymeric quality for biomedical applications [64].

In some cases, the biomass recovered by centrifugation is first washed with an organic solvent to remove fatty acids and oils left from the culture medium. Subsequently, the biomass may be freeze-dried prior to extracting the polymer with a solvent such as chloroform [4]. Cold methanol is then generally used to precipitate the polymer from chloroform [65]. Alternatively, a freshly harvested biomass paste may be washed with acetone and dried under vacuum at ambient temperature prior to solvent extraction of the polymer [66]. PHB-co-PHV has been recovered from *Halomonas campisalis* cells using a similar process [65] (Table 2). P3HB-co-4HB has been similarly extracted [66] and a similar extraction has been reported for poly-3HB-co-3HV from *Pseudomonas oleovorans* cells [67]. Variations of solvent extraction methods have been used by others [27, 44, 68] (Table 2). In some processes dichloromethane has been used for extraction instead of chloroform [69].

Some studies have used mechanical disruption by ultrasonication of cells in combination with solvent extraction [70]. Use of other mechanical disruption methods has been reported [62]. Use of chemicals to digest the

**Table 2** PHA recovery processes

| Recovery method   | Advantages   | Recovery agent   | Microorganism  | Yield <sup>a</sup><br>(purity)<br>(%) | References |
|---|--|--|--|---------------------------------------|------------|
| Solvent extraction  | High purity; endotoxin removal; limited polymer degradation                              | Chloroform, methanol                                       | <i>Halomonas campisalis</i> MCM B-1027                 | 36.82                                 | [64]       |
|   |  | Chloroform, hexane   | <i>Cupriavidus necator</i> A-04                        | 78                                    | [27]       |
|   |  | Chloroform, hexane   | <i>Wautersia eutropha</i> ATCC 17699                   | 90                                    | [67]       |
|   |  | Dichloromethane, hexane                                    | <i>Pseudomonas oleovorans</i>                          | 38                                    | [68]       |
|   |  | Chloroform   | Mixed microbial culture                                | 77                                    | [43, 44]   |
| Mechanical disruption   | Less use of chemicals; reduced polymer degradation                                       | Sonication, chloroform                                     | <i>Alcaligenes lata</i> DSM1123                        | 95                                    | [70]       |
| Chemical digestion  | No polymer degradation; high purity; applicable to large volumes and high cell densities | NaClO, chloroform/ethanol                                  | <i>Escherichia cloacae</i> SU-1                        | 94                                    | [71]       |
|   |  | SDS, LAS-99, ES702, AOS-04, Brij <sup>®</sup> 58, NaOH     | <i>Ralstonia eutropha</i> ,<br><i>Escherichia coli</i> | 99(90)                                | [72]       |
|   |  |  |  |                                       |            |
| Enzymatic digestion<br>(with or without mechanical treatment) | Good polymer recovery; high purity; reduced use of chemicals other than enzymes          | Alcalase, SDS, EDTA  | <i>Pseudomonas putida</i>                              | 90(92.6)                              | [75]       |
|   |  | Benzonase, Alcalase, lysozyme, flavourzyme; microfluidizer | <i>P. putida</i> PGA1                                  | (99.2)                                | [76]       |
| Supercritical fluids  | Low toxicity; low cost; high polymer purity  | CO <sub>2</sub>  | Bacterial cells  | 90(99)                                | [79]       |

<sup>a</sup> Yield is given in terms of PHA content (% of cell dry weight)

cell envelope to facilitate solvent extraction has been reported for PHA recovery from *Enterobacter cloacae* cells [71] as well as from other microorganisms.

A variety of digestive detergents have been evaluated for PHA recovery [72] with varying efficacy. Presumably, the effectiveness of a particular detergent in dissolving the cell envelope depends on the microbial species, but there is no information on this. Detergents such as sodium dodecylsulfate (SDS) have been used to rupture cell membranes to recover granules of the crude PHA polymers [62]. Incubation of *R. eutropha* and *E. coli* cells with 5 % (w/v) SDS for 3 to 6 h has allowed recovery of 95 % of the intracellular PHA [72], but the purity of the recovered polymer was improved by extending the detergent treatment to longer than 6 h. Digestion of the cells was enhanced by increasing the incubation temperature. Digestion of cells with alkali (NaOH) has been used for PHA recovery [62, 72] and there is evidence that overzealous treatment with alkali damages the polymer. A treatment regimen for PHA recovery from *E. coli* may be the use of 1 M NaOH at 50 °C with gentle mixing for 10 min [73].

A comparison of chemical digestion and solvent extraction suggest the latter to afford a greater purity of the PHA product, but if the cells contain a high level of PHA (e.g. >80 % (w/w) of cell mass) digestion with chemicals may give as high a purity as solvent extraction [72]. A case-based evaluation is always necessary in selecting a preferred recovery method.

Enzymatic digestion of *Pseudomonas putida* cells to recover mcl-PHA with a purity of nearly 93 % was reported by Kathiraser et al. [74]. Solvent extraction gave a product of a somewhat higher purity (~96 % pure). The recovery of mcl-PHA from *P. putida* cells by combined enzymatic-chemical digestion has been reported [75]. Alcalase and lysozyme enzymes were effective in digesting the cellular material. Chemicals such as sodium dodecylsulfate (SDS) and ethylenediamine tetra-acetic acid (EDTA) helped in solubilizing the non-PHA materials. This combined treatment allowed nearly 90 % of the PHA to be recovered with a purity of nearly 93 % [75]. Enzymes in general may be too expensive for use in a large-scale extraction process. Some enzymes may digest the PHA polymer [74]. Also, cell wall digesting enzymes tend to be microorganism specific [58]; therefore, a case-based evaluation is necessary.

Combinations of enzymatic and mechanical cell disruption treatments have also been used for recovering the intracellular PHAs [76]. Bacteria contain a significant proportion of their biomass as DNA, a jelly-like polymer, and disruption of the cells releases this DNA in the cell homogenate. Therefore, the homogenate can be quite viscous and difficult to process. Thus, enzymes such as

benzonase (a commercial nuclease) may need to be added, for example at a concentration of 10 µL/L cell broth at pH 10, to reduce viscosity by digesting DNA and ease processing through certain mechanical cell disruption devices [76]. In some cases, the PHA pellet recovered from the digested cells has been further treated with ozone or peroxide to remove contaminants [76].

Supercritical fluids have attracted attention for PHA recovery [64, 77–79] (Table 2). Of particular interest is supercritical CO<sub>2</sub> as it is inexpensive, readily available, does not leave behind a toxic residue, has a low reactivity, is nonflammable and has a moderate critical temperature (31 °C) and pressure (7.29 MPa). Supercritical fluids have been used to extract nearly 90 % of the PHA in the biomass at purities ranging from 86 to 99 % [64, 79] (Table 2). A variety of other relatively less used methods of recovering PHA exist [64].

### PHA Production in Genetically Modified Plants

Cost of the carbon source is a substantial contributor to the cost of producing PHAs by microbial processes [80]. Furthermore, recovering the microbial biomass from the fermentation broth and further processing to extract the PHA are expensive. A potentially cheaper production option is to use atmospheric carbon dioxide and sunlight to produce PHAs in genetically modified plants [9, 81, 82]. Plants are easily harvested and a large amount of water does not need to be removed from plant biomass for extracting PHAs. Plant platforms for producing PHA have been extensively reviewed [80, 83, 84]. Some recent studies on PHA biosynthesis in plants are summarized in Table 3.

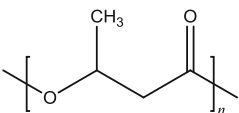
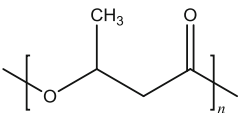
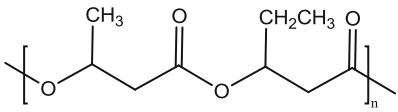
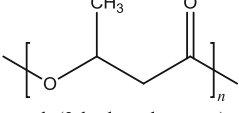
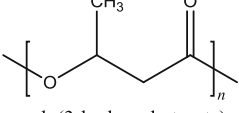
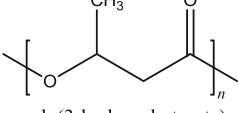
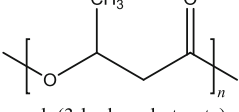
Synthesis of PHB in genetically modified tobacco plant (*Nicotiana tabacum*) has been reported [85]. The plant had been transformed with a plasmid construct containing genes from *Acinetobacter* sp. and *Bacillus megaterium* to code the enzymes required for PHA synthesis. The modified tobacco produced between 17 and 19 % (w/w) PHB in leaf tissue and nearly 9 % in the total plant biomass.

Matsumoto et al. [86] used the codon optimization method to improve expression of PHA in tobacco inserted with the PHA synthesis genes of *R. eutropha*. The codon-optimization of *phaB* gene resulted in a two-fold increase in PHB content of the plant tissue compared to the case for the non-optimized gene (Table 3) [86]. In contrast, the codon-optimization of *phaC* gene had no significant effect on PHB accumulation [86]. This led to the conclusion that *phaB* gene product had a rate determining influence on PHB production in tobacco leaves [86].

Ariffin et al. [81] reported the transfection of immature palm oil seedlings with *Agrobacterium tumefaciens* carrying pRMIN and pLMIN plasmids harboring the various PHA



**Table 3** PHA biosynthesis in plants

| Plant                                     | PHA genes  | Product  | Yield   | References |
|---|--|--|---|------------|
| <i>Nicotiana tabacum</i>                  | <i>Acinetobacter</i> sp. thiolase ( <i>phaA</i> ), synthase ( <i>phaC</i> )  | <br>poly(3-hydroxybutyrate)                       | 17.3–18.8 % DW in leaf tissues                                  | [9]        |
| <i>Nicotiana tabacum</i>                  | <i>Bacillus megaterium</i> reductase ( <i>phaB</i> )   | <br>poly(3-hydroxybutyrate)                       | 8.8 % DW in total plant biomass                                 | [85]       |
| <i>Elaeis guineensis</i>                  | <i>bktB</i> , <i>phaB</i> , <i>phaC</i> and <i>tdcB</i>  | <br>poly(3-hydroxybutyrate-co-3-hydroxyvalerate) | About 91.2 % PHB GUS positive test transformation               | [81]       |
| <i>Panicum virgatum</i> L                 | <i>phaA</i> , <i>phaB</i> of <i>R. eutropha</i> hybrid <i>phaC</i> <i>P. oleovorans</i> / <i>Zoogloea ramigera</i> | <br>poly(3-hydroxybutyrate)                       | 3.72 % DW in leaves and 1.23 % DW from stalk and sprouts        | [87]       |
| <i>Arabidopsis thaliana</i>               | <i>phaA</i> , <i>phaB</i> , <i>phaC</i>  | <br>poly(3-hydroxybutyrate)                       | 14.3 % (w/w) PHB in younger leaves; 7 % (w/w) PHB in older ones | [88]       |
| <i>Nicotiana tabacum</i>                  | <i>R. eutropha</i> <i>phaA</i> , <i>phaB</i> , <i>phaC</i>   | <br>poly(3-hydroxybutyrate)                     | 2 mg g <sup>-1</sup> DW   | [86]       |
| <i>A. thaliana</i> , <i>Saccharum</i> sp. | <i>R. eutropha</i> <i>phaA</i> , <i>phaB</i> , <i>phaC</i>   | <br>poly(3-hydroxybutyrate)                     | 1.6–1.8 % in the leaves   | [11]       |

DW dry weight

synthesis genes. Nearly 90 % of the transfected calli were successfully transformed (Table 3). A PHB yield of 3.7 % of leaf dry weight and 1.2 % of stalk dry weight has been reported for production in genetically engineered switch-grass *Panicum virgatum* L harboring genes of *Ralstonia eutropha* and a hybrid gene construct from *Pseudomonas oleovorans*/*Zoogloea ramigera* [87] (Table 3).

A high level of PHB expression in plants causes chlorosis, a condition characterized by a reduced chlorophyll production, consequently reduced production of carbohydrate and reduced plant growth [80]. This problem may be alleviated by delaying the synthesis of PHB until the photosynthetic tissues of the plant are well developed. This may be achieved, for example, by using a chemically induced gene-switch ([88]. The gene switching approach

has been demonstrated in *Arabidopsis thaliana* [88]. With this approach, a PHB level of around 14 % (w/w) was obtained in younger leaves and 7 % in older ones [89] (Table 3).

Gene switching is not the only strategy for reducing or overcoming chlorosis. An alternative approach is to produce PHA within the plant peroxisomes [11]. Peroxisomal production of PHA has been reported in *A. thaliana* and *Saccharum* sp. (sugarcane) using *R. eutropha* genes [11]. PHB yields of 1.6 % (w/w) and 1.8 % (w/w) based on dry biomass were obtained in sugarcane leaves and *A. thaliana* seedlings, respectively (Table 3). Although, peroxisomes were the targeted production sites, in sugarcane PHB accumulated throughout most of the leaf cell including in the peroxisomes and the vacuoles.

## Enzymatic Synthesis of PHA In Vitro

Enzyme catalyzed synthesis of PHAs in vitro without involving any microorganisms is an alternative production method [21]. Enzymatic syntheses are generally highly stereoselective, chemoselective, regioselective and enantioselective. This ensures a well-defined structure of the synthesized polymer. Furthermore, enzyme catalyzed reactions typically occur under ambient reaction conditions and the separation of the polymer from the reaction mixture is straightforward.

PHA polymers can be produced in vitro from a wide range of substrates including cyclic lactones and carbonates (Table 4). PHAs such as poly-3-hydroxypropionate, poly-4-hydroxybutyrate and poly-6-hydroxyhexanoate have been produced this way. Enzymes used in PHA synthesis include cutinases [20], oxidoreductases [90–92] and hydrolases, especially the serine hydrolases such as lipase (EC 3.1.1.3) [20, 93]. Lipases function as hydrolases in aqueous media to hydrolyze ester bonds [94]; however, in microaqueous media, lipases can catalyze the formation of ester bonds (Fig. 2). Immobilized lipase B of *Candida antarctica* has proved to be especially effective in production of PHAs via ring opening polymerization of cyclic lactones [91, 95, 96].

Cutinase of the soft-rot fungus *Humicola insolens* has been used to catalyze polycondensations and ring-opening polymerizations of lactones [97]. The optimal activity temperature for this enzyme was 70 °C. The enzyme, immobilized on beads of an ion exchange resin, catalyzed the ring-opening polymerization of both  $\epsilon$ -caprolactone (PCL) and  $\omega$ -pentadecalactone (PDL) in toluene to poly( $\epsilon$ -caprolactone) and poly( $\omega$ -pentadecalactone), respectively [97]. Polymerization did not occur if the monomers were changed to (*R,S*)- $\beta$ -butyrolactone and *L*-lactide. In ring-opening polymerization of  $\epsilon$ -caprolactone at 70 °C, a monomer conversion of nearly 99 % was achieved (Table 4). The number averaged molecular weight and the polydispersity index of the product depended on whether the polymerization occurred in toluene or in the bulk substrate as the solvent [97].

Using  $\omega$ -pentadecalactone monomer in toluene, a polymer with a high molecular weight of 44,600 Da could be produced [97]. Lactones with 7- and 16-carbon rings were found to be good monomers for ring-opening polymerization with the immobilized cutinase of *H. insolens* [97]. The enzyme also catalyzed polycondensation of diols and diacids with good activity depending on the chain length of the substrate [97].

Feder and Gross [98] explored the chain length selectivity of *H. insolens* cutinase immobilized on Amberzyme oxirane resin, in polycondensation of  $\omega$ -hydroxyalkanoic acids having 6, 10, 12 and 16 carbons. The catalytic

activity increased as the chain length increased from C12 to C16. No polymerization occurred with C6 and C10 substrates. The C16 substrate could be polymerized to a product with a number averaged molecular weight of 40,400 Da. Using the C16 substrate and immobilized *C. antarctica* lipase B (Novozym 435) as the catalyst, the polymer produced had a number averaged molecular weight of only 25,500 Da [98]. The lipase catalyzed the polymerization of the C12 substrate as effectively as it did that of the C16 substrate, but had no polymerization activity with the C6 substrate [98].

Advances in enzyme catalysis have made possible the production of functionalized PHAs without the need for protection/deprotection of the functional group during the polymerization reaction. Takwa et al. [99] reported the synthesis of  $\omega$ -functionalized polypentadecalactone containing dithiol, thiol acrylate, diacrylate or dimethacrylate end groups. A single-step solvent-free lipase catalyzed polymerization process was used (Table 4). Two approaches were explored for the synthesis. In the first approach, a difunctionalized polymer with dithiol or thiolacrylate end groups was obtained by mixing the lipase, the lactone and an equimolar mixture of the functional initiator (6-mercapto-1-hexanol) and terminator (11-mercapto-1-undecanoic acid or vinyl acrylate). This way, about 96 % of the polymer was functionalized with dithiol or thiol-methacrylate end groups. In the second approach, a functional diester (ethylene glycol diacrylate or ethylene glycol dimethacrylate) was mixed with lactone and non-dehydrated lipase, allowing the enzymatic water content to serve as initiator. After 2 h of reaction, the pressure was reduced to evaporate the accumulated water so that the reaction could be driven further towards polymerization. This way, more than 96 % of the polymer product could be functionalized with diacrylate or dimethacrylate end groups.

Lipase-catalyzed synthesis of functionalized poly- $\omega$ -pentadecalactone-co-butylene-co-carbonate has been reported [19]. A two-stage synthesis was used (Table 4). In the first stage, oligomerization was carried out under a low vacuum (600 mmHg, 18 h, 80 °C). This was followed by the second stage in which polymerization occurred under a high vacuum (2.4 mmHg, 48 h, 80 °C). The copolymer yield from the monomers was nearly 92 % and the product had a high molecular weight of nearly 33,000 Da. The composition of the copolymer could be influenced by varying the ratio of the monomers in the feed [19].

Lipase catalyzed synthesis of a copolymer made of 3-hydroxybutyric acid (3HA) and D-glucono- $\delta$ -lactone monomers, has been reported [100] (Table 4). Of the several lipases tested for this reaction, the Novozym 435 lipase B from *Candida antarctica* proved to be the best. The reaction was carried out at 80 °C and did not require a

**Table 4** Enzyme-catalyzed polymerization

| Enzyme   | Reaction conditions | Monomer  | Solvent  | Yield                       | References |
|--|---------------------|--|--|-----------------------------|------------|
| <i>Hemicola insolens</i> cutinase                        | 70 °C, 24 h         | Both $\epsilon$ -caprolactone (PCL), $\omega$ -pentadecalactone (PDL), (R,S)- $\beta$ -butyrolactone L-lactide | Toluene, bulk substrate  | ~99 %                       | [97]       |
| <i>Hemicola insolens</i> cutinase                        | 70 °C, 8 h          | $\omega$ -Hydroxyalkanoic acids  | Diphenyl ether   | ~83 %                       | [98]       |
| <i>Fervidobacterium nodosum</i> lipase                   | 90 °C, 72 h         | $\epsilon$ -Caprolactone   | Dioxane, acetone, THF, dichloromethane, chloroform, toluene, cyclohexane, <i>n</i> -hexane, bulk substrate | 45–94 %                     | [38]       |
| <i>Candida antarctica</i> lipase B                       | 60 °C, 48 h         | D,D-lactide 1-phenylethanol  | D <sub>8</sub> -Toluene  | 11 % monomer conversion;    | [112]      |
| <i>C. antarctica</i> lipase B mutant Q157A               |                     |  |  | 71 % monomer conversion;    |            |
| <i>C. antarctica</i> lipase B mutant Q157A, I189A, L278A |                     |  |  | 89 % monomer conversion     |            |
| <i>Candida antarctica</i> lipase B 435                   | 80 °C, 24 h         | 3-Hydroxybutyric acid D-glucono- $\delta$ -lactone   | <i>tert</i> -butanol/dimethylsulfoxide [Bmim]PF <sub>6</sub> , bulk substrate                              | 99 % 3HA monomer conversion | [100]      |
| <i>Candida antarctica</i> lipase B 435                   | 80 °C, 66 h         | $\omega$ -Pentadecalactone (PDL), diethyl carbonate 1,4-butanediol   | Diphenyl ether   | 92 %                        | [19]       |
| <i>Candida antarctica</i> lipase B 435                   | 65 °C, 168 h        | $\epsilon$ -Caprolactone, $\delta$ -valerolactone  | Supercritical CO <sub>2</sub> (scCO <sub>2</sub> ) and 1,1,1,2-tetrafluoroethane (R-134a), bulk substrate  | 70.5–89.4 %                 | [114]      |

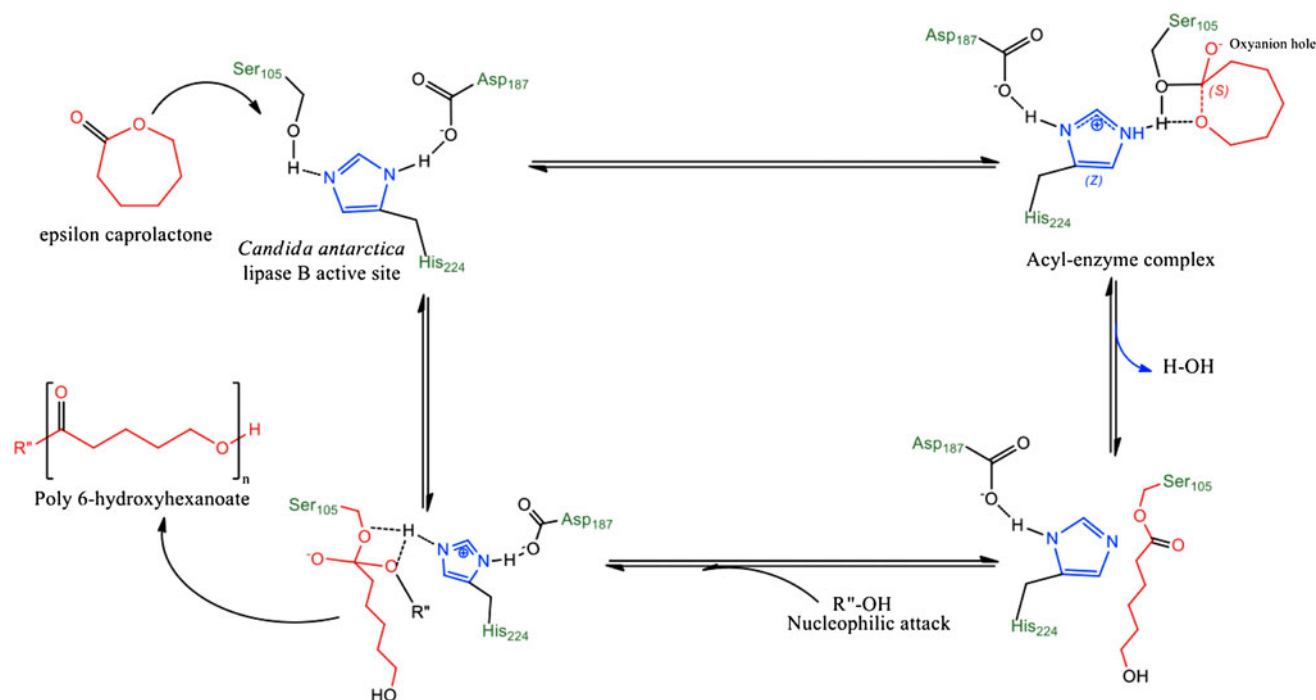
prior derivatization of the monomers. The composition of the product was strongly influenced by the nature of the reaction medium: using a blended *tert*-butanol/dimethylsulfoxide solvent or a medium of the ionic liquid [Bmim]PF<sub>6</sub>, around 99 % of the 3HA monomer was converted to product. However, the same reaction carried out in the bulk substrate (i.e., without any solvent) resulted in an almost 1.5 fold reduced conversion of the 3HA monomer [100]. The product had a low molecular weight ( $\leq 470$  Da) and this was attributed to a poor specificity of the lipase towards 3-hydroxybutyric acid [100].

Controlling the concentration of the initiator in the reaction medium in an enzyme catalyzed polymerization can provide some control over the molecular weight of the polymer formed [101]. For example, in the absence of water (an initiator), the polymer formed tends to have a high molecular weight, but the molecular weight is reduced as the concentration of water in the solvent increases. The use of specific initiators may allow an improved tailoring of the polymerization with a better defined outcome in molecular weight and improved fidelity in the terminating end.

Lipases and cutinases are not the only enzymes capable of polymerizing substrates in vitro. Purified PHA synthase has been shown to polymerize substrates in vitro [102]. Using class II PHA synthase (PhaC1<sub>PP</sub>) from *Pseudomonas putida* and class III PHA synthase (PhaEC<sub>AV</sub>) from *Allochrochromatium vinosum*, polyhydroxyalkanoates could be synthesized on a hydrophobic support of highly oriented pyrolytic graphite (HOPG) [102]. A poly-3-hydroxyoctanoate film of a few nanometers thickness was formed on the HOPG support when PhaC1<sub>PP</sub> and 3-hydroxyoctanoyl-CoA were used. Using the synthase PhaEC<sub>AV</sub> and 3-hydroxybutyryl-CoA, a homogenous poly-3-hydroxybutyrate was formed on the support. This technology provides a method of forming an ultra-thin PHA film on a hydrophobic support and may have other industrial applications in surface-coatings.

Although enzyme-mediated in vitro polymerization has important advantages, problems remain. Hazardous organic solvents are generally required for achieving high activity with enzymes such as lipases [18, 103]. Also, as polymerization progresses, the concentration of the dissolved polymer increases and so does the viscosity of medium. This imposes diffusion limitations and leads to a polymer with a characteristically low molecular weight [15]. In vitro polymerization with enzymes may be improved by some of the following approaches: (1) microwave irradiation of the reaction mixture [23, 104, 105]; (2) ultrasonic irradiation [96]; (3) replacement of conventional organic solvents with supercritical fluids [106–108] and ionic liquids [104, 109, 110]; (4) use of co-solvent blends [18]; and (5) the use of continuous flow microreactors [111]. In addition, enzyme catalysts themselves may be improved, for example, through molecular





**Fig. 2** Substrate–enzyme interaction at the active site during enzyme-catalyzed ring opening polymerization

engineering [112, 113], modification of immobilization methods [114] and co-lyophilization with non-buffer salts.

Functionalized linear hyperbranched polymers have been produced in supercritical fluids from lactones using lipase-catalyzed synthesis [115]. Supercritical  $\text{CO}_2$  ( $\text{scCO}_2$ ), the bulk substrates (i.e., lactones) and 1,1,1,2-tetrafluoroethane (R-134a) were compared as media for this reaction. Polymerization occurred in both solvents, but was faster in supercritical carbon dioxide. The maximum yield in  $\text{scCO}_2$  was 89.4 % at 120 h compared to 71.2 % in R-134a and 70.4 % in the bulk substrate. Beyond 120 h of reaction, the yield began to decline in both solvents, but particularly strongly in  $\text{scCO}_2$  [115]. This was attributed to polymer degradation presumably through hydrolysis.

Enzyme-catalyzed polymerization in a continuous flow microreactor has been reported [111]. The reactor was configured to provide a high catalyst surface area compared to the reactor volume, to improve contact of the substrate with the immobilized enzyme and mass transfer was enhanced through flow. The reaction medium was toluene and the catalyst was Novozym 435 lipase. The reaction occurred at 70 °C. A monomer conversion of >90 % was achieved in less than 5 min in the microreactor whereas a batch process took 30 min to attain a monomer conversion of about 70 % [111].

Molecular modeling techniques have been used to design a mutant lipase of *Candida antarctica* with a 90-fold increased activity relative to the wild-type enzyme during ring-opening polymerization of D,D-lactide [113]. Simulations of molecular

dynamics were used to identify steric hindrances preventing effective catalysis at the active site of the native enzyme. Site-specific mutagenesis was then used to delete three amino acids at the entrance of the enzyme's active site. This modification caused the aforementioned increase in enzyme activity relative to the wild-type enzyme and improved monomer conversion. Similar approaches have been used to improve the performance of *Rhizomucor miehei* lipase [116].

A thermophilic lipase from *Fervidobacterium nodosum* has been reported to catalyze the ring opening polymerization of  $\epsilon$ -caprolactone [38]. This enzyme had optimal activity at 90 °C compared to an optimum temperature of 60 °C for most other lipases. The thermophilic enzyme achieved a near 100 % conversion of the monomer and yielded a product with a number averaged molecular weight of 2,340 Da. The *F. nodosum* lipase (FNL) had a higher affinity towards  $\epsilon$ -caprolactone monomer compared to the commonly used *Candida antarctica* lipase B (CALB). However, in ring-opening polymerization of  $\epsilon$ -caprolactone, the specificity and selectivity of FNL were far below those of CALB [38].

A naturally occurring alkaline lipase isolated from *Acinetobacter* sp. has been reported to be stable in a variety of solvents (ethanol, methanol, isopropyl alcohol, dimethylformamide, dimethylsulfoxide, *n*-hexane, acetone), retaining 80 % of its initial activity after 90 min at pH 10 and 50 °C [112].

The selectivity of Novozym 435 in ring-opening polymerization of lactones has been found to depend on the conformation of the substrate: in *cisoid* lactones, the

enzyme shows *S*-selectivity whereas in *transoid* lactones it has a pronounced *R*-selectivity. Iterative tandem catalysis has been used to polymerize 6-methyl- $\epsilon$ -caprolactone [117]. In iterative tandem catalysis, two different catalysts work together to accomplish polymer propagation. For example, combining Novozym 435 with a racemization catalyst results in turning the unreactive terminal alcohols with an *S*-configuration into reactive ones with an *R*-configuration that can be propagated. Using this approach, a racemic monomer could be quantitatively converted into a homochiral polymer [117]. In vitro production of PHAs has been further reviewed [21].

### Chemo-Biosynthesis

Chemical, morphological and physical properties of polymers can be usefully modified by functionalization with different structural and chemical motifs. Synthesis of novel functionalized polymers has been shown to be possible by using a combination of chemical and enzymatic processes [91, 118].

Synthesis of symmetric quintuplet CBABC-type pentablock copolymers has been achieved with a combination of lipase catalysis and atom transfer radical polymerization (ATRP) [118]. The lipase Novozym 435 and  $\epsilon$ -caprolactone were used in a first step to produce a tri-block copolymer of di-hydroxyl terminated polycaprolactone block polyethylene oxide (PCL-*b*-PEO-*b*-PCL) using the terminal hydroxyl of di-hydroxyl-capped polyethylene oxide (PEO) as initiator (Fig. 3). Further chemical esterification of this tri-block copolymer with  $\alpha$ -bromopropionyl bromide in the presence of dichloromethane gave bromine ended tri-block microinitiator that accepted ATRP of styrene in the presence of copper (I) chloride and 2, 2'-bipyridine, forming quintuplate pentablock copolymer (PSt-*b*-PCL-*b*-PEO-*b*-PCL-*b*-PSt). The number averaged molecular weight of this product was around 38,900 Da. The polymer was capable of assuming different self assembled aggregate morphologies in aqueous media. Similar synthetic processes have been reported for H-shaped block copolymers (Fig. 4) [119] and a Y-shaped ABA<sub>2</sub>-type tri-block copolymer (Fig. 5) [120]. Chemo-enzymatic synthesis of biodegradable PHA copolymers with an excellent shape memory has been reported [121].

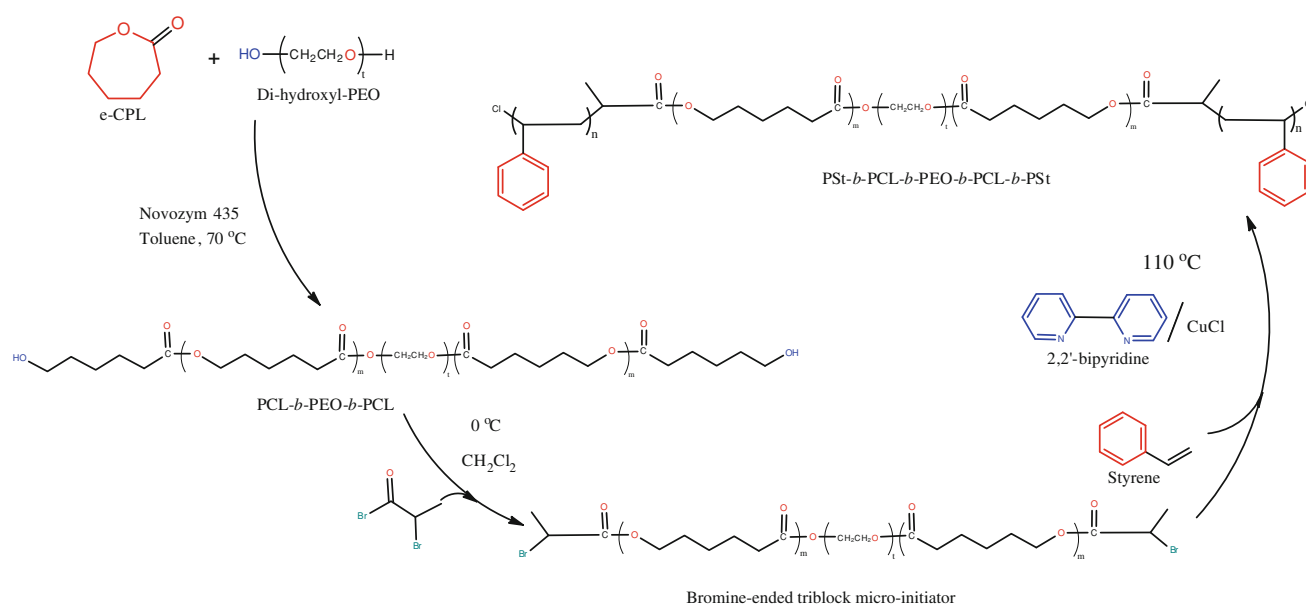
Most of the copolymerization processes require two consecutive steps. After the formation of the first block, an intermediate transformation step is used to convert the end-groups of the block into active micro-initiators for the next block. An alternative one-pot cascade synthesis has been reported for making block copolymers using a bifunctional initiator to allow consecutive polymerization without the need for intermediate transformation steps [122]. However, the one-pot cascade approach does present major

challenges in production of copolymers with a high molecular weight [120, 122].

Tajima et al. [123] reported a chemo-enzymatic synthesis of poly-lactate-co-3-hydroxybutyrate in a water-organic solvent two-phase reaction system (Fig. 6). Chemically synthesized thiophenyl (*R*)-lactate [(*R*)-LATP] and thiophenyl (*R*)-3-hydroxybutyrate [(*R*)-3HBTP] were used as substrate precursors to first produce hydroxyalkanoylCoA (HACoA) by the ester exchange reaction between the thiophenyl alkanoate and CoA. Then an engineered lactate-polymerizing PHA synthase was used to polymerize the hydroxyalkanoyl-CoA (HACoA) to PHA. This resulted in a copolymer with a number averaged molecular weight of 11,000 Da and a polydispersity index of 1.4. The ratio of the monomers in the copolymer could be controlled by varying the molar ratio of (*R*)-LATP and (*R*)-3HBTP fed to the process. Other similar schemes involving a two-phase reaction system have been reported [124].

### Functionalized Biopolymers

Biodegradable polymers are continuously finding applications in numerous fields especially biomedical. However, most of the synthesized biopolymers lack biological stimulus found in either intra or extra cellular matrix, thus specialized biopolymers are needed to be applied for this purpose. Recent advances in biopolymer engineering resulted in significant efforts towards the synthesis of biopolymers with specific functional groups capable of coupling bioactive ligands (Table 5). For example, stimuli responsive biopolymers having an ability to mimic the cellular response process were reported [125–127]. It is not surprising that these biopolymers have attracted much attention recently due to their ability to respond to specific changes in basic environmental stimuli such as temperature [128], pH [129–131], photo [132] and eletro [133] stimuli while others were reported to respond to multiple stimuli [134]. Recently, a thermo-sensitive triblock of PLA-*b*-PNIPAAm-*b*-PLA having low critical solution temperature (LSCT) of 31.15–32.62 °C has been reported [128]. It has been reported that the thermal stimuli of these polymers to have arisen as a result of the hydrophobic interactions among PNIPAAm molecular chains, the intermolecular hydrogen bonding between the PNIPAAm chains, water molecules, and the intramolecular hydrogen bonding between the –CONH<sub>2</sub> groups [125]. Poly-3-hydroxybutyrate macro initiator was used in ATRP to initiate the synthesis of a novel thermo sensitive amphiphilic triblock hydrophobic PHB flanks by hydrophilic PNIPAAm (Table 5) [135]. Zhu et al. [136] reported the synthesis of polycaprolactone based temperature sensitive



**Fig. 3** Chemo-enzymatic synthesis of a symmetric quintuplet CBABC-type pentablock copolymer. Adapted from [118]

polymer (PNIPAM-*b*-(HEMA-PCL)) using PNIPAAm as the macroinitiator in RAFT polymerization process. Differences in cellular pH have been utilized in designing novel drug delivery devices (Table 5). For instance, Bawa et al. [130] reported the general blood and tissue pH to be about 7.4 while in carcinogenic cells the pH was found to be about 1.0. Yin et al. [137] recently observed the physico-chemical characteristics of pH sensitive PHF-*b*-PEG micelles (Table 5). The researchers reported that the  $pK_a$  value of the copolymer can generally be controlled by changing the ratio of the amino acid residue to that of the lactide and ethylene glycol. Taking these biopolymers as drug delivery devices for example, differences in stomach acidic pH to that of intestinal basic pH could determine their target site for delivering the drug. Thus, serve as pH dependent specific delivery devices. Despite their poor biodegradability, poor polymer-cellular interaction and low solubility in most organic solvents; electro conductive polymers were reported to be used as scaffold in nerve regeneration culture and other biomedical fields [138]. Wei et al. [139] reported the synthesis of specialty polymer with enhanced PC-12 cellular attachment and differentiation using a film of PANi functionalized with bioactive laminin-derived adhesion peptide. Plant bioactive coumarin is reported to be used as photoinduced cross linker in the synthesis of photosensitive polymers [140]. Coumarin encapped PCL-co-TMC were used as photocurable precursors in biomedical devices fabrication and drug encapsulation devices [125, 141]. Polyethyleneglycole functionalized gadolinium ion ( $\text{Gd}^{3+}$ ) has been reported to be used as in vivo paramagnetic probe for magnetic resonance imaging [142].

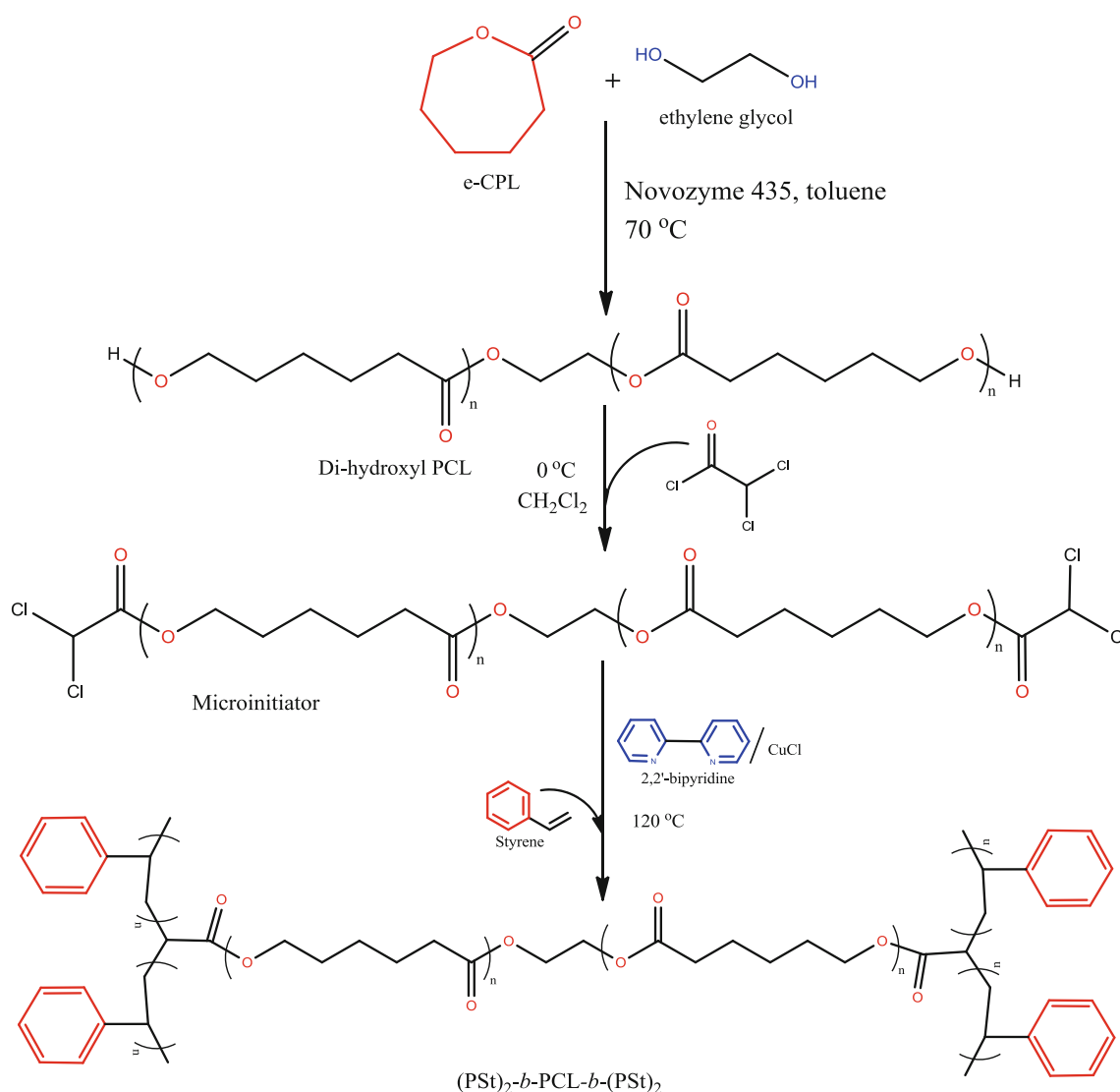
Sugars such as galactose and mannose were reported to be specific ligands to the ASGPR receptor, which is overexpressed in hepatocellular carcinoma [143]. Jiang et al. [144] observed the solution behavior of PCL functionalized hydroxyethyl cellulose (HEC). Previously, Lu et al. [145] reported the synthesis of poly(1'-O-vinyladipoyl-sucrose) in chemo-enzymatic process resulting in polymer with molecular weight as high as 53 kDa having improved solvation properties that can be explored as promising biomaterial. In general, polymer functionalization has resulted in recent increasing demand of biodegradable polymers in diverse industrial applications. Functionalization of polymer has opened a new avenue for the production of novel polymers with specific application that were not possible earlier.

## Applications of Polyhydroxyalkanoates

### Biomedical Applications

PHAs have attracted much attention as materials for biodegradable implants in biomedical and tissue engineering applications. Specifically, PHB has been reported to be biocompatible with various kinds of cells [146] (Table 6).

Use of PHAs as drug delivery systems (Table 6) for prolonged release of therapeutics into systemic circulation is receiving attention [147]. Polyhydroxyesters such as block copolymer of PEG-*b*-PCL in the form of micelles and nanoparticles have been used for parenteral delivery of taxanes [148] (Table 6). A matrix of nanoparticles of poly-3-hydroxybutyrate-*co*-3-hydroxyhexanoate (PHBHHx) has



**Fig. 4** Chemo-enzymatic synthesis of H-shaped block copolymer. Adapted from [119]

been used to deliver antineoplastic agents to cancer cells [149] (Table 6). PHB nanoparticles functionalized with a tumor-specific ligand have been examined for specifically targeting certain breast cancer cells [150]. The non-steroidal anti-inflammatory drug ibuprofen has been conjugated to nontoxic oligo(3-hydroxybutyrate), in attempts to improve drug delivery but this novel formulation remains to be thoroughly assessed [151].

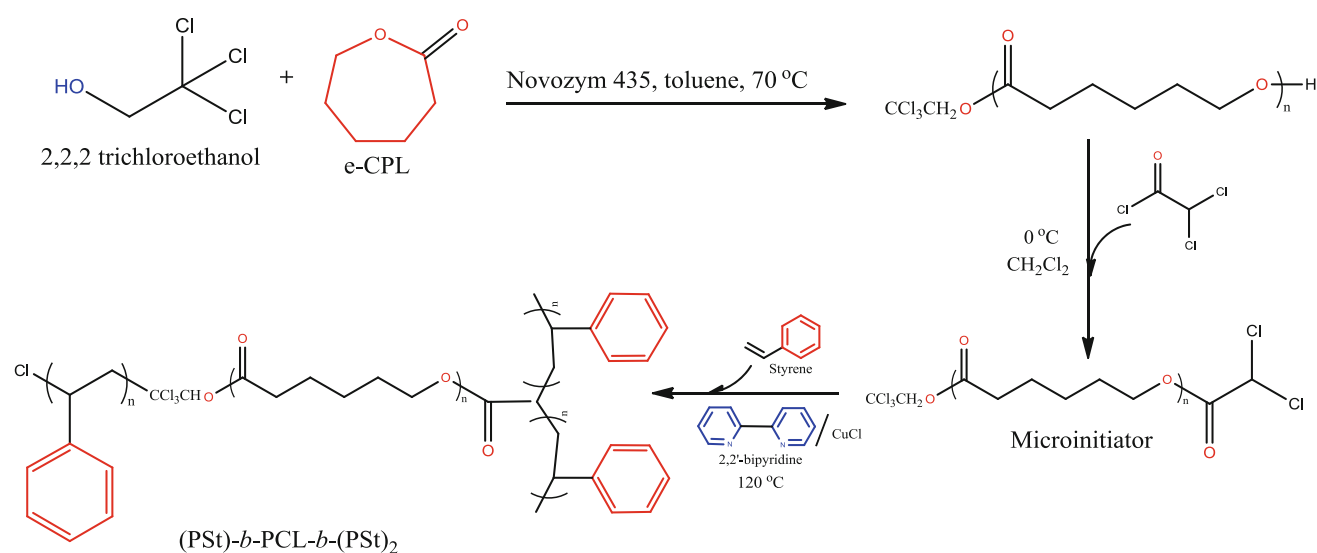
Poly-3-hydroxybutyrate microspheres have been tested in vitro for releasing the antibiotics gentamycin and tetracycline [152]. Multifunctional PHB/45S5Bioglass composite system has been discussed as drug delivery agents and for use in certain bone tissue engineering applications [152].

Polycaprolactone (PCL) tends to be highly permeable and this is an attractive feature in some drug delivery applications. Use of PCL in certain drug delivery applications has been approved by the US Food and Drug

Administration [146]. PCL degrades slowly (2–4 years) in vivo and is therefore useful for developing drug release implants for long-term use [153].

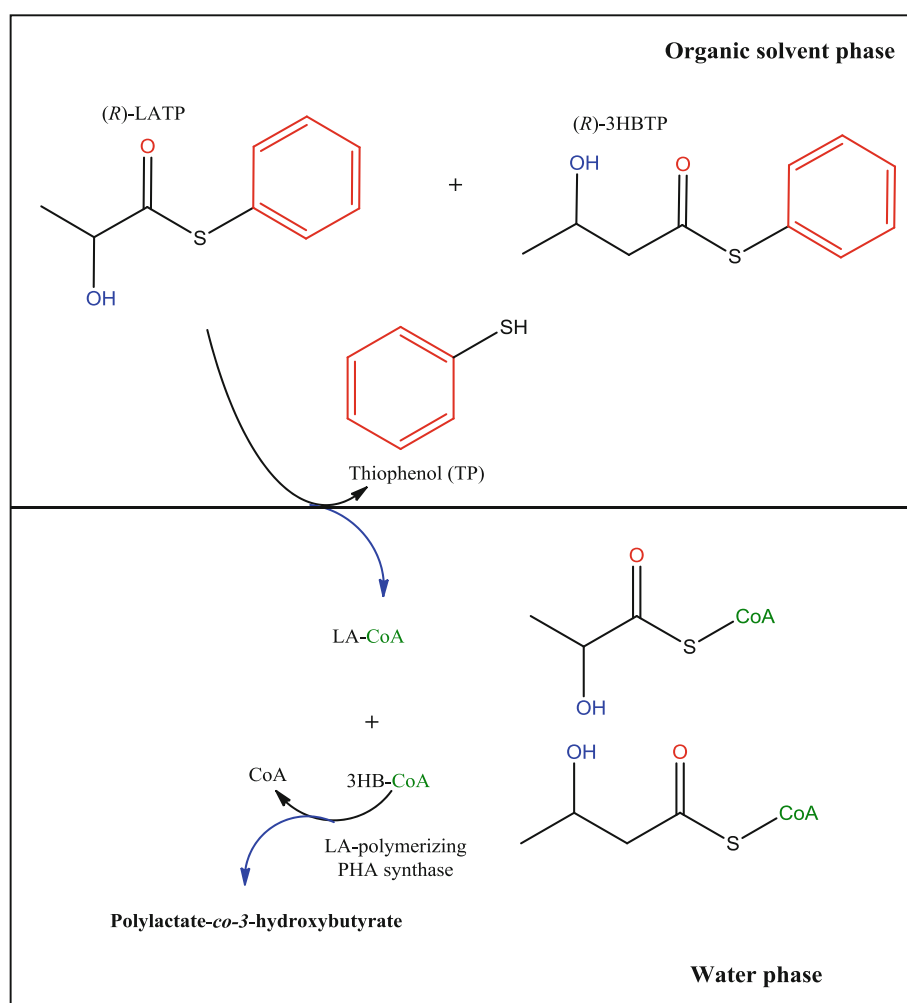
Silver nanoparticles have attracted much attention because of their antibacterial properties [154–156], but slurries of such particles tend to be unstable. Use of polyhydroxyalkanoates in prolonging stability of such slurries has been reported [157].

Poly-3-hydroxybutyrate-*co*-3-hydroxyhexanoate scaffolds have been evaluated for use in eyelid reconstruction in experimental animals [158] (Table 6). Although the scaffold performed satisfactorily, it produced some inflammation that took about 2 weeks to clear. Poly-3-hydroxybutyrate-*co*-3-hydroxyhexanoate was found to induce cartilage development from mouse mesenchymal stem cells and preserve the chondrocytic phenotype of the cells [159] (Table 6).

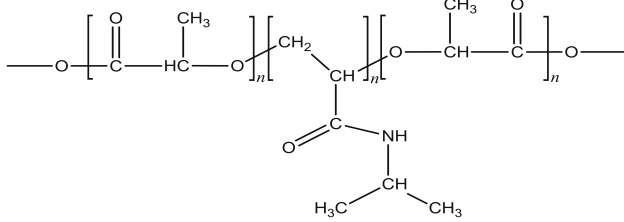
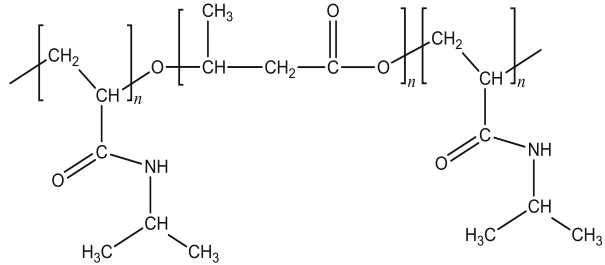
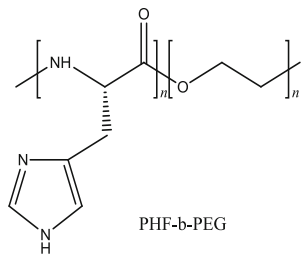
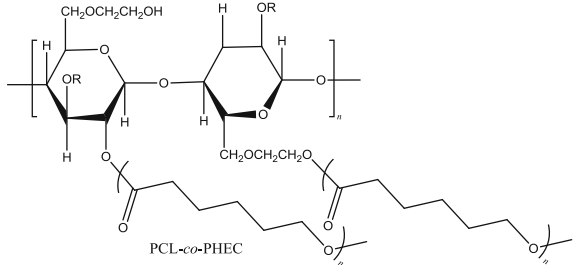


**Fig. 5** Chemo-enzymatic synthesis of Y-shaped block copolymer. Adapted from [120]

**Fig. 6** Chemo-enzymatic synthesis of polylactate-co-3-hydroxybutyrate in a two-phase reaction system. Adapted from [123]



**Table 5** Functionalized biopolymers

| Functionalized character | Polymer   | Application          | References |
|--------------------------|---|----------------------|------------|
| Temperature responsive   |  <p>PLA-<i>b</i>-PNIPAAm-<i>b</i>-PLA</p>     | Drug delivery device | [128]      |
|                          |  <p>PNIPAAm-<i>b</i>-PHB-<i>b</i>-PNIPAAm</p> | Drug delivery device | [135]      |
| pH responsive            |  <p>PHF-<i>b</i>-PEG</p>                      | Drug delivery device | [137]      |
| Specific binding         |  <p>PCL-<i>co</i>-PHEC</p>                  | Drug delivery device | [144]      |

The use of a terpolyester of 3-hydroxybutyrate-*b*-3-hydroxyvalerate-*b*-3-hydroxyhexanoate (PHBVHHx) as scaffold for promoting differentiation of human bone marrow mesenchymal stem cell into nerve cells (Table 6) has been reported [160]. PHBVHHx scaffolds with a pore size of 30–60  $\mu\text{m}$  were found to be best.

PCL reinforced with phosphate glass fibers has been used to make fixation pins for intramedullary fractures, craniofacial repairs and general bone repair [146]. PCL can be modified in various ways to improve mechanical strength and alter properties such as degradability, compatibility, hydrophilicity and crystallinity. For example, poly- $\epsilon$ -caprolactone functionalized polyethylene glycol copolymer has been reported to have a strong

amphiphilicity, a controlled biodegradability and excellent biocompatibility.

PCL blended with poly-glycerol sebacate has been used as a fibrous scaffold for aortic valve regeneration [161]. Use of both PCL and PHA has been reported as substrates for cardiovascular tissue engineering [162] (Table 6). The diverse biomedical applications of PCL have been further reviewed by others [163, 164]. Among the various other biomedical applications, PHA is being used in tablet formulations [165, 166], surgical sutures [39], wound dressings [167, 168], surgical implants to join tubular body parts [169, 170], controlled release contraceptive devices [171–173], lubricating powders, blood vessels, tissue scaffolds, and bone fracture fixation plates [39, 174–177]. Of these

**Table 6** Applications of polyhydroxyalkanoates

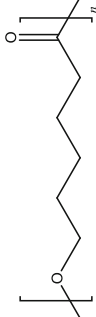
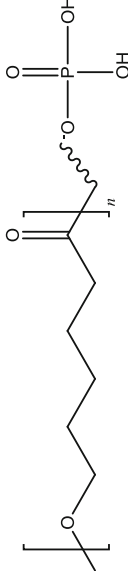
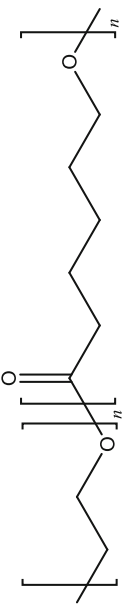
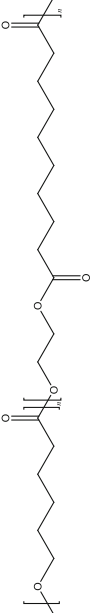
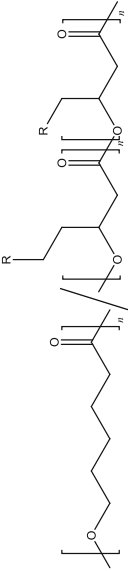
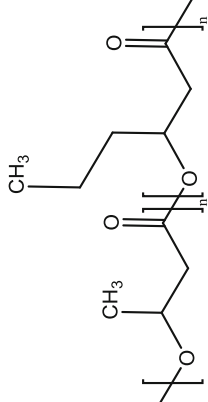
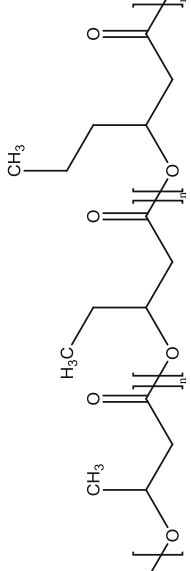
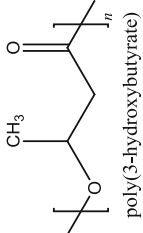
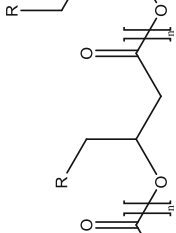
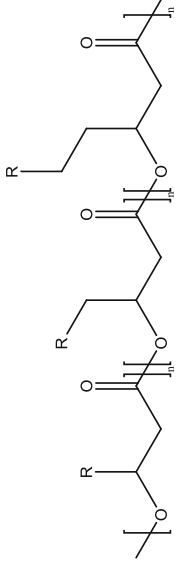

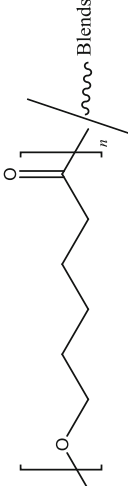
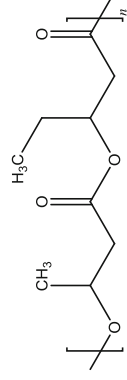
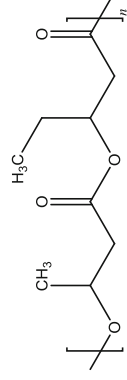
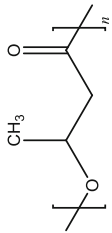
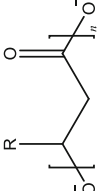
| Polymer                    | Chemical structure   | Polymer form used     | Applications   | References |
|----------------------------|--|-----------------------|--|------------|
| Biomedical applications    |  |                       |  |            |
| PCL                        |   | Drug delivery devices | Chemopreventive curcumin delivery  | [147]      |
| PCL/phosphate glass fibers |    | Fibers                | Fracture fixation pins, craniofacial repair and general bone regeneration            | [146]      |
| PEG-b-PCL                  |    | Fibrous scaffolds     | Antineoplastic taxanes delivery  | [148]      |
| PCL/PEG sebacate blends    |    | Fibrous scaffolds     | Aortic valve regeneration  | [161]      |
| PCL/PHA blends             |    | Scaffolds             | Cardiovascular tissue engineering  | [162]      |
| PHBHHx                     |  | Nanoparticles matrix  | Antineoplastic agents carrier  | [149]      |
|                            |  | Scaffolds             | Eye lid tissue regeneration  | [158]      |
|                            |  |                       | Induce chondrogenesis of mesenchymal stem cells                                      | [159]      |
| PHBHVHHx                   |  | Scaffold              | Differentiation of human bone marrow mesenchymal stem cells (hBMSC) into nerve cells | [160]      |

Table 6 continued

| Polymer                                      | Chemical structure  | Polymer form used                  | Applications   | References     |
|--|---|------------------------------------|--|----------------|
| PHB/(RGD4C)                                  |    | Functionalized nanoparticles       | Breast cancer therapy                                | [150]          |
| PHB/45S5 <sup>®</sup> bioglass composite     |    | Microsphere                        | Tissue engineering                                   | [152]          |
| PHA  |    | Colloids                           | Stabilizes silver nanoparticles                      | [157]          |
| Industrial applications<br>PHA methyl esters |    | 3-Hydroxy alkanolate methyl esters | Biofuel and fuel additives                           | [53, 179, 180] |
| PCL blends                                   |    | Nanocomposites                     | Packaging  | [183]          |
| PHBHV  |   | Copolymer film                     | Packaging  | [182]          |
| PHB  |   | Granules in-feed                   | Pathogenic bacterial growth inhibitor in aquaculture | [183–185]      |
| PHA  |  | Micro and nanoparticles            | Herbicides controlled release carrier                | [186]          |
|  |  | Composite Granules                 | Biomimetic absorbent                                 | [187]          |
|  |   |                                    | Paper sizing   | [181]          |



applications, surgical sutures constitute perhaps the largest use category with a 2010 market value exceeding US\$1.3 billion annually [178].

### Industrial Applications

In addition to their biomedical applications, PHAs can potentially replace petrochemicals-based plastics in diverse other applications (Table 6).

A recently suggested application is the use of PHAs as precursors of biofuels. Like bioethanol from sugars, PHAs can be made into renewable biofuels. Hydrolysis of PHAs followed by methyl esterification provides 3-hydroxyalkanoates methyl esters with an energy content that is comparable to that of bioethanol [53, 179, 180]. Whether hydroxyalkanoate esters would be as cheap as bioethanol in fuel blends is debatable. This is because in making a PHA-based fuel, a carbon source first needs to be polymerized, the polymer then needs to be hydrolyzed and a subsequent methylation step is required. In contrast, glucose and other sugars can be directly fermented to bioethanol.

Polyhydroxyalkanoate latexes have been used in the paper industry for surface coating of paper and as sizing agents [181] (Table 6). PHB has had limited applications in packaging because of its high glass transition temperature which results in brittleness under typical use conditions. PHB's utility in packaging has been improved by copolymerizing with various levels (5–20 %) of valerate to produce PHBV polymers with glass transition temperatures of 4 °C at 5 % and 1 °C at 20 % valerate content [182] (Table 6). Novel polymeric materials for food packaging consisting of PCL blends have been developed [183]. They have been reported to have an excellent durability and a remarkable tensile strength [183] (Table 6). Uses of PHAs in the food industry have been discussed elsewhere [184, 185].

PHAs appear to be potentially useful in controlling bacterial pathogens in certain aquaculture applications [186–188]. For example, administration in the feed of 1,000 mg L<sup>-1</sup> of PHB particles of an average diameter of 30 µm, or addition of inactivated cells (10<sup>7</sup> cells mL<sup>-1</sup>) of PHB-containing *Brachymonas* bacteria (equivalent to ~10 mg L<sup>-1</sup> PHB) to the culture water of brine shrimp (*Artemia nauplii*) larvae, conferred a complete protection from a virulent strain of the intestinal pathogen *Vibrio campbellii* [187]. Other similar reports have claimed an inhibitory effect of PHB on certain gut microflora of the giant freshwater prawn (*Macrobrachium rosenbergii*) larvae [188]. Administration of PHB (5 g L<sup>-1</sup>) in the feed significantly increased the survival of the prawn larvae and improved their development. The total bacterial counts and *Vibrio* spp. counts were significantly reduced in PHB-fed larvae compared to the control larvae.

Polyhydroxyalkanoates have been used as controlled release agents for herbicides in agricultural. Controlled release potentially reduces the impact of the herbicides on nontarget species and reduces the need for repeated applications [189]. Micro- and nanoparticles of PHB and PHBV were used in a controlled release formulation of the herbicide ametryn [189] (Table 6). PHB has been successfully tested for removing lipid-soluble organic pollutants from water by adsorption [190] (Table 6).

### Concluding Remarks

PHAs are versatile biopolymers with diverse applications. PHAs are biodegradable and they may be produced in a sustainable way using renewable feedstocks. PHAs can be produced in vitro using enzymes without involving microbial cells. Alternatively, they may be produced by microbial fermentation processes and using recombinant plants. Production of PHAs using microorganisms and enzymes remains relatively expensive compared to plastics derived from petroleum. Production in plants is likely to establish itself as the least expensive option for certain PHAs, but does not currently offer the molecular versatility of the products that can be made using microbial fermentations and enzymes. In view of their relatively high cost, PHAs are likely to be used first in high-value niche applications, particularly in biomedicine, but their broader industrial use will increase as the cost of production declines.

**Acknowledgments** University of Malaya is acknowledged for supporting this work through the research grants RG165-11AFR and UM.C/625/1/HIR/MOHE/05.

### References

1. Bauwens T (2011) First estimates suggest around 4% increase in plastics global production from 2010. Plastics Europe. <http://www.plasticseurope.org/information-centre/press-room-1351/press-releases-2012/first-estimates-suggest-around-4-increase-in-plastics-global-production-from-2010.aspx>. Accessed 18 July 2012
2. Piet LPJ (2010) World-wide production of crude steel and plastics 1950–2010. Eindhoven University of Technology, Netherlands
3. Prieto MA (2007) From oil to bioplastics, a dream come true? J Bacteriol 189(2):289
4. Ko-Sin N, Wong Y-M, Tsuge T, Sudesh K (2011) Biosynthesis and characterization of poly(3-hydroxybutyrate-co-3-hydroxyvalerate) and poly(3-hydroxybutyrate-co-3-hydroxyhexanoate) copolymers using jatropha oil as the main carbon source. Process Biochem 46(8):1572–1578. doi:10.1016/j.procbio.2011.04.012
5. Ni Y-Y, Kim DY, Chung MG, Lee SH, Park H-Y, Rhee YH (2010) Biosynthesis of medium-chain-length poly(3-hydroxyalkanoates) by volatile aromatic hydrocarbons-degrading *Pseudomonas fulva* TY16. Bioresour Technol 101(21):8485–8488. doi:10.1016/j.biortech.2010.06.033

6. Hofer P, Vermette P, Groleau D (2011) Production and characterization of polyhydroxyalkanoates by recombinant *Methylobacterium extorquens*: combining desirable thermal properties with functionality. *Biochem Eng J* 54(1):26–33
7. Abu-Elreesh G, Zaki S, Farag S, Elkady MF, Abd-El-Haleem D (2011) Exobiopolymer from polyhydroxyalkanoate-producing transgenic yeast. *Afr J Biotechnol* 10(34):6558–6563
8. Sabirova J, Golyshin P, Ferrer M, Lunsdorf H, Abraham W, Timmis K (2011) Extracellular polyhydroxyalkanoates produced by genetically engineered microorganisms. US Patent 20,110,183,388
9. Bohmert-Tatarev K, McAvoy S, Daughtry S, Peoples OP, Snell KD (2011) High levels of bioplastic are produced in fertile transplastomic tobacco plants engineered with a synthetic operon for the production of polyhydroxybutyrate. *Plant Physiol* 155(4):1690
10. Brumbley S, Petrasovits LA, McQualter RA, Zhou L, Nielsen LK (2008) Sugarcane: an industrial crop for the production of polyhydroxyalkanoates. In: *ComBio2008*, Canberra, Australia, 21–25 Sept 2008
11. Tilbrook K, Gebbie L, Schenk PM, Poirier Y, Brumbley SM (2011) Peroxisomal polyhydroxyalkanoate biosynthesis is a promising strategy for bioplastic production in high biomass crops. *Plant Biotechnol J* 9(9):958–969
12. Van Beilen JB, Poirier Y (2008) Production of renewable polymers from crop plants. *Plant J* 54(4):684–701
13. Otari S, Ghosh J (2009) Production and characterization of the polymer polyhydroxy butyrate-co-polyhydroxy valerate by *Bacillus megaterium* NCIM 2475. *Curr Res J Biol Sci* 1(2): 23–26
14. Bhubalan K, Chuah JA, Shozui F, Brigham CJ, Taguchi S, Sinskey AJ, Rha CK, Sudesh K (2011) Characterization of the highly active polyhydroxyalkanoate synthase of *Chromobacterium* sp. strain USM2. *Appl Environ Microbiol* 77(9):2926
15. Kobayashi S (2010) Lipase-catalyzed polyester synthesis—a green polymer chemistry. *Proc Jpn Acad Ser B* 86(4):338–365
16. Schultz A (2011) Consumers push plastics industry to find bio-based solutions. *CNBC News*. [http://www.cnbc.com/id/42194558/Consumers\\_Push\\_Plastics\\_Industry\\_to\\_Find\\_Bio-Based\\_Solutions](http://www.cnbc.com/id/42194558/Consumers_Push_Plastics_Industry_to_Find_Bio-Based_Solutions). Accessed 4 Aug 2011
17. Mohan AM (2010) Biodegradable polymers market packaging world report. <http://www.packworld.com/news-29339>
18. Gumel AM, Annuar MSM, Heidelberg T, Chisti Y (2011) Thermo-kinetics of lipase-catalyzed synthesis of 6-O-glucosyldecanoate. *Bioresour Technol* 102(19):8727–8732
19. Jiang Z (2011) Lipase-catalyzed copolymerization of dialkyl carbonate with 1, 4-butanediol and  $\omega$ -pentadecalactone: synthesis of poly ( $\omega$ -pentadecalactone-co-butylene-co-carbonate). *Biomacromolecules* 12:1912–1919
20. Miletic N, Loos K, Gross RA (2011) Enzymatic polymerization of polyester. In: Katja L (ed) *Biocatalysis in polymer chemistry*. Wiley-VCH, pp 84–128
21. Thomson N, Roy I, Summers D, Sivaniah E (2010) In vitro production of polyhydroxyalkanoates: achievements and applications. *J Chem Technol Biotechnol* 85(6):760–767
22. Yao D, Li G, Kuila T, Li P, Kim NH, Kim SI, Lee JH (2011) Lipase catalyzed synthesis and characterization of biodegradable polyester containing L-malic acid unit in solvent system. *J Appl Polym Sci* 120(2):1114–1120
23. Matos TD, King N, Simmons L, Walker C, McClain AR, Mahapatro A, Rispoli FJ, McDonnell KT, Shah V (2011) Microwave assisted lipase catalyzed solvent-free poly- $\epsilon$ -caprolactone synthesis. *Green Chem Lett Rev* 4(1):73–79
24. Akaraonye E, Keshavarz T, Roy I (2010) Production of polyhydroxyalkanoates: the future green materials of choice. *J Chem Technol Biotechnol* 85(6):732–743
25. Suriyamongkol P, Weselake R, Narine S, Moloney M, Shah S (2007) Biotechnological approaches for the production of polyhydroxyalkanoates in microorganisms and plants—a review. *Biotechnol Adv* 25(2):148–175
26. Annuar MSM, Tan IKP, Ramachandran KB (2008) Evaluation of nitrogen sources for growth and production of medium-chain-length poly-(3-hydroxyalkanoates) from palm kernel oil by *Pseudomonas putida* PGA 1. *Asia Pac J Mol Biol Biotechnol* 16(1):11–15
27. Chanprateep S, Buasri K, Muangwong A, Utiswannakul P (2010) Biosynthesis and biocompatibility of biodegradable poly(3-hydroxybutyrate-co-4-hydroxybutyrate). *Polym Degrad Stab* 95(10):2003–2012. doi:10.1016/j.polymdegradstab.2010.07.014
28. Franz A, Song HS, Ramkrishna D, Kienle A (2011) Experimental and theoretical analysis of poly ([beta]-hydroxybutyrate) formation and consumption in *Ralstonia eutropha*. *Biochem Eng J* 55(1):49–58
29. Grothe E, Chisti Y (2000) Poly ( $\beta$ -hydroxybutyric acid) thermoplastic production by *Alcaligenes latus*: behavior of fed-batch cultures. *Bioproc Biosys Eng* 22(5):441–449
30. Grothe E, Moo-Young M, Chisti Y (1999) Fermentation optimization for the production of poly ([beta]-hydroxybutyric acid) microbial thermoplastic. *Enzyme Microb Technol* 25(1–2): 132–141
31. Salim YS, Abdullah AA-A, Nasri CSSM, Ibrahim MNM (2011) Biosynthesis of poly(3-hydroxybutyrate-co-3-hydroxyvalerate) and characterisation of its blend with oil palm empty fruit bunch fibers. *Bioresour Technol* 102(3):3626–3628. doi:10.1016/j.bior tech.2010.11.020
32. Tian P, Shang L, Ren H, Mi Y, Fan D, Jiang M (2010) Biosynthesis of polyhydroxyalkanoates: current research and development. *Afr J Biotechnol* 8(5):709–714
33. Quillaguamán J, Guzmán H, Van-Thuoc D, Hatti-Kaul R (2010) Synthesis and production of polyhydroxyalkanoates by halophiles: current potential and future prospects. *Appl Microbiol Biotechnol* 85(6):1687–1696
34. Sudesh K, Bhubalan K, Chuah JA, Kek YK, Kamilah H, Sridewi N, Lee YF (2011) Synthesis of polyhydroxyalkanoate from palm oil and some new applications. *Appl Microbiol Biotechnol* 89(5):1373–1386
35. Jensen TE, Sicko LM (1971) Fine structure of poly-{beta}-hydroxybutyric acid granules in a blue-green alga, *Chlorogloea fritschii*. *J Bacteriol* 106(2):683
36. Yan Q, Zhao M, Miao H, Ruan W, Song R (2010) Coupling of the hydrogen and polyhydroxyalkanoates (PHA) production through anaerobic digestion from Taihu blue algae. *Bioresour Technol* 101(12):4508–4512. doi:10.1016/j.biortech.2010.01.073
37. Gumel AM, Annuar MSM, Heidelberg T (2012) Effects of carbon substrates on biodegradable polymer composition and stability produced by *Delftia tsuruhatensis* Bet002 isolated from palm oil mill effluent. *Polym Degrad Stab* 97(8):1227–1231. doi:10.1016/j.polymdegradstab.2012.05.041
38. Li Q, Li G, Yu S, Zhang Z, Ma F, Feng Y (2010) Ring-opening polymerization of  $\epsilon$ -caprolactone catalyzed by a novel thermophilic lipase from *Fervidobacterium nodosum*. *Process Biochem* 46(1):253–257
39. Rai R, Keshavarz T, Roether J, Boccaccini A, Roy I (2011) Medium chain length polyhydroxyalkanoates, promising new biomedical materials for the future. *Mater Sci Eng R Reports* 72(3):29–47
40. Ramalingam S, Vikram M, Vigneshbabu M, Sivasankari M (2011) Flux balance analysis for maximizing polyhydroxyalkanoate production in *Pseudomonas putida*. *Indian J Biotechnol* 10(1):70–74
41. Hori K, Ichinohe R, Unno H, Marsudi S (2011) Simultaneous syntheses of polyhydroxyalkanoates and rhamnolipids by

- Pseudomonas aeruginosa* IFO3924 at various temperatures and from various fatty acids. *Biochem Eng J* 53:196–202
42. de Almeida A, Giordano AM, Nickel PI, Pettinari MJ (2010) Effects of aeration on the synthesis of poly (3-hydroxybutyrate) from glycerol and glucose in recombinant *Escherichia coli*. *Appl Environ Microbiol* 76(6):2036–2040
  43. Albuquerque MGE, Concas S, Bengtsson S, Reis MAM (2010) Mixed culture polyhydroxyalkanoates production from sugar molasses: the use of a 2-stage CSTR system for culture selection. *Bioresour Technol* 101(18):7112–7122. doi:10.1016/j.biortech.2010.04.019
  44. Albuquerque MGE, Martino V, Pollet E, Avérous L, Reis MAM (2011) Mixed culture polyhydroxyalkanoate (PHA) production from volatile fatty acid (VFA)-rich streams: effect of substrate composition and feeding regime on PHA productivity, composition and properties. *J Biotechnol* 151(1):66–76. doi:10.1016/j.jbiotec.2010.10.070
  45. Matsumoto K, Kobayashi H, Ikeda K, Komanoya T, Fukuoka A, Taguchi S (2011) Chemo-microbial conversion of cellulose into polyhydroxybutyrate through ruthenium-catalyzed hydrolysis of cellulose into glucose. *Bioresour Technol* 102:3564–3567
  46. Zúñiga C, Morales M, Le Borgne S, Revah S (2011) Production of poly-[beta]-hydroxybutyrate (PHB) by *Methylobacterium organophilum* isolated from a methanotrophic consortium in a two-phase partition bioreactor. *J Hazard Mater* 190(1–3):876–882
  47. Xu Z, Chen H, Wu H, Li L (2010) 7 mT static magnetic exposure enhanced synthesis of poly-3-hydroxybutyrate by activated sludge at low temperature and high acetate concentration. *Process Saf Environ Prot* 88(4):292–296
  48. Shrivastav A, Mishra SK, Mishra S (2010) Polyhydroxyalkanoate (PHA) synthesis by *Spirulina subsalsa* from Gujarat coast of India. *Int J Biol Macromol* 46(2):255–260
  49. Filippou PS, Koini EN, Calogeropoulou T, Kalliakmani P, Panagiotidis CA, Kyriakidis DA (2011) Regulation of the *E. coli* AtoSC two component system by synthetic biologically active 5, 7, 8-trimethyl-1, 4-benzoxazine analogues. *Bioorg Med Chem* 19(16):5061–5070
  50. Theodorou EC, Theodorou MC, Kyriakidis DA (2011) AtoSC two-component system is involved in cPHB biosynthesis through fatty acid metabolism in *E. coli*. *BBA Gen Subj* 1810(5):561–568
  51. Theodorou EC, Theodorou MC, Samali MN, Kyriakidis DA (2011) Activation of the AtoSC two-component system in the absence of the AtoC N-terminal receiver domain in *E. coli*. *Amino Acids* 40(2):1–10
  52. Jian J, Zhang SQ, Shi ZY, Wang W, Chen GQ, Wu Q (2010) Production of polyhydroxyalkanoates by *Escherichia coli* mutants with defected mixed acid fermentation pathways. *Appl Microbiol Biotechnol* 87(6):1–10
  53. Gao X, Chen JC, Wu Q, Chen GQ (2011) Polyhydroxyalkanoates as a source of chemicals, polymers, and biofuels. *Curr Opin Biotechnol* 22(6):768–774
  54. Kang Z, Du L, Kang J, Wang Y, Wang Q, Liang Q, Qi Q (2011) Production of succinate and polyhydroxyalkanoate from substrate mixture by metabolically engineered *Escherichia coli*. *Biores Technol* 102(11):6600–6604
  55. Liu Q, Luo G, Zhou XR, Chen GQ (2011) Biosynthesis of poly(3-hydroxydecanoate) and 3-hydroxydodecanoate dominating polyhydroxyalkanoates by  $\beta$ -oxidation pathway inhibited *Pseudomonas putida*. *Metab Eng* 13:11–17
  56. Chung AL, Jin HL, Huang LJ, Ye HM, Chen JC, Wu Q, Chen GQ (2011) Biosynthesis and characterization of Poly (3-hydroxydodecanoate) by  $\beta$ -oxidation inhibited mutant of *Pseudomonas entomophila* L48. *Biomacromolecules* 12(10):3559–3566
  57. Bhubalan K, Rath D-N, Abe H, Iwata T, Sudesh K (2010) Improved synthesis of P(3HB-co-3HV-co-3HHx) terpolymers by mutant *Cupriavidus necator* using the PHA synthase gene of *Chromobacterium* sp. USM2 with high affinity towards 3HV. *Polym Degrad Stab* 95(8):1436–1442. doi:10.1016/j.polyimdegradstab.2009.12.018
  58. Chisti Y, Moo-Young M (1986) Disruption of microbial cells for intracellular products. *Enzyme Microb Technol* 8(4):194–204
  59. Buelhamd A, Abd-El-Haleem D, Zaki S, Amara A, GMS A (2007) Genetic engineering of *Schizosaccharomyces pombe* to produce bacterial polyhydroxyalkanoates. *J Appl Sci Environ Manag* 11(2):83–90
  60. Desuoky A, El-Haleem A, Zaki S, Abuelhamd A, Amara A, Aboelreesh G (2007) Biosynthesis of polyhydroxyalkanoates in wildtype yeasts. *J Appl Sci Environ Manag* 11(3):1119–8362
  61. Sabirova JS, Haddouche R, Van Bogaert I, Mulaa F, Verstraete W, Timmis K, Schmidt Dannert C, Nicaud J, Soetaert W (2011) The ‘LipoYeasts’ project: using the oleaginous yeast *Yarrowia lipolytica* in combination with specific bacterial genes for the bioconversion of lipids, fats and oils into high value products. *Microb Biotechnol* 4(1):47–54
  62. Tamer IM, Moo-Young M, Chisti Y (1998) Disruption of *Alcaligenes latus* for recovery of poly ( $\beta$ -hydroxybutyric acid): comparison of high-pressure homogenization, bead milling, and chemically induced lysis. *Ind Eng Chem Res* 37(5):1807–1814
  63. Kunasundari B, Sudesh K (2011) Isolation and recovery of microbial polyhydroxyalkanoates. *eXPRESS Pol Lett* 5(7):620–634. doi:10.3144/expresspolymlett.2011.60
  64. Jacquel N, Lo C-W, Wei Y-H, Wu H-S, Wang SS (2008) Isolation and purification of bacterial poly(3-hydroxyalkanoates). *Biochem Eng J* 39(1):15–27. doi:10.1016/j.bej.2007.11.029
  65. Kulkarni SO, Kanekar PP, Jog JP, Patil PA, Nilegaonkar SS, Sarnaik SS, Kshirsagar PR (2011) Characterisation of copolymer, poly (hydroxybutyrate-co-hydroxyvalerate) (PHB-co-PHV) produced by *Halomonas campisalis* (MCM B-1027), its biodegradability and potential application. *Bioresour Technol* 102(11):6625–6628. doi:10.1016/j.biortech.2011.03.054
  66. Rao U, Sridhar R, Sehgal PK (2010) Biosynthesis and biocompatibility of poly(3-hydroxybutyrate-co-4-hydroxybutyrate) produced by *Cupriavidus necator* from spent palm oil. *Biochem Eng J* 49(1):13–20. doi:10.1016/j.bej.2009.11.005
  67. Allen AD, Anderson WA, Ayorinde FO, Eribo BE (2010) Biosynthesis and characterization of copolymer poly (3HB-co-3HV) from saponified *Jatropha curcas* oil by *Pseudomonas oleovorans*. *J Ind Microbiol Biot* 37(8):849–856
  68. López-Cuellar M, Alba-Flores J, Rodríguez J, Pérez-Guevara F (2011) Production of polyhydroxyalkanoates (PHAs) with canola oil as carbon source. *Int J Biol Macromol* 48(1):74–80
  69. Chardron S, Bruzard S, Lignot B, Elain A, Sire O (2010) Characterization of bionanocomposites based on medium chain length polyhydroxyalkanoates synthesized by *Pseudomonas oleovorans*. *Polym Test* 29(8):966–971. doi:10.1016/j.polymer testing.2010.08.009
  70. Penloglou G, Chatzidoukas C, Kiparissides C (2012) Microbial production of polyhydroxybutyrate with tailor-made properties: an integrated modelling approach and experimental validation. *Biotechnol Adv* 30(1):329–337. doi:10.1016/j.biotechadv.2011.06.021
  71. Samrot A, Avinesh R, Sukeetha S, Senthilkumar P (2011) Accumulation of poly[(R)-3-hydroxyalkanoates] in *Enterobacter cloacae* SU-1 during growth with two different carbon sources in batch culture. *Appl Biochem Biotechnol* 163(1):195–203. doi:10.1007/s12010-010-9028-7
  72. Yang YH, Brigham C, Willis L, Rha CK, Sinskey A (2011) Improved detergent-based recovery of polyhydroxyalkanoates (PHAs). *Biotechnol Lett* 1–6
  73. Lo C-W, Wu H-S, Wei Y-H (2011) High throughput study of separation of poly(3-hydroxybutyrate) from recombinant



- Escherichia coli* XL1 blue. J Taiwan Inst Chem E 42(2):240–246. doi:10.1016/j.jtice.2010.08.001
74. Kathiraser Y, Aroua MK, Ramachandran KB, Tan IKP (2007) Chemical characterization of medium chain length polyhydroxyalkanoates (PHAs) recovered by enzymatic treatment and ultrafiltration. J Chem Technol Biot 82(9):847–855
  75. Yasotha K, Aroua MK, Ramachandran KB, Tan IKP (2006) Recovery of medium-chain-length polyhydroxyalkanoates (PHAs) through enzymatic digestion treatments and ultrafiltration. Biochem Eng J 30(3):260–268. doi:10.1016/j.bej.2006.05.008
  76. Horowitz DM, Brennan EM (2010) Methods for the separation and purification of biopolymers. European Patents 1(070):135
  77. Darani KK, Reza Mozafari M (2010) Supercritical fluids technology in bioprocess industries: a review. J Biochem Technol 2(1):144–152
  78. Khosravi-Darani K (2010) Research activities on supercritical fluid science in food biotechnology. Crit Rev Food Sci Nutr 50(6):479–488
  79. Posada JA, Naranjo JM, López JA, Higuera JC, Cardona CA (2011) Design and analysis of poly-3-hydroxybutyrate production processes from crude glycerol. Process Biochem 46(1):310–317. doi:10.1016/j.procbio.2010.09.003
  80. Reemmer J (2009) Advances in the synthesis and extraction of biodegradable polyhydroxyalkanoates in plant systems—a review. MMG 445 Basic Biotechnol eJ 5(1):44–49
  81. Ariffin N, Abdullah R, Rashdan Muad M, Lourdes J, Emran NA, Ismail MR, Ismail I, Fadzil MFM, Ling KL, Siddiqui Y, Amir AA, Berahim Z, Husni Omar M (2011) Constructions of expression vectors of polyhydroxybutyrate-co-hydroxyvalerate (PHBV) and transient expression of transgenes in immature oil palm embryos. Plasmid 66(3):136–143. doi:10.1016/j.plasmid.2011.07.002
  82. Snell KD (2010) Multi-gene expression construct containing modified intein. European Patents 1(255):846
  83. Börnke F, Broer I (2010) Tailoring plant metabolism for the production of novel polymers and platform chemicals. Curr Opin Plant Biol 13(3):353–361
  84. Poirier Y, Brumbley S (2010) Metabolic engineering of plants for the synthesis of polyhydroxyalkanoates plastics from bacteria. In: Chen GG-Q (ed) vol 14. Microbiology Monographs. Springer Berlin / Heidelberg, pp 187–211. doi:10.1007/978-3-642-03287-5\_8
  85. Bohmert-Tatarev K, McAvoy S, Daughtry S, Peoples OP, Snell KD (2011) Focus issue on plastid biology: high levels of bioplastic are produced in fertile transplastomic tobacco plants engineered with a synthetic operon for the production of polyhydroxybutyrate. Plant Physiol 155(4):1690
  86. Matsumoto K, Morimoto K, Gohda A, Shimada H, Taguchi S (2010) Improved polyhydroxybutyrate (PHB) production in transgenic tobacco by enhancing translation efficiency of bacterial PHB biosynthetic genes. J Biosci Bioeng 111(4):485–488
  87. Somleva MN, Snell KD, Beaulieu JJ, Peoples OP, Garrison BR, Patterson NA (2008) Production of polyhydroxybutyrate in switchgrass, a value added co product in an important lignocellulosic biomass crop. Plant Biotechnol J 6(7):663–678
  88. Kourtz L, Peoples OP, Snell KD (2010) Chemically inducible expression of biosynthetic pathways. US Patent App. 20,100/196,974
  89. Kourtz L, Dillon K, Daughtry S, Peoples OP, Snell KD (2007) Chemically inducible expression of the PHB biosynthetic pathway in *Arabidopsis*. Transgenic Res 16(6):759–769
  90. Gogoi P, Hazarika S, Dutta N (2010) Kinetics and mechanism on laccase catalyzed synthesis of poly (allylamine) catechin conjugate. Chem Eng J 163(12):86–92
  91. Kadokawa J, Kobayashi S (2010) Polymer synthesis by enzymatic catalysis. Curr Opin Chem Biol 14(2):145–153
  92. Kim S, Silva C, Evtuguin DV, Gamelas JAF, Cavaco-Paulo A (2011) Polyoxometalate/laccase-mediated oxidative polymerization of catechol for textile dyeing. Appl Microb Biot 89(4):981–987
  93. Liu W, Chen B, Wang F, Tan T, Deng L (2011) Lipase-catalyzed synthesis of aliphatic polyesters and properties characterization. Process Biochem 46(10):1993–2000. doi:10.1016/j.procbio.2011.07.008
  94. Sharma R, Chisti Y, Banerjee UC (2001) Production, purification, characterization, and applications of lipases. Biotechnol Adv 19(8):627–662
  95. Arumugasamy SK, Ahmad Z (2011) *Candida antarctica* as catalyst for polycaprolactone synthesis: effect of temperature and solvents. Asia Pac J Chem Eng 6:398–405. doi:10.1002/apj.583
  96. Gumel AM, Annur MSM, Chisti Y, Heidelberg T (2012) Ultrasound assisted lipase catalyzed synthesis of poly-6-hydroxyhexanoate. Ultrason Sonochem 19(3):659–667
  97. Hunsen M, Azim A, Mang H, Wallner SR, Ronkvist A, WENCHUN X, Gross RA (2008) Cutinase: a powerful biocatalyst for polyester synthesis by polycondensation of diols and diacids and ROP of lactones. In: Polymer biocatalysis and biomaterials II, vol 999. ACS symposium series, vol 999. American Chemical Society, pp 263–274
  98. Feder D, Gross RA (2010) Exploring chain length selectivity in HIC-catalyzed polycondensation reactions. Biomacromolecules 11(3):690–697
  99. Takwa M, Hult K, Martinelle M (2008) Single-step, solvent-free enzymatic route to  $\omega$ -functionalized polypentadecalactone macromonomers. Macromolecules 41(14):5230–5236
  100. Kakasi-Zsurka S, Todea A, But A, Paul C, Boeriu CG, Davidescu C, Nagy L, Kuki Á, Kéki S, Péter F (2011) Biocatalytic synthesis of new copolymers from 3-hydroxybutyric acid and a carbohydrate lactone. J Mol Catal B Enzym 71:22–28
  101. Veld M, Palmans A (2011) Hydrolases part I: enzyme mechanism, selectivity and control in the synthesis of well-defined polymers. In: Palmans ARA, Heise A (eds) Enzymatic polymerisation. Adv Polym Sci 237:55–78. doi:10.1007/12\_2010\_86
  102. Sato S, Minato M, Kikkawa Y, Abe H, Tsuge T (2010) In vitro synthesis of polyhydroxyalkanoate catalyzed by class II and III PHA synthases: a useful technique for surface coatings of a hydrophobic support with PHA. J Chem Technol Biot 85(6):779–782
  103. Gumel AM, Annur MSM, Heidelberg T, Chisti Y (2011) Lipase mediated synthesis of sugar fatty acid esters. Process Biochem 46:2079–2090
  104. Mallakpour S, Rafiee Z (2011) New developments in polymer science and technology using combination of ionic liquids and microwave irradiation. Prog Polym Sci 36(12):1754–1765
  105. Sosnik A, Gotelli G, Abraham GA (2011) Microwave-assisted polymer synthesis (MAPS) as a tool in biomaterials science: how new and how powerful. Prog Polym Sci 36:1050–1078
  106. García-Arrazola R, López-Guerrero DA, Gimeno M, Bárzana E (2009) Lipase-catalyzed synthesis of poly-L-lactide using supercritical carbon dioxide. J Supercrit Fluid 51(2):197–201
  107. Matsuda T (2011) Asymmetric catalytic synthesis in supercritical fluids. Catal Meth Asym Synth 373–390
  108. Thurecht KJ, Villarroya S (2010) Biocatalytic polymerization in exotic solvents. In: Loos K (ed) Biocatalysis in polymer chemistry. Wiley-VCH Verlag GmbH & Co. KGaA, pp 323–348. doi:10.1002/9783527632534.ch13
  109. Gorke J, Srienc F, Kazlauskas R, Flickinger MC (2010) Enzyme-catalyzed reactions in ionic liquids. In: Encyclopedia of

- industrial biotechnology: bioprocess, bioseparation and cell technology. Wiley, New York. doi:[10.1002/9780470054581.eib271](https://doi.org/10.1002/9780470054581.eib271)
110. Mallakpour S, Dinari M (2011) High performance polymers in ionic liquid: a review on prospects for green polymer chemistry. Part II: polyimides and polyesters. *Iranian Polym J* 20(4): 259–279
  111. Kundu S, Bhargale AS, Wallace WE, Flynn KM, Guttman CM, Gross RA, Beers KL (2011) Continuous flow enzyme-catalyzed polymerization in a microreactor. *J Am Chem Soc* 133(15): 6006–6011
  112. Ahmed EH, Raghavendra T, Madamwar D (2010) An alkaline lipase from organic solvent tolerant *Acinetobacter* sp. EH28: application for ethyl caprylate synthesis. *Bioresour Technol* 101(10):3628–3634
  113. Takwa M, Larsen MW, Hult K, Martinelle M (2011) Rational redesign of *Candida antarctica* lipase B for the ring opening polymerization of d, d-lactide. *Chem Comm* 47:7392–7394
  114. Karagoz B, Bayramoglu G, Altintas B, Bicak N, Arica MY (2010) Poly (glycidyl methacrylate)-polystyrene diblocks copolymer grafted nanocomposite microspheres from surface-initiated atom transfer radical polymerization for lipase immobilization: application in flavor ester synthesis. *Ind Eng Chem Res* 49(20):9655–9665
  115. López-Luna A, Gallegos JL, Gimeno M, Vivaldo-Lima E, Bárcana E (2010) Lipase-catalyzed syntheses of linear and hyperbranched polyesters using compressed fluids as solvent media. *J Mol Catal B Enzym* 67(1–2):143–149. doi:[10.1016/j.molcatb.2010.07.020](https://doi.org/10.1016/j.molcatb.2010.07.020)
  116. Han S-Y, Zhang J-H, Han Z-l, Zheng S-P, Lin Y (2011) Combination of site-directed mutagenesis and yeast surface display enhances *Rhizomucor miehei* lipase esterification activity in organic solvent. *Biotechnol Lett* 33(12):2431–2438. doi: [10.1007/s10529-011-0705-6](https://doi.org/10.1007/s10529-011-0705-6)
  117. Palmans ARA, van As BAC, van Buijtenen J, Meijer E (2008) Ring-opening of  $\omega$ -substituted lactones by Novozym 435: selectivity issues and application to iterative tandem catalysis. In: *Polymer biocatalysis and biomaterials II*, vol 999. American Chemical Society Publications, pp 230–244
  118. Sha K, Li D, Li Y, Zhang B, Wang J (2008) The chemoenzymatic synthesis of a novel CBABC-type pentablock copolymer and its self-assembled “crew-cut” aggregation. *Macromolecules* 41(2):361–371
  119. Zhang B, Li Y, Xu Y, Wang S, Ma L, Wang J (2008) Chemoenzymatic synthesis and characterization of H-shaped triblock copolymer. *Polym Bull* 60(6):733–740. doi:[10.1007/s00289-008-0906-x](https://doi.org/10.1007/s00289-008-0906-x)
  120. Zhang B, Li Y, Wang W, Wang J, Chen X (2011) ABA 2-type triblock copolymer composed of PCL and PSt: synthesis and characterization. *Polym Bull* 67(8):1507–1518
  121. Xue L, Dai S, Li Z (2010) Biodegradable shape-memory block co-polymers for fast self-expandable stents. *Biomaterials* 31(32):8132–8140
  122. de Geus M, Palmans Anja RA, Duxbury Christopher J, Villarroya S, Howdle Steven M, Heise A (2008) Chemoenzymatic synthesis of block copolymers. In: *Polymer biocatalysis and biomaterials II*, vol 999. ACS symposium series, vol 999. American Chemical Society, pp 216–229. doi:[10.1021/bk-2008-0999.ch014](https://doi.org/10.1021/bk-2008-0999.ch014)
  123. Tajima K, Satoh Y, Satoh T, Itoh R, Han X, Taguchi S, Kakuchi T, Munekata M (2009) Chemo-enzymatic synthesis of poly (lactate-co-(3-hydroxybutyrate)) by a lactate-polymerizing enzyme. *Macromolecules* 42(6):1985–1989
  124. Han X, Satoh Y, Tajima K, Matsushima T, Munekata M (2009) Chemo-enzymatic synthesis of polyhydroxyalkanoate by an improved two-phase reaction system (TPRS). *J Biosci Bioeng* 108(6):517–523
  125. Tian H, Tang Z, Zhuang X, Chen X, Jing X (2012) Biodegradable synthetic polymers: preparation, functionalization and biomedical application. *Prog Polym Sci* 37(2):237–280. doi: [10.1016/j.progpolymsci.2011.06.004](https://doi.org/10.1016/j.progpolymsci.2011.06.004)
  126. Motornov M, Roiter Y, Tokarev I, Minko S (2010) Stimuli-responsive nanoparticles, nanogels and capsules for integrated multifunctional intelligent systems. *Prog Polym Sci* 35(1–2): 174–211
  127. Jocić D, Tourrette A, Lavrić PK (2010) Biopolymer-based stimuli-responsive polymeric systems for functional finishing of textiles. In: Elnashar MM (ed) *Biopolymers*. Sciyo, Croatia, pp 37–40. doi:[10.5772/286](https://doi.org/10.5772/286)
  128. Xu F, Yan TT, Luo YL (2011) Synthesis and micellization of thermosensitive PNIPAAm-b-PLA amphiphilic block copolymers based on a bifunctional initiator. *Macromol Res* 19(12): 1287–1295
  129. Meng F, Zhong Z, Feijen J (2009) Stimuli-responsive polymersomes for programmed drug delivery. *Biomacromolecules* 10(2):197–209
  130. Bawa P, Pillay V, Choonara YE, du Toit LC (2009) Stimuli-responsive polymers and their applications in drug delivery. *Biomed Mater* 4:022001
  131. Stuart MAC, Huck WTS, Genzer J, Müller M, Ober C, Stamm M, Sukhorukov GB, Szleifer I, Tsukruk VV, Urban M (2010) Emerging applications of stimuli-responsive polymer materials. *Nature Mater* 9(2):101–113
  132. Cui W, Qi M, Li X, Huang S, Zhou S, Weng J (2008) Electrospun fibers of acid-labile biodegradable polymers with acetal groups as potential drug carriers. *Int J Pharm* 361(1–2):47–55
  133. Barinov V, Dabrowski R, Levon K (2006) Methods and apparatus for modifying gel adhesion strength. WO Patent WO/2006/ 050,340
  134. Costa RR, Custódio CA, Arias FJ, Rodríguez-Cabello JC, Mano JF (2011) Layer-by-layer assembly of chitosan and recombinant biopolymers into biomimetic coatings with multiple stimuli-responsive properties. *Small* 7(18):2640–2649
  135. Loh XJ, Cheong WCD, Li J, Ito Y (2009) Novel poly (N-isopropylacrylamide)-poly [(R)-3-hydroxybutyrate]-poly (N-isopropylacrylamide) triblock copolymer surface as a culture substrate for human mesenchymal stem cells. *Soft Matter* 5(15):2937–2946
  136. Zhu JL, Zhang XZ, Cheng H, Li YY, Cheng SX, Zhuo RX (2007) Synthesis and characterization of well-defined, amphiphilic poly (N-isopropylacrylamide)-b-[2-hydroxyethyl methacrylate-poly ( $\epsilon$ -caprolactone)]<sub>n</sub> graft copolymers by RAFT polymerization and macromonomer method. *J Polym Sci, Part A: Polym Chem* 45(22):5354–5364
  137. Yin H, Lee ES, Kim D, Lee KH, Oh KT, Bae YH (2008) Physicochemical characteristics of pH-sensitive poly (L-histidine)-b-poly (ethylene glycol)/poly (L-lactide)-b-poly (ethylene glycol) mixed micelles. *J Control Release* 126(2):130–138
  138. Guo Y, Li M, Mylonakis A, Han J, MacDiarmid AG, Chen X, Lelkes PI, Wei Y (2007) Electroactive oligoaniline-containing self-assembled monolayers for tissue engineering applications. *Biomacromolecules* 8(10):3025–3034
  139. Wei Y, Lelkes PI, MacDiarmid AG, Guterman E, Cheng S, Palouian K, Bidez P (2004) Electroactive polymers and nanostructured materials for neural tissue engineering. In: Qifeng Z, Cheng SZD (eds) *Contemporary topics in advanced polymer science and technology*. Peking University Press, Beijing, China, pp 430–436
  140. Yamamoto H, Kitsuki T, Nishida A, Asada K, Ohkawa K (1999) Photoresponsive peptide and polypeptide systems. 13. Photoinduced cross-linked gel and biodegradation properties of copoly-

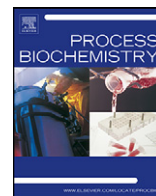
- (L-lysine) containing  $\epsilon$ -7-Coumaryloxyacetyl-L-lysine residues. *Macromolecules* 32(4):1055–1061
141. Kwon IK, Matsuda T (2005) Photo-polymerized microarchitectural constructs prepared by microstereolithography ( $\mu$ SL) using liquid acrylate-end-capped trimethylene carbonate-based prepolymers. *Biomaterials* 26(14):1675–1684
  142. Gupta H, Wilkinson RA, Bogdanov AA Jr, Callahan RJ, Weissleder R (1995) Inflammation: imaging with methoxy poly(ethylene glycol)-poly-L-lysine-DTPA, a long-circulating graft copolymer. *Radiology* 197(3):665–669
  143. Ross JF, Chaudhuri PK, Ratnam M (1994) Differential regulation of folate receptor isoforms in normal and malignant tissues in vivo and in established cell lines. Physiologic and clinical implications. *Cancer* 73(9):2432–2443
  144. Jiang C, Wang X, Sun P, Yang C (2011) Synthesis and solution behavior of poly ( $\epsilon$ -caprolactone) grafted hydroxyethyl cellulose copolymers. *Int J Biol Macromol* 48(1):210–214
  145. Lu D, Wu Q, Lin X (2002) Chemoenzymatic synthesis of biodegradable poly (1'-O-vinyladipoyl-sucrose). *Chinese J Polym Sci* 20(6):579–584
  146. Puppi D, Chiellini F, Piras AM, Chiellini E (2010) Polymeric materials for bone and cartilage repair. *Prog Polym Sci* 35(4):403–440. doi:10.1016/j.progpolymsci.2010.01.006
  147. Bansal SS, Goel M, Aqil F, Vadhanam MV, Gupta RC (2011) Advanced drug-delivery systems of curcumin for cancer chemoprevention. *Cancer Prev Res* 4:1158
  148. Gaucher G, Marchessault RH, Leroux JC (2010) Polyester-based micelles and nanoparticles for the parenteral delivery of taxanes. *J Control Release* 143(1):2–12
  149. Kiliçay E, Demirbilek M, Türk M, Güven E, Hazer B, Denkbaz EB (2011) Preparation and characterization of poly(3-hydroxybutyrate-co-3-hydroxyhexanoate) (Phbhxx) based nanoparticles for targeted cancer therapy. *Eur J Pharm Sci* 44(3):310–320. doi:10.1016/j.ejps.2011.08.013
  150. Lee J, Jung S-G, Park C-S, Kim H-Y, Batt CA, Kim Y-R (2011) Tumor-specific hybrid polyhydroxybutyrate nanoparticle: surface modification of nanoparticle by enzymatically synthesized functional block copolymer. *Bioorg Med Chem Lett* 21(10):2941–2944. doi:10.1016/j.bmcl.2011.03.058
  151. Zawidlak-Wegrzynska B, Kawalec M, Bosek I, Luczyk-Juzwa M, Adamus G, Rusin A, Filipczak P, Glowala-Kosinska M, Wolanska K, Krawczyk Z (2010) Synthesis and antiproliferative properties of ibuprofen-oligo (3-hydroxybutyrate) conjugates. *Eur J Med Chem* 45(5):1833–1842
  152. Francis L (2011) Biosynthesis of polyhydroxyalkanoates and their medical applications. University of Westminster, Westminster
  153. Seyednejad H, Ghassemi AH, van Nostrum CF, Vermonden T, Hennink WE (2011) Functional aliphatic polyesters for biomedical and pharmaceutical applications. *J Control Release* 152:168–172
  154. Li W-R, Xie X-B, Shi Q-S, Duan S-S, Ouyang Y-S, Chen Y-B (2011) Antibacterial effect of silver nanoparticles on *Staphylococcus aureus*. *Biometals* 24(1):135–141. doi:10.1007/s10534-010-9381-6
  155. Li WR, Xie XB, Shi QS, Zeng HY, Ou-Yang YS, Chen YB (2010) Antibacterial activity and mechanism of silver nanoparticles on *Escherichia coli*. *Appl Microbiol Biotechnol* 85(4):1115–1122
  156. Mirzajani F, Ghassempour A, Aliahmadi A, Esmaeili MA (2011) Antibacterial effect of silver nanoparticles on *Staphylococcus aureus*. *Res Microbiol* 162(5):542–549
  157. Phukon P, Saikia JP, Konwar BK (2011) Enhancing the stability of colloidal silver nanoparticles using polyhydroxyalkanoates (PHA) from *Bacillus circulans* (MTCC 8167) isolated from crude oil contaminated soil. *Colloids Surf B Biointerfaces* 86(2):314–318. doi:10.1016/j.colsurfb.2011.04.014
  158. Zhou J, Peng S-W, Wang Y-Y, Zheng S-B, Wang Y, Chen G-Q (2010) The use of poly(3-hydroxybutyrate-co-3-hydroxyhexanoate) scaffolds for tarsal repair in eyelid reconstruction in the rat. *Biomaterials* 31(29):7512–7518. doi:10.1016/j.biomaterials.2010.06.044
  159. Yan C, Wang Y, Shen X-Y, Yang G, Jian J, Wang H-S, Chen G-Q, Wu Q (2011) MicroRNA regulation associated chondrogenesis of mouse MSCs grown on polyhydroxyalkanoates. *Biomaterials* 32(27):6435–6444. doi:10.1016/j.biomaterials.2011.05.031
  160. Wang L, Wang Z-H, Shen C-Y, You M-L, Xiao J-F, Chen G-Q (2010) Differentiation of human bone marrow mesenchymal stem cells grown in terpolyesters of 3-hydroxyalkanoates scaffolds into nerve cells. *Biomaterials* 31(7):1691–1698. doi:10.1016/j.biomaterials.2009.11.053
  161. Butcher JT, Mahler GJ, Hockaday LA (2011) Aortic valve disease and treatment: the need for naturally engineered solutions. *Adv Drug Del Rev* 63:242–268
  162. Bouten C, Dankers P, Driessen-Mol A, Pedron S, Brizard A, Baaijens F (2011) Substrates for cardiovascular tissue engineering. *Adv Drug Del Rev* 63:221–241
  163. Wei XW, Gong CY, Gou ML, Fu SZ, Guo QF, Shi S, Luo F, Guo G, Qiu LY, Qian ZY (2009) Biodegradable poly ( $\epsilon$ -caprolactone)-poly (ethylene glycol) copolymers as drug delivery system. *Int J Pharm* 381(1):1–18
  164. Woodruff MA, Hutmacher DW (2010) The return of a forgotten polymer-polycaprolactone in the 21st century. *Prog Polym Sci* 35(10):1217–1256
  165. Patel A, Velikov K (2011) Colloidal delivery systems in foods: a general comparison with oral drug delivery. *LWT Food Sci Technol* 44(9):1958–1964
  166. Riekes MK, Barboza FM, Vecchia DD, Bohatch M Jr, Farago PV, Fernandes D, Silva MAS, Stulzer HK (2011) Evaluation of oral carvedilol microparticles prepared by simple emulsion technique using poly (3-hydroxybutyrate-co-3-hydroxyvalerate) and polycaprolactone as polymers. *Mater Sci Eng C* 31(5):962–968
  167. Öztürk F, Ermertcan AT (2011) Wound healing: a new approach to the topical wound care. *Cutan Ocul Toxicol* 30(2):92–99
  168. Uppal R, Ramaswamy GN, Arnold C, Goodband R, Wang Y (2011) Hyaluronic acid nanofiber wound dressing—production, characterization, and in vivo behavior. *J Biomed Mater Res Part B Appl Biomater* 97B(1):20–29
  169. Bodmeier R (2011) Implants particles. US Patents
  170. Howe J (2011) Suture anchor inserter. US Patents
  171. Bansal SS, Vadhanam MV, Gupta RC (2011) Development and in vitro-in vivo evaluation of polymeric implants for continuous systemic delivery of curcumin. *Pharm Res* 28(5):1121–1130
  172. Wakis V, Jonnalagadda S (2011) Novel poly-DL-lactide-polycaprolactone copolymer based flexible drug delivery system for sustained release of ciprofloxacin. *Drug Deliv* 18(4):236–245
  173. Wong VG, Wood LL (2011) Conveniently implantable sustained release drug compositions. US Patents
  174. Thuaksuban N, Nuntanarant T, Pattanachot W, Suttapreyasri S, Cheung LK (2011) Biodegradable polycaprolactone-chitosan three-dimensional scaffolds fabricated by melt stretching and multilayer deposition for bone tissue engineering: assessment of the physical properties and cellular response. *Biomed Mater* 6:015009
  175. Williams SF, Martin DP, Gerngross T, Horowitz DM (2011) Polyhydroxyalkanoates for in vivo applications. US Patents
  176. Williams SF, Martin DP, Gerngross T, Horowitz DM (2011) Medical device comprising polyhydroxyalkanoate having pyrogen removed. US Patents
  177. Woodruff MA, Hutmacher DW (2010) Resorbable composite scaffolds for bone tissue engineering. In: Tissue and cell engineering society (TCES), Manchester, 28–30 July 2010. TCES

178. Pillai CKS, Sharma CP (2010) Absorbable polymeric surgical sutures: chemistry, production, properties, biodegradability, and performance. *J Biomater Appl* 25(4):291–366. doi:[10.1177/0885328210384890](https://doi.org/10.1177/0885328210384890)
179. Wang SY, Wang Z, Liu MM, Xu Y, Zhang XJ, Chen GQ (2010) Properties of a new gasoline oxygenate blend component: 3-hydroxybutyrate methyl ester produced from bacterial poly-3-hydroxybutyrate. *Biomass Bioenerg* 34(8):1216–1222
180. Zhang X, Luo R, Wang Z, Deng Y, Chen GQ (2009) Application of (R)-3-hydroxyalkanoate methyl esters derived from microbial polyhydroxyalkanoates as novel biofuels. *Biomacromolecules* 10(4):707–711
181. Bourbonnais R, Marchessault RH (2010) Application of polyhydroxyalkanoate granules for sizing of paper. *Biomacromolecules* 11(4):989–993. doi:[10.1021/bm9014667](https://doi.org/10.1021/bm9014667)
182. Modi S, Koelling K, Vodovotz Y (2011) Assessment of PHB with varying hydroxyvalerate content for potential packaging applications. *Eur Polym J* 47:179–186
183. Johansson C (2011) Bio-nanocomposites for food packaging applications. *Nanocomposites with biodegradable polymers: synthesis, properties, and future perspectives*. Oxford University Press, UK
184. Del Nobile MA, Conte A, Buonocore GG, Incoronato AL, Massaro A, Panza O (2009) Active packaging by extrusion processing of recyclable and biodegradable polymers. *J Food Eng* 93(1):1–6
185. Siracusa V, Rocculi P, Romani S, Rosa MD (2008) Biodegradable polymers for food packaging: a review. *Trends Food Sci Technol* 19(12):634–643
186. De Schryver P, Dierckens K, Bahn Thi QQ, Amalia R, Marzorati M, Bossier P, Boon N, Verstraete W (2011) Convergent dynamics of the juvenile European sea bass gut microbiota induced by polyhydroxybutyrate. *Environ Microbiol* 13(4):1042–1051
187. Defoirdt T, Sorgeloos P, Bossier P (2011) Alternatives to antibiotics for the control of bacterial disease in aquaculture. *Curr Opin Microbiol* 14(3):251–258
188. Nhan DT, Wille M, De Schryver P, Defoirdt T, Bossier P, Sorgeloos P (2010) The effect of poly [beta]-hydroxybutyrate on larviculture of the giant freshwater prawn *Macrobrachium rosenbergii*. *Aquaculture* 302(1–2):76–81. doi:[10.1016/j.aquaculture.2010.02.011](https://doi.org/10.1016/j.aquaculture.2010.02.011)
189. Grillo R, AdES Pereira, de Melo NFS, Porto RM, Feitosa LO, Tonello PS, Filho NLD, Rosa AH, Lima R, Fraceto LF (2011) Controlled release system for ametryn using polymer microspheres: preparation, characterization and release kinetics in water. *J Hazard Mater* 186(2–3):1645–1651. doi:[10.1016/j.jhazmat.2010.12.044](https://doi.org/10.1016/j.jhazmat.2010.12.044)
190. Zhang X, Wei C, He Q, Ren Y (2010) Enrichment of chlorobenzene and o-nitrochlorobenzene on biomimetic adsorbent prepared by poly-3-hydroxybutyrate (PHB). *J Hazard Mater* 177(1–3):508–515

## Lipase mediated synthesis of sugar fatty acid esters

Editing and co-author of manuscript





## Review

## Lipase mediated synthesis of sugar fatty acid esters

A.M. Gumel<sup>a</sup>, M.S.M. Annuar<sup>a,\*</sup>, T. Heidelberg<sup>b</sup>, Y. Chisti<sup>c</sup><sup>a</sup> Institute of Biological Sciences, Faculty of Science, University of Malaya, Kuala Lumpur 50603, Malaysia<sup>b</sup> Department of Chemistry, Faculty of Science, University of Malaya, Kuala Lumpur 50603, Malaysia<sup>c</sup> School of Engineering, PN 456, Massey University, Private Bag 11 222, Palmerston North, New Zealand

## ARTICLE INFO

## Article history:

Received 26 May 2011

Received in revised form 7 July 2011

Accepted 27 July 2011

Available online 4 August 2011

## Keywords:

Sugar esters

Esterification

Surfactants

Lipase

Water activity

Nonaqueous media

## ABSTRACT

This review is concerned with lipase catalyzed synthesis of sugar fatty acid esters in water immiscible organic solvents. Sugar esters are widely used nonionic and nontoxic biosurfactants. Certain sugar esters inhibit microbial growth and have other activities. Lipase mediated synthesis has important advantages over conventional chemical synthesis of sugar esters. Lipase catalyzed synthesis is typically carried out in organic solvents having a low water activity to drive the reaction towards synthesis instead of towards ester hydrolysis. The impact of the various reaction conditions on enzymatic synthesis of sugar esters in nonaqueous media is discussed. Considered in particular are the solvent effects; the effects of water activity; the influence of the nature and concentration of the reactants (sugars and fatty acids); the influence of temperature; and the effects associated with the specific nature of the lipase catalyst used.

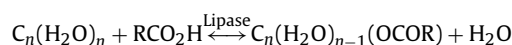
© 2011 Elsevier Ltd. All rights reserved.

## Contents

|   |      |
|---|------|
| 1. Introduction.....                        | 2079 |
| 2. Lipases .....                            | 2080 |
| 3. The reactants .....                      | 2080 |
| 4. The solvents .....                       | 2082 |
| 5. Effects of temperature .....             | 2083 |
| 6. Effects of water activity .....          | 2085 |
| 7. Chemical versus enzymatic synthesis..... | 2087 |
| 8. Concluding remarks.....                  | 2088 |
| References .....                            | 2088 |

## 1. Introduction

The review is focused on the use of lipases for the synthesis of sugar esters. Sugar fatty acid esters (SFAEs) are produced by an esterification reaction between a sugar ( $C_n(H_2O)_n$ ) and a fatty acid ( $RCO_2H$ ) as shown below:



SFAEs are tasteless and odorless nonionic surfactants. They are biodegradable, nontoxic and nonirritant. These properties and their antimicrobial activity have made them attractive for use in foods, pharmaceuticals and cosmetics [1–6]. Certain sugar esters

are insecticidal and miticidal [7]. Various other functional and biological properties have been associated with them [1,8].

Sugar fatty acid esters can be produced by nonenzymatic chemical routes [5,9,10]. The chemical routes require more energy than the enzymatic route and have a low selectivity [6]. In addition, the combination of high temperature and alkaline catalyst used in chemical processes, causes discoloration of the product and the formation of toxic byproducts [6]. Some of the byproducts are allergenic and possibly carcinogenic [10]. As a consequence, lipase catalyzed synthesis is the preferred option for producing sugar fatty acid esters.

Extensive literature exists on lipase mediated synthesis of sugar fatty acid esters [1,2,11–14], but important aspects of this reaction remain to be clarified. For example, why certain combinations of solvents favor synthesis, the effect of the fatty acid chain length on the reaction and the maximum water activity within the reaction

\* Corresponding author. Tel.: +60 6 03 7967 4003; fax: +60 6 03 7967 4178.

E-mail addresses: [suffian.annuar@um.edu.my](mailto:suffian.annuar@um.edu.my), [suffian.annuar@yahoo.com](mailto:suffian.annuar@yahoo.com) (M.S.M. Annuar).

mixture at which the equilibrium shifts from synthesis to hydrolysis. This review discusses these aspects of enzymatic synthesis of SFAE. A brief overview is provided of the relevant lipases. The effects of temperature, solvents and water activity are discussed. The effects of the structures of the reactants involved on the rate and other attributes of the reaction are considered. Guidelines are provided for the lipase-mediated synthesis of SFAE.

## 2. Lipases

Lipases (triacyl glycerol hydrolases, EC 3.1.1.3) are widely used in organic syntheses in the production of specialty chemicals and polymeric materials (Table 1) [1,2,10,12–19]. Lipases typically catalyze the hydrolysis of lipids in aqueous media, but this equilibrium reaction shifts towards synthesis, or esterification, in nonaqueous solvents in the presence of a sparing amount of water. A certain amount of water is essential for hydration of the enzyme even though water is not required for the synthesis of SFAE.

The catalytic activity and stability of lipases depend on their three dimensional conformation. The hydration state of the enzyme influences its activity and stability. The active site of the enzyme involves a movable lid-region [20,21]. The enzyme is active only at the interface between a hydrophobic solvent and an aqueous medium as this interaction is associated with the opening of the lid [22–24]. Different lipases differ in structure, including the structure of the lid region [21]. Differences in the structure of lid region affect lipase activity, regioselectivity and stereoselectivity (Fig. 1) [21,30]. Rational design of lipases has been shown to enhance their enantioselectivity [25], and the use of such engineered lipases in synthesis may have advantages. Specifically engineered lipases have been shown to have greatly enhanced specificity towards branched chain fatty acids [26], for example. Simple chemical modification of lipases can sometimes improve their activity, specificity and selectivity [27–29]. For instance, the use of a detergent-modified lipase powder afforded much greater yields of several SFAE compared to the use of the untreated powder of the same lipase [27].

In synthesis of SFAE, lipases are almost always used in an immobilized form, typically attached to porous beads of a plastic material. Increasing concentration of lipase in the reaction mixture is known to enhance the rate of the initial reaction, but too high a concentration of the immobilized enzyme makes mixing of the reaction slurry difficult. This reduces the reaction rate by adversely affecting mass

transfer [30]. Therefore using excessive enzyme is expensive and counterproductive.

Most of the lipases used in ester synthesis in nonaqueous media appear to be of microbial origin [20,31,32]. Lipases from *Candida antarctica*, *Candida rugosa*, *Candida cylindracea*, *Rhizomucor miehei*, *Bacillus subtilis*, and *Bacillus licheniformis* are commonly used. Porcine pancreatic lipase is also frequently used. Lipases and their action have been previously reviewed [20,33–36]. Production of microbial lipases has been discussed [20,31,32,37] and characteristics of specific microbial lipases have received some attention [23,24,32–34,38–40]. Methods for detecting and characterizing lipases have been discussed by others [20,41].

## 3. The reactants

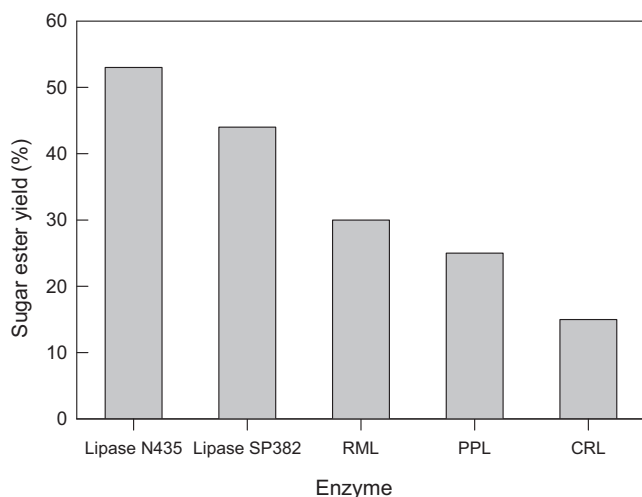
Sugars and fatty acids are the substrates involved in the synthesis of sugar esters. How efficiently a given lipase catalyzes a given esterification process depends on the characteristics of the substrates. Lipases from different sources exhibit different catalytic efficiency towards different substrates. Some lipases have a high selectivity for long and medium chain fatty acids, but others are selective towards short and branched chain fatty acids [11,38]. Ionic and steric effects of the substrates (substitution, unsaturation, branching, carbon chain length) influence the selectivity and activity [11,12].

The effect of the chain length of the fatty acid (the acyl donor) on lipase activity is difficult to generalize. The commonly used lipase Novozyme 435 (*C. antarctica* lipase B [42] immobilized on a macroporous acrylic polymer resin) has a higher specificity towards the unbranched long chain fatty acids [26,43,44]. Kumar et al. [45] reported an increase in activity with increasing carbon chain length of the acyl donor for lipases from *Staphylococcus warneri* and *Staphylococcus xylosus*. In contrast, for *Thermomyces lanuginosus* lipase (Lipolase 100T), increasing chain length of the acyl donor led to reduced rates of esterification. The nature of the support material used in immobilizing a lipase can also affect its selectivity [29,46].

The molar ratio of the two reacting substrates significantly influences the esterification reaction (Table 2). This is because the solubility of a substrate in the reaction medium is affected by the concentration of the other substrate as dissolution of a substrate affects the polarity of the reaction medium. Yan et al. [17] reported that in reaction of glucose with a saturated long chain fatty acid (stearic acid) an excess of the fatty acid in the reaction mixture significantly increased the yield of the sugar ester. The optimal molar ratio of the fatty acid to glucose appeared to be ~3 [17]. In contrast, the yield was reduced by decreasing the chain length of the fatty acid in a reaction involving glucose [6]. *C. antarctica* lipase B immobilized on polymer beads was used in these studies at 50–78 °C [6,17].

In esterification of fructose, increasing excess of short chain fatty acids (e.g. capric acid) favored the esterification reaction in 2-methyl-2-butanol (*tert*-amyl alcohol) [44]. For the same sugar, an increasing excess of long chain fatty acids (e.g. stearic acid) decreased the conversion rate [44]. This effect was attributed to the saturation of the catalytic site of the *C. antarctica* lipase B by a large quantity of the long chain fatty acid which blocked the access of fructose to the active site. An alternate explanation for this phenomena has invoked the differences in viscosities of solutions of fatty acids of different chain lengths at a fixed molar concentration [47].

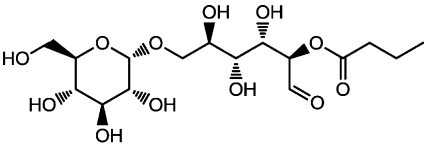
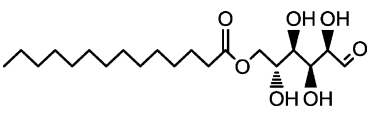
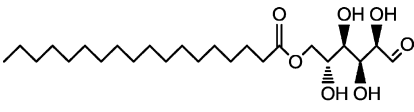
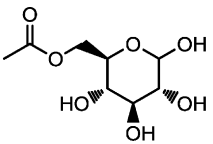

In equimolar mixtures of fructose and fatty acids, increasing chain length of the fatty acid enhances the conversion, but the conversion rate decreases with an increasing molar ratio of the fatty acid to sugar [43,44]. In esterification of glucose with hexadecanoic acid (palmitic acid), an increasing glucose concentration at a



**Fig. 1.** Effect of the type of lipase on the yield of sugar esters [30,69]. *Rhizomucor miehei* lipase (RML), immobilized porcine pancreatic lipase (PPL) and immobilized *Candida rugosa* lipase (CRL).

**Table 1**

Some sugar esters produced by lipase catalyzed enzymatic synthesis.

| Lipase type                        | Acyl donor                      | Acyl acceptor                 | Product   | Time (h) | Yield (%)              | Refs. |
|------------------------------------|---------------------------------|-------------------------------|---|----------|------------------------|-------|
| <i>Candida antarctica</i> SP-435   | Ethyl butanoate                 | Maltose                       | <br>6- <i>O</i> -monobutryl-D-Glucopyranosyl-D-glucose | 24       | 93                     | [82]  |
| <i>Candida antarctica</i> SP-435   | Tetradecanoic acid              | D-Glucose monohydrate         | <br>6- <i>O</i> -glucose tetradecanoate                | 24       | 34 mg mL <sup>-1</sup> | [85]  |
| <i>Mucor miehei</i> Lipozyme TM 20 | Octadecanoic acid               | D-Glucose                     | <br>6- <i>O</i> -glucose octadecanoate                 | 46       | 9.32                   | [52]  |
| Porcine pancreatic lipase IIII     | Vinyl acetate                   | D-Glucose                     | <br>6- <i>O</i> -acetyl glucopyranoside               | 72       | 62                     | [59]  |
| <i>Candida antarctica</i> N 435    | Icosa-5,8,11,14-tetraenoic acid | Isopropylidene-D-xylofuranose | <br>xylose-5-arachidonoate                           | 20       | 83                     | [138] |

**Table 2**  
Effects of reactants type, mole ratio and enzyme type on yield of sugar esters.

| Acyl donor                | Acyl acceptor | Acyl donor:acceptor ratio | Enzyme                      | Yield (%)            | Refs. |
|---------------------------|---------------|---------------------------|-----------------------------|----------------------|-------|
| (9Z)-Octadec-9-enoic acid | Fructose      | 5:1                       | Novozym 435                 | 17 g L <sup>-1</sup> | [2]   |
| (9Z)-Octadec-9-enoic acid | Fructose      | 1:1                       | Novozym 435                 | 6 g L <sup>-1</sup>  |       |
| Hexadecanoic acid         | Fructose      | 1:1                       | Novozym 435                 | 53                   | [30]  |
| Hexadecanoic acid         | Fructose      | 1:1                       | Lipozyme IM                 | 30                   |       |
| Hexadecanoic acid         | Fructose      | 1:1                       | Lipase B SP 382             | 44                   |       |
| Dodecanoic acid           | Fructose      | 1:1                       | Lipase B SP 435             | 55                   |       |
| Octadecanoic acid         | Glucose       | 1:1                       | <i>C. antarctica</i> lipase | 28.8                 | [40]  |
| Octadecanoic acid         | Fructose      | 1:1                       | Lipase SP 435               | 80                   | [44]  |
| Octadecanoic acid         | Fructose      | 1:5                       | Lipase SP 435               | 26                   |       |
| Octanoic acid             | Fructose      | 1:1                       | Lipase SP 435               | 46                   |       |
| Hexadecanoic acid         | Glucose       | 1:1                       | Platase M R. <i>miehei</i>  | 30                   | [48]  |
| Hexadecanoic acid         | Glucose       | 1:2                       | Platase M R. <i>miehei</i>  | 15                   |       |

fixed concentration of the fatty acid initially promoted the reaction [48]. The conversion rate attained a maximum at a substrate molar ratio of 1:1. Further increase in glucose concentration reduced the conversion rate. This reduction was associated with either the substrate (glucose) inhibition of the enzyme or the removal of water by adsorption on glucose to levels that affected the enzyme activity [48]. In contrast, in acylation of glucose with capric acid, Yan et al. [17] reported a considerable increase of the conversion from 18% to 64% as the sugar to fatty acid molar ratio increased from 1:1 to 6:1.

In acylation of isoquercitrin with fatty acids of various carbon chain lengths dissolved in 2-methyl-2-butanol, Salem et al. [49] reported that the conversion yield and the initial rate decreased from 66% to 38% and from 17.7 to 10.1 mmol h<sup>-1</sup>, respectively, as the carbon chain length of the fatty acid increased from C4 to C18. Novozyme 435 lipase was used in this study.

Changes in concentration of the product of the esterification reaction may also affect the solubility of the reactants. For example, Cauglia and Canepa [10] observed that the initial low solubility of glucose (1.6 g L<sup>-1</sup> at 60 °C) in 2-methyl-2-butanol was increased significantly with an increasing concentration of the product (i.e. glucose myristate) during the reaction. The increased solubilization of glucose led to an increased rate of product formation [10].

In general, the conversion rate of lipase catalyzed transesterifications involving fatty acids with 10 or fewer carbons can be improved by supplying an excess of the fatty acid (Table 2). In contrast, for a reaction involving longer fatty acids, e.g. 16 or more carbons in the hydrocarbon chain, a lower molar ratio of fatty acid to sugar is preferable, as a high concentration of a nonpolar fatty acid decreases the solubility of the sugar in the reaction medium.

Sugars tend to be poorly soluble in nonpolar organic reaction media. Reduced polarity derivatives of sugars (e.g. alkyl and acetal derivatives) have been used as substrates to enhance solubility [50,51]. Some of the studies used preprepared sugar derivatives, but suitable derivatives may be made *in situ* during the esterification reaction by adding sugar solubilizing reagents (e.g. organo-boronic acids) to the reaction mixture [52,53]. Highly polar nonaqueous organic solvents can be used for the esterification reaction to improve the solubility of the reactants. This is discussed in the next section of this review.

Other approaches for improving the reaction include the use of activated acyl donors [54–56] and the use of sugar substrate in the form of a solid phase [6,17,43,57–60]. Suspended particles of the sugar continuously replenish the dissolved pool of the substrate as it is consumed by the reaction. Substrates such as glucose have the potential to inhibit certain lipases, but not others [61].

Accumulation of the product in the reaction solvent suppresses its rate of formation. Therefore, a continuous removal of the product

ester is desired. Various simultaneous reaction–extraction schemes have been developed for this purpose [62].

#### 4. The solvents

A nonaqueous solvent is essential for lipase catalyzed synthesis of sugar fatty esters. A suitable solvent must be able to dissolve sufficient amounts of both the substrates, i.e. the sugar and the fatty acid. The solubilities of sugars and fatty acids in organic solvents are generally markedly different and this complicates the esterification reaction as a high concentration of both the reactants within a single phase is difficult to achieve. In addition, the solvent must not adversely affect the stability of the enzyme and its activity. Solvent selection is known to affect the enantioselectivity and specificity of lipase catalyzed reactions [63–66].

In water immiscible organic solvents, the solvent induced drying of the hydration layer of the enzyme [49,67] reduces its catalytic power, activity and stability. Synthetic activity declines progressively with time partly as a consequence of the solvent effect. Removal of the hydration water is said to increase the enzyme rigidity [67]. Lipases that can better withstand prolonged exposure to organic solvents are needed. Immobilization of lipases appears to improve their resistance to organic solvents. Ideally, the product solubility in the solvent should be low so that it is continuously removed by precipitation and the reaction equilibrium is driven towards the product [68].

In an organic solvent, the three dimensional conformation of the enzyme is altered relative to that in an aqueous solution. This affects the catalytic activity, stereoselectivity, regioselectivity as well as stability. The reported differences in the activity of an enzyme in different organic solvents have been attributed to the differences in the extent of enzyme hydration. In general, organic solvents significantly influence the various reaction parameters such as the reaction rate, the maximum reaction velocity (i.e.  $v_{\max}$ ), the catalyst turnover rate (i.e.  $K_{\text{cat}}$ ), the substrate affinity for the catalyst (i.e.  $K_M$ ) and the specificity constant ( $K_{\text{cat}}/K_M$ ), by affecting the hydration status of the enzyme [12].

The influence of organic solvents in enzymatic ester syntheses has been studied extensively and interpreted in various ways [15,69]. Some studies suggest that a solvent's dielectric constant affects the polar and ionic interactions within the three dimensional structure of the enzyme, thus altering the rigidity of the enzyme thereby affecting activity [70,71]. The Hildebrand parameter  $\delta$  is a widely used measure of the solvent polarity, although it is a poor measure [12]. In lipase mediated synthesis, a low polarity ( $\delta \approx 8 \text{ cal}^{1/2} \text{ cm}^{-3/2}$ ) of the solvent is generally accepted to enhance the reaction rate. Other studies suggest that by modifying the polarity at the enzyme active site, a solvent may contribute to

stabilization of the charged transition states during the reaction [72]. Variations in the total free energy associated with the differences in solvation energies of the different solvents have been claimed to be the possible reasons for the solvent effect in non-aqueous media [73].

Because of differences in polarities, solvents differ in their partition coefficient ( $P$ ) values (Table 3). Differences in solvent log  $P$  have been used to explain their effect on the catalytic activity and specificity of enzymes [15,74]. Highest enzyme activities and stabilities are generally observed in solvents with high log  $P$  values [16,75], but others have argued that log  $P$  is not necessarily well correlated with enzyme activity in a given solvent [76,77]. Parameters such as the solvent dielectric constant [70,71], polarity and electron acceptance index [78], as well as the aforementioned Hildebrand solubility parameter [79] have all been used to explain the effect of different solvents on the rate of an enzymatic reaction. Compared to the other parameters mentioned, the solvent log  $P$  appears to generally better correlate the observed lipase activity [74].

A strongly hydrophobic solvent is not always a good choice for lipase mediated syntheses because the hydrophilic sugars such as glucose tend to be poorly soluble in them [1,80,81] and this can adversely affect the product yield of the reaction [82]. The polarity and ionization capacity of a nonaqueous reaction medium may be favorably modified by blending two or more solvents [75,81,83].

Early work on the enzymatic synthesis of sugar fatty acid esters identified relatively polar water-immiscible organic solvents as suitable. Hazardous solvents such as pyridine, dimethyl formamide (DMF) and dimethylpyrrolidone (DMP) were commonly used [80–84]. Environmental and health risks of these solvents [52,86–89] have driven the search for other suitable reaction solvents. For example, Yan et al. [60] achieved reasonably good conversion yields in production of glucose caprylate in ethyl methyl ketone (66%) and acetone (90%). Similarly, Adnani et al. [90] attained good conversions (88–96%) of several fatty acids to xylitol fatty acid esters using hexane as the solvent and Novozyme 435 immobilized lipase. Jia et al. [83] used a mixture of hexane and acetone for lipase-catalyzed synthesis of dilauroyl maltose.

Degn and Zimmermann [81] reported the synthesis of myristate ester of different carbohydrates using immobilized lipase of *C. antarctica*. The production rate of myristyl glucose was improved from 222 to 1212 mmol g<sup>-1</sup> h<sup>-1</sup> by changing the solvent from pure *tert*-butanol to a mixture of *tert*-butanol and pyridine (55:45, v/v). The yield of myristyl glucose was highest when an excess of unsolubilized glucose was present in the reactor [81]. No synthetic activity was detected if glucose was replaced with maltotriose, cellobiose, sucrose and lactose probably because of the poor solubility of these sugars in the *tert*-butanol/pyridine (55:45, v/v) solvent system [81]. Use of sugar derivatives with improved solubility relative to the native sugar offers another means of improving the rate of the enzyme catalyzed synthesis [1]. In some cases, a suspension of undissolved sugars in a solvent has been used to provide a continuous supply of the sugar as it is consumed by the reaction in the solvent [81,91,92].

Ionic liquids are being increasingly used as solvents in lipase mediated synthesis of fatty acid sugar esters [1,14,93–99] (Table 3). Ionic liquids are generally nonvolatile. They are composed of ions instead of the neutral molecules of solvents such as acetone. Ionic liquids dissolve sugars and other complex carbohydrates well [100]. For example, the solubility of sugars such as glucose, sucrose and lactose in an ionic liquid may exceed 100 g L<sup>-1</sup> [95,96]. Whereas polar organic solvents such as methanol inactivate lipases, ionic liquids with similar polarities do not [97]. It has been reported that additives such as aqueous sodium carbonate can be used to further modify the suitability of ionic liquids for lipase catalyzed reactions [97]. This way, reactions that would not normally occur without

the additive can be made to occur at rates comparable to those in nonpolar organic solvents [97].

Ionic liquids also affect the enzyme activity. Lee et al. [96] studied the stability and activity of *C. antarctica* lipase B435 in different ionic liquids and their mixtures. The enzyme activity was reported to be stable in 1-[2-(2-methoxyethoxy)-ethyl]-2,3-dimethylimidazolium tetrafluoronitrate [Bmim][Tf2N], but the activity decreased rapidly in 1-[2-(2-methoxyethoxy)-ethyl]-2,3-dimethylimidazolium tetrafluorooxide [Bmim][TfO] [96]. The stability of the enzyme could be increased by adding [Bmim][Tf2N] to ionic liquid mixtures [96]. For example, the stability of lipase in a 1:1 (v/v) mixture of [Bmim][Tf2N] and [Bmim][TfO] was similar to its stability in pure [Bmim][Tf2N].

Using a supersaturated solution of glucose in [Bmim][TfO], Lee et al. [96] could attain an 86% conversion of the fatty acid to ester, but the conversion dropped to 61% when the enzyme was reused a second time. Carrying out the reaction in a 1:1 (v/v) mixture of [Bmim][Tf2N] and [Bmim][TfO] reduced the initial conversion to 69%, but the activity of the enzyme remained high in subsequent cycles of use. The results suggest that compared to conventional nonaqueous solvents, ionic liquids are substantially superior for use in lipase-mediated syntheses [96]. Supercritical fluids have also been used as reaction solvents [45,94,101,102]. Lipase catalysis in ionic liquids and supercritical fluids has been reviewed by Fan and Qian [94].

## 5. Effects of temperature

Temperature of the reaction affects the stability of the enzyme, the solubilities of the reactants and that of the product, the rate of the reaction and the position of the equilibrium. Most of the commonly used lipases are reasonably thermostable. For example, the *C. antarctica* immobilized lipase B (Novozyme 435) can be used at temperatures of between 60 °C and 80 °C without a significant loss of catalytic activity [17,103].

With Novozyme 435 as the catalyst, a low solubility and conversion of the substrate have been reported at temperatures of <30 °C. With the same catalyst, a temperature of >70 °C greatly reduced the enzyme activity and therefore the conversion of the substrate [15,52,53,71,104]. Therefore, a suitable temperature range for synthesis using Novozyme 435 appears to be between 30 °C and 70 °C although in specific cases a temperature of up to 80 °C may be used [103].

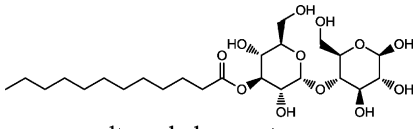
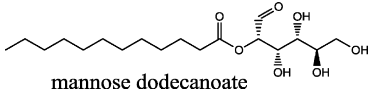
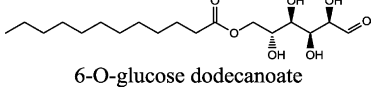
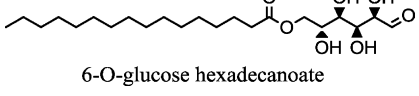
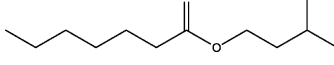
For enzymatic synthesis of glucose ester, Yu et al. [40] reported an increase in the enzymatic activity as the reaction temperature was raised from 35 to 45 °C. In this temperature range, the activation energy ( $E_a$ ) for the formation of the acyl-enzyme complex was estimated to be 52.9 kJ mol<sup>-1</sup> [40]. In comparison with this, the activation energy for the formation of the glucose monoester was only 19.4 kJ mol<sup>-1</sup>. In addition to affecting the reaction rate directly, the use of an elevated reaction temperature likely improves the relevant mass transfer rates.

Solubility of glucose in ethyl-methyl ketone is enhanced as the temperature is raised from 25 to 60 °C [17]. In the same temperature range, the solubility of the ester (glucose caprylate), also increases substantially from 2.98 to 69.3 mg mL<sup>-1</sup> [17]. The increased solubility makes the product removal by crystallization/precipitation difficult and this in turn shifts the reaction equilibrium towards hydrolysis. A consideration of how solubilities of the reactants and the product depend on temperature is required for deciding a suitable reaction temperature. Temperature dependence of dissolution kinetics of glucose and fructose in 2-methyl-2-butanol has been described [105].

In one study of enzyme mediated esterification, a 78% conversion of fructose to its palmitate ester was achieved in 72 h at 60 °C



**Table 3**  
Reaction solvent effects on yield of sugar esters in lipase catalyzed syntheses.

| Solvent   | Log <i>P</i> | Enzyme        | Yield (%) | Time (h) | Product  | Refs. |
|---|--------------|---------------|-----------|----------|--|-------|
| DMSO  | −1.30**      | CAL B 435     | 0         | 72       | <br>maltose dodecanoate       | [83]  |
| <i>tert</i> -Pentanol                                     | 1.30**       | CAL B 435     | 19        | 72       |  |       |
| n-Hexane  | 3.50**       | CAL B 435     | 0         | 72       |  |       |
| <i>tert</i> -Pentanol: DMSO (19:1, v/v)                   | 1.20**       | CAL B 435     | <80       | 72       |  |       |
| <i>tert</i> -Pentanol: DMSO (4:1, v/v)                    | 0.80**       | CAL B 435     | 39        | 72       |  |       |
| n-Hexane: acetonitrile (4:1, v/v)                         | <3.00**      | CAL B 435     | <4        | 72       |  |       |
| n-Hexane: 70% acetonitrile                                | 1.00**       | CAL B 435     | 11        | 72       | <br>mannose dodecanoate       | [139] |
| Acetonitrile  | −0.36**      | CAL B 435     | 59        | 30       |  |       |
| Acetone   | −0.26**      | CAL B 435     | 38        | 30       |  |       |
| <i>tert</i> -Butanol                                      | 0.35*        | CAL B 435     | 47        | 30       |  |       |
| 2 Methyl 2 butanol  | 0.89*        | CAL B 435     | 24        | 24       | <br>6-O-glucose dodecanoate   | [96]  |
| [Bmim][TfO]   | –            | Novozym 435   | 86        | 11       |  |       |
| [Bmim][Tf <sub>2</sub> N]                                 | –            | Novozym 435   | <20       | 11       |  |       |
| [Bmim][TfO]: [Bmim][Tf <sub>2</sub> N] (1:1, v/v)         | –            | Novozym 435   | 69        | 11       |  |       |
| [Bmim][TfO]: [Bmim][Tf <sub>2</sub> N] (3:1, v/v)         | –            | Novozym 435   | 82        | 11       | <br>6-O-glucose hexadecanoate | [95]  |
| [Bmim][PF <sub>6</sub> ]: <i>tert</i> -butanol (4:1, v/v) | –            | CAL B L2 C2   | 9         | 72       |  |       |
| [Bmim][PF <sub>6</sub> ]: <i>tert</i> -butanol (3:2, v/v) | –            | CAL B L2 C2   | 45        | 72       |  |       |
| Supercritical CO <sub>2</sub>                             | –            | Lipolase 100T | 37        | 12       |  |       |
| Supercritical CO <sub>2</sub>                             | –            | HPL           | 11        | 12       | <br>isoamyl heptanoate       | [45]  |
| Supercritical CO <sub>2</sub>                             | –            | Novozym 435   | 47        | 12       |  |       |

Abbreviations: 1-butyl-3-methylimidazolium trifluoromethane sulfonate [Bmim][TfO]; 1-butyl-3-methylimidazolium bis (trifluoromethylsulfonyl)imide [Bmim][Tf<sub>2</sub>N]; 1-butyl-3-methyl imidazolium hexafluorophosphate [BMIM][PF<sub>6</sub>]; hog pancreas lipase (HPL); *Candida antarctica* lipase B (CALB).

\* Log *P* calculated online at Virtual Computational Chemistry Laboratory <http://www.vcclab.org/alogps/start.html>.

\*\* Log *P* values reported by Jia et al. [83].

[30]. Increasing the temperature to 70 °C, reduced the conversion dramatically to only 1.3% after 72 h because of thermal deactivation of the enzyme and the increased solubility of the sugar ester (Table 4). At temperatures of above 90 °C, the deactivation enthalpy of the enzyme ( $107.8 \times 10^3 \text{ kJ mol}^{-1}$ ) exceeded the activation energy ( $67.5 \times 10^3 \text{ kJ mol}^{-1}$ ) [30].

In lipase catalyzed synthesis of glucose esters of short chain fatty acids such as caprylic acid, best conversion was attained by keeping the reaction temperature between 35 and 45 °C. In this range of temperature the solubility of the product was low and it could be removed from the reaction mixture by precipitation. If the reaction involves long chain fatty acids, the temperature can be raised to 60 °C [17]. Thus the optimal temperature of the reaction depends on the carbon chain length of the fatty acid molecules being reacted [44]. Clearly, the temperature for the optimal stability of the enzyme is not necessarily optimal for the reaction (Table 4). An empirical case-by-case evaluation is necessary within the 30–80 °C range to establish the optimal operating temperature for a given combination of the solvent, the enzyme, and the reactants.

## 6. Effects of water activity

In lipase catalyzed production of sugar esters, the activity of water in the nonaqueous reaction medium is an important consideration. Ester formation itself does not require water, but a minimal amount of water is necessary for hydration of the enzyme, its stability and catalytic activity [10,106]. Water is also a product of the esterification reaction. An accumulation of water produced by the reaction forces the reaction equilibrium towards hydrolysis, instead of towards ester synthesis. The amount of water also influences the activity and the selectivity of the enzyme. The amount of water must remain at extremely low levels for ester synthesis to occur (Table 5). This necessitates the use of nonaqueous reaction solvents.

The effect of water is sometimes discussed in terms of its concentration, but it is the thermodynamic water activity that actually influences the reaction equilibrium [15,47,107–111]. In a reaction mixture with multiple phases in equilibrium, the water activity in all the phases is identical, but not the water concentration. The activity of water ( $a_w$ ) in a solvent is given by the following equation:

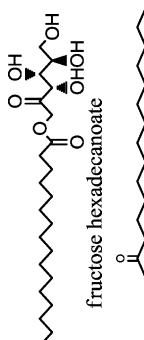
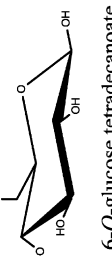
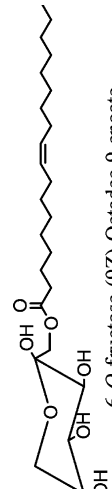
$$a_w = \frac{f_w \gamma_w x_w}{f_w^0} = [\text{H}_2\text{O}] a_f = \gamma_w x_w \quad (1)$$

where  $f_w$  and  $f_w^0$  are the fugacity of water in solvent and in pure state,  $a_f$  is the activity factor,  $\gamma_w$  is the activity coefficient and  $x_w$  is the mole fraction of water in the solvent respectively [111].

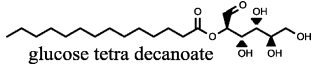
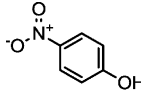
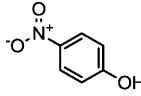
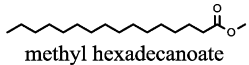
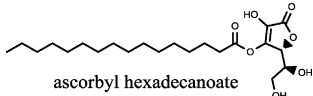
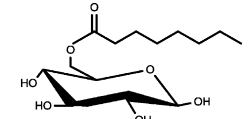
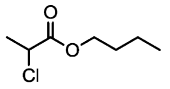
As the synthetic reaction produces water, any strategy to favor synthesis over hydrolysis requires a continuous removal of the water from the reaction [10,112,113]. As nucleophile for the hydrolysis reaction, water is also a competitive inhibitor of the lipase-catalyzed synthesis of sugar esters in organic media [39,44,47,70,79,107,108,114–119].

Various strategies have been used to limit the amount of water in the reaction medium [6,15,17,22,60,113,120–123]. Water may be removed continuously by bleeding a portion of the solvent from the reaction system, regenerating it by distillation and recycling it [6,17,60,122]. Pervaporation [120,121] and microwave irradiation [22,123] have also been used for water removal. Another way of controlling the water activity is to equilibrate the reaction medium with a saturated salt solution of known water activity [81]. This could be done either prior to the reaction to adjust the initial water activity, or during the reaction by continuously contacting the reaction medium with the saturated salt solution via a silicon membrane [124].

**Table 4**  
Effect of temperature on yield of sugar esters.

| Temperature (°C) | Enzyme      | Time (h) | Yield (%)            | Product   | Refs. |
|------------------|-------------|----------|----------------------|---|-------|
| 30               | Novozym 435 | 72       | 48                   | <br>fructose hexadecanoate             | [30]  |
| 60               | Novozym 435 | 72       | 78                   |   | [95]  |
| 70               | Novozym 435 | 72       | 1.3                  |   |       |
| 40               | CAL-B       | 72       | 18                   |   |       |
|                  |             |          |                      | <br>6-O-glucose tetradecanoate         |       |
| 50               | CAL-B       | 72       | 60                   |   | [118] |
| 60               | CAL-B       | 72       | 11                   |   |       |
| 60               | Novozym 435 | 4        | 32 g L <sup>-1</sup> |   |       |
|                  |             |          |                      | <br>6-O-fructose-(9Z)-Octadec-9-enoate |       |
| 80               | Novozym 435 | 4        | 43 g L <sup>-1</sup> |   |       |

**Table 5**Effects of water activity ( $a_w$ ) or water content on initial rate and product yield.

| $a_w$                | H <sub>2</sub> O control technique                 | Time (h) | Enzyme                  | Initial rate                             | Yield (%)              | Product  | Refs. |
|----------------------|--|----------|-------------------------|--|------------------------|--|-------|
| 5 μL g <sup>-1</sup> | Preequilibration Mg(NO <sub>3</sub> ) <sub>2</sub> | 12       | Novozym 435             | 2 mmol h <sup>-1</sup> g <sup>-1</sup>   | 38                     | <br>glucose tetra decanoate         | [10]  |
|                      | Preequilibration Mg(NO <sub>3</sub> ) <sub>2</sub> | 1        |                         |  | 18                     |  |       |
|                      | Mol. sieve 4 Å                                     | 7        |                         | 3.9 mmol h <sup>-1</sup> g <sup>-1</sup> | 38 mg mL <sup>-1</sup> |  |       |
|                      | Equilibration CaCl <sub>2</sub>                    | 7        |                         | 2 mmol h <sup>-1</sup> g <sup>-1</sup>   | 18                     |  |       |
|                      | Equilibration CaSO <sub>4</sub>                    | 7        |                         |  | >5                     |  |       |
| 0.79                 | Untreated  | N.G.     | <i>C. rugosa</i> lipase | 840 units                                | 1 fold                 | <br>p-nitrophenol                   | [22]  |
| N.G.                 | pH-tuned   |          |                         | 1995 units                               | 2.4 fold               | <br>p-nitrophenol                   |       |
|                      | pH-tuned + TPP                                     |          | 3247 units              | 3.8 fold                                 |                        |  |       |
|                      | pH-tune + TPP+ MW                                  | 10 s     | 4514 units              | 5.4 fold                                 |                        |  |       |
| 0.07                 | Saturated salts equilibration                      | 35       | Novozym 435             | 18 g L <sup>-1</sup> h <sup>-1</sup>     | N.G.                   | <br>methyl hexadecanoate            | [47]  |
| 0.58                 |  |          |                         | 5 g L <sup>-1</sup> h <sup>-1</sup>      |                        | <br>ascorbyl hexadecanoate          |       |
| 0.07                 |  |          |                         | 5.8 g L <sup>-1</sup> h <sup>-1</sup>    |                        |  |       |
| 0.78                 |  |          |                         | 1 g L <sup>-1</sup> h <sup>-1</sup>      |                        |  |       |
| N.G.                 | Azeotropic distillation                            | N.G.     | CAL-B EP100             | N.G.                                     | ~76                    | <br>6- <i>O</i> -glucose octanoate | [60]  |
|                      | Without distillation                               |          |                         |  | 50                     |  |       |
| 0.1%                 | Pervaporation                                      | N.G.     | <i>C. rugosa</i> lipase | N.G.                                     | 6.3                    | <br>butyl 2-chloropropanoate      | [120] |
| 0.5%                 |  |          |                         |  | 36.6                   |  |       |
| 0.6%                 |  |          |                         |  | 25.4                   |  |       |

TPP: three phase partitioning, MW: microwave irradiation, N.G.: data not given.



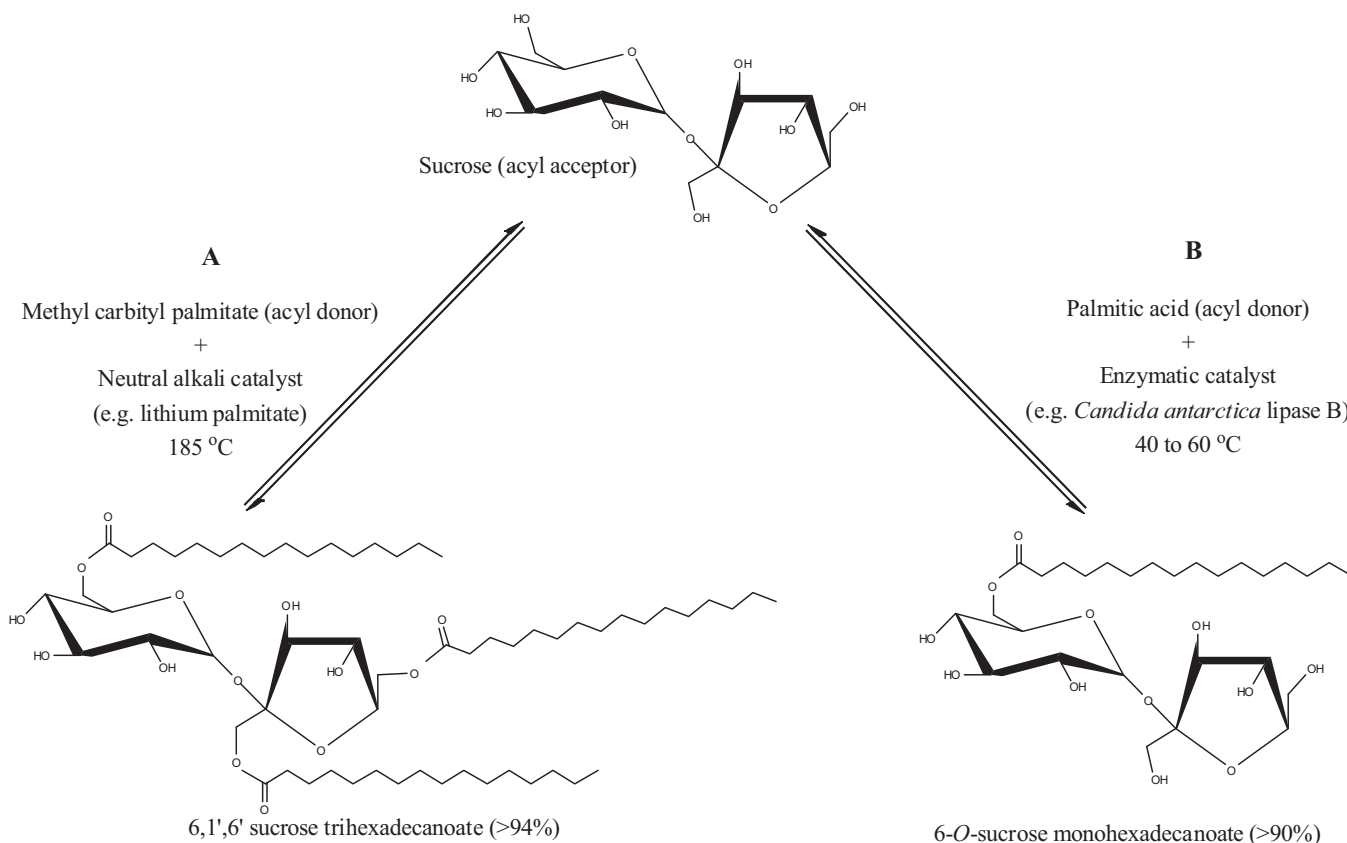


Fig. 2. Comparison of (A) chemical and (B) enzymatic syntheses of sugar esters.

Two-phase solvent systems (e.g. reverse micelles) have been effectively used for water removal [15,112,125]. Water may be removed also by using molecular sieves [10,27,48,90,126], but this method requires replacement of the sieves before they become saturated with water. Molecular sieves of 4 Å pore size have been reported to have a superior water removal capability compared to adsorbing agents such as zeolite and molecular sieves of a 3 Å pore size [10,48]. The efficacy of the molecular sieves depends on the reaction solvent used and the sieves have been suggested to have a detrimental effect on the enzyme catalyst [124,127]. In a reaction mixture at equilibrium, a dramatic increase in the rate of synthesis was observed on addition of a water adsorbent material [10].

In synthesis of sugar esters, the conversion yield and the initial reaction rate have been reduced by an increase of water activity to >0.6 [107]. In one study, the maximum yield of the product was reported at an initial water activity of 0.23 [60]. The initial rate of the synthetic reaction was not affected by changes in the water concentration in reaction medium from 5 to 10  $\mu\text{L g}^{-1}$  [10]. A reduction in the initial rate of reaction occurred for water concentration values of <2  $\mu\text{L g}^{-1}$ . These observations reinforce the need for the water activity to be maintained within a certain range during the entire reaction in order to maximize the product yield [47,107,128,129]. Control of water activity in lipase catalyzed esterifications has been reviewed [112,113].

## 7. Chemical versus enzymatic synthesis

Sugar fatty acid esters can be made also via the nonenzymatic chemical synthesis and, therefore, a comparison of the chemical and enzymatic routes is pertinent.

Industrial synthesis of sugar esters of glucose, fructose and sucrose is performed by trans-esterification of the methyl esters of the corresponding fatty acid in presence of a basic or metallic

catalyst. This reaction normally requires a temperature of >100 °C and a reduced pressure [130]. For example, Liu et al. [131] reported the synthesis of a sucrose ester, achieving a final yield of nearly 38% within 30 min of reaction at temperatures of 170–185 °C and reduced pressures of 133–400 Pa, using lithium oleate as catalyst. When sodium oleate and potassium palmitate were used as catalysts, the sucrose ester yield was lower at around 21% and 10%, respectively [131]. Sucrose ester could not be produced using lithium palmitate as a catalyst [131]. Martin [132] patented the use of a method to produce sugar esters at a reaction temperature of around 115 °C.

The use of high temperature in chemical synthesis implies a high energy cost for the overall production process. In addition, the chemical process requires difficult and multistep separations. The esters synthesized by such high-temperature processes are contaminated with undesirable byproducts and commonly contain a heterogeneous mixture of products of different degrees of esterification and different positions of acylation (Fig. 2) [130,131]. For example, in chemical processing there is difficulty in achieving regioselective acylation of sucrose due to a similar reactivity of the three primary and the eight secondary hydroxyl groups [130]. In addition there is the problem of intramolecular migration of the acyl group during processing [130]. Intramolecular migration can of course be prevented by protection and deprotection but this complicates the synthesis [130,141]. In comparison to chemical catalysis, enzymatic sugar ester synthesis is a one-step process that does not typically involve protection/deprotection of the hydroxyl groups [141].

Enzymatic synthesis offers a low-energy (e.g. reaction temperatures of 40–60 °C) and environmentally benign alternative to chemical synthesis and has been widely reported [1,5,6,10,17,30,133–137,59,138,139]. Enzymatic route offers a high degree of chemo-, regio-, enantio- and diastereoselectivity. The

product is typically a monoester (Fig. 2), although traces of diesters may occur. A relatively simple product mixture simplifies further downstream purification. The enzymatic route can achieve high yields. For example, Ferrer et al. [3] reported a conversion yield of about 98% for 6-O-laurylsucrose at 40 °C using immobilized *T. lanuginosus* lipase. The reaction required 12 h.

Hazardous solvents such as pyridine and dimethyl formamide (DMF) are the norm in chemical catalysis [132,140] and have been used also in enzymatic catalysis. Increasingly, this is changing especially in relation to enzymatic processes. Some of the catalysts used in chemical synthesis are potentially hazardous. For example, certain diatomaceous earth catalysts [130], if improperly handled, have the potential to cause pneumoconiosis.

## 8. Concluding remarks

Overcoming the challenges posed by lipase catalyzed esterification can improve access to many useful products including biosurfactants, drug-carriers, flavor esters, cosmetics and fragrance esters [12]. The need persists for suitable nonaqueous and safe solvents for use in this reaction. Ionic liquids and supercritical fluids provide new opportunities. Lipases themselves may be improved by protein engineering [25,75,143–147]. Rational design of lipases remains largely unexplored, but has the potential for enhancing the enzyme thermostability, improving its solvent tolerance, increasing its specificity and heightening its activity. Performance of existing lipases can be enhanced by operational methods such as ultrasonication [98,148–150] and microwave irradiation [22,123,149]. *In situ* control of water activity continues to demand novel solutions.

## References

- [1] Chang SW, Shaw JF. Biocatalysis for the production of carbohydrate esters. *New Biotechnology* 2009;26:109–16.
- [2] Coulon D, Ghoul M. The enzymatic synthesis of non-ionic surfactants: the sugar esters – an overview. *Agro Food Industry Hi-Tech* 1998;9:22–6.
- [3] Ferrer M, Soliveri J, Plou FJ, López-Cortés N, Reyes-Duarte D, Christensen M, et al. Synthesis of sugar esters in solvent mixtures by lipases from *Thermomyces lanuginosus* and *Candida antarctica* B, and their antimicrobial properties. *Enzyme and Microbial Technology* 2005;36:391–8.
- [4] Furukawa S, Akiyoshi Y, O'Toole GA, Ogihara H, Morinaga Y. Sugar fatty acid esters inhibit biofilm formation by food-borne pathogenic bacteria. *International Journal of Food Microbiology* 2010;138:176–80.
- [5] Queneau Y, Chambert S, Besset C, Cheaib R. Recent progress in the synthesis of carbohydrate-based amphiphilic materials: the examples of sucrose and isomaltulose. *Carbohydrate Research* 2008;343:1999–2009.
- [6] Yan Y. Enzymatic production of sugar fatty acid esters. Germany: University of Stuttgart; Ph.D. Thesis; 2001.
- [7] Puterka GJ, Farone W, Palmer T, Barrington A. Structure-function relationships affecting the insecticidal and miticidal activity of sugar esters. *Journal of Economic Entomology* 2003;96:636–44.
- [8] Schiefelbein L, Keller M, Weissmann F, Lubert M, Bracher F, Frie W. Synthesis, characterization and assessment of suitability of trehalose fatty acid esters as alternatives for polysorbates in protein formulation. *European Journal of Pharmaceutics and Biopharmaceutics* 2010;76:342–50.
- [9] Bromann R, König B, Fischer L. Regioselective synthesis of sugar esters without catalyst using alpha-hydroxycarboxylic acids. *Synthetic Communications* 1999;29:951–7.
- [10] Cauglia F, Canepa P. The enzymatic synthesis of glucosylmyristate as a reaction model for general considerations on 'sugar esters' production. *Biore-source Technology* 2008;99:4065–72.
- [11] Adachi S, Kobayashi T. Synthesis of esters by immobilized-lipase-catalyzed condensation reaction of sugars and fatty acids in water-miscible organic solvent. *Journal of Bioscience and Bioengineering* 2005;99:87–94.
- [12] Divakar S, Manohar B. Use of lipases in the industrial production of esters. *Industrial Enzymes* 2007:283–300.
- [13] Karmee SK. Lipase catalyzed synthesis of ester based surfactants from biomass derivatives. *Biofuels, Bioproducts and Biorefining* 2008;2:144–54.
- [14] Hernandez-Fernandez FJ, de los Rios AP, Lozano-Blanco LJ, Godínez C. Biocatalytic ester synthesis in ionic liquid media. *Journal of Chemical Technology and Biotechnology* 2010;85:1423–35.
- [15] Lortie R. Enzyme catalyzed esterification. *Biotechnology Advances* 1997;15:1–15.
- [16] Loughlin WA. Biotransformations in organic synthesis. *Biore-source Technology* 2000;74:49–62.
- [17] Yan Y, Bornscheuer UT, Stadler G, Lutz-Wahl S, Reuss M, Schmid RD. Production of sugar fatty acid esters by enzymatic esterification in a stirred-tank membrane reactor: optimization of parameters by response surface methodology. *Journal of the American Oil Chemists' Society* 2001;78:147–53.
- [18] Kennedy JF, Kumar H, Panesar PS, Marwaha SS, Goyal R, Parmar A, et al. Enzyme catalyzed regioselective synthesis of sugar esters and related compounds. *Journal of Chemical Technology and Biotechnology* 2006;81:866–76.
- [19] Ghanem A. Trends in lipase-catalyzed asymmetric access to enantiomerically pure/enriched compounds. *Tetrahedron* 2007;63:1721–54.
- [20] Sharma R, Chisti Y, Banerjee UC. Production, purification, characterization, and applications of lipases. *Biotechnology Advances* 2001;19:627–62.
- [21] Secundo F, Carrea G, Tarabiono C, Gatti-Lafranconi P, Brocca S, Lotti M, et al. The lid is a structural and functional determinant of lipase activity and selectivity. *Journal of Molecular Catalysis B: Enzymatic* 2006;39:166–70.
- [22] Saifuddin N, Raziah AZ. Enhancement of lipase enzyme activity in non-aqueous media through rapid three phase partitioning and microwave irradiation. *e-Journal of Chemistry* 2008;5:864–71.
- [23] Tejo BA, Salleh AB, Pleiss J. Structure and dynamics of *Candida rugosa* lipase: the role of organic solvent. *Journal of Molecular Modeling* 2004;10:358–66.
- [24] Cajal Y, Svendsen A, Girona V, Patkar SA, Alsina MA. Interfacial control of lid opening in *Thermomyces lanuginosus* lipase. *Biochemistry* 2000;39:413–23.
- [25] Magnusson AO, Rotticci-Mulder JC, Santagostino A, Hult K. Creating space for large secondary alcohols by rational redesign of *Candida antarctica* lipase B. *European Journal of Chemical Biology* 2005;6:1051–6.
- [26] Juhl PB, Doderer K, Hollmann F, Thum O, Pleiss J. Engineering of *Candida antarctica* lipase B for hydrolysis of bulky carboxylic acid esters. *Journal of Biotechnology* 2010;150:474–80.
- [27] Tsuzuki W, Kitamura Y, Suzuki T, Kobayashi S. Synthesis of sugar fatty acid esters by modified lipase. *Biotechnology and Bioengineering* 1999;64:267–71.
- [28] Lee SB, Kim KJ. Effect of water activity on enzyme hydration and enzyme reaction rate in organic solvents. *Journal of Fermentation and Bioengineering* 1995;79:473–8.
- [29] Cabrera Z, Gutarra MLE, Guisan JM, Palomo JM. Highly enantioselective biocatalysts by coating immobilized lipases with polyethyleneimine. *Catalysis Communications* 2010;11:964–7.
- [30] Sabeder S, Habulin M, Knez Z. Lipase-catalyzed synthesis of fatty acid fructose esters. *Journal of Food Engineering* 2006;77:880–6.
- [31] Shu ZY, Jiang H, Lin RF, Jiang YM, Lin L, Huang JZ. Technical methods to improve yield, activity and stability in the development of microbial lipases. *Journal of Molecular Catalysis B: Enzymatic* 2010;62:1–8.
- [32] Treichel H, de Oliveira D, Mazutti MA, Di Luccio M, Oliveira JV. A review on microbial lipases production. *Food and Bioprocess Technology* 2010;3:182–96.
- [33] Contesini FJ, Lopes DB, Macedo GA, Nascimento MG, Carvalho PO. *Aspergillus* sp. lipase: potential biocatalyst for industrial use. *Journal of Molecular Catalysis B: Enzymatic* 2010;67:163–71.
- [34] Guncheva M, Zhiryakova D. Catalytic properties and potential applications of *Bacillus* lipases. *Journal of Molecular Catalysis B: Enzymatic* 2011;68:1–21.
- [35] Krishna SH, Karanth NG. Lipases and lipase-catalyzed esterification reactions in nonaqueous media. *Catalysis Reviews* 2002;44:499–591.
- [36] Rodrigues RC, Fernandez-Lafuente R. Lipase from *Rhizomucor miehei* as an industrial biocatalyst in chemical process. *Journal of Molecular Catalysis B: Enzymatic* 2010;64:1–22.
- [37] Singh M, Singh S, Singh RS, Chisti Y, Banerjee UC. Transesterification of primary and secondary alcohols using *Pseudomonas aeruginosa* lipase. *Biore-source Technology* 2008;99:2116–20.
- [38] Alhir S, Manjrekajis S, Chandan R. Lipase of *Penicillium caseicolum*. *Journal of Agric and Food Chemistry* 1990;38:598–601.
- [39] Boutur O, Dubreucq E, Galzy P. Factors influencing ester synthesis catalysed in aqueous media by the lipase from *Candida deformans* (zach) langeron and guerra. *Journal of Biotechnology* 1995;42:23–33.
- [40] Yu J, Zhang J, Zhao A, Ma X. Study of glucose ester synthesis by immobilized lipase from *Candida* sp. *Catalysis Communications* 2008;9:1369–74.
- [41] Hasan F, Shah AA, Hameed A. Methods for detection and characterization of lipases: a comprehensive review. *Biotechnology Advances* 2009;27:782–98.
- [42] Anderson EM, Larsson KM, Kirk O. One biocatalyst – Many applications: the use of *Candida antarctica* B-lipase in organic synthesis. *Biocatalysis Biotransformation* 1998;16:181–204.
- [43] Cao L, Bornscheuer UT, Schmid RD. Lipase-catalyzed solid-phase synthesis of sugar esters. Influence of immobilization on productivity and stability of the enzyme. *Journal of Molecular Catalysis B: Enzymatic* 1999;6:279–85.
- [44] Soultani S, Engasser J-M, Ghoul M. Effect of acyl donor chain length and sugar/acyl donor molar ratio on enzymatic synthesis of fatty acid fructose esters. *Journal of Molecular Catalysis B: Enzymatic* 2001;11:725–31.
- [45] Kumar R, Modak J, Madras G. Effect of the chain length of the acid on the enzymatic synthesis of flavours in supercritical carbon dioxide. *Biochemical Engineering Journal* 2005;23:199–202.
- [46] Séverac E, Galy O, Turon F, Pantel CA, Condoret JS, Monsan P, et al. Selection of Cal B immobilization method to be used in continuous oil transesterification: analysis of the economical impact. *Enzyme and Microbial Technology* 2010;48:61–70.

- [47] Humeau C, Girardin M, Rovel B, Miclo A. Effect of the thermodynamic water activity and the reaction medium hydrophobicity on the enzymatic synthesis of ascorbyl palmitate. *Journal of Biotechnology* 1998;63:1–8.
- [48] Tarahomjoo S, Alemzadeh I. Surfactant production by an enzymatic method. *Enzyme and Microbial Technology* 2003;33:33–7.
- [49] Salem JH, Humeau C, Chevalot I, Harscoat-Schiavo C, Vanderesse R, Blanchard F, et al. Effect of acyl donor chain length on isoquercitrin acylation and biological activities of corresponding esters. *Process Biochemistry* 2010;45:382–9.
- [50] Adelhorst K, Fredrik B, Godtfredsen SE, Kirk O. Enzyme catalysed preparation of 6-O-acetylglucopyranosides. *Synthesis* 1990;2:112–5.
- [51] De Goede A, Oosterom MV, Van Deurzen MPJ, Sheldon RA, Bekkum HV, Rantwijk FV. Selective lipase-catalyzed esterification of alkyl glycosides. *Biocatalysis and Biotransformation* 1994;9:145–55.
- [52] Oguntimain GB, Erdmann H, Schmid RD. Lipase catalyzed synthesis of sugar ester in organic solvents. *Biotechnology Letters* 1993;15:175–80.
- [53] Schlottbeck A, Lang S, Wray V, Wagner F. Lipase-catalyzed monoacylation of fructose. *Biotechnology Letters* 1993;15:61–4.
- [54] Pulido R, López FO, Gotor V. Enzymatic regioselective acylation of hexoses and pentoses using oxime esters. *Journal of the American Chemical Society* 1992;114:2981–8.
- [55] Therisod M, Klivanov AM. Facile enzymatic preparation of monoacylated sugars in pyridine. *Journal of the American Chemical Society* 1986;108:5638–40.
- [56] Chenevert R, Pelchat N, Jacques F. Stereoselective enzymatic acylations (transesterifications). *Current Organic Chemistry* 2006;10:1067–94.
- [57] Cao L, Fischer A, Bornscheuer UT, Schmid RD. Lipase-catalyzed solid phase synthesis of sugar fatty acid esters. *Biocatalysis and Biotransformations* 1997;14:262–9.
- [58] Cao L, Bornscheuer UT, Schmid RD. Lipase-catalyzed solid-phase synthesis of sugar esters IV: selectivity of lipases towards primary and secondary hydroxyl groups in carbohydrates. *Biocatalysis and Biotransformation* 1998;16:249–57.
- [59] Sharma A, Chattopadhyay S. Lipase catalysed acylation of carbohydrates. *Biotechnology Letters* 1993;15:1145–93.
- [60] Yan Y, Bornscheuer UT, Cao L, Schmid RD. Lipase-catalyzed solid-phase synthesis of sugar fatty acid esters: removal of byproducts by azeotropic distillation. *Enzyme and Microbial Technology* 1999;25:725–8.
- [61] Tsuzuki W, Kitamura Y, Suzuki T, Mase T. Effects of glucose on lipase activity. *Bioscience, Biotechnology and Biochemistry* 1999;63:1467–70.
- [62] Zhang W, Wang Y, Hayat K, Zhang X, Shabbar A, Feng B, et al. Efficient lipase-selective synthesis of dilauryl mannoses by simultaneous reaction–extraction system. *Biotechnology Letters* 2009;31:423–8.
- [63] Klivanov AM. Asymmetric transformations catalysed by enzymes in organic solvents. *Accounts of Chemical Research* 1990;23:114–20.
- [64] Sakurai T, Margolin AL, Russell AJ, Klivanov AM. Control of enzyme enantioselectivity by the reaction medium. *Journal of the American Chemical Society* 1988;110:7236–7.
- [65] Wescott CR, Klivanov AM. The solvent dependence of enzyme specificity. *Biochimica et Biophysica Acta* 1994;1206:1–9.
- [66] Liu Y, Wang F, Tan T. Effects of alcohol and solvent on the performance of lipase from *Candida* sp. in enantioselective esterification of racemic ibuprofen. *Journal of Molecular Catalysis B: Enzymatic* 2009;56:126–30.
- [67] Hudson EP, Eppler RK, Clark DS. Biocatalysis in semi-aqueous and nearly anhydrous conditions. *Current Opinion in Biotechnology* 2005;16:637–43.
- [68] Rubio E, Fernandez-Mayorales A, Klivanov AM. Effects of solvents on enzyme regioselectivity. *Journal of American Chemical Society* 1991;113:695–6.
- [69] Paula AV, Barboza JC, Castro HF. Study of the influence of solvent, carbohydrate and fatty acid in the enzymatic synthesis of sugar esters by lipases. *Química Nova* 2005;28:792–6.
- [70] Affleck R, Haynes CA, Clark DS. Solvent dielectric effects on protein dynamics. *Proceedings of the National Academy of Sciences of the United States America* 1992;89:167–70.
- [71] Affleck R, Xu ZF, Suzawa V, Focht K, Clark DS, Dordick JS. Enzymatic catalysis and dynamics in low water environments. *Proceedings of the National Academy of Sciences of the United States America* 1992;89:1100–4.
- [72] Xu ZF, Attleck R, Wangikar P, Suzawa V, Dordick JS, Clark DS. Transition state stabilization of subtilisin in organic media. *Biotechnology and Bioengineering* 1994;43:515–20.
- [73] Ryu K, Dordick JS. Free energy relationships of substrate and solvent hydrophobicities with enzymatic catalysis in organic media. *Journal of the American Chemical Society* 1989;111:8026–7.
- [74] Lu J, Nie K, Wang F, Tan T. Immobilized lipase *Candida* sp 99-125 catalyzed methanolysis of glycerol trioleate: Solvent effect. *Bioresource Technology* 2008;99:6070–4.
- [75] Akoh CC, Mutua LM. Synthesis of alkyl glucoside fatty acid esters: effect of reaction parameters and the incorporation of n-3 polyunsaturated fatty acids. *Enzyme and Microbial Technology* 1994;16:115–9.
- [76] Ghatore AS, Guerra MJ, Bell G, Halling PJ. Immiscible organic solvent inactivation of urease, chymotrypsin, lipase, and ribonuclease: separation of dissolved solvent and interfacial effects. *Biotechnology and Bioengineering* 1994;44:1355–61.
- [77] Narayan VS, Klivanov AM. Are water immiscibility and apolarity of the solvent relevant to enzyme efficiency? *Biotechnology and Bioengineering* 1993;41:390–3.
- [78] Valivety RH, Halling PJ, Peilow AD, Macrae AR. Relationship between water activity and catalytic activity of lipases in organic media. effects of supports, loading and enzyme preparation. *European Journal of Biochemistry* 1994;222:461–6.
- [79] Brink LES, Tramper J. Optimization of organic solvent in multiphase biocatalysis. *Biotechnology and Bioengineering* 1985;27:1258–69.
- [80] Akkara JA. Enzymatic synthesis and modification of polymers in nonaqueous solvents. *Trends in Biotechnology* 1999;17:67–73.
- [81] Degn P, Zimmermann W. Optimization of carbohydrate fatty acid ester synthesis in organic media by a lipase from *Candida antarctica*. *Biotechnology and Bioengineering* 2001;74:483–91.
- [82] Oosterom WM, van Rantwijk F, Sheldon RA. Regioselective acylation of disaccharides in t-butyl alcohol catalysed by *Candida antarctica* lipase. *Biotechnology and Bioengineering* 1996;49:328–33.
- [83] Jia C, Zhao J, Feng B, Zhang X, Xia W. A simple approach for the selective enzymatic synthesis of dilauryl maltose in organic media. *Journal of Molecular Catalysis B: Enzymatic* 2010;62:265–9.
- [84] Chopineau J, McCafferty FD, Therisod M, Klivanov AM. Production of bio-surfactants from sugar alcohols and vegetable oils catalyzed by lipases in a nonaqueous medium. *Biotechnology and Bioengineering* 1988;31:208–14.
- [85] Degn P, Pedersen LH, Duus J, Zimmermann W. Lipase-catalysed synthesis of glucose fatty acid esters in tertbutanol. *Biotechnology Letters* 1999;21:275–80.
- [86] Janssen AEM, Klabbers C, Franssen MCR, Reijt KV. Enzymatic synthesis of carbohydrate esters in 2-pyrrolidone. *Enzyme Microbial Technology* 1991;13:565–71.
- [87] Lambriani A. Understanding the formation of sugar fatty acid esters. North Carolina: University of North Carolina, M.Sc. Dissertation; 2006.
- [88] Riva S, Chopineau J, Kieboom APG, Klivanov AM. Protease-catalyzed regioselective esterification of sugars and related compounds in anhydrous dimethylformamide. *Journal of American Chemical Society* 1988;110:584–9.
- [89] Park O-J, Park HG, Yang J-W. Enzymatic trans-esterification of monosaccharides and amino acid esters in organic solvents. *Biotechnology Letters* 1996;18:473–8.
- [90] Adnani A, Basri M, Chaibakhsh N, Salleh A, Rahman M. Lipase-catalyzed synthesis of a sugar alcohol-based nonionic surfactant. *Asian Journal of Chemistry* 2011;23:388–92.
- [91] Paradkar VM, Dordick JS. Aqueous-like activity of alphachymotrypsin dissolved in nearly anhydrous organic solvents. *Journal of the American Chemical Society* 1994;116:5009–10.
- [92] Xie J, Hsieh YL. Enzyme catalyzed transesterification of vinyl esters on cellulose solids. *Journal of Polymer Science Part A: Polymer Chemistry* 2001;39:1931–9.
- [93] Chen Z, Zong M, Gu Z. Enzymatic synthesis of sugar esters in ionic liquids. *Chinese Journal of Organic Chemistry* 2007;27:1448–52.
- [94] Fan Y, Qian J. Lipase catalysis in ionic liquids/supercritical carbon dioxide and its applications. *Journal of Molecular Catalysis B: Enzymatic* 2010;66:1–7.
- [95] Ganske F, Bornscheuer UT. Lipase-catalyzed glucose fatty acid ester synthesis in ionic liquids. *Organic Letters* 2005;7:3097–8.
- [96] Lee SH, Ha SH, Hiep NM, Chang W-J, Koo Y-M. Lipase-catalyzed synthesis of glucose fatty acid ester using ionic liquids mixtures. *Journal of Biotechnology* 2008;133:486–9.
- [97] Park S, Kazlauskas RJ. Improved preparation and use of room-temperature ionic liquids in lipase-catalyzed enantio- and regioselective acylations. *The Journal of Organic Chemistry* 2001;66:8395–401.
- [98] Lee SH, Nguyen HM, Koo YM, Ha SH. Ultrasound-enhanced lipase activity in the synthesis of sugar ester using ionic liquids. *Process Biochemistry* 2008;43:1009–12.
- [99] Moniruzzaman M, Nakashima K, Kamiya N, Goto M. Recent advances of enzymatic reactions in ionic liquids. *Biochemical Engineering Journal* 2010;48:295–314.
- [100] Fort DA, Remsing RC, Swatloski RP, Moyna P, Moyna G, Rogers RD. Can ionic liquids dissolve wood? Processing and analysis of lignocellulosic materials with 1-n-butyl-3-methylimidazolium chloride. *Green Chemistry* 2006;9:63–9.
- [101] Habulin M, Sabeder S, Paljevac M, Primožic M, Knez Z. Lipase-catalyzed esterification of citronellol with lauric acid in supercritical carbon dioxide/co-solvent media. *The Journal of Supercritical Fluids* 2007;43:199–203.
- [102] Lozano P, Villora G, Gomez D, Gayo AB, Sánchez-Conesa JA, Rubio M, et al. Membrane reactor with immobilized *Candida antarctica* lipase B for ester synthesis in supercritical carbon dioxide. *The Journal of Supercritical Fluids* 2004;29:121–8.
- [103] Yoshida Y, Kimura Y, Kadota M, Tsuno T, Adachi S. Continuous synthesis of alkyl ferulate by immobilized *Candida antarctica* lipase at high temperature. *Biotechnology Letters* 2006;28:1471–4.
- [104] Ljunger G, Adlercreutz P, Mattiasson B. Enzymatic synthesis of octyl-[beta]-glucoside in octanol at controlled water activity. *Enzyme and Microbial Technology* 1994;16:751–5.
- [105] Engasser JM, Chamoulaeu F, Chebil L, Ghoul M. Kinetic modeling of glucose and fructose dissolution in 2-methyl-2-butanol. *Biochemical Engineering Journal* 2008;42:159–65.
- [106] Halling PJ. What can we learn by studying enzymes in non-aqueous media. *Philosophical Transactions of the Royal Society of the Biological Sciences B: London* 2004;359:1287–96.

- [107] Chamouleau F, Coulon D, Girardin M, Ghoul M. Influence of water activity and water content on sugar esters lipase-catalyzed synthesis in organic media. *Journal of Molecular Catalysis B: Enzymatic* 2001;11:949–54.
- [108] Cheng Y-C, Tsai S-W. Effects of water activity and alcohol concentration on the kinetic resolution of lipase-catalyzed acyl transfer in organic solvents. *Enzyme and Microbial Technology* 2003;32:362–8.
- [109] Halling PJ. Thermodynamic predictions for biocatalysis in nonconventional media: theory, tests, and recommendations for experimental design and analysis. *Enzyme and Microbial Technology* 1994;16:178–206.
- [110] Halling PJ. Biocatalysis in low-water media: understanding effects of reaction conditions. *Current Opinion in Chemical Biology* 2000;4:74–80.
- [111] Kang IJ, Pfromm PH, Rezac ME. Real time measurement and control of thermodynamic water activities for enzymatic catalysis in hexane. *Journal of Biotechnology* 2005;119:147–54.
- [112] Gandhi NN, Patil NS, Sawant SB, Joshi JB, Wangikar PP, Mukesh D. Lipase-catalyzed esterification. *Catalysis Reviews* 2000;42:439–80.
- [113] Rhee JS. Water activity control in lipase-catalyzed reaction system. *Journal of Microbiology and Biotechnology* 1998;8:191–6.
- [114] Arroyo M, Moreno J, Sinisterra J. Alteration of the activity and selectivity of immobilized lipases by the effect of the amount of water in the organic medium. *Journal of Molecular Catalysis A: Chemical* 1995;97:195–201.
- [115] Berendsen HJC, Postma JPM, Van Gunsteren WF, DiNola A, Haak JR. Molecular dynamics with coupling to an external bath. *Journal of Chemical Physics* 1984;81:3684.
- [116] Bhattacharyya SM, Wang ZG, Zewail AH. Dynamics of water near a protein surface. *Journal of Physical Chemistry B* 2003;107:13218–28.
- [117] Chowdary GV, Prapulla SG. The influence of water activity on the lipase catalyzed synthesis of butyl butyrate by transesterification. *Process Biochemistry* 2002;38:393–7.
- [118] Coulon D, Ismail A, Girardin M, Rovel B, Ghoul M. Effect of different biochemical parameters on the enzymatic synthesis of fructose oleate. *Journal of Biotechnology* 1996;51:115–21.
- [119] Jönsson Å, van Breukelen W, Wehtje E, Adlercreutz P, Mattiasson B. The influence of water activity on the enantioselectivity in the enzyme-catalyzed reduction of 2-pentanone. *Journal of Molecular Catalysis B: Enzymatic* 1998;5:273–6.
- [120] Bélafi-Bakó K, Dörm N, Ulbert O, Gubicza L. Application of pervaporation for removal of water produced during enzymatic esterification in ionic liquids. *Desalination* 2002;149:267–8.
- [121] Sakaki K, Aoyama A, Nakane T, Ikegami T, Negishi H, Watanabe K, et al. Enzymatic synthesis of sugar esters in organic solvent coupled with pervaporation. *Desalination* 2006;193:260–6.
- [122] Yan Y, Bornscheuer UT, Schmid RD. Efficient water removal in lipase catalyzed esterifications using a low boiling point azeotrope. *Biotechnology and Bioengineering* 2002;78:31–4.
- [123] Yu D, Tian L, Ma D, Wu H, Wang Z, Wang L, et al. Microwave-assisted fatty acid methyl ester production from soybean oil by Novozym 435. *Green Chemistry* 2010;12:844–50.
- [124] Wehtje E, Kaur J, Adlercreutz P, Chand S, Mattiasson B. Water activity control in enzymatic esterification processes. *Enzyme and Microbial Technology* 1997;21:502–10.
- [125] Park O-J, Jeon G-J, Yang J-W. Protease-catalyzed synthesis of disaccharide amino acid esters in organic media. *Enzyme and Microbial Technology* 1999;25:455–62.
- [126] Zhang X, Adachi S, Watanabe Y, Kobayashi T, Matsuno R. Prediction of the equilibrium conversion for the synthesis of acyl hexose through lipase catalyzed condensation in water miscible solvent in the presence of molecular sieve. *Biotechnology Progress* 2003;19:293–7.
- [127] Wehtje E, Svensson I, Adlercreutz P, Mattiasson B. Continuous control of water activity during biocatalysis in organic media. *Biotechnology Letters* 1993;7:873–8.
- [128] Clara LA, Donya S, Alejandro GM. A new assay for lipase activity in organic solvents. Lipase-catalyzed synthesis of octyl-linolenate in a hexane microaqueous reaction system. *Enzyme and Microbial Technology* 1995;17:131–5.
- [129] Coulon D, Ismail A, Girardin M, Ghoul M. Enzymatic synthesis of alkylglycoside fatty acid esters catalyzed by an immobilized lipase. *Journal of Molecular Catalysis B: Enzymatic* 1998;5:45–8.
- [130] Ferrer M, Cruces MA, Plou FJ, Pastor E, Fuentes G, Bernabé M, et al. Chemical versus enzymatic catalysis for the regioselective synthesis of sucrose esters of fatty acids. In: Avelino Corma FVMSM, José Luis GF, editors. *Studies in Surface Science and Catalysis*, vol. 130. Elsevier; 2000. p. 509–14.
- [131] Liu X, Gong L, Xin M, Liu J. The synthesis of sucrose ester and selection of its catalyst. *Journal of Molecular Catalysis A: Chemical* 1999;147:37–40.
- [132] Martin JB. Method for preparing fatty esters of non-reducing oligosaccharides in the presence of pyridine. United States Patents: Procter and Gamble; 1958.
- [133] Patil DR, Rethwisch DG, Dordick JS. Enzymatic synthesis of a sucrose containing linear polyester in nearly anhydrous organic media. *Biotechnology and Bioengineering* 1991;37:639–46.
- [134] Pedersen NR, Wimmer R, Matthiesen R, Pedersen LH, Gessesse A. Synthesis of sucrose laurate using a new alkaline protease. *Tetrahedron: Asymmetry* 2003;14:667–73.
- [135] Carrea G, Riva S, Secundo F, Danieli B. Enzymatic synthesis of various 1 [prime or minute]-O-sucrose and 1-O-fructose esters. *Journal of the Chemical Society, Perkin Transactions* 1989;1:1057–61.
- [136] Pu MAO, Yong-mei X, Jun-hua LI, Jin-wei Y, Ling-bo QU. Research process in enzymatic synthesis of sucrose ester. Liaoning Chemical Industry; 2011.
- [137] Boeckh D, Hauer B, Häring D. Enzymatic synthesis of sugar acrylates: United States Patent, Patent No. US7,767,425B2, August 3, 2010.
- [138] Ward OP, Fang J, Li Z. Lipase-catalyzed synthesis of a sugar ester containing arachidonic acid. *Enzyme and Microbial Technology* 1997;20:52–6.
- [139] Watanabe Y, Miyawaki Y, Adachi S, Nakanishi K, Matsuno R. Equilibrium constant for lipase-catalyzed condensation of mannose and lauric acid in water-miscible organic solvents. *Enzyme and Microbial Technology* 2001;29:494–8.
- [140] Chauvin C, Baczko K, Plusquellec D. New highly regioselective reactions of unprotected sucrose. Synthesis of 2-O-acylsucroses and 2-O-(N-alkylcarbamoyl) sucroses. *Journal of Organic Chemistry* 1993;58:2291–5.
- [141] Arcos JA, Bernabé M, Otero C. Quantitative enzymatic production of 6-O-acylglucose esters. *Biotechnology and Bioengineering* 1998;57:505–9.
- [142] Fischer M, Pleiss J. The Lipase Engineering Database: a navigation and analysis tool for protein families. *Nucleic Acids Research* 2003;31:319.
- [143] Frenken LGJ, Egmond MR, Batenburg AM, Verrips CT. *Pseudomonas glumae* lipase: increased proteolytic stability by protein engineering. *Protein Engineering* 1993;6:637.
- [144] Kourist R, Brundiek H, Bornscheuer UT. Protein engineering and discovery of lipases. *European Journal of Lipid Science and Technology* 2010;112:64–74.
- [145] Rotticci D, Rotticci-Mulder JC, Denman S, Norin T, Hult K. Improved enantioselectivity of a lipase by rational protein engineering. *European Journal of Chemical Biology* 2001;2:766–70.
- [146] Svensson I, Hernández I, Virto M, de Renobales M. Determination of lipase activity in cheese using trivalerin as substrate. *International Dairy Journal* 2006;16:423–30.
- [147] Chisti Y. Sonobioreactors: using ultrasound for enhanced microbial productivity. *Trends in Biotechnology* 2003;21:89–93.
- [148] Rufino AR, Biaggio FC, Santos JC, De Castro HF. Screening of lipases for the synthesis of xylitol monoesters by chemoenzymatic esterification and the potential of microwave and ultrasound irradiations to enhance the reaction rate. *International Journal of Biological Macromolecules* 2010;47:5–9.
- [149] Xiao Y-M, Wu Q, Cai Y, Lin X-F. Ultrasound-accelerated enzymatic synthesis of sugar esters in nonaqueous solvents. *Carbohydrate Research* 2005;340:2097–103.

## CHAPTER 4

# Current application of controlled degradation processes in polymer modification and functionalization

---

**Ahmad Mohamad Gumel<sup>1</sup>, M. Suffian M. Annuar<sup>1\*</sup> and Thorsten Heidelberg<sup>2</sup>**

*<sup>1</sup>Institute of Biological Sciences, <sup>2</sup>Department of Chemistry*

*Faculty of Science, University of Malaya, 50603 Kuala Lumpur, Malaysia*

**Published:** *Journal of Applied Polymer Science* (2013) 129 (6) :3079-3088

(ISI cited publication: tier 2)

### Statement of contributions of joint Authorship

**Ahmad Mohammed Gumel:** (Candidate)

Writing and compilation of the review literature. Main author of the manuscript

**M. Suffian M. Annuar:** (Principal Supervisor)

Supervised and assisted with manuscript compilation, editing and co-author of the manuscript.

**Thorsten Heidelberg :** (Co-Supervisor)

Supervised and assisted with chemical analyses, structure elucidation and co-author of the manuscript

## Current Application of Controlled Degradation Processes in Polymer Modification and Functionalization

Ahmad Mohamad Gumel,<sup>1</sup> M. Suffian M. Annuar,<sup>1</sup> Thorsten Heidelberg<sup>2</sup>

<sup>1</sup>Institute of Biological Sciences, Faculty of Science, University of Malaya, 50603 Kuala Lumpur, Malaysia

<sup>2</sup>Department of Chemistry, Faculty of Science, University of Malaya, 50603 Kuala Lumpur, Malaysia

Correspondence to: M. S. M. Annuar (E-mail: suffian\_annuar@um.edu.my)

**ABSTRACT:** Ecological concerns over the accumulation of polymeric waste material and the demand for functionalized polymers in specialty applications have promoted extensive research on different controlled degradation processes and their use. The production of functionalized or modified polymers by conventional synthetic routes is expensive and time consuming. However, advances in degradation technology have become an enabling factor in the production of modified polymers and their functionalization. Mild irradiation, ozonization, and enzymatic routes are among the processes that have been explored for polymer modification. Biopolymers, such as chitosan, hyaluronic acids, and polyhydroxyalkanoates, are known to be suitable for a diverse number of applications, ranging from biomedical to organic-electronics. At the same time, their high molecular weight, crystallinity, and shelf degradability limit their utility. Controlled degradation processes can be used to prepare these types of polymers with reasonably low molecular weights and to generate radical species that help to stabilize these polymers or to initiate further beneficial reactions. In this article, we review the application of controlled degradation processes for polymer modification and functionalization. © 2013 Wiley Periodicals, Inc. *J. Appl. Polym. Sci.* 129: 3079–3088, 2013

**KEYWORDS:** applications; biodegradable; biopolymers and renewable polymers; degradation; functionalization of polymers

Received 21 October 2012; accepted 21 December 2012; published online 12 February 2013

DOI: 10.1002/app.39006

### INTRODUCTION

Polymers are being increasingly used for more and more diverse purposes; they are particularly important in food, cosmetics, and biomedical applications.<sup>1–3</sup> The rise in the utilization of polymers has health and (often negative) ecological implications, especially from biomedical and environmental perspectives. The demand for the control of the precise delivery targets for therapeutic drugs and the capability of polymeric drug carriers to release their drugs on an independent timescale is growing; polymeric waste disposal can cause severe environmental pollution when they are poorly degradable materials. Both of these warrant an intense research exploration into controlled degradation processes for polymer functionalization and modification. The recent momentum in the use of biodegradable polymers over nondegradable ones is among the measures taken toward environmental friendliness and an increase in the sophistication of biomedical applications. However, at present, most of these biodegradable polymers lack many of the attributes of their nondegradable counterparts. These issues are further compounded by the fact that the production of tailor-made or functionalized biodegradable polymers may be costly because of difficult synthetic steps that are often required for their

production. Although several approaches to the development of simpler and more cost-effective means to improve the quality of these biodegradable polymers, including dual biosynthesis<sup>4</sup> and blending,<sup>5</sup> have been reported, additional options need to be explored. In view of this, researchers have turned to the use of the opposite route of degradation processes to either improve the degradability of these important polymers or to customize the process for the production of specialty polymers for niche applications. Among recently reported methods have been the use of high-energy radiation,<sup>6</sup> ozonization,<sup>7</sup> ultrasonic irradiation,<sup>8</sup> microwave irradiation,<sup>9</sup> oxidation,<sup>10,11</sup> biodegradation,<sup>12</sup> and photodegradation.<sup>13</sup>

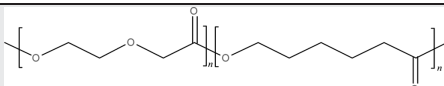
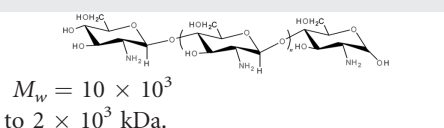
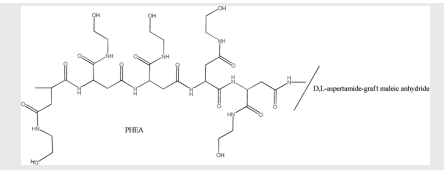
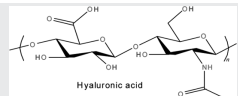
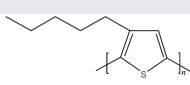
In this article, we review current research approaches in the application of controlled degradation processes as alternative and viable routes toward enhanced polymer degradation, modification, and functionalization. In most cases, the mechanisms and biochemistry of the degradation process are also presented.

### USE OF BIODEGRADATION AND ORGANOMODIFIERS

Biodegradation is known to be an effective method of completely removing degradable polymers and their constituents



**Table I.** Application of Controlled Degradation Processes for Polymer Degradation and/or Modification

| Degradation method                     | Degradation agent         | Polymer   | Application                              | Reference |
|--|---------------------------|---|--|-----------|
| Selective enzymatic degradation        | <i>Pseudomonas lipase</i> |   | Multifunctional polymers                 | 23        |
| Radiation induced partial degradation  | $\gamma$                  | <br>$M_w = 10 \times 10^3$<br>to $2 \times 10^3$ kDa.                       | Plant growth promoters                   | 50        |
| Radiation induced graft polymerization | $\gamma$                  | <br>PBLA<br>1,1'-bis(2-hydroxyethyl)-2,2'-bis(hydroxymethyl)ethane-1,2-diol | Pulsatile protein release                | 54        |
| Ozonization                            | Ozone                     | <br>Hyaluronic acid<br>$M_w = 1535-87$ kDa.                                  | Antioxidant and wound healing activities | 7         |
| Ozonization                            | Ozone                     |   | Improved electroconductivity             | 61 and 62 |

from the environment.<sup>14</sup> Several approaches have been developed that either employ the use of enzymes<sup>12,15,16</sup> or microbial consortia<sup>17-19</sup> to affect polymer degradation and modification. The metabolic degradation mechanism of polymers has been reported to use several enzymes, such as dehydrogenases, hydrolases, and oxidases, whereas the process is mostly based on either hydroxyl group oxidation to yield ketones or the hydrolysis of the carbonyl structure followed by the final mineralization of the components. The hydroxyl group oxidation is reported to be based on one of two steps, either the oxidation of one adjacent hydroxyl group to yield monoketone structure or the oxidation of two adjacent hydroxyl groups to form  $\beta$ -diketones structures.<sup>20</sup>

Extensive research on a plethora of microbial enzymes that are normally involved in polymer degradation has been reported recently.<sup>16-18</sup> For example, controlling the rate of silk-based polymeric material degradation is vital to its potential use in biomedical applications, such as drug delivery and tissue engineering scaffolding. Recently, Pritchard et al.<sup>21</sup> reported the use of protease type XIV and ethylenediamine tetraacetic acid (EDTA) as biocontrolling switches to control the *in vitro* degradation of silk-based drug-carrier devices. The researchers observed the effects of the protease concentration on accelerating degradation and the use of EDTA on reducing the rates of degradation and controlling drug release from silk-based biomaterials. They reported an increased rate of proteolysis with increasing protease concentration; this resulted in an increased

dye release from silk carriers. On the other hand, the release of EDTA from the silk carriers inhibited proteolysis, which in turn controlled the proteolytic rate and, hence, the drug release.

The important step in polymer degradation, especially that of polyhydroxyalkanoate, is the degradation of the polymeric lamellar crystal.<sup>12,22</sup> It has been reported that in most cases, the extracellular enzymes, such as polymerases and hydrolases secreted by the microbial consortia, are responsible for polymer biodegradation. Kulkarni et al.<sup>23</sup> reported the selective enzymatic degradation of a block copolymer [polycaprolactone-*b*-poly(*p*-dioxanone)] with *Pseudomonas lipase* (Table I). The researchers reported that after they subjected the material to 200 h of enzymatic degradation, the poly(*p*-dioxanone) copolymer part was completely stable and not tampered with, whereas the degradation affected the polycaprolactone (PCL) part. They demonstrated that degradation properties of multifunctional polymers could be manipulated and controlled with selective enzymatic degradation; this results in unique polymers with specific properties for specialized applications. They further reported that the degree of enzymatic degradation relies heavily on the apparent enzyme penetration depth and the initial molecular weight of the block copolymer; a suggestion substantiated further by Numata et al.<sup>12</sup> and Tanuma et al.<sup>24</sup> In addition, the chemical structure,<sup>12,25</sup> molecular branches,<sup>12</sup> and degree of acetylation<sup>26</sup> are among the parameters suggested to exert influence on the enzymatic degradation of polymeric

materials. Recently, the controlled enzymatic degradation of PCL was reported with a polymer-embedded *Candida antarctica* lipase B solution (1.6%) in both continuous fluid exchange flow and controlled humidity chamber processes.<sup>27</sup> With 20 mM potassium phosphate buffer at pH 7.1 and a flow rate of 0.2 mL/min, researchers were able to achieve a polymer weight loss of about 85% in 3 days, an increase that was more greater in the process without the flow, where a bulk weight loss of 70% within 9 days of incubation was observed. The researchers suggested that the increase in the degradation rate under the flow conditions could be attributed to the more efficient removal of the degradation products that could act as competitive inhibitors. However, they observed a slower decrease in the polymer weight loss (70% in 7 days) as the flow rate was further increased to 0.5 mL/min; they attributed this to the negative influence of the increased flow rate on the enzyme stability.<sup>27</sup> When studying the rate of enzymatic degradation at controlled relative humidities (RHs) of 20, 75, and 95% with the same polymer-embedded 1.6% *C. antarctica* lipase B, researchers observed an insignificant polymer weight loss in the 20% RH condition.<sup>27</sup> However, at 75 and 95% RH, the polymer film was observed to exhibit weight losses of 25 and 58% after 28 days of incubation, respectively. The application of this controlled enzymatic degradation of polymeric materials under controlled humidity conditions could be an advantage in applications where the unique degradation properties of enzyme-embedded biodegradable films are exploited for the release of active materials such as fragrances, flavors, and therapeutic agents.

The biodegradation of waterborne polyurethane was reported to be enhanced by the incorporation of vinyl trimethoxysilane modified starch.<sup>28</sup> When the chemically hybridized polymer was incubated with 10% modified starch in an  $\alpha$ -amylase solution for 10 days, a maximum weight loss of 15% and a decrease in the tensile strength of 60% were observed. This result was reported to be much bigger than that of the polymer containing the unmodified starch (5% weight loss and  $\sim$ 17% tensile strength decrease). Extracellular poly(hydroxybutyrate depolymerase) purified from *Ralstonia pickettii* T1 was used to degrade a film of poly[(R)-3-hydroxybutyrate-co-4-hydroxybutyrate] that was prepared by uniaxial cold-drawing from an amorphous polymer at a temperature just below the glass transition.<sup>29</sup> In this type of polymer, the researchers observed the degradation rate to range from 0.14 to 0.67 mg cm<sup>-2</sup> h<sup>-1</sup>, depending on the polymer mechanical structure. The degree of enzymatic degradation was observed to increase with increasing draw ratio and 4-hydroxybutyric acid (4HB) content; this was mostly attributed to the decrease in the polymer crystallinity. They further reported that the enzyme preferably attacked the  $\beta$  form over the  $\alpha$  form; this was attributed to the lower steric hindrance against the ester bonds in the planar zigzag conformation of the  $\beta$  form as compared to the  $\alpha$ -form helical conformation.<sup>29</sup> The controlled enzymatic degradation of poly(3-hydroxybutyrate-co-4-hydroxybutyrate) was studied with commercial lipases,<sup>16</sup> wherein the researchers employed the use of nonregio-specific Amano lipase AK and 1,3-regiospecific Novozym lipopan BG to control the degradation of Poly(3-hydroxybutyrate-co-4-hydroxybutyrate) (P3HB-co-4HB) from 400 kDa to low-molecular-weight polymers of 1–5 kDa within 72 h to

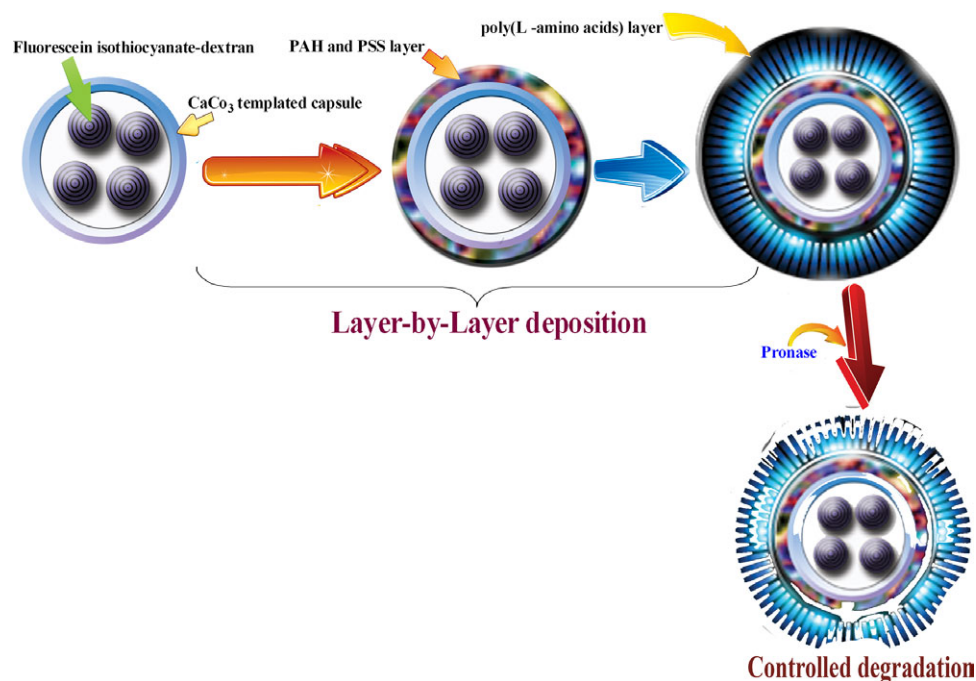
make it suitable as a drug-release device. In another study, the use of a nonspecific protease (pronase) to catalyze the controlled degradation of CaCO<sub>3</sub>-templated capsules that were prepared via layer-by-layer deposition techniques was reported.<sup>30</sup> The researchers showed that by either increasing the number of biodegradable layers in the capsules or inserting a synthetic polyelectrolyte of poly(allylamine hydrochloride) (PAH) and poly(sodium-4-styrene sulfonate) (PSS) to form multicompartiment polyelectrolyte multilayer capsules (Figure 1), the pronase-induced degradation of the capsules could be slowed down on the order of hours, and this resulted in the controlled detachment of subcompartments of multicompartiment capsules, with the potential for intracellular delivery or *in vivo* applications. Furthermore, the degradation rate was observed to increase with increasing pronase concentration.<sup>30</sup>

In addition to extracellular and *in vitro* enzymatic degradation, whole-cell microbial polymer degradation has been reported.<sup>20,31</sup> Poly(vinyl alcohol) (PVA) is considered to be an excellent compatible polymer blend with other polyhydroxyalkanoates because of its water solubility, biodegradability, and diverse applications. Jecu et al.<sup>32</sup> observed the degradation of poly(vinyl alcohol) by fungal strains belonging to genera of *Aspergillus*, *Monilia*, *Penicillium*, *Aureobasidium*, and *Trichoderma*. The researchers observed that of all the species tested, *Aspergillus niger* came out to be the best at degrading the PVA composite, with the degree of degradation largely depending on the media and polymer compositions. A higher degradation ( $\geq$ 60%) of a copolymer of sucrose polyesters was also reported with *A. niger*.<sup>33</sup> The increasing demand for soft wood, especially in current infrastructural developments, has been a point of ecological concern. It has been suggested that a polymer composite of fast-growing herbs, such as kenaf, grass, palm oil leaves, and bamboo, could serve as an alternative to wood.<sup>34</sup> A bio-composite polymer of polylactide and *Hibiscus cannabinus* (kenaf) was said to have a similar properties to that of particle-board and, as such, has been considered as a softwood alternative.<sup>35</sup> Recently, mycelia of *Pleurotus ostreatus* immobilized on calcium alginate beads was used by Hidayat and Tachibana<sup>35</sup> to degrade a composite polymer of polylactide and kenaf fiber; they achieved a 48% degradation after 6 months as compared an 84% fiber degradation in a noncomposite. They reported that the degradation of the PLA/kenaf composite by *P. ostreatus* mycelia occurred via oxidation and caused the rupture of hydroxyl groups and the formation of carboxylic acids groups.

In contrast to eukaryotic fungal species, several bacterial genera, such as *Bacillus*, *Comamonas*, *Pseudomonas*, *Staphylococcus*, and *Streptococcus*, are among those that have been used in polymer biodegradation.<sup>31</sup> Schneider et al.<sup>36</sup> observed the effects of the oleic acid concentration on poly(3-hydroxybutyrate) (P3HB) biodegradation produced by *Cupriavidus necator*. They observed that the polymer crystallinity decreased with increasing oleic acid concentration in the feed; this increased the degradability of the produced polymer.

The presence of impurities, organomodifiers, and plasticizers have been reported to affect the biodegradability of polymers. Researchers reported the use of organomodifiers such as clay to manipulate the polymer degradability and stability. Clay





**Figure 1.** Controlled enzymatic degradation of the multilayer capsule in drug-delivery devices. [Color figure can be viewed in the online issue, which is available at [www.interscience.wiley.com](http://www.interscience.wiley.com).]

nanoparticles were reported to modulate the biodegradability of gluten-based agromaterials<sup>37</sup> and result in a degree of degradation as high as 92%. Heteroaromatic ring derivatives were used to control the degree of degradation in polypropylene.<sup>38</sup> The researchers reported that the degradation rate was highly influenced by the electron density of the C=C bond in the heteroaromatic derivatives. Low-electron-density heteroaromatic derivatives such as 2-(furan-2-ylmethylene) malononitrile were found to restrict the  $\beta$  scission of polypropylene macroradicals by converting them to stable-resonance macroradicals. In comparison, changing the aromatic rings with high-electron-density derivatives such as 2-cyano-3-(pyrrole-2-yl)-2-propionic acid ethyl ester resulted in a high degradation rate.<sup>38</sup>

### HIGH-ENERGY RADIATION

High-energy radiation has been proven to be a useful tool in polymer degradation and/or the manipulation of the physicochemical structure of many industrially important polymers.<sup>39,40</sup> For instance, high-energy radiation has been applied to cause chain scission and branching in polypropylene.<sup>41</sup> High-melt-strength polypropylene grains were synthesized by Olani et al.<sup>42</sup> using  $\gamma$  radiation. The same radiation was also shown to degrade poly(lactide-co-glycolide) (PLGA).<sup>40</sup> It has also been used to enhance the electric conductivity of polymer electrolytes<sup>43</sup> and polyaniline-[poly(vinylidene chloride)-co-(vinyl acetate)] blends.<sup>44</sup> An electron beam was employed to degrade PLGA by chain scission;<sup>45</sup> it has also been reported to have been used to achieve controlled surface degradation in biodegradable polymers.<sup>39,46</sup> Carbon ion beams were reported to modify the physicochemical structures of both poly(allyl diglycol) carbonate and poly(ethylene terephthalate) polymer films.<sup>47</sup> An informative review of the effects of irradiation on controlled

drug-delivery and release systems was compiled by Ražem and Katušin-Ražem.<sup>48</sup>

Galovic et al.<sup>49</sup> studied the effect of  $\gamma$  radiation on polyethylenes of different densities with temperature-modulated differential scanning calorimetry. The researchers observed increases in the crystallinity and stability of the polymer at radiation doses up to 200 kGy; beyond this value, decreases in these parameters were observed. They suggested that the low radiation favored polymer macromolecular breakage over crosslinking, which in turn led to an increased perfection of the crystals because of the alleviation of tension at the sites of the lamellae surfaces where the molecules entered the lattice. On the other hand, the high radiation doses favored the increase in the macromolecular surface free energy that induced crosslinking at the lateral grain boundaries and resulted in a lower crystallinity because of lattice distortion and expansion.<sup>49</sup> El-Sawy et al.<sup>50</sup> employed  $\gamma$  radiation to degrade chitosan with a molecular weight of about  $10 \times 10^3$  kDa into water-soluble chitosan with an average molecular weight of less than  $2 \times 10^3$  kDa and that was suitable for use as a growth promoter in agricultural fields (Table I). Using initiators such as ammonium persulfate and hydrogen peroxide, the researchers showed that the degree of degradation depended not only on the radiation dose but also on the concentration of the initiator. Technically, by modulating the radiation dose and initiator concentration, one can achieve a specific oligomeric chitosan polymer. The production of high-performance carbon fibers mostly depends on the precursors, among which polyacrylonitrile (PAN) is the most important. Unfortunately, the use of PAN as a precursor involves peroxidation to achieve the oligomerization of the nitrile groups to form a ladder chain structure, which improves the thermal stability of the fibers. The conventional method is time consuming, requires

the use of chemicals, and is a highly exothermic process.<sup>6</sup> Gamma radiation has recently been reported to induce the formation of free radicals and crosslinking in PAN fibers and improve both the thermal stability and cyclization (oligomerization) efficiency of the fibers.<sup>6,51</sup>

Polymer ion-beam irradiation liberates hydrogen and other volatile gasses that are suggested to influence the formation of free radicals and unsaturation; this in turn improves the polymer dielectric constant and conductivity. Singh et al.<sup>52</sup> employed this phenomenon to improve the electrical conductivity of copper-doped poly(methyl methacrylate) for applications in organoelectronic components. High-energy radiation was used to induce graft polymerization (Table I) because of its simplicity, and it requires no catalyst or additives over the conventional methods and, hence, results in an almost pure product.<sup>53</sup> Recently, the mild condition of  $\gamma$  radiation was used to crosslink poly(*N*-2-hydroxyethyl)-DL-aspartamide with maleic anhydride to produce a functionalized hydrogel that was used as a drug-delivery device by the encapsulation and pulsatile release of proteins.<sup>54</sup>

Lotfy<sup>55</sup> studied the controlled degradation of low-molecular-weight dextrin in the presence of  $\gamma$  irradiation (5–100 kGy). Using both electron spin resonance and X-ray diffraction spectra, the researchers reported the dextrin to undergo oxidative degradation at the crystalline regions of the amylopectin chains. Furthermore, they revealed that the polymer weight loss of the irradiated sample occurred at lower temperatures compared to that of the unirradiated samples; this resulted in oligomeric dextrin components with melting temperatures that decreased with increasing irradiation dose.<sup>55</sup>

Flocculation is an efficient and cost-effective process for water treatment; polymers are popularly used as flocculating agents because of their ability to destabilize colloidal suspensions.<sup>56</sup> Ironically, the biodegradability of natural polymers reduces their shelf life in this process, whereas synthetic polymers are costly and nonbiodegradable. In view of this,  $\gamma$  radiation was used as a cost-effective route to produce a novel flocculant by the grafting of 2-methacryloyloxyethyl trimethyl ammonium chloride onto chitosan; this resulted in a copolymer with high cationic properties that was able to treat water over a wide range of pHs.<sup>56</sup>

Gamma-radiation graft polymerization was also applied in the preparation of a thermosensitive and pH-sensitive copolymer of polypropylene that was prepared by the grafting of *N*-isopropyl acrylamide and acrylic acid onto polypropylene films.<sup>53</sup> The researchers observed that the degree of grafting increased with increasing radiation dose to 20 kGy; above this value, the increase was insignificant, which they reported to be due to an increased free-radical concentration, which resulted in a high probability of radical recombination.<sup>53</sup> Previously, the  $\gamma$ -induced controlled release of clonazepam by the radiolysis of poly(D,L-lactide-co-glycolide)-loaded microspheres was investigated with matrix electron paramagnetic resonance spectroscopy in a vacuum temperature range of 77–298 K.<sup>57</sup> The researchers observed that increasing the radiation resulted in an increase in the generation of the drug-free radicals and reported the stabilization of the polymer matrix in the mixed system with respect to the radiation damage.<sup>57</sup>

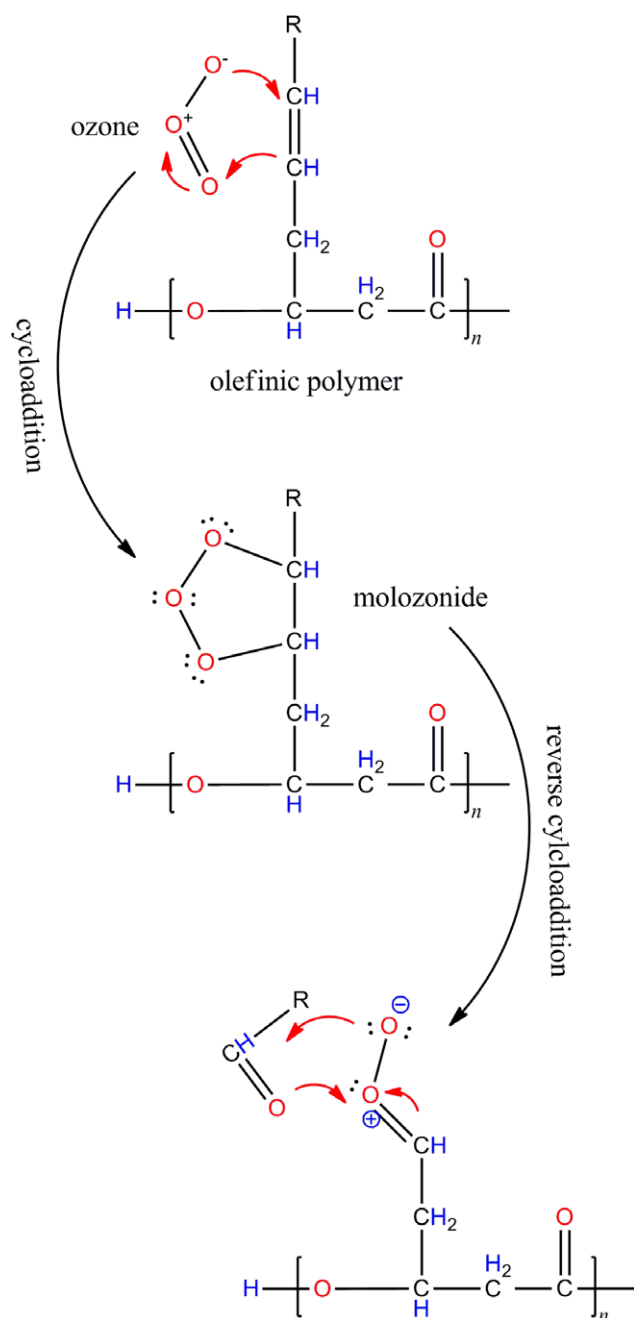
The tensile strength and stability of starch-based thermoplastic was enhanced by crosslinking with aromatic cinnamyl alcohol using electron-beam irradiation.<sup>58</sup> The macromolecular chain scission due to the electron-beam irradiation was observed to be counterbalanced by the induced interchain covalent linkage bridged by the cinnamyl alcohol, which led to a grafted polymer with superior properties.

## OZONIZATION

Ozonization is among the most important aspects in polymer degradation as a result of atmospheric exposure. Under strained conditions, a nonresistance elastomer can be attacked by ozone concentrations as little as 1 ppb.<sup>59</sup> Polymer degradation by ozonolysis has been reported to occur mostly by the cleavage of bonds between  $sp^2$  or  $sp$  carbon atoms in olefinic polymers.<sup>59,60</sup> However, the  $sp^3$  carbon–hydrogen bonds of polymers containing labile hydrogen atoms are also attacked but at much slower rates.<sup>59</sup> The ozonolysis mechanism is said to involve steps such as the cycloaddition of ozone to the olefinic double bond to form unstable molozonide (Figure 2), which is decomposed into carbonyl compounds and carbonyl oxide moieties via a cycloreversion process. Lastly, a stereoselective cycloaddition occurs as a result of the carbonyl oxide, which flips over with the nucleophilic oxyanion attacking the carbon atom of the carbonyl group, resulting in the formation of a peroxidic ozonolysis product.<sup>59</sup>

Although reactive and degradative to polymers, ozone still finds applications in polymer modification. Hyaluronic acids, especially those of low molecular weight, have electron-scavenging antioxidant activities and promote excisional wound healing.<sup>7</sup> Recently, ozone treatment was used to prepare low-molecular-weight hyaluronic acid.<sup>7</sup> Using ozonization (Table I), the researchers reported a reduction in the native hyaluronic acid molecular weight as large as 94.3% (from 1535 to 87 kDa within 120 min at 40°C), and they further observed that the heterogeneous reaction between the gaseous-phase ozone and the hyaluronic acid solution affected the polydispersity of the polymer. Experimental parameters, such as the reaction temperature, ozone concentration, media pH, ionic strength, and agitation speed are among the factors that have been reported to influence the ozonization process.<sup>7</sup>

Ozonization has further been reported to be used in the production of organoconductive polymers. It has been reported to influence the electrical conductivity of poly(3-pentylthiophene) films because of the formation of charge-transfer complexes.<sup>61</sup> However, the conductivity was observed to drop significantly with time as a result of the oxidative degradation of the polymer. In contrast to this observation, Nowaczyk et al.<sup>62</sup> reported the use of ozonization to induce both permanent and temporary increases in the electrical specific conductivity of a gold-sandwiched poly(3-pentylthiophene) polymer. The researchers observed that a permanent increase in the conductivity could be induced by the ozonization effect on the polymer morphology, which resulted in the formation of polymer grains aggregates, due to grain boundary resistance on polymer expansion. Whereas a temporary increase in the conductivity was observed to be a result of induced *p*-doping by ozonization, which took



**Figure 2.** Mechanism of polymer ozonization. [Color figure can be viewed in the online issue, which is available at [www.interscience.wiley.com](http://www.interscience.wiley.com).]

place because the high electronegativity of the ozone readily captured electrons from the delocalized  $\pi$  orbitals in the polymer backbone to form charge-transfer complexes, which operated as excess charge carriers.<sup>62</sup>

Polyethylene has been widely used in a number of industrial applications. Unfortunately, the polymer is characterized by poor dye adhesion to its surface, especially high-density polyethylene. Currently employed chemical surface modification methods, such as thermal oxidation and the use of strong electrical fields, are costly and time consuming. The surface functionalization of ultra-high-molecular-weight polyethylene with oxygen-bearing moieties was successfully achieved via ozoniza-

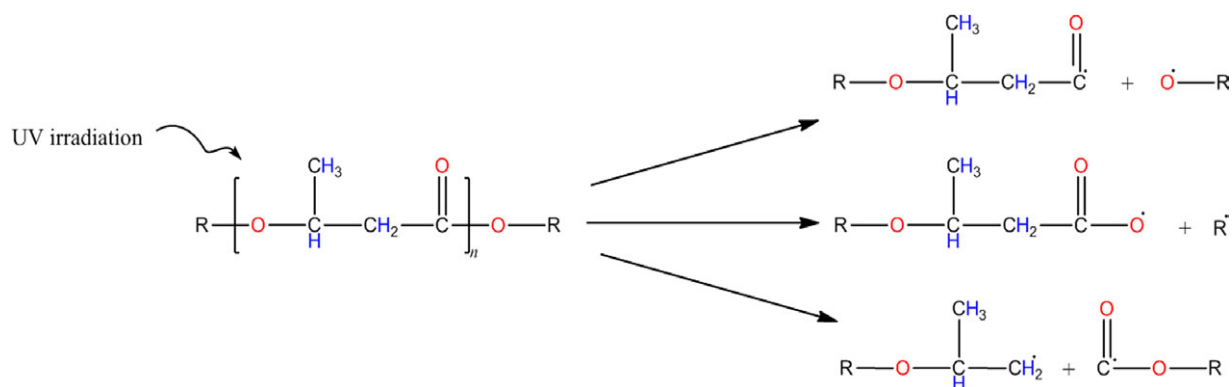
tion process with 10% ozone in oxygen under mild conditions.<sup>63</sup> In this process, the researchers reported that the ozonization mostly affected the amorphous phase of the polymer while preserving the crystalline phase. A similar report of polymer surface modification by ozonization was reported for styrenic triblock copolymers of elastomeric poly(ethylene-butylene) capped by polystyrene.<sup>64</sup> The researchers observed that prolonged exposure to ozone-induced crystallization and conferred a higher oxidative thermal stability to the polymer; this resulted in a qualitative polymer with a wide range of applications from organoelectronics to biopatterning.<sup>64</sup>

## PHOTODEGRADATION

The diverse applications of polymers in almost all aspects of human endeavors, ranging from spacecraft down to agricultural irrigation materials, has exposed applied polymers to adverse environmental conditions that warrant research concerning polymer degradation and stability. Although some of these polymers are biodegradable, environmental plastic wastes are usually thermally decomposed. The thermal degradation process is known to be costly and releases carcinogenic volatile gasses, and as such, the process is normally discouraged. The basis of polymer photolysis arises because of the presence of repeating carbonyl groups in polyesters, which results in photochemical cleavage by a Norrish-type reaction to degrade the polymer.<sup>65–67</sup> The ability of light photons, such as UV and IR irradiation, to degrade polymers has previously been reported.<sup>65,68,69</sup>

Previously, Tsuji et al.<sup>69</sup> studied the photodegradation of polylactide and polycaprolactone (PCL) for 200 h. They reported that UV radiation penetrated the polymer sample without a reduction in the intensity, regardless of the crystallinity or chemical structure, and degraded the polymer through a bulk erosion mechanism. However, they reported that the chemical structure adjacent to the carbonyl oxygen played a role in the photodegradability of the polymer. The effect of UV radiation on PHB was reported.<sup>70</sup> It was observed that in PHB, UV irradiation degraded the polymer by predominant chain scission into oligomers that could easily be functionalized (Figure 3) with lesser crosslinking reactions. The researchers further reported that when the UV irradiation was operated at temperatures higher than that of polymer's glass transition, the crystallinity increased as a result of the degraded reolecules' mobility in the amorphous region, which tended to rearrange themselves by crystallization.<sup>70</sup> Klinger and Landfester<sup>71</sup> observed the effect of UV-induced degradation on dual-stimuli poly(2-hydroxyethyl methacrylate-*co*-methacrylic acid) microgels. They reported the degradation rate to depend on parameters such as the media pH, intensity and wavelength of the applied irradiation, molecular structure of the crosslinking molecules, and overall molecular weight of the copolymer.

The control of protein adsorption onto a polymer surface is known to be a difficult challenge in biotechnological applications because of the strong adsorption that is irreversible and makes protein patterning almost impossible.<sup>72</sup> It has been reported that polymer brushes of oligo(ethylene glycol) methacrylate showed an exceptional resistance to protein adsorption. Ahmad et al.<sup>72</sup> used UV radiation at 244 nm to modify



**Figure 3.** Schematic diagram of UV-induced progressive chain scission in PHB. [Color figure can be viewed in the online issue, which is available at [www.interscience.wiley.com](http://www.interscience.wiley.com).]

poly[oligo(ethylene glycol)] methacrylate under mild conditions to break the oligo(ethylene glycol) chain to aldehyde that covalently bound protein and enhanced the patterning process.

Low-molecular-weight chitosan has been reported to increase the postharvest quality of citrus and exhibit antimycotic, antibacterial, and anticarcinogenic activities.<sup>73–75</sup> The deacetylation of chitin gives a chitosan of high molecular weight that has a low solubility in aqueous media, and this limits its industrial applications in many fields.<sup>76</sup> Recently, Yue et al.<sup>76</sup> reported the use of UV irradiation to induce accelerated degradation of chitosan during ozonolization to produce low-molecular-weight chitosan, which could be used in agrobases, biomedical, cosmetics, and food applications.

Silk fiber was reported to have a tensile strength of up to 4.5 GPa and an elasticity of about 35%; this makes it the toughest fiber known to man.<sup>77</sup> Silk fibroins are known to be surprisingly soluble in salt-containing aqueous, aqueous–organic, and organic solvents; unfortunately, the process is said to be time consuming. UV radiation was used to generate the silk fibroin in water within a shorter time to yield fibroin that was biocompatible and, at the same time, possessed remarkable physico-mechanical properties for use in diverse applications, such as surgical sutures, three-dimensional porous sponges, and microcapsules.<sup>77</sup>

### THERMOMECHANICAL AND OXIDATIVE DEGRADATION

Polymeric physical and chemical structures are known to influence the thermomechanical properties of polymers. It has been reviewed earlier that mechanical action induces chemical changes in polymers.<sup>78</sup> Moreover, the fermentation of substrates, especially ammonium cations in polyhydroxyalkanoates, have been reported to greatly influence the thermomechanical degradation of polymers.<sup>79,80</sup> Hydroxyalkanoic acids (HAs) are reported to have a wide range of industrial applications, such as metal corrosion inhibitors<sup>81</sup> and antibacterial agents.<sup>82</sup> These HAs are said to be chiral building blocks of several therapeutic drugs such as  $\beta$ -lactam, captopril, elaiophyllin, and hydroxyacyl hydrazine in viscosin; and fungicides such as vermuculin and norpyrenophorin.<sup>83</sup> Conventionally, HAs are produced by the

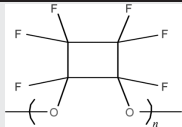
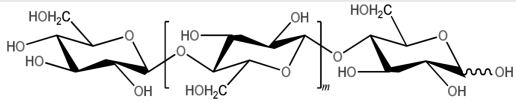
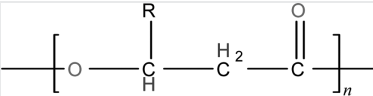
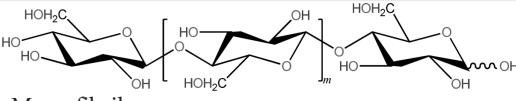
acid/base hydrolysis or methanolysis of high-molecular-weight polyhydroxyalkanoates, a process that mostly results in traces of impurities within the final products. Thermal degradation is seen as an alternative process because of the generation of pure HA. Sin et al.<sup>84</sup> reported the use of moderately high temperatures (160–190°C) to produce oligomeric HAs from medium-chain-length polyhydroxyalkanoates. They proposed the degradation mechanism to occur via hydrolytic chain cleavage initiated at the  $-\text{COO}-\text{CH}-\text{alkyl}$  group.<sup>85</sup> The researchers observed a loss of crystallinity when the PHA was heated at 180–190°C; ascribing the effects to the degradation of the polymer crystalline phase, which caused an increase in the mobility of the degraded polymeric units as the temperature approached the decomposition point.<sup>84</sup> In contrast to this observation, Sadi et al.<sup>70</sup> reported that an increased mobility of degraded polymeric molecules caused increased crystallinity because the molecules tended to rearrange themselves by crystallization.

Thermal degradation with microwave irradiation (Table II) to induce the controlled production of oligoesters (number-average molecular weight  $\leq 1000$  g/mol) in polyhydroxyalkanoates was recently reported.<sup>9</sup> The researchers observed the process to be 100 times faster than the conventional thermal degradation process and to occur within a very short time ( $<15$  min). They attributed the faster rate of degradation to be due to the generated highly efficient internal heating as a result of the direct coupling of microwave energy with the polar molecules; this led to the carboxyl–ester linkage.<sup>9</sup> The researchers suggested that for effective control of the degradation rate, microwave power should be modulated with the application of simultaneous cooling.

The mechanical ultrasonic degradation of commercially important polymers, such as polystyrene, polybutadiene, polystyrene–butadiene, PAN–butadiene, and polystyrene–acrylonitrile was reported.<sup>86</sup> Pinheiro et al.<sup>87</sup> proposed that chain scission was a starting point in the thermomechanical degradation of longer chains of high-density polyethylene, where their higher probability of entanglements resulted in macroradicals that could be functionalized. However, they noticed that the chain scission mechanism was less prominent in the shorter chains as a result



**Table II.** Thermomechanical and Oxidative Degradation in Polymer Modification

| Degradation method               | Polymer  | Application  | Reference |
|----------------------------------|--|--|-----------|
| Pulse ultrasonication            |                 | 1,4-Diradical intermediate for polymer functionalization | 88        |
| Ultrasound fragmentation         |                 | Improved crystallinity for the biocomposite polymer      | 90        |
| Microwave irradiation            |                 | Oligoesters for functionalization                        | 9         |
| TEMPO chemooxidative degradation | <br>Macrofibril | Surface-oxidized cellulosic nanofibril                   | 11        |

of their mobility but was rather useful for grafting the macro-radicals and, thus, increased the molecular weight.<sup>87</sup>

Recently, Klukovich et al.<sup>88</sup> studied the mechanical effects of pulsed ultrasound on perfluorocyclobutane polymers (Table II); this led to mechanically induced chain scission and molecular weight degradation via a stepwise mechanism with a 1,4-diradical intermediate. It yielded a polymer for localized functionalization and crosslinking.<sup>88</sup> The high crystallinity and extensive hydrogen bonding within the cellulosic polymer backbone conferred to it the advantage of being a natural fiber composite. However, because of the presence of an amorphous region in these naturally occurring celluloses, their tensile strength was highly limited. Hence, for the efficient application of these materials, a modification in the polymeric properties, especially the crystallinity, is needed. Goodwin et al.<sup>89</sup> reported the use of ultrasound irradiation to produce customized-molecular-weight pharmaceutical cellulosic ethers. The rate of degradation was observed to depend on the type of polymeric material and the irradiation time.<sup>89</sup> Recently, prolonged ultrasound fragmentation was reported to alter the crystallinity and molecular weight of cellulosic materials.<sup>90</sup> Using plant and bacterial cellulosic samples having a weight-average molecular weights of about 100 and 200 kDa, respectively, the researchers observed a continuous increase in the crystallinity index and a reduction in the molecular weight of the materials within 60 min of ultrasound irradiation to about 46 and 47 kDa, respectively. Pectin, which is a complex heteropolysaccharide commonly found in plant cell walls and middle lamella, has a wide application in the food and pharmaceutical industries as gelling, thickening, texturizing, stabilizing, and emulsifying agent.<sup>91</sup> However, the strong resistance of pectin to degradation by other physicochemical processes, such as ultrasound irradiation and some me-

chanical degradation methods, limits its optimal utilization. Chen et al.<sup>91</sup> reported the use of dynamic high-pressure microfluidization (DHPM) to induce controlled degradation in high-methoxyl pectin. The researchers observed a reduction of about 50% in molecular weight through the application of a DHPM of 80 MPa at pH 3.7, whereas an increase in the DHPM to 200 MPa at the same pH resulted in a molecular weight reduction of about 74%. However, a change in the pH to more acidic conditions appeared to highly influence the degradation. For instance, the application of 160 MPa of DHPM at pH 1.0 resulted in about an 89% degradation of the methoxyl pectin.<sup>91</sup> This reduction in the pectin's average molecular weight with the treatments was attributed to the breakdown of the covalent bonds inside the polymer chain.

The chemooxidative degradation of cellulose microfibrils with 2,2,6,6-tetramethylpiperidiny-1-oxy (TEMPO) radical derivatives and its analogous compounds were employed by Iwamoto et al.<sup>11</sup> to produce surface-oxidized cellulosic nanofibrils via hydromechanical treatment. When the oxidative effect of the TEMPO and its derivatives on wood cellulose surface oxidation were compared, researchers observed that both TEMPO and those analogous compounds of 4-acetamide and 4-methoxy derivatives showed an efficient catalytic surface oxidation of nanofibrils (>56%) compared to those of 4-hydroxyl and 4-oxo derivatives (<2%). The researchers reported that the observed differences in the catalytic efficiency among the TEMPO and its derivatives was probably due to their low redox potential, catalyst stability to media system, and affinity to cellulose type.

## CONCLUSIONS

The demand for specific degradability traits and functionalized/modified polymers in niche applications, and the difficulty

encountered in their *de novo* preparations under conventional syntheses has brought about the current interest in polymer modification and functionalization via controlled degradation processes. A successful degradation program depends on the ability to exert a certain degree of control over major parameters such as the rate and selectivity/specificity. This can be achieved through the manipulation of the degradation environment, for example, the (bio)catalyst concentration, modulation of irradiation intensity, humidity, and pH, for a particular process. Preparation methods of polymers before degradation can also be used as means to affect another level of control; this may involve the tailoring of the composition of the polymer, degree of crystallinity in different parts of the polymer, molecular weight, functional groups, and so on. It is possible to achieve a specific degradation outcome through a combination of these distinct techniques. There is also an opportunity to combine tandem physicochemical and enzymatic degradation steps, and this opens up wider possibilities for modified products.

## ACKNOWLEDGMENTS

The authors thank the University of Malaya for financial support (research grants PV036/2012A, RG165-11AFR, UM.C/625/1/HIR/MOHE/05, and RP024-2012A).

## REFERENCES

1. Iwata, T.; Tanaka, T. In *Microbiology Monographs*; Chen, G. G.-Q., Ed.; Springer: Berlin, **2010**; p 257.
2. Simanek, E. *Mol. Pharm.* **2010**, *7*, 921.
3. Tian, H.; Tang, Z.; Zhuang, X.; Chen, X.; Jing, X. *Prog. Polym. Sci.* **2012**, *37*, 237.
4. Numata, K.; Doi, Y. *Polym. J.* **2011**, *43*, 642.
5. Kabe, T.; Tsuge, T.; K.-Kasuya, I.; Takemura, A.; Hikima, T.; Takata, M.; Iwata, T. *Macromolecules* **2012**, *45*, 1858.
6. Liu, W.; Wang, M.; Xing, Z.; Qi, Y.; Wu, G. *Radiat. Phys. Chem.* **2012**, *81*, 622.
7. Wu, Y. *Carbohydr. Polym.* **2012**, *89*, 709.
8. Wong, S.-S.; Kasapis, S.; Tan, Y. M. *Carbohydr. Polym.* **2009**, *77*, 280.
9. Ramier, J.; Grande, D.; Langlois, V.; Renard, E. *Polym. Degrad. Stab.* **2012**, *97*, 322.
10. Kruželák, J.; Hudec, I.; Dosoudil, R. *Polym. Degrad. Stab.* **2012**, *97*, 921.
11. Iwamoto, S.; Kai, W.; Isogai, T.; Saito, T.; Isogai, A.; Iwata, T. *Polym. Degrad. Stab.* **2010**, *95*, 1394.
12. Numata, K.; Finne-Wistrand, A.; Albertsson, A.-C.; Doi, Y.; Abe, H. *Biomacromolecules* **2008**, *9*, 2180.
13. Bocchini, S.; Fukushima, K.; Blasio, A. D.; Fina, A.; Frache, A.; Geobaldo, F. *Biomacromolecules* **2010**, *11*, 2919.
14. Luckachan, G. E.; Pillai, C. K. S. *J. Polym. Environ.* **2011**, *1*.
15. Zhao, Z.; Yang, L.; Hu, Y.; He, Y.; Wei, J.; Li, S. *Polym. Degrad. Stab.* **2007**, *92*, 1769.
16. Rodríguez-Contreras, A.; Calafell-Monfort, M.; Marqués-Calvo, M. S. *Polym. Degrad. Stab.* **2012**, *97*, 597.
17. Mohan, K. J. *Biochem. Technol.* **2011**, *2*, 210.
18. Loredó-Treviño, A.; Gutiérrez-Sánchez, G.; Rodríguez-Herrera, R.; Aguilar, C. N. *J. Polym. Environ.* **2012**, *1*.
19. Doi, Y.; Kitamura, S.; Abe, H. *Macromolecules* **1995**, *28*, 4822.
20. Kawai, F.; Hu, X. *Appl. Microbiol. Biotechnol.* **2009**, *84*, 227.
21. Pritchard, E. M.; Valentin, T.; Boisson, D.; Kaplan, D. L. *Bio-materials* **2011**, *32*, 909.
22. Numata, K.; Abe, H.; Iwata, T. *Materials* **2009**, *2*, 1104.
23. Kulkarni, A.; Reiche, J.; Hartmann, J.; Kratz, K.; Lendlein, A. *Eur. J. Pharm. Biopharm.* **2008**, *68*, 46.
24. Tanuma, H.; Saito, T.; Nishikawa, K.; Dong, T.; Yazawa, K.; Inoue, Y. *Carbohydr. Polym.* **2010**, *80*, 260.
25. Jiang, N.; Jiang, S.; Hou, Y.; Yan, S.; Zhang, G.; Gan, Z. *Polymer* **2010**, *51*, 2426.
26. Verheul, R. J.; Amidi, M. M.; van Steenberg, J.; van Riet, E.; Jiskoot, W.; Hennink, W. E. *Biomaterials* **2009**, *30*, 3129.
27. Ganesh, M.; Gross, R. A. *Polymer* **2012**, *53*, 3454.
28. Lee, S. J.; Kim, B. K. *Carbohydr. Polym.* **2012**, *87*, 1803.
29. Zhang, J.; Kasuya, K.; Hikima, T.; Takata, M.; Takemura, A.; Iwata, T. *Polym. Degrad. Stab.* **2011**, *96*, 2130.
30. Marchenko, I.; Yashchenok, A.; Borodina, T.; Bukreeva, T.; Konrad, M.; Möhwald, H.; Skirtach, A. J. *Controlled Release* **2012**, *162*, 599.
31. Bhardwaj, H.; Gupta, R.; Tiwari, A. J. *Polym. Environ.* **2012**, *1*. DOI 10.1007/s10924-012-0456-z.
32. Jecu, L.; Gheorghe, A.; Rosu, A.; Raut, I.; Grosu, E.; Ghiurea, M. *J. Polym. Environ.* **2010**, *18*, 284.
33. Barros, M. T.; Petrova, K. T.; Singh, R. P. *Eur. Polym. J.* **2010**, *46*, 1151.
34. Pamuła, E.; Błażewicz, M.; Paluszkiwicz, C.; Dobrzyński, P. *J. Mol. Struct.* **2001**, *596*, 69.
35. Hidayat, A.; Tachibana, S. *Int. Biodeterior. Biodegrad.* **2012**, *71*, 50.
36. Schneider, A. L. S.; Silva, D. D.; Garcia, M. C. F.; Grigull, V. H.; Mazur, L. P.; Furlan, S. A.; Aragao, G. F.; Pezzin, A. P. T. *J. Polym. Environ.* **2010**, *18*, 401.
37. Chevillard, A.; Angellier-Coussy, H.; Cuq, B.; Guillard, V.; César, G.; Gontard, N.; Gastaldi, E. *Polym. Degrad. Stab.* **2011**, *96*, 2088.
38. Wan, D.; Ma, L.; Zhang, Z.; Xing, H.; Wang, L.; Jiang, Z.; Zhang, G.; Tang, T. *Polym. Degrad. Stab.* **2012**, *97*, 40.
39. Cairns, M.-L.; Dickson, G. R.; Orr, J. F.; Farrar, D.; Hawkins, K.; Buchanan, F. J. *Polym. Degrad. Stab.* **2011**, *96*, 76.
40. Jo, S.-Y.; Park, J.-S.; Gwon, H.-J.; Shin, Y.-M.; Khil, M.-S.; Nho, Y.-C.; Lim, Y.-M. *Radiat. Phys. Chem.* **2012**, *81*, 846.
41. Otaguro, H.; de Lima, L. F. C. P.; Parra, D. F.; Lugão, A. B.; Chinelatto, M. A.; Canevarolo, S. V. *Radiat. Phys. Chem.* **2010**, *79*, 318.
42. Oliani, W. L.; Parra, D. F.; Lugão, A. B. *Radiat. Phys. Chem.* **2010**, *79*, 383.

43. Nanda, P.; Maity, S.; Pandey, N.; Ray, R.; Thakur, A. K.; Tarafdar, S. *Radiat. Phys. Chem.* **2011**, *80*, 22.
44. Bodugöz-Sentürk, H.; Güven, O. *Radiat. Phys. Chem.* **2011**, *80*, 153.
45. Chye Joachim Loo, S.; Ping Ooi, C.; Chiang, Freddy Boey, Y. *Biomaterials* **2005**, *26*, 3809.
46. Cairns, M.-L.; Sykes, A.; Dickson, G. R.; Orr, J. F.; Farrar, D.; Dumba, A. F.; Buchanan, J. *Acta Biomater.* **2011**, *7*, 548.
47. Kumar, V.; Sonkawade, R. G.; Chakarvarti, S. K.; Singh, P.; Dhaliwal, A. S. *Radiat. Phys. Chem.* **2012**, *81*, 652.
48. Ražem, D.; Katusin-Ražem, B. *Radiat. Phys. Chem.* **2008**, *77*, 288.
49. Galovic, S.; Secerov, B.; Trifunovic, S.; Milicevic, D.; Suljovrujic, E. *Radiat. Phys. Chem.* **2012**, *81*, 1374. <http://dx.doi.org/10.1016/j.radphyschem.2011.11.054>
50. El-Sawy, N. M.; Abd El-Rehim, H. A.; Elbarbary, A. M.; Hegazy, E. S. A. *Carbohydr. Polym.* **2010**, *79*, 555.
51. Liu, W.; Wang, M.; Xing, Z.; Wu, G. *Radiat. Phys. Chem.* **2012**, *81*, 835.
52. Singh, D.; Singh, N. L.; Qureshi, A.; Kulriya, P.; Tripathi, A.; Avasthi, D. K.; Gulluoglu, A. N. *J. Non-Cryst. Solids* **2010**, *356*, 856.
53. Ramírez-Fuentes, Y. S.; Bucio, E.; Burillo, G. *Nucl. Instrum. Methods Phys. Res. Sect. B* **2007**, *265*, 183.
54. LoPresti, C.; Vetri, V.; Ricca, M.; Foderà, V.; Tripodo, G.; Spadaro, G.; Dispenza, C. *React. Funct. Polym.* **2011**, *71*, 155.
55. Lotfy, S. *Int. J. Biol. Macromol.* **2009**, *44*, 57.
56. Wang, J. P.; Chen, Y. Z.; Ge, X. W.; Yu, H. Q. *Chemosphere* **2007**, *66*, 1752.
57. Fautitano, A.; Buttafava, A.; Montanari, L.; Cilurzo, F.; Conti, B.; Genta, I.; Valvo, L. *Radiat. Phys. Chem.* **2003**, *67*, 61.
58. Khandal, D.; Mikus, P.-Y.; Dole, P.; Bliard, C.; Soulestin, J.; Lacrampe, M.-F.; Baumberger, S.; Coqueret, X. *Radiat. Phys. Chem.* **2012**, *81*, 986. <http://dx.doi.org/10.1016/j.radphyschem.2011.10.028>
59. Allen, N. S.; Edge, M.; Mourelatou, D.; Wilkinson, A.; Liauw, C. M.; Dolores Parellada, M.; Barrio, J. A.; Ruiz Santa Quiteria, V. *Polym. Degrad. Stab.* **2003**, *79*, 297.
60. Hintz, H.; Egelhaaf, H. J.; Peisert, H.; Chassé, T. *Polym. Degrad. Stab.* **2010**, *95*, 818.
61. Nowaczyk, J.; Olszowy, P.; Cysewski, P.; Nowaczyk, A.; Czerwiński, W. *Polym. Degrad. Stab.* **2008**, *93*, 1275.
62. Nowaczyk, J.; Blockhuys, F.; Czerwiński, W. *Mater. Chem. Phys.* **2012**, *132*, 823.
63. Cataldo, F.; Rosati, A.; Lilla, E.; Ursini, O. *Polym. Degrad. Stab.* **2011**, *96*, 955.
64. Peinado, C.; Corrales, T.; Catalina, F.; Pedrón, S.; Santa Quiteria, V. R.; Parellada, M. D.; Barrio, J. A.; Olmos, D.; González-Benito, J. *Polym. Degrad. Stab.* **2010**, *95*, 975.
65. Ikada, E. *J. Photopolym. Sci. Technol.* **1998**, *11*, 23.
66. Scaiano, J. C.; Stampelcoskie, K. G.; Hallett-Tapley, G. L. *Chem. Commun.* **2012**, *48*, 4798.
67. Yasuda, N.; Wang, Y.; Tsukegi, T.; Shirai, Y.; Nishida, H. *Polym. Degrad. Stab.* **2010**, *95*, 1238.
68. Lucki, J.; Rabek, J. F.; Rånby, B.; Ekström, C. *Eur. Polym. J.* **1981**, *17*, 919.
69. Tsuji, H.; Echizen, Y.; Nishimura, Y. *Polym. Degrad. Stab.* **2006**, *91*, 1128.
70. Sadi, R. K.; Fehine, G. J. M.; Demarquette, N. R. *Polym. Degrad. Stab.* **2010**, *95*, 2318.
71. Klinger, D.; Landfester, K. *Macromolecules* **2011**, *44*, 9758.
72. Ahmad, A. S.; Hucknall, A.; Chilkoti, A.; Leggett, G. *J. Langmuir* **2010**, *26*, 9937.
73. Chien, P.-J.; Sheu, F.; Lin, H.-R. *Food Chem.* **2007**, *100*, 1160.
74. Hernández-Muñoz, P.; Almenar, E.; Valle, V. D.; Velez, D.; Gavara, R. *Food Chem.* **2008**, *110*, 428.
75. Zhang, H.; Li, R.; Liu, W. *Int. J. Mol. Sci.* **2011**, *12*, 917.
76. Yue, W.; He, R.; Yao, P.; Wei, Y. *Carbohydr. Polym.* **2009**, *77*, 639.
77. Sionkowska, A.; Planecka, A. *Polym. Degrad. Stab.* **2011**, *96*, 523.
78. Caruso, M. M.; Davis, D. A.; Shen, Q.; Odom, S. A.; Sottos, N. R.; White, S. R.; Moore, J. S. *Chem. Rev.* **2009**, *109*, 5755.
79. Hablot, E.; Bordes, P.; Pollet, E.; Avérous, L. *Polym. Degrad. Stab.* **2008**, *93*, 413.
80. Gumel, A. M.; Annur, M. S. M.; Heidelberg, T. *Polym. Degrad. Stab.* **2012**, *97*, 1227.
81. Kiely, D. E.; Hash, K. R.; Kramer-Presta, K.; Smith, T. U.S. Pat. 20120,035,356 ( **2012**).
82. Otto, R.; Ramirez, A. M.; Kremer, D. R. U.S. Pat. US8329638 B2 ( **2012**).
83. Ren, Q.; Ruth, K.; Thöny-Meyer, L.; Zinn, M. *Appl. Microbiol. Biotechnol.* **2010**, *87*, 41.
84. Sin, M. C.; Tan, I. K. P.; Annur, M. S. M.; Gan, S. N. *Int. J. Polym. Anal. Charact.* **2011**, *16*, 337.
85. Sin, M. C.; Gan, S. N.; Annur, M. S. M.; Tan, I. K. P. *Polym. Degrad. Stab.* **2011**, *96*, 1705.
86. Sathiskumar, P. S.; Madras, G. *Ultrason. Sonochem.* **2012**, *19*, 503.
87. Pinheiro, L. A.; Chinelatto, M. A.; Canevarolo, S. V. *Polym. Degrad. Stab.* **2004**, *86*, 445.
88. Klukovich, H. M.; Kean, Z. S.; Iacono, S. T.; Craig, S. L. *J. Am. Chem. Soc.* **2011**, *133*, 17882.
89. Goodwin, D. J.; Picout, D. R.; Ross-Murphy, S. B.; Holland, S. J.; Martini, L. G.; Lawrence, M. *J. Carbohydr. Polym.* **2011**, *83*, 843.
90. Wong, S.-S.; Kasapis, S.; Huang, D. *Food Hydrocolloids* **2012**, *26*, 365.
91. Chen, J.; Liang, R.-H.; Liu, W.; Liu, C.-M.; Li, T.; Tu, Z.-C.; Wan, J. *Food Hydrocolloids* **2012**, *28*, 121.

## CHAPTER 5

# Ultrasound assisted lipase catalyzed synthesis of poly-6-hydroxyhexanoate

**A. M. Gumel<sup>1</sup>, M. S. M. Annuar<sup>1\*</sup>, T. Heidelberg<sup>2</sup>, Y. Chisti<sup>3</sup>**

<sup>1</sup> Institute of Biological Sciences,    <sup>2</sup> Department of Chemistry

*Faculty of Science, University of Malaya, Kuala Lumpur 50603, Malaysia*

<sup>3</sup> School of Engineering, PN 456, Massey University, Private Bag 11 222, Palmerston North, New Zealand

**Published:** *Ultrasonics Sonochemistry* (2011) **19**(3): 659-667

(ISI cited publication: tier 1)

### Statement of contributions of joint Authorship

**Gumel, A.M:** (Candidate)

Writing and compilation of manuscript, established methodology, data collection, presentation and analyses. Main author of the manuscript

**Annuar, M.S.M:** (Principal Supervisor)

Supervised and assisted with manuscript compilation, editing and co-author of the manuscript.

**Heidelberg, T:** (Co-Supervisor)

Supervised and assisted with chemical analyses, structure elucidation and co-author of the manuscript

**Chisti, Y:** (Research collaborator)

Editing and co-author of manuscript





Contents lists available at SciVerse ScienceDirect

## Ultrasonics Sonochemistry

journal homepage: [www.elsevier.com/locate/ultsonch](http://www.elsevier.com/locate/ultsonch)

## Ultrasound assisted lipase catalyzed synthesis of poly-6-hydroxyhexanoate

A.M. Gumel<sup>a</sup>, M.S.M. Annuar<sup>a,\*</sup>, Y. Chisti<sup>c</sup>, T. Heidelberg<sup>b</sup><sup>a</sup> Institute of Biological Sciences, Faculty of Science, University of Malaya, 50603 Kuala Lumpur, Malaysia<sup>b</sup> Department of Chemistry, Faculty of Science, University of Malaya, 50603 Kuala Lumpur, Malaysia<sup>c</sup> School of Engineering, PN 456, Massey University, Private Bag 11 222, Palmerston North, New Zealand

## ARTICLE INFO

## Article history:

Received 19 August 2011

Received in revised form 24 October 2011

Accepted 27 October 2011

Available online 7 November 2011

## Keywords:

Lipase

Polycaprolactone

Polyhydroxyalkanoates

Ultrasound

Kinetics

Biopolymers

## ABSTRACT

Ultrasonic irradiation greatly improved the *Candida antarctica* lipase B mediated ring opening polymerization of  $\epsilon$ -caprolactone to poly-6-hydroxyhexanoate in the ionic liquid 1-ethyl-3-methylimidazolium tetrafluoroborate. Compared to the conventional nonsonicated reaction, sonication improved the monomer conversion by 63% and afforded a polymer product of a narrower molecular weight distribution and a higher degree of crystallinity. Under sonication, the polydispersity index of the product was  $\sim 1.44$  compared to a value of  $\sim 2.55$  for the product of the conventional reaction. With sonication, nearly 75% of the monomer was converted to product, but the conversion was only  $\sim 16\%$  for the reaction carried out conventionally. Compared to conventional operation, sonication enhanced the rate of polymer propagation by  $>2$ -fold and the turnover number of the lipase by  $>3$ -fold.

© 2011 Elsevier B.V. All rights reserved.

## 1. Introduction

This work is concerned with enzyme-mediated sonication-enhanced production of the biodegradable polymer poly-6-hydroxyhexanoate, a polyhydroxyalkanoates (PHA). Polymers such as PHA are important in many industrial and biomedical applications because of their biocompatibility, biodegradability and attractive mechanical properties [1,2]. Temporary prostheses, controlled drug delivery devices, resorbable implants and tissue engineering scaffolds are some of the products made from biodegradable polymers [3]. Poly-6-hydroxyhexanoate (poly- $\epsilon$ -caprolactone) is a semi crystalline polymer that can be inexpensively produced by ring-opening polymerization (ROP) of the monomer  $\epsilon$ -caprolactone [4,5].

Ring-opening polymerization of lactones and lactides can be achieved with conventional chemical catalysis or by using biocatalysts [6]. Chemical catalysis relies on organometallic compounds [7] that can contaminate the product and are potentially toxic in biomedical applications. In contrast, the products of enzyme mediated biocatalytic ring opening polymerization have little or no potential for an adverse health impact. In addition, enzymatic biocatalysis offers an excellent enantiomeric selectivity, specificity and catalytic activity under mild reaction conditions. Enzyme catalyzed ROP can make use of a wide range of substrates including

cyclic lactones. The lipase B enzyme of *Candida antarctica* has proved to be a highly effective catalyst for ROP of cyclic lactones [8–11].

Enzyme mediated synthesis of PHAs by ring opening polymerization is conventionally carried out in potentially hazardous volatile organic solvents such as tetrahydrofuran [12,13]. An alternative is to use nonvolatile and highly thermostable ionic liquids as solvents. PHAs and the corresponding monomers tend to be highly soluble in ionic liquids [4]. Furthermore, enzymes such as lipases have a longer lifespan in ionic liquids than in conventional organic solvents [4,14].

Earlier studies of lipase mediated ROP were characterized by poor stability of the enzyme, a slow rate of reaction, and a low molecular weight of the polymer product. These problems continue to limit large-scale commercial use of lipase mediated ROP [15]. Attempts have been made to improve the performance of lipase mediated ROP through the use of microwave irradiation [16,17], supercritical fluids [18], and ionic solvents [12,19,20]. Use of ultrasound holds a substantial potential for enhancing the performance of biocatalytic processes [21], but sonication has not been evaluated for lipase mediated ROP. This paper reports on ultrasound-assisted lipase-catalyzed ROP of  $\epsilon$ -caprolactone to poly-6-hydroxyhexanoate and aims to study its kinetics relative to the non-sonicated process. The product conversion yield and its selected characteristics were also studied in comparison with the non-sonicated treatment. The reaction is carried out in a nonconventional ionic liquid.

\* Corresponding author. Tel.: +60 379674003; fax: +60 379674178.

E-mail address: [suffian\\_annuar@um.edu.my](mailto:suffian_annuar@um.edu.my) (M.S.M. Annuar).

## 2. Materials and methods

### 2.1. Materials

All chemicals used were of analytical grade, unless otherwise stated. The ionic solvent 1-ethyl 3-methylimidazolium tetrafluoroborate [Emim][BF<sub>4</sub>] (purity >99%) and  $\epsilon$ -caprolactone monomer were obtained from Merck ([www.merck.com](http://www.merck.com)). Standard poly- $\epsilon$ -caprolactone of different molecular weights, tetrahydrofuran, chloroform and methanol were purchased from Sigma–Aldrich ([www.sigmaaldrich.com](http://www.sigmaaldrich.com)). *C. antarctica* lipase B 435 was purchased from Novozymes ([www.novozymes.com](http://www.novozymes.com)). The enzyme was supplied immobilized on beads of a macroporous acrylic resin [22].

### 2.2. Methods

#### 2.2.1. Enzymatic ring opening of $\epsilon$ -caprolactone

Reactions were performed in triplicate. [Emim][BF<sub>4</sub>] (6.54 M) and  $\epsilon$ -caprolactone (9.02 M) of known water activity were mixed in 20 mL capped reaction vials. Lipase B (1.5% w/v, g/100 mL) was added to initiate the reaction except in the primary control vials. The initial water content and water activity of each reaction mixture were measured using Metrohm® Karl Fisher coulometric titrator (831 KF-coulometer; [www.mt.com](http://www.mt.com)) and Rotronic HygroPalm water activity meter (HP23-AW; [www.rotronic.co.uk](http://www.rotronic.co.uk)), respectively.

A batch of the reaction vials was subjected to ultrasound irradiation by immersing in a sonicated water bath (Transsonic Tp690/H, Elma, Germany) operated at a frequency of 35 kHz and a maximum ultrasound rated power of 320 W. The vials were irradiated for 20 min. Then, they were taken out of the sonication bath and the reaction was allowed to progress until specified time in automatic shaking incubator (Daihan LabTech®, Korea) at 200 rpm, 55 °C. A second batch of vials (without sonication) was incubated in the automatic shaking incubator for 20 min at 200 rpm and 55 °C, and then the reaction was allowed to progress until specified time under the same experimental conditions. These nonsonicated vials served as secondary controls.

At specific intervals, vials were removed and 20 mL of chloroform was added to the viscous reaction mixture in each vial to stop the reaction. The mixture was then immediately suction filtered through a 0.40  $\mu$ m PTFE filter membrane to remove the lipase beads. The final water content and the water activity in each reaction vial were measured prior to quenching, as specified above.

#### 2.2.2. Product recovery

The product (poly-6-hydroxyhexanoate) was recovered by concentrating the filtrate from the previous section to about 4 mL at 40 °C in a rotary evaporator (LABOROTA C-311; [www.heidolph-instruments.com](http://www.heidolph-instruments.com)) under reduced pressure. Cold methanol (methanol to reaction mixture ratio of 2:1 by vol) was then added to precipitate the product and the solids were filtered. The crude white precipitate of the poly-6-hydroxyhexanoate was re-dissolved in 10 mL of chloroform, concentrated to 4 mL as above, precipitated again with methanol and recovered. This process was repeated a further three times to purify the product. The recovered product was dried overnight under vacuum and subsequently subjected to <sup>1</sup>H NMR and FTIR analyzes. The same extraction and purification steps were used to monitor the increase in weight of the polymer during the reaction.

#### 2.2.3. Qualitative analysis of the product

**2.2.3.1. FTIR spectroscopy.** Spectra were recorded using a Perkin Elmer FTIR RX 1 spectrometer (Perkin-Elmer Inc., Wellesley, MA, USA). About 0.01 mg of the synthesized poly-6-hydroxyhexanoate

sample was ground with 0.02 mg of dried potassium bromide (KBr) pellets as carrier and cast on a FTIR carrier-nut as a thin transparent film. Poly- $\epsilon$ -caprolactone standard (CAS 24980-41-4, Sigma–Aldrich) was subjected to the same treatment. The spectra were recorded at room temperature between 4000 and 400 cm<sup>−1</sup> with 4 cm<sup>−1</sup> resolution running 10 scans.

**2.2.3.2. <sup>1</sup>H NMR analyzes.** The proton NMR spectra were recorded on a JEOL JNM-GSX 270 FT-NMR (JOEL Ltd., Tokyo, Japan) machine at 250 MHz. Deuterated chloroform (CDCl<sub>3</sub>) was used as the solvent and tetramethylsilane (TMS) was the internal reference standard. The sample was prepared by dissolving 5 mg of it in 2 mL of deuterated chloroform. About 1.5 mL of this solution was withdrawn using a borosilicate glass syringe and filtered into an NMR tube via a 0.02  $\mu$ m disposable filter cartridge.

**2.2.3.3. Gel permeation chromatography (GPC).** GPC analyzes were carried out on a Waters 600-GPC (Waters Corp., Milford, MA, USA) instrument equipped with a Waters refractive index detector (model 2414). The instrument was equipped with following gel columns (7.8 mm internal diameter  $\times$  300 mm) connected in series: HR1, HR2, HR5E and HR5E Waters Styrogel HR-THF. The GPC measurements were used to characterize the weight averaged molecular weight ( $M_w$ ), the number averaged molecular weight ( $M_n$ ) and the polymer distribution index (polydispersity index, *PDI*) of both the synthesized polymer samples and the secondary control polymer samples. Monodisperse polystyrene standards of different molecular weights ( $3.72 \times 10^2$ ,  $2.63 \times 10^3$ ,  $9.10 \times 10^3$ ,  $3.79 \times 10^4$ ,  $3.55 \times 10^5$ ,  $7.06 \times 10^5$ ,  $3.84 \times 10^6$  and  $6.77 \times 10^6$  Da) were used to generate the calibration curve. The polymer samples were dissolved in tetrahydrofuran (THF) at a concentration of 2.0 mg mL<sup>−1</sup>, filtered through a 0.22  $\mu$ m filter and injected (100  $\mu$ L) at 40 °C. THF at a flow rate of 1.0 mL min<sup>−1</sup> was the mobile phase. The polydispersity index (*PDI*) was calculated as follows:

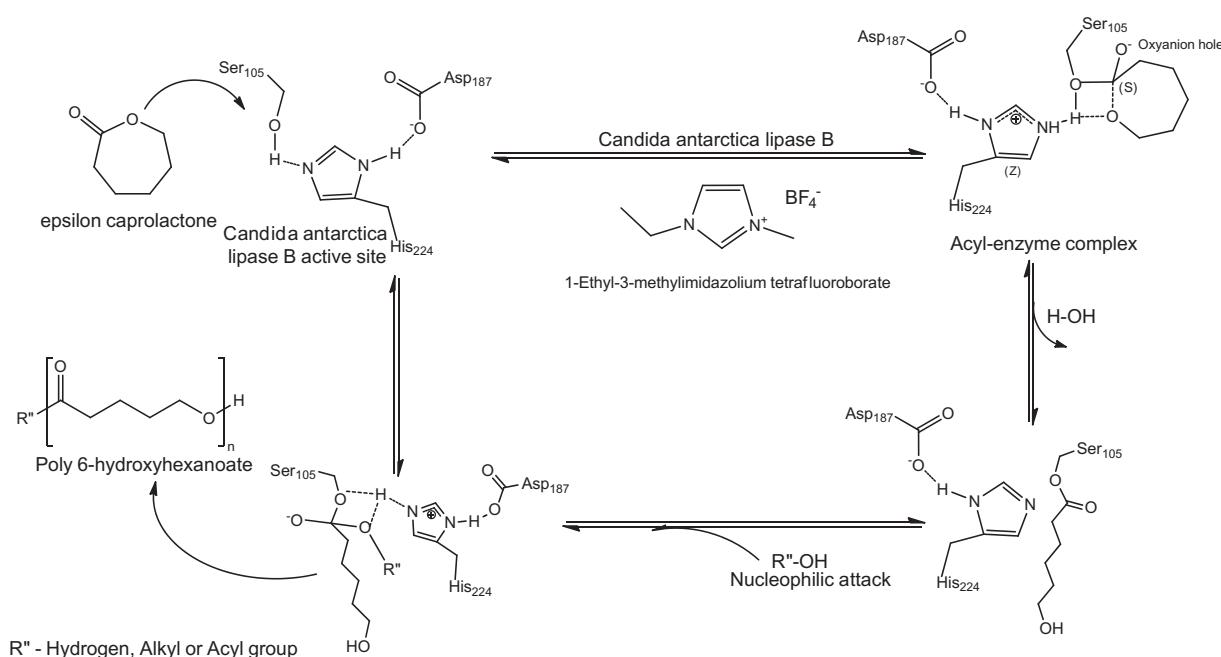
$$PDI = \frac{M_w}{M_n} \quad (1)$$

**2.2.3.4. Differential scanning calorimetry (DSC).** DSC analyzes of the synthesized poly-6-hydroxyhexanoate were performed using a Perkin-Elmer differential scanning calorimeter (DSC 6; Perkin-Elmer Inc., Wellesley, MA, USA). Scans were made under a nitrogen flow rate of 50 mL min<sup>−1</sup>. The temperature range of the scans was between −65 °C and 125 °C. Heating/cooling rate was 20 °C min<sup>−1</sup>. The melting temperature ( $T_m$ ) was taken at the peak of the DSC thermogram endotherm.

**2.2.3.5. Thermogravimetric analysis (TGA).** TGA analysis was performed on a Perkin-Elmer TGA 4000 instrument (Perkin-Elmer Inc., Wellesley, MA, USA). The samples were heated from 50 °C to 900 °C at a heating rate of 10 °C min<sup>−1</sup> under a nitrogen flow rate of 20 mL min<sup>−1</sup>.

## 3. Results and discussion

The catalytic action of lipases has been previously reviewed [23]. The active site of the enzyme consists of a catalytic triad of the amino acid residues of serine<sub>105</sub>, histidine<sub>224</sub> and aspartate<sub>187</sub> (Fig. 1). These catalytic residues are involved in the ring opening polymerization of  $\epsilon$ -caprolactone in the ionic solvent [Emim][BF<sub>4</sub>], as postulated in Fig. 1. The utilization of  $\epsilon$ -caprolactone for the polymerization reaction obeys Michaelis–Menten kinetics as shown later in this paper. The kinetics of the overall polymerization process suggests that the rate-determining step is the formation



**Fig. 1.** Proposed mechanism of lipase catalyzed ring-opening-polymerization of  $\epsilon$ -caprolactone in [Emim][BF<sub>4</sub>] (R' = H- or alkyl group or acyl group).

of the acyl-enzyme intermediate complex [24–26] (Fig. 1). The reaction to produce  $\omega$ -hydroxycarboxylic acid, probably the shortest polymer propagating species is initiated by a nucleophilic attack of the water present in the reaction medium on the acyl carbon of the acyl-enzyme intermediate. The acyl-enzyme intermediate undergoes further nucleophilic attack by the terminal hydroxyl of the propagating polymer (or water molecule) to result in elongation of the polymer chain by one unit (or chain termination). This process continues.

The basic polymerization process is the same irrespective of whether ultrasound is involved, but sonication affects both the catalytic characteristics of the enzyme and how it interacts with the monomer and the growing polymer. Thus the characteristics of the polymer produced differ depending on whether sonication is used. The characteristics of the polymer produced under various conditions and the impact of sonication on the kinetics of polymerization are discussed in the following sections.

### 3.1. Product characterization

#### 3.1.1. FTIR analysis

Fig. 2 compares of the FTIR spectra of the product produced under sonication, the product produced without sonication and the authentic polymer standard. In the spectra (Fig. 2a and b), the absorption bands at 3438.19 cm<sup>-1</sup> indicate the presence of hydroxyl groups confirming the formation of a linear polymer chain [27]. The absorption bands at 2945.12 cm<sup>-1</sup> and 2866.16 cm<sup>-1</sup> were attributed to the expected asymmetric and symmetric CH<sub>2</sub> stretching vibrations, respectively. In all spectra (Fig. 2), the absorption band at 1724.15 cm<sup>-1</sup> was attributed to carbonyl (C=O) stretching vibrations. The band at 1369.27 cm<sup>-1</sup> was assigned to CH<sub>3</sub> groups. The absorption band at 1240.77 cm<sup>-1</sup> was due to asymmetric COC stretching vibrations. The bands at 1196 and 1195 cm<sup>-1</sup> were associated with the OC–O stretching vibrations. The bands from 1169 to 1174 cm<sup>-1</sup> were assigned to symmetric COC stretching vibrations. The series of absorption bands from 1108 cm<sup>-1</sup> to 453 cm<sup>-1</sup> were attributed to C–O and C–C stretching vibrations in the amorphous phase. These spectral observations were consistent with data previously reported by Elzein et al. [28] for the same polymer.

The absence of an absorption band at 870 cm<sup>-1</sup> revealed this polymer to be not syndiotactic and the absorption bands at 840, 842 and 1047 cm<sup>-1</sup> confirmed the synthesized polymer to be isotactic [29]. Both synthesized polymer samples (Fig. 2a and b) showed evidence of a crystalline character in view of the absorption bands in the region of 1296–1294 cm<sup>-1</sup>. The spectra of the synthesized products agreed well with the spectrum of the standard poly- $\epsilon$ -caprolactone of a similar number averaged molecular weight ( $M_n \approx 10,000$  Da) and with the data reported in the literature [27,30,31].

#### 3.1.2. Proton NMR analysis

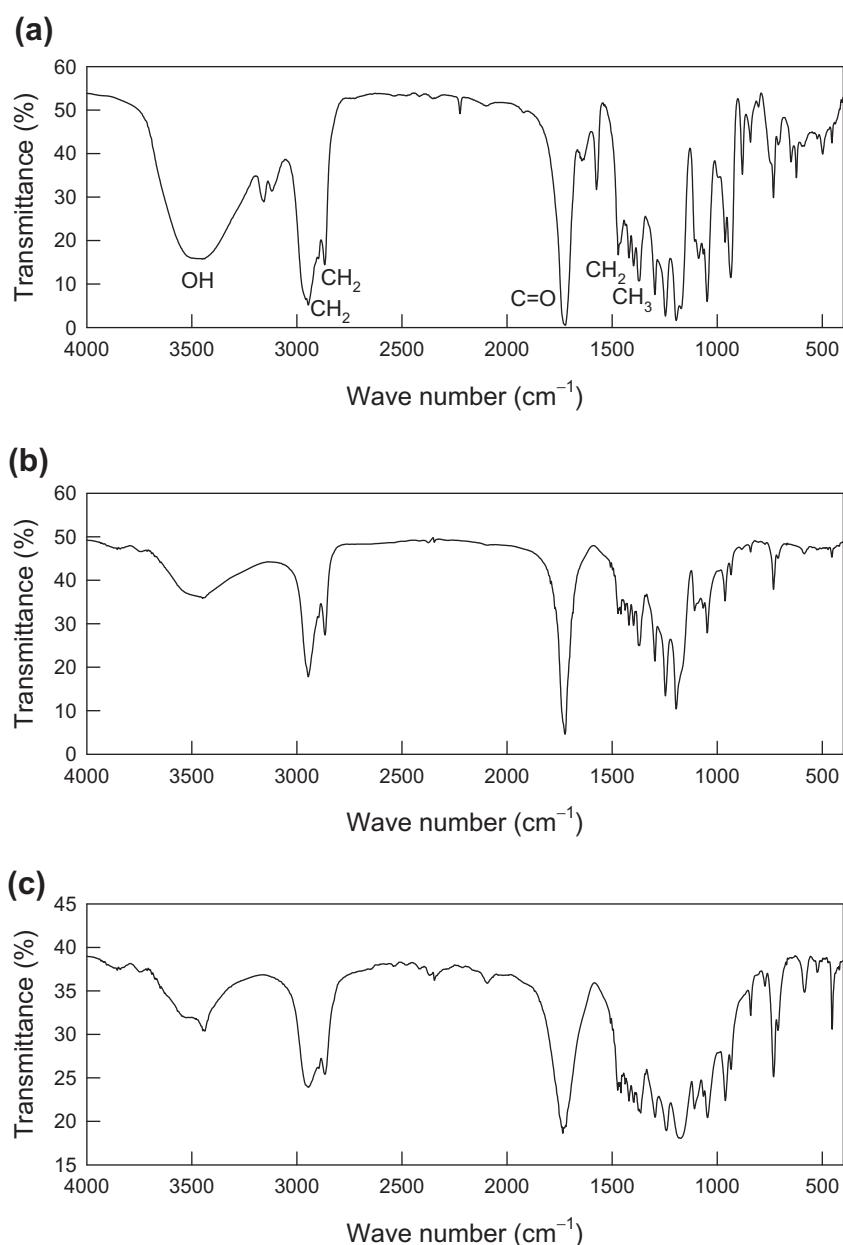
A comparison of the <sup>1</sup>H NMR spectra of the synthesized products (Fig. 3a and b) with the spectrum of the poly-6-hydroxyhexanoate standard (Fig. 3c), and the other literature data [6,30] confirmed the product samples to be poly-6-hydroxyhexanoate.

In the spectra in Fig. 3, the triplet chemical shifts *a* ( $\delta = 2.39$  ppm) were due to the methylene protons located at the  $\alpha$ -positions of the ester carbonyl carbons. The broad quartet chemical shifts *b*, *d* at 1.66 ppm (Fig. 3a–c) were attributed to the methylene protons located at positions  $\beta$  and  $\delta$  of the ester group, respectively. The broad quartet chemical shifts *c* at 1.37 ppm were assigned to protons of methylene at the  $\gamma$ -position of the carbonyl ester. The triplets *e* at 4.17 ppm were ascribed to the methylene protons of position  $\epsilon$  of the ester group. The narrow triplet chemical shifts *f* (3.66 ppm) were due to the carbinol protons. The further triplets at 4.20 ppm originated from the methylene protons in the dimer [30,32].

### 3.2. Thermal analysis

Differential scanning calorimetry (DSC) and thermogravimetric analysis (TGA) were used to further characterize the synthesized polymers. The DSC thermograms of the polymer samples are shown in Fig. 4.

The polymer produced via ultrasound assisted synthesis had a melting temperature ( $T_m$ ) of 58.46 °C (Fig. 4) which was in good agreement with the literature [33]. The melting temperature of the polymer produced using the nonsonicated synthesis was



**Fig. 2.** FTIR spectra of poly-6-hydroxyhexanoate synthesized at 55 °C: (a) 8 h of reaction after 10 min of sonication; (b) 24 h of reaction without sonication; (c) standard poly-6-hydroxyhexanoate ( $M_n \approx 10,000$  Da).

significantly lower at 49.84 °C (Fig. 4). This lower than expected melting temperature could be explained by a low molecular weight ( $M_w$ ) of the product formed in the absence of sonication as clearly seen in Table 1. In sonicated synthesis, polymerization reaction proceeded faster (Table 1) and for longer because the microstreaming associated with sonication improved mass transfer of the monomer to the active site of the enzyme in a reaction mixture that became increasingly viscous with time and therefore increasingly mass transfer limited [34].

The higher molecular weight of the polymer formed under sonication was confirmed directly by gel permeation chromatography as well as by a higher DSC endothermic enthalpy of fusion ( $\Delta H_f$ ) of 86.38 J g<sup>-1</sup> compared to a much lower  $\Delta H_f$  value of 39.29 J g<sup>-1</sup> for the product formed via nonsonicated synthesis. Endothermic enthalpy of melting is known to decrease with a decrease in molecular weight of a polymer [35].

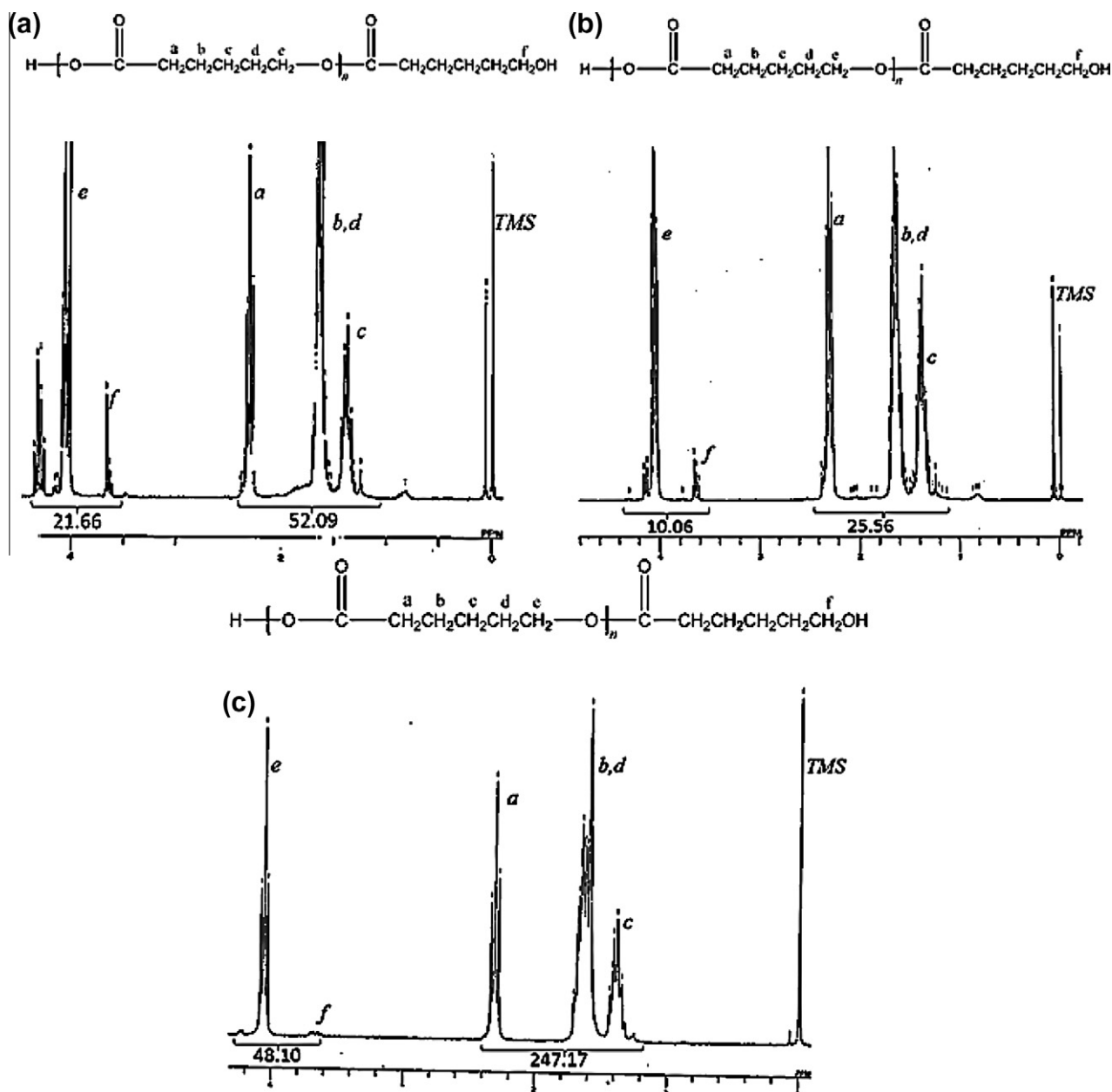
Using the measured endothermic melting enthalpy ( $\Delta H_f$ ) and the melting temperature ( $T_m$ ), the entropy of fusion ( $\Delta S_f$ ) could be calculated as follows:

$$\Delta S_f = \frac{\Delta H_f}{T_m} \quad (2)$$

The  $\Delta S_f$  values were 1.48 J g<sup>-1</sup> °C<sup>-1</sup> for the polymer produced under sonication and 0.79 J g<sup>-1</sup> °C<sup>-1</sup> for the material produced without sonication. Therefore, the polymer produced by sonicated synthesis had a higher degree of crystallinity compared to the polymer produced without using ultrasound.

The degree of crystallinity ( $X_c$ ) of the polymer samples could be calculated directly from the DSC thermogram data using the following equation:

$$X_c = \frac{\Delta H_f}{\Delta H_f^0} \quad (3)$$



**Fig. 3.**  $^1\text{H}$  NMR spectra of poly-6-hydroxyhexanoate synthesized at 55 °C: (a) 8 h of reaction after 10 min of sonication; (b) 24 h of reaction without sonication; (c) standard poly-6-hydroxyhexanoate ( $M_n \approx 10,000$  Da). The numbers at baselines of the peaks represent the integrated areas of the peaks.

where  $\Delta H_f^\circ$  is the endothermic melting enthalpy of the 100% crystalline poly-6-hydroxyhexanoate ( $142 \text{ J g}^{-1}$ ) as reported in the literature [28]. Using the above equation, the polymer made via sonicated synthesis was found to have an  $X_c$  value of 0.61 (or crystallinity of 61%). In contrast, the polymer formed without the use of ultrasound had a much lower crystallinity of 28%. The higher crystallinity achieved under sonication is explained by the microstreaming motions that occur under sonication [21] helping to align the polymer molecules to pack them more tightly together. Ultrasound has been previously reported to affect interactions between polymer molecules [34,36].

Based on thermogravimetric measurements (data not shown), the polymer samples displayed appreciable durability to thermal degradation. Most (>99%) of the polymer produced under sonication had an initial thermal degradation temperature ( $T_i$ ) of about 380 °C and a maximum thermal degradation temperature ( $T_d$ ) of

about 509 °C. The highest rate of change on the weight loss curve occurs at 420 °C. In comparison with this, only 89% of the polymer produced under nonsonicated conditions had a  $T_i$  of about 330 °C and a  $T_d$  of about 464 °C. The highest rate of change on the weight loss curve was observed at 380 °C. These differences in resistance to thermal degradation are explained primarily by the differences in the average molecular weights and the degrees of crystallinity of the different polymer samples.

### 3.3. Reaction kinetics

The  $\epsilon$ -caprolactone monomer conversion to poly-6-hydroxyhexanoate was calculated using the weight of vacuum dried product formed and the initial weight of the monomer charged into the reaction flasks. The volumetric productivity ( $\phi$ ,  $\text{g L}^{-1} \text{ h}^{-1}$ ) of the reaction system was calculated using the following equation:



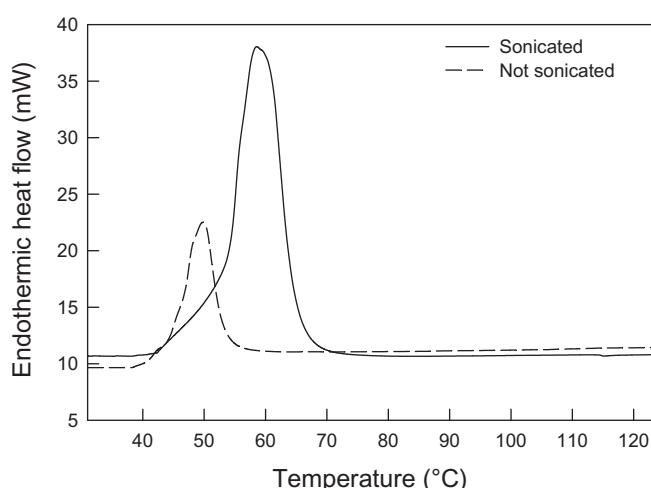


Fig. 4. Evolution of endothermic heat flow as a function of temperature.

$$\phi = \frac{[P]}{\Delta t} \quad (4)$$

where  $[P]$  is the final concentration of the polymer and  $\Delta t$  is time required for the synthesis.

The reaction conversion was calculated as the percentage of the initial monomer converted to the product. The molar rate of polymer production was calculated as the initial rate of increase in the weight of the polymer in the reaction mixture at a specified concentration of the enzyme.

The measured initial rate of monomer consumption ( $v_p$ ) in the polymerization reaction at various initial concentrations of the monomer fitted the Michaelis–Menten kinetics; thus,

$$v_p = \frac{v_{\max}[M]}{K_M + [M]} \quad (5)$$

where  $[M]$  is the concentration of the monomer,  $v_{\max}$  is the constant maximum possible reaction rate at a given concentration of the enzyme, and  $K_M$  is Michaelis constant. The  $K_M$  and  $v_{\max}$  values were determined by nonlinear regression of the data using the Polymath 6.0 software ([www.polymath-software.com](http://www.polymath-software.com)).

The catalytic constant ( $k_{\text{cat}}$ ) could be calculated from the  $v_{\max}$  value using the following equation:

$$k_{\text{cat}} = \frac{v_{\max}}{[E]_0} \quad (6)$$

where  $[E]_0$  is the concentration of the enzyme. The enzyme concentration was calculated from the known concentration of the immobilized enzyme placed in the reaction vial, the known molecular weight of the lipase B of 33,000 g mol<sup>−1</sup> and the knowledge that the immobilized enzyme preparation contained 2% (g/100 g) of active protein as reported in literature [33,37,38].

The polymer concentration is related to the monomer conversion and the number averaged molecular weight of the polymer ( $\bar{M}_n$ ), as follows:

$$[P_n] = \frac{([M]_0 - [M]_t)MW}{\bar{M}_n} \quad (7)$$

where  $[M]_0$  is the initial concentration of the monomer,  $[M]_t$  is the monomer concentration at time  $t$  and  $MW$  is the molecular weight of the monomer ( $MW = 114.14$  g mol<sup>−1</sup>). The degree of polymerization ( $X_n$ ) was calculated by using the following equation:

$$X_n = \frac{\bar{M}_n}{MW} \quad (8)$$

where  $\bar{M}_n$  is the number average molecular weight and  $MW$  is the molecular weight of the monomer.

The kinetic parameters for the reaction ( $v_{\max}$ ,  $K_M$ ,  $k_{\text{cat}}$ ,  $\phi$ ) are summarized in Table 1 for both the sonicated and nonsonicated treatments. In the monomer concentration range of 4.51–13.53 M, the catalytic constant value ( $k_{\text{cat}}$ , Table 1) for the enzyme was higher under sonicated conditions than for the nonsonicated reaction. The enzyme's specificity constant ( $k_{\text{cat}}/K_M$ ) for both the sonicated and nonsonicated treatments vary within a very narrow range. Under sonicated conditions, therefore, the enzyme was a better catalyst. Sonication likely improved the mass transfer of the monomer to the active site of the enzyme by inducing cavitation-associated microturbulence [21]. In addition, sonication may have contributed to enhancing the pulsating motions that occur within an enzyme molecule, to improve its binding–unbinding interactions with the substrate and the reactant [21]. Liu et al. [34] reported similar observations in relation to the effects of ultrasound on lipase-catalyzed hydrolysis of soy oil in a solvent-free system.

### 3.4. Volumetric productivity and monomer conversion

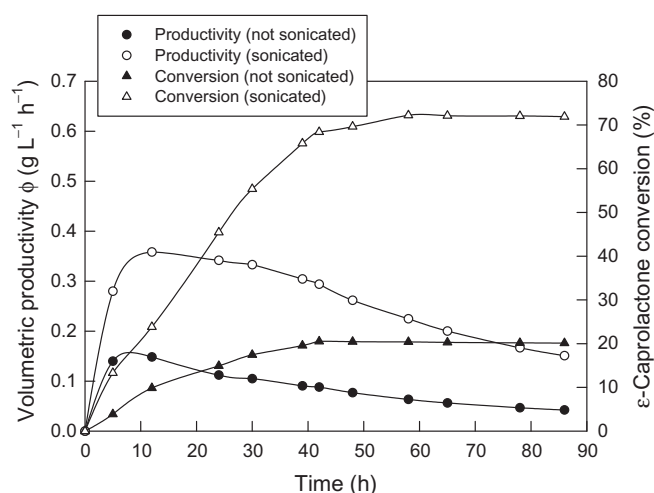
Time profiles of the volumetric productivity ( $\phi$ ) of the polymer and the monomer conversion to the product during the reaction are shown in Fig. 5. In the sonicated reaction, both the initial rate of increase in productivity and the final value are significantly greater than in the nonsonicated polymerization (Fig. 5). In both cases, after the maximum productivity has been attained, the productivity declines with time. In other words, the rate of polymerization gradually slows. This is attributed to two factors. First, as the polymer concentration in the solvent and the average molecular weight of the polymer increase, the viscosity of the reaction mixture increases and the mass transfer of the monomer to the enzyme progressively slows down. Secondly, the increasing size of the polymer molecules with time slows the diffusive transport of the polymer molecule irrespective of the viscosity of the solvent and this contributed to slowing the reaction.

The percentage conversion of the monomer increased hyperbolically with reaction time until further reaction became effectively impossible because of mass transfer limitations (Fig. 5). The maximum value of the monomer conversion was at most 20% (Fig. 5) in the nonsonicated reaction and was attained after 42 h of reaction. In contrast, under the sonicated conditions, the maximum value of the monomer conversion was nearly 2.7-fold higher at 73.2% and was attained by around 45 h (Fig. 5).

**Table 1**  
Kinetic parameters for the synthesis of poly-6-hydroxyhexanoate.

| Synthesis    | $\bar{v}_p$<br>( $\times 10^{-5}$ mol L <sup>−1</sup> s <sup>−1</sup> ) | $v_{\max}$<br>( $\times 10^{-4}$ mol L <sup>−1</sup> s <sup>−1</sup> ) | $K_M$<br>(M) | $k_{\text{cat}}$<br>( $\times 10^2$ s <sup>−1</sup> ) | $k_{\text{cat}}/K_M$<br>L (mol s) <sup>−1</sup> | $\bar{\phi}$<br>(g L <sup>−1</sup> h <sup>−1</sup> ) | $\bar{X}_n$ | $\bar{M}_n$<br>(Da) | $\bar{M}_w$<br>(Da) | Maximum<br>conversion (%) |
|--------------|---|--|--------------|---|---|--|-------------|---------------------|---------------------|---------------------------|
| Sonicated    | 5.7   | 10.1   | 17.2         | 11.1  | 64.8  | 0.20   | 53.4        | 6037                | 11,469              | 73.5                      |
| Nonsonicated | 5.3   | 0.9  | 14.4         | 10.1  | 72.2  | 0.08   | 11.4        | 1294                | 4369                | 15.7                      |

The bar above the various symbols indicates an averaged value. The maximum standard deviation was  $\pm 5\%$  of the average values shown.



**Fig. 5.** Dependence of volumetric productivity and monomer conversion on reaction time (18.04 M  $\epsilon$ -caprolactam, 1 mL [Emim][BF<sub>4</sub>], 55 °C).

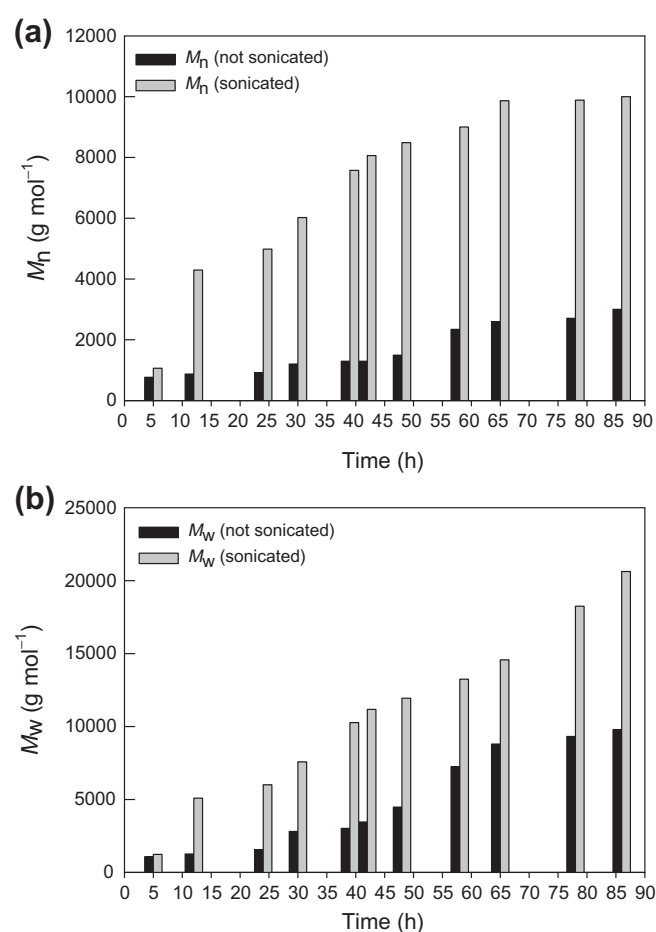
The poor conversion in the absence of sonication has been observed in prior work and has been attributed at least partly to a progressive loss of activity of the enzyme with time [39,40]. A comparable activity loss should occur also in the sonicated conditions as many enzymes are susceptible to damage by ultrasound [21]. In processes where ultrasound has damaged enzymes, sonication has nevertheless often increased the rate of the enzyme catalyzed reaction and the conversion of the substrate. This happens because the activity enhancing effect of sonication on the enzyme can commonly outweigh the damaging effect during the course of a reaction.

Another explanation for a reducing substrate conversion with time under nonsonicated conditions has been the accumulation of water produced by the reaction. As the water content of the reaction mixture increases, the reaction equilibrium tends to move towards polymer hydrolysis rather than synthesis and this reduces the net production of the polymer [41,42]. Perhaps the most important factor in slowing down the conversion, or the rate of reaction, is the progressively reduced mass transfer of the substrate to the enzyme as a consequence of the increase in viscosity because of the formation of the polymer. Sonication of course is well known to greatly enhance mixing and mass transfer in reaction systems [21,43] and therefore contributes to increasing the reaction rate and conversion relative to the nonsonicated conditions (Fig. 5).

### 3.5. Influence of sonication on the molecular weight of the polymer

Both the number average molecular weight ( $M_n$ ) of the polymer and the weight average molecular weight ( $M_w$ ) increased as the reaction progressed (Fig. 6). The final  $M_n$  and  $M_w$  values were both higher in the sonicated reaction compared to the reaction carried out conventionally (Fig. 6). Therefore, sonication clearly contributed to an increased average length of the polymer molecules. This was attributed to sonication improving the supply of the monomer to the growing polymer molecule at the active site of the enzyme, a direct consequence of improved mass transfer through microstreaming.

Sonication affected the  $M_n$  and  $M_w$  values and therefore the polydispersity index ( $PDI$ ) of the polymer. The  $PDI$  of the final product produced under sonication was substantially lower than for the product produced under conventional conditions (Table 2). A low value of  $PDI$  implies a polymer with a narrow distribution of molecular weights and better defined properties. Thus, in nonsonicated synthesis, the polymer size distribution was less well controlled.



**Fig. 6.** Number average molecular weight ( $M_n$ ) of polymer as a function of reaction time (a) and weight average molecular weight ( $M_w$ ) of polymer as a function of reaction time (b) (18.04 M  $\epsilon$ -caprolactam, 1 mL [Emim][BF<sub>4</sub>], 55 °C).

**Table 2**

Gel permeation chromatography molecular weight of poly-6-hydroxyhexanoate as a function of reaction time.

| Time (h) | Nonsonicated synthesis |            |       | Sonicated synthesis |            |       |
|----------|------------------------|------------|-------|---------------------|------------|-------|
|          | $M_n$ (Da)             | $M_w$ (Da) | $PDI$ | $M_n$ (Da)          | $M_w$ (Da) | $PDI$ |
| 5        | 766                    | 1075       | 1.40  | 1066                | 1235       | 1.16  |
| 12       | 874                    | 1260       | 1.44  | 4294                | 5091       | 1.19  |
| 24       | 921                    | 1558       | 1.69  | 4983                | 6003       | 1.20  |
| 30       | 1202                   | 2804       | 2.33  | 6024                | 7573       | 1.26  |
| 39       | 1294                   | 3015       | 2.33  | 7575                | 10,268     | 1.36  |
| 42       | 1294                   | 3456       | 2.67  | 8061                | 11,177     | 1.40  |
| 48       | 1492                   | 4477       | 3.00  | 8489                | 11,942     | 1.41  |
| 58       | 2345                   | 7245       | 3.09  | 9001                | 13,245     | 1.47  |
| 65       | 2596                   | 8795       | 3.39  | 9867                | 14,567     | 1.48  |
| 78       | 2707                   | 9321       | 3.44  | 9887                | 18,243     | 1.85  |
| 86       | 3003                   | 9785       | 3.26  | 9998                | 20,626     | 2.06  |

During the early part of the reaction, the  $PDI$  values for the polymer produced under both sonicated and nonsonicated conditions were relatively low and similar (Table 2). This was attributed to a high solvation power of the ionic solvent for the polymer being formed [44]. In a reaction medium with a high solvation power, the polymer being produced remains dissolved and the polymer molecules remain relatively well dispersed so that mass transfer of the monomer to the growing polymer remains good. As the polymerization reaction progresses, the polymer concentration and the average molecular weight become such that mass transfer becomes poorer unless an external agent such as ultrasound is used to counter this effect.

Ultrasound also has the potential for increasing the effective nucleophile concentration in a reaction medium by splitting water to create hydrogen and hydroxyl radicals [45] and this can result in an enhanced rate of chain propagation and monomer conversion. This can also result in an increased rate of polymer hydrolysis and chain cleavage to reduce the average molecular weight [46,47].

### 3.6. Effects of enzyme loading

In separate studies, the ring opening polymerization reaction to produce poly-6-hydroxyhexanoate was carried out at the immobilized lipase concentrations ranging from 8 to 20 g L<sup>-1</sup>. The effects of enzyme concentration on the rate of polymerization ( $v_p$ ) and the monomer conversion are shown in Fig. 7 for the sonicated and nonsonicated reaction systems.

In view of Eq. (6), an increased loading of the enzyme is expected to increase the value of the constant  $v_{\max}$  and, therefore, the rate of the polymerization is expected to increase for a given initial concentration of the monomer, as in Eq. (5). The results in Fig. 7a for the sonicated synthesis therefore concur with expectations. For the nonsonicated synthesis, increasing the enzyme concentration had a relatively minor impact on the conversion (Fig. 7b) and barely any effect on the rate of polymerization once the enzyme concentration was  $\geq 12$  g L<sup>-1</sup>. Similar results were reported [34] in a study of the effects of ultrasound on lipase-catalyzed hydrolysis of soy oil in a solvent-free system. This behavior

is readily explained. As the enzyme is added in the form of particles, a high concentration of the enzyme produces relatively viscous slurry, which is difficult to mix. Poor mixing reduces mass transfer and the rate of reaction fails to increase with increasing concentration of the enzyme. As a consequence of the turbulence enhancing effect of ultrasound, the sonicated reaction system remains well mixed up to a high concentration of the enzyme and the reaction rate therefore continues to increase as more enzyme is added. In a sonicated system, the rate of hydrolysis of soy oil was found [34] to increase linearly with increasing concentration of the lipase particles up to an enzyme loading of 20 g L<sup>-1</sup>. Concomitantly, the results also indicated that for a particular enzyme concentration used, the turnover number (mol product (mol enzyme)<sup>-1</sup>) is consistently higher for the sonicated treatments as compared to the non-sonicated ones (Fig. 7b).

## 4. Conclusions

In lipase-mediated synthesis of poly-6-hydroxyhexanoate via ring opening polymerization of  $\epsilon$ -caprolactone in an ionic solvent, ultrasonic irradiation of the reaction system greatly enhanced the rate of polymerization and the extent of the monomer conversion to the product. Sonication improved the quality of the polymer produced, by enhancing its molecular weight, increasing its crystallinity and reducing its polydispersity relative to the polymer formed under nonsonicated control conditions. The observed effects of ultrasound could be explained by an improved mass transfer in the reaction system and an enhanced turnover number of the enzyme subjected to sonication-induced microstreaming.

## Acknowledgement

The authors acknowledged the financial assistance from the University of Malaya (Grant No. UM.C/625/1/HIR/MOHE/05).

## References

- [1] E. Grothe, M. Moo-Young, Y. Chisti, Fermentation optimization for the production of poly( $\beta$ -hydroxybutyric acid) microbial thermoplastic, *Enzyme and Microbial Technology* 25 (1999) 132–141.
- [2] P. Zinck, One-step synthesis of polyesters specialties for biomedical applications, *Reviews in Environmental Science and Biotechnology* 8 (2009) 231–234.
- [3] M.A. Woodruff, D.W. Hutmacher, Resorbable composite scaffolds for bone tissue engineering, in: *Tissue and Cell Engineering Society (TCES), TCES, Manchester, 2010*.
- [4] J.T. Gorko, K. Okrasa, A. Louwagie, R.J. Kazlauskas, F. Sreinc, Enzymatic synthesis of poly(hydroxyalkanoates) in ionic liquids, *Journal of Biotechnology* 132 (2007) 306–313.
- [5] L.S. Nair, C.T. Laurencin, Biodegradable polymers as biomaterials, *Progress in Polymer Science* 32 (2007) 762–798.
- [6] F. He, S. Li, H. Garreau, M. Vert, R. Zhuo, Enzyme-catalyzed polymerization and degradation of copolymers of [ $\epsilon$ ]-caprolactone and [ $\gamma$ ]-butyrolactone, *Polymer* 46 (2005) 12682–12688.
- [7] A.C. Albertsson, R.K. Srivastava, Recent developments in enzyme-catalyzed ring-opening polymerization, *Advanced Drug Delivery Reviews* 60 (2008) 1077–1093.
- [8] S.K. Arumugasamy, Z. Ahmad, *Candida antarctica* as catalyst for polycaprolactone synthesis: effect of temperature and solvents, *Asia-Pacific Journal of Chemical Engineering* 6 (2011) 398–405.
- [9] D. Knani, A.L. Gutman, D.H. Kohn, Enzymatic polyesterification in organic media. Enzyme catalyzed synthesis of linear polyesters. I. Condensation polymerization of linear hydroxyesters. II. Ring opening polymerization of caprolactone, *Journal of Polymer Science Part A: Polymer Chemistry* 31 (1993) 1221–1232.
- [10] A. Kumar, R.A. Gross, *Candida antarctica* lipase B catalyzed polycaprolactone synthesis: effects of organic media and temperature, *Biomacromolecules* 1 (2000) 133–138.
- [11] H. Uyama, S. Kobayashi, Enzymatic ring-opening polymerization of lactones catalyzed by lipase, *Chemistry Letters* (1993) 1149–1150.
- [12] J. Gorko, F. Sreinc, R. Kazlauskas, Toward advanced ionic liquids. Polar, enzyme-friendly solvents for biocatalysis, *Biotechnology and Bioprocess Engineering* 15 (2010) 40–53.

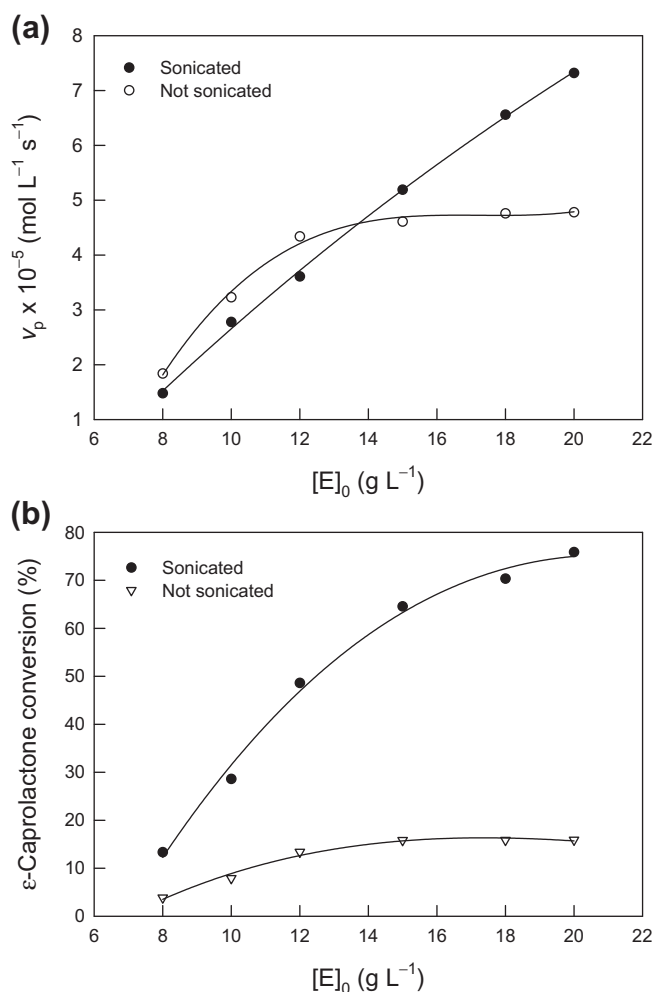


Fig. 7. Polymerization reaction rate  $v_p$  (a) and monomer conversion (b) as functions of enzyme loading  $[E]_0$  (18.04 M  $\epsilon$ -caprolactam, 1 mL [Emim][BF<sub>4</sub>], 55 °C).



- [13] N. Jacquél, C.W. Lo, H.S. Wu, Y.H. Wei, S.S. Wang, Solubility of polyhydroxyalkanoates by experiment and thermodynamic correlations, *AIChE Journal* 53 (2007) 2704–2714.
- [14] P. Wasserscheid, T. Welton, *Ionic Liquids in Synthesis*, Wiley Online Library, 2003.
- [15] S. Kobayashi, Lipase-catalyzed polyester synthesis – a green polymer chemistry, *Proceedings of the Japan Academy Series B: Mathematical Sciences* 86 (2010) 338–365.
- [16] T.D. Matos, N. King, L. Simmons, C. Walker, A.R. McClain, A. Mahapatro, F.J. Rispoli, K.T. McDonnell, V. Shah, Microwave assisted lipase catalyzed solvent-free poly-ε-caprolactone synthesis, *Green Chemistry Letters and Reviews* 4 (2011) 73–79.
- [17] A. Sosnik, G. Gotelli, G.A. Abraham, Microwave-assisted polymer synthesis (MAPS) as a tool in biomaterials science: how new and how powerful, *Progress in Polymer Science* 36 (2011) 1050–1078.
- [18] R. García-Arrazola, D.A. López-Guerrero, M. Gimeno, E. Bárzana, Lipase-catalyzed synthesis of poly-L-lactide using supercritical carbon dioxide, *The Journal of Supercritical Fluids* 51 (2009) 197–201.
- [19] P. Kubisa, Ionic liquids as solvents for polymerization processes – progress and challenges, *Progress in Polymer Science* 34 (2009) 1333–1347.
- [20] K.J. Thurecht, S. Villarroya, Biocatalytic polymerization in exotic solvents, *Biocatalysis in Polymer Chemistry*, Wiley VCH Verlag GmbH & Co. KGaA, 2010, pp. 323–348.
- [21] Y. Chisti, Sonobioreactors: using ultrasound for enhanced microbial productivity, *Trends in Biotechnology* 21 (2003) 89–93.
- [22] E.M. Anderson, K.M. Larsson, O. Kirk, One biocatalyst-many applications: the use of *Candida antarctica* B-lipase in organic synthesis, *Biocatalysis and Biotransformation* 16 (1998) 181–204.
- [23] R. Sharma, Y. Chisti, U.C. Banerjee, Production, purification, characterization, and applications of lipases, *Biotechnology Advances* 19 (2001) 627–662.
- [24] P. Dubois, O. Coulembier, J.M. Raquez, *Handbook of Ring-Opening Polymerization*, Wiley Online Library, 2009.
- [25] C. Li, T. Tan, H. Zhang, W. Feng, Analysis of the conformational stability and activity of *Candida antarctica* lipase B in organic solvents, *Journal of Biological Chemistry* 285 (2010) 28434.
- [26] J. Ottosson, *Enthalpy and Entropy in Enzyme-Catalysis: A Study of Lipase Enantioselectivity*, Royal Institute of Technology, Stockholm, Sweden, 2001, p. 12.
- [27] J. Ma, Q. Li, B. Song, D. Liu, B. Zheng, Z. Zhang, Y. Feng, Ring-opening polymerization of μ-caprolactone catalyzed by a novel thermophilic esterase from the archaeon *Archaeoglobus fulgidus*, *Journal of Molecular Catalysis B: Enzymatic* 56 (2009) 151–157.
- [28] T. Elzein, M. Nasser-Eddine, C. Delaite, S. Bistac, P. Dumas, FTIR study of polycaprolactone chain organization at interfaces, *Journal of Colloids and Interface Science* 273 (2004) 381–387.
- [29] B.H. Stuart, *Polymer Analysis*, Wiley, 2002.
- [30] F.C. Oliveira, M.L. Dias, L.R. Castilho, D.M.G. Freire, Characterization of poly(3-hydroxybutyrate) produced by *Cupriavidus necator* in solid-state fermentation, *Bioresource Technology* 98 (2007) 633–638.
- [31] M.C. Sin, M.S.M. Annuar, I.K.P. Tan, S.N. Gan, Thermodegradation of medium-chain-length poly(3-hydroxyalkanoates) produced by *Pseudomonas putida* from oleic acid, *Polymer Degradation and Stability* 95 (2010) 2334–2342.
- [32] K.J. Thurecht, A. Heise, d. Matthijs, S. Villarroya, J. Zhou, M.F. Wyatt, S.M. Howdle, Kinetics of enzymatic ring-opening polymerization of ε-caprolactone in supercritical carbon dioxide, *Macromolecules* 39 (2006) 7967–7972.
- [33] L. van der Mee, F. Helmich, R. de Bruijn, J.A.J.M. Vekemans, A.R.A. Palmans, E.W. Meijer, Investigation of lipase-catalyzed ring-opening polymerizations of lactones with various ring sizes: kinetic evaluation, *Macromolecules* 39 (2006) 5021–5027.
- [34] Y. Liu, Q. Jin, L. Shan, W. Shen, X. Wang, The effect of ultrasound on lipase-catalyzed hydrolysis of soy oil in solvent-free system, *Ultrasonics Sonochemistry* 15 (2008) 402–407.
- [35] H.Y. Kweon, M.K. Yoo, I.K. Park, T.H. Kim, H.C. Lee, H.S. Lee, J.S. Oh, T. Akaike, C.S. Cho, A novel degradable polycaprolactone networks for tissue engineering, *Biomaterials* 24 (2003) 801–808.
- [36] L. Gebicka, J.L. Gekicki, The effect of ultrasound on heme enzymes in aqueous solution, *Journal of Enzyme Inhibition and Medicinal Chemistry* 12 (1997) 133–141.
- [37] F. Secundo, G. Carrea, C. Soregaroli, D. Varinelli, R. Morrone, Activity of different *Candida antarctica* lipase B formulations in organic solvents, *Biotechnology and Bioengineering* 73 (2001) 157–163.
- [38] H.K. Weber, H. Stecher, K. Faber, Some properties of commercially available crude lipase preparations, *Preparative Biotransformations* (1995) 5–21.
- [39] A.G. Marangoni, *Enzyme Kinetics: A Modern Approach*, John Wiley and Sons, 2003.
- [40] S. Schnell, P.K. Maini, Enzyme kinetics at high enzyme concentration, *Bulletin of Mathematical Biology* 62 (2000) 483–499.
- [41] M. Matsumoto, D. Odachi, K. Kondo, Kinetics of ring-opening polymerization of lactones by lipase, *Biochemical Engineering Journal* 4 (1999) 73–76.
- [42] Y. Mei, A. Kumar, R.A. Gross, Probing water-temperature relationships for lipase-catalyzed lactone ring-opening polymerizations, *Macromolecules* 35 (2002) 5444–5448.
- [43] Y. Xiao, Q. Wu, Y. Cai, X. Lin, Ultrasound-accelerated enzymatic synthesis of sugar esters in nonaqueous solvents, *Carbohydrate Research* 340 (2005) 2097–2103.
- [44] S.J. Nara, J.R. Harjani, M.M. Salunkhe, A.T. Mane, P.P. Wadgaonkar, Lipase-catalysed polyester synthesis in 1-butyl-3-methylimidazolium hexafluorophosphate ionic liquid, *Tetrahedron Letters* 44 (2003) 1371–1373.
- [45] J. Kurja, Some Outstanding Problems Concerning Heterogeneous Polymerization in Aqueous Media, Eindhoven University of Technology, Eindhoven, The Netherlands, 1997.
- [46] L.A. Henderson, Y.Y. Svirkin, R.A. Gross, D.L. Kaplan, G. Swift, Enzyme-catalyzed polymerizations of ε-caprolactone: effects of initiator on product structure, propagation kinetics, and mechanism, *Macromolecules* 29 (1996) 7759–7766.
- [47] S. Namekawa, S. Suda, H. Uyama, S. Kobayashi, Lipase-catalyzed ring-opening polymerization of lactones to polyesters and its mechanistic aspects, *International Journal of Biological Macromolecules* 25 (1999) 145–151.

# CHAPTER 6

## Lipase catalyzed ultrasonic synthesis of poly-4-hydroxybutyrate-co-6-hydroxyhexanoate

---

**A. M. Gumel<sup>1</sup>, M. S. M. Annuar<sup>1\*</sup>, Y. Chisti<sup>2</sup>**

*<sup>1</sup> Institute of Biological Sciences,*

*Faculty of Science, University of Malaya, Kuala Lumpur 50603, Malaysia*

*<sup>2</sup> School of Engineering, PN 456, Massey University, Private Bag 11 222, Palmerston North, New Zealand*

**Published:** *Ultrasonics Sonochemistry* (2013) **20(3)**:937-947

(ISI cited publication: tier 1)

### Statement of contributions of joint Authorship

**Gumel, A.M:** (Candidate)

Writing and compilation of manuscript, established methodology, data collection, presentation and analyses. Main author of the manuscript

**Annuar, M.S.M:** (Principal Supervisor)

Supervised and assisted with manuscript compilation, editing and co-author of the manuscript.

**Chisti, Y:** (Research collaborator)

Editing and co-author of manuscript



Contents lists available at SciVerse ScienceDirect

## Ultrasonics Sonochemistry

journal homepage: [www.elsevier.com/locate/ultson](http://www.elsevier.com/locate/ultson)

## Lipase catalyzed ultrasonic synthesis of poly-4-hydroxybutyrate-co-6-hydroxyhexanoate

A.M. Gumel<sup>a</sup>, M.S.M. Annuar<sup>a,\*</sup>, Y. Chisti<sup>b</sup><sup>a</sup> Institute of Biological Sciences, Faculty of Science, University of Malaya, 50603 Kuala Lumpur, Malaysia<sup>b</sup> School of Engineering, PN 456, Massey University, Private Bag 11 222, Palmerston North, New Zealand

## ARTICLE INFO

## Article history:

Received 6 June 2012

Received in revised form 5 September 2012

Accepted 14 September 2012

Available online 23 November 2012

## Keywords:

Biocopolymers

Lipases

Polyhydroxyalkanoates

Ultrasound

## ABSTRACT

Four different lipases were compared for ultrasound-mediated synthesis of the biodegradable copolymer poly-4-hydroxybutyrate-co-6-hydroxyhexanoate. The copolymerization was carried out in chloroform. Of the enzymes tested, Novozym 435 exhibited the highest copolymerization rate, in fact the reaction rate was observed to increase with about 26-fold from 30 to 50 °C ( $7.9 \times 10^{-3} \text{ M s}^{-1}$ ), sonic power intensity of  $2.6 \times 10^3 \text{ W m}^{-2}$  and dissipated energy of  $130.4 \text{ J ml}^{-1}$ . Copolymerization rates with the *Candida antarctica* lipase A, *Candida rugosa* lipase, and Lecitase Ultra™ were lower at  $2.4 \times 10^{-4}$ ,  $1.3 \times 10^{-4}$  and  $3.5 \times 10^{-4} \text{ M s}^{-1}$ , respectively. The catalytic efficiency depended on the enzyme. The efficiency ranged from  $4.15 \times 10^{-3} \text{ s}^{-1} \text{ M}^{-1}$  for Novozym 435– $1.48 \times 10^{-3} \text{ s}^{-1} \text{ M}^{-1}$  for *C. rugosa* lipase. Depending on the enzyme and sonication intensity, the monomer conversion ranged from 8.2% to 48.5%. The sonication power, time and temperature were found to affect the rate of copolymerization. Increasing sonication power intensity from  $1.9 \times 10^3$  to  $4.5 \times 10^3 \text{ W m}^{-2}$  resulted in an increased in acoustic pressure ( $P_a$ ) from  $3.7 \times 10^8$  to  $5.7 \times 10^8 \text{ N m}^{-2}$  almost 2.4–3.7 times greater than the acoustic pressure ( $1.5 \times 10^8 \text{ N m}^{-2}$ ) that is required to cause cavitation in water. A corresponding acoustic particle acceleration ( $a$ ) of  $9.6 \times 10^3$ – $1.5 \times 10^4 \text{ m s}^{-2}$  was calculated i.e. approximately 984–1500 times greater than under the action of gravity.

© 2012 Elsevier B.V. All rights reserved.

## 1. Introduction

Polyhydroxyalkanoates are polyesters that can be produced from various monomers by the action of lipases [1,2]. In aqueous media, lipases catalyze the hydrolysis of ester bonds, but in a milieu with sparing quantities of water they catalyze ester synthesis to produce polyesters and other products [1]. A wide range of PHA homopolymers, copolymers and functionalized copolymers can be produced using enzyme catalysis [2]. Compared to nonenzymatic forms of catalysis, lipases offer an excellent enantiomeric selectivity, specificity and catalytic activity under mild reaction conditions [2,3], but lipase-catalyzed production of copolymers is often slow and troubled by low yields. The copolymer formed often has a relatively low molecular weight. Some of these problems are associated with a poor mass transfer of the monomer to the growing copolymer chain at the active site of the enzyme. The mass transfer becomes poorer as the reaction proceeds, the copolymer chain lengthen and the viscosity of the reaction medium increases. Attempts have been made to improve lipase-mediated copolymerization through various methods [4–6]. In this respect, the use of

ultrasonic irradiation of the reaction mixture has proven to be particularly promising [1,7–12]. It has been mentioned that the chemical effects of ultrasound process are derived primarily from acoustic cavitation [13,14]. In this process the cavitation bubble collapse results in the release of an enormous amount of energy and temperature into the dissipating liquids. The induction of these short-lived high temperatures and pressures, combined with extraordinarily rapid cooling are said to highly influence the derivation of chemical reactions [13].

Ultrasound has been used to improve many biocatalytic processes [4,6,9,15]. Sonication generates extreme and rapid cyclic pressure changes in a fluid [9,11,12]. During the rarefaction phase of sonication microbubbles of gas and vapor are produced by cavitation [15–17]. In the compression phase, these bubbles implode to generate a violent shock wave that propagates through the fluid [18,19]. Intense turbulence is produced. This improves the mass transfer, dispersion of phases and promotes deagglomeration of the reactants [20]. Motion at the level of enzyme and monomeric molecules may be induced by sonication to influence the interactions of the reactants at the active site [1]. All these factors affect the rate of the reaction. Activity and stability of enzymes is also affected by sonication [21], especially at high transmission of acoustic power (high cavitation threshold), which result in the

\* Corresponding author. Tel.: +60 379674003; fax: +60 379677182.

E-mail address: [suffian\\_annuar@um.edu.my](mailto:suffian_annuar@um.edu.my) (M.S.M. Annuar).

## Nomenclature

|                |   |                      |   |
|----------------|---|----------------------|---|
| $A$            | volumetric area ( $\text{cm}^2$ )                                     | $K_M^{\text{CB}}$    | equilibrium constant (M)  |
| $a$            | particle acceleration ( $\text{m s}^{-2}$ )                           | $K_M^{\text{BC}}$    | equilibrium constant (M)  |
| $[B]$          | concentration of $\gamma$ -butyrolactone (M)                          | $k$                  | ultrasonic polymer degradation rate constant ( $\text{s}^{-1}$ )            |
| $[B]_0$        | initial value of $[B]$ (M)  | $k_{\text{cat}}$     | turnover number ( $\text{s}^{-1}$ )   |
| $[B]_t$        | value of $[B]$ at time $t$ (M)  | $M_n$                | number averaged molecular weight (Da)                                       |
| $[C]$          | concentration of $\epsilon$ -caprolactone (M)                         | $M_w$                | weight averaged molecular weight (Da)                                       |
| $[C]_0$        | initial value of $[C]$ (M)  | PDI                  | polydispersity index  |
| $[C]_t$        | value of $[C]$ at time $t$ (M)  | PHA                  | polyhydroxyalkanoate  |
| $c$            | speed of sound ( $\text{m s}^{-1}$ )                                  | $P_A$                | amplitude pressure ( $\text{N m}^{-2}$ )                                    |
| DSC            | differential scanning calorimeter                                     | $P_a$                | acoustic pressure (atm)   |
| $[E]$          | concentration of enzyme (M)   | ROP                  | ring opening copolymerization   |
| $[EB]$         | concentration of the enzyme–butyrolactone complex EB (M)              | $\Delta S_f$         | endothermic entropy of fusion ( $\text{J g}^{-1} \text{ } ^\circ\text{C}$ ) |
| $[EC]$         | concentration of the enzyme–caprolactone complex EC (M)               | TGA                  | thermogravimetric analysis  |
| $[ECB]$        | concentration of the enzyme–monomer complex ECB (M)                   | $T_d$                | average degradation temperature ( $^\circ\text{C}$ )                        |
| $[E_T]$        | total concentration of the enzyme (M)                                 | $T_m$                | melting temperature ( $^\circ\text{C}$ )                                    |
| $f$            | frequency (Hz)  | $v$                  | rate of copolymerization ( $\text{M s}^{-1}$ )                              |
| GPC            | gel permeation chromatography   | $v_{\text{max}}$     | the maximum reaction rate ( $\text{M s}^{-1}$ )                             |
| $\Delta H_f$   | endothermic melting enthalpy ( $\text{J g}^{-1}$ )                    | $V$                  | reaction volume (ml)  |
| $\Delta H_f^0$ | endothermic melting enthalpy of the 100% crystalline polycaprolactone | $v_p$                | maximum particle velocity ( $\text{M s}^{-1}$ )                             |
| $I$            | sonic power intensity ( $\text{W m}^{-2}$ )                           | $X_p$                | apparent degree of crystallinity  |
| $K_S^B$        | equilibrium constant (M)  | <b>Greek letters</b> |   |
| $K_S^C$        | equilibrium constant (M)  | $\eta$               | catalytic efficiency ( $\text{s}^{-1} \text{ m}^{-1}$ )                     |
|                |   | $\sigma$             | variance  |
|                |   | $\rho$               | bulk density ( $\text{kg m}^{-3}$ )   |
|                |   | $\xi$                | particle displacement (m)   |

deleterious effect on the reactant and the products due to the excessive increase in cavitation bubbles violent collapse [15].

This work is concerned with ultrasound-mediated lipase-catalyzed copolymerization of the biodegradable copolymer poly-4-hydroxybutyrate-co-6-hydroxyhexanoate from a mixture of  $\gamma$ -butyrolactone and  $\epsilon$ -caprolactone. Four different lipases are compared for use in this reaction, including three soluble lipases and one immobilized lipases. The use of the lipase preparation Lecitase Ultra™ for the copolymerization of polyhydroxyalkanoates is reported for the first time.

## 2. Materials and methods

### 2.1. Materials

All materials used were of analytical grade, unless otherwise stated. The organic solvents (chloroform, tetrahydrofuran, methanol) and the monomers ( $\gamma$ -butyrolactone,  $\epsilon$ -caprolactone) were purchased from Merck (Merck, USA). The lipases (*Candida antarctica* lipase B, Novozym® 435; *C. antarctica* lipase A; *Candida rugosa* lipase; Lecitase Ultra™, phospholipase A1 from *Thermomyces lanuginosus*) were purchased from Sigma Aldrich (Sigma Aldrich, USA). Of the enzymes used, the Novozym® 435 was an immobilized preparation and the others were used as dissolved enzymes.

### 2.2. Methods

#### 2.2.1. Enzyme activity

The activities of the lipases were measured as reported by Teng and Xu [22] in both ultrasonic bath (Elmasonic P30H; Elma, Germany) and conventional automatic shaking incubator (Daihan Lab-Tech® Korea). Thus the enzymes (immobilized Novozym® 435 and unbound Lecitase Ultra™, *C. antarctica* lipase A and *C. rugosa* lipase) each at  $20 \text{ U mL}^{-1}$  of reaction mixture was added to a vial

containing 10 mL of a 10 mM 4-nitrophenyl palmitate solution in *n*-hexane. To this mixture 60  $\mu\text{L}$  of 1 M absolute ethanol was added. The resulting slurry was sonicated at 37 kHz,  $30^\circ\text{C}$ , 1.2 W of sonication power and  $0.38 \text{ W cm}^{-2}$  power intensity; or at 200 rpm,  $30^\circ\text{C}$  in conventional automatic shaking process. In each system, the reaction was allowed to proceed for a period of 80 min. Aliquots (30  $\mu\text{L}$  each) of the reaction mixture were withdrawn at intervals and quenched by mixing with 1 mL of 0.1 M NaOH in a quartz cuvette. The 4-nitrophenol liberated by the reaction was measured at 412 nm (UV–Vis spectrophotometer V-630; Jasco, Japan) against a blank of distilled water. The enzyme activity was calculated as the slope of a plot of 4-nitrophenol released versus time.

#### 2.2.2. Ultrasonic assisted enzymatic ring opening copolymerization (ROP)

Triplicate reaction vials of 20 mL volume were used in all experiments. Each vial contained chloroform (10 mL),  $\epsilon$ -caprolactone (5 mM) and  $\gamma$ -butyrolactone (3 mM). To this mixture, 0.2 g of the enzyme catalyst was added to initiate the reaction. All reaction vials were sonicated in an ultrasound bath (Elmasonic P30H; Elma, Germany) operated at 37 kHz,  $40^\circ\text{C}$ , and 0.8 W of the sonication power and  $0.19 \text{ W cm}^{-2}$  power intensity, unless stated otherwise. Aliquot samples (20  $\mu\text{L}$ ) of the reaction mixture were withdrawn at specific intervals, mixed with 5  $\mu\text{L}$  of absolute ethanol, diluted with 1.0 mL chloroform and immediately filtered. The residual monomers were then measured.

At the end of the reaction, the copolymer was extracted by diluting the reaction mixture with 20 mL of chloroform, followed by filtration using glass fritted Buchner filter funnel. The filtrate was then concentrated to about 3 mL at  $50^\circ\text{C}$  under reduced pressure. Subsequently, the copolymer was precipitated by adding to the concentrate 10 mL of cold methanol ( $4^\circ\text{C}$ ). The solvent was then decanted and the precipitated copolymer was washed with ethoxyethane. A minimum of three washes was used to remove

traces of the unreacted monomers and oligomers from the copolymer. The copolymer was purified by a further three-stage precipitation. At each stage, the copolymer was dissolved in chloroform (3 mL), added to cold methanol (10 mL, 4 °C) and the white precipitate is recovered. The final extracted product was dried to a constant weight at room temperature at 30 °C under vacuum. A portion of the dried sample was subsequently subjected to further authentication analyses.

### 2.2.3. Quantification of residual monomers

The residual monomers were quantified by GCMSMS. An Agilent triple quadrupole 7000B instrument (Agilent, USA) equipped with GCMSMS triple axis detector carrying Agilent HP-5 ms column (30 m long  $\times$  0.25 mm internal diameter  $\times$  0.25  $\mu$ m film thickness), was used. A sample (1  $\mu$ L) was automatically injected into the GCMSMS at a split ratio of 1:50. The injection temperature was 280 °C. The column oven temperature profile was as follows: 40 °C for 1 min then increased to 120 °C at 15 °C min<sup>-1</sup>; held at 120 °C for 2 min then increased to 250 °C at 10 °C min<sup>-1</sup>; then held at 250 °C for 10 min. Helium (0.41 bar) was used as the carrier gas at a flow rate of 48.3 mL min<sup>-1</sup>. Mass spectra were acquired at 1250 scan speed using electron impact energy of 70 eV at 200 °C ion-source temperature and 280 °C interface temperature. The data obtained was used to quantify the residual monomers by comparing with the relevant calibration plots prepared by analyzing standard solutions of the monomers in chloroform. Analysis of the standard solution also provided the reference peak retention time, the ion mass data and the relationship between concentration and the area under the peak.

### 2.2.4. Product authentication

FTIR-ATR spectra were recorded at room temperature (25 °C) over a range of 4000–400 cm<sup>-1</sup> using a Perkin-Elmer FTIR RX 1 spectrometer (Perkin-Elmer Inc., Wellesley, MA, USA). A sample (0.01 g) of the synthesized copolymer was dissolved in dichloromethane and smeared on the NaCl crystal window of the instrument. The spectrum was recorded after the sample had been dried under vacuum.

Proton NMR spectra were recorded on a JEOL JNM-GSX 270 FT-NMR (JOEL Ltd., Tokyo, Japan) machine at 250 MHz. About 2 mg sample was dissolved in Chloroform-D (2 mL) with tetramethylsilane (TMS) as the internal reference standard. About 1.5 mL of the dissolved mixture was filtered into an NMR tube by using a glass syringe equipped with a 0.22  $\mu$ m PTFE disposable filter (11807-25, Sartorius Stedim, Germany).

Copolymer average molecular weights were recorded on Waters 600 (Waters Corp, Milford, MA, USA) equipped with a Waters refractive index detector (model 2414) and the following gel columns (7.8 mm internal diameter  $\times$  300 mm each) in series: HR1, HR2, HR5E and HR5E Waters Styrogel HR-THF. Monodisperse polystyrene of different molecular weights ( $3.72 \times 10^2$ ,  $2.63 \times 10^3$ ,  $9.10 \times 10^3$ ,  $3.79 \times 10^4$ ,  $3.55 \times 10^5$ ,  $7.06 \times 10^5$ ,  $3.84 \times 10^6$  and  $6.77 \times 10^6$  Da) were used as standards to produce the calibration curve. The copolymer samples were dissolved in tetrahydrofuran (THF) at a concentration of 2.0 mg mL<sup>-1</sup>, filtered through a 0.22  $\mu$ m PTFE filter and then injected into the GPC (100  $\mu$ L) at 40 °C. THF at a flow rate of 1.0 mL min<sup>-1</sup> was used as the mobile phase.

Differential scanning calorimetric analyses of the synthesized copolymer were carried out using a Perkin-Elmer differential scanning calorimeter (DSC 6; Perkin-Elmer Inc., Wellesley, MA, USA). Scans were made under a nitrogen gas flow rate of 50 mL min<sup>-1</sup> and at temperatures ranging from -60 °C to 150 °C. The heating-cooling rate was 20 °C min<sup>-1</sup>.

Thermal gravimetric analyses were performed on a Perkin-Elmer TGA4000 instrument (Perkin-Elmer Inc., Wellesley, MA,

USA). The samples were heated from 50 to 900 °C at a rate of 10 °C min<sup>-1</sup> under a nitrogen gas flow rate of 20 mL min<sup>-1</sup>.

### 2.3. Calculations

The copolymerization reaction involving two monomeric substrates was assumed to follow a random sequential bi bi mechanism according to reported literature [23,24]. The reversible binding of the monomers, either  $\epsilon$ -caprolactone (C) or  $\gamma$ -butyrolactone (B), to the enzyme (E) was assumed to be rapid. The overall scheme of the reaction was hypothesized to be as in Fig. 1 where decomposition of the complex ECB to the product P is the rate-limiting step.

In view of the scheme in Fig. 1, the rate of the product formation ( $v$ ) depends on the concentration of the enzyme–monomer complex ECB, as follows:

$$v = k_{\text{cat}}[\text{ECB}] \quad (1)$$

where  $k_{\text{cat}}$  is the turnover number. From Fig. 1, the total concentration  $[\text{E}_T]$  of the enzyme in the reaction vessel is as follows:

$$[\text{E}_T] = [\text{E}] + [\text{EB}] + [\text{EC}] + [\text{ECB}] \quad (2)$$

Using Eq. (1), Eq. (2) and the definitions of the equilibrium constants  $K_S^C$ ,  $K_S^B$ ,  $K_M^{CB}$  and  $K_M^{BC}$ , the rate equation :

$$\frac{v}{v_{\text{max}}} = \frac{[\text{C}][\text{B}]}{K_S^C K_M^{CB} + K_M^{CB}[\text{C}] + K_M^{BC}[\text{B}] + [\text{C}][\text{B}]} \quad (3)$$

where the constant maximum reaction rate  $v_{\text{max}}$  is

$$v_{\text{max}} = k_{\text{cat}}[\text{E}_T] \quad (4)$$

In Eq. (3),  $K_S^B$  is related to the other equilibrium constants as follows:

$$K_S^B = \frac{K_M^{CB} K_S^C}{K_M^{BC}} \quad (5)$$

Nonlinear regression (Polymath® 6.0 software; www.polymath-software.com) was used to calculate the values of the equilibrium constants and  $v_{\text{max}}$ . The regression used the Levenberg–Marquardt (LM) algorithm involving 64 iterations.

The catalytic efficiency  $\eta$  (s<sup>-1</sup> M<sup>-1</sup>) for the complex ECB is given by

$$\eta = \frac{k_{\text{cat}}}{K_M^{BC}} \quad (6)$$

The endothermic melting enthalpy ( $\Delta H_f$ ) and the melting temperature  $T_m$  are related to endothermic entropy of fusion ( $\Delta S_f$ ) as follows:

$$\Delta S_f = \frac{\Delta H_f}{T_m} \quad (7)$$

The apparent degree of crystallinity ( $X_p$ ) of the copolymer was calculated using the following equation:

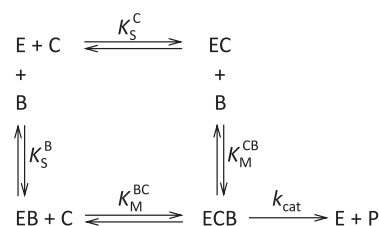


Fig. 1. Reaction scheme for the enzyme catalyzed polymerization of  $\epsilon$ -caprolactone (C) and  $\gamma$ -butyrolactone (B) to the product P.

$$X_p = \frac{\Delta H_f}{\Delta H_f^0} \quad (8)$$

where  $\Delta H_f^0$  is the endothermic melting enthalpy of the 100% crystalline polycaprolactone ( $142 \text{ J g}^{-1}$ ) as given in the literature [25]. The monomer conversion percentage was calculated as follows:

$$\text{Conversion (\%)} = \left( \frac{([C]_0 + [B]_0) - ([C]_t + [B]_t)}{[C]_0 + [B]_0} \right) \times 100\% \quad (9)$$

The polydispersity index (PDI) of the copolymer was calculated as follows:

$$PDI = \frac{M_w}{M_n} \quad (10)$$

The colorimetric analysis of the ultrasonic power,  $P$  was determined according to Eq. (11) as given in literature [16]

$$P = \frac{m \times c_p \times \Delta T}{\Delta t} \quad (11)$$

where  $P$  is power (W),  $m$  is the mass of the water (g),  $c_p$  is the specific heat capacity of water ( $4.18 \text{ J g}^{-1} \text{ K}^{-1}$ ),  $T$  is the temperature (K) and  $t$  is the sonication time (s).

The sonic power intensity,  $I$  ( $\text{W cm}^{-2}$ ) was calculated according to,

$$I = \frac{P}{A} \quad (12)$$

where  $A$  is the reaction volumetric area ( $\text{cm}^2$ )

The sonication-dissipated energy,  $E$  ( $\text{J ml}^{-1}$ ) is given by Eq. (13).

$$E = \frac{P \times t}{V} \quad (13)$$

where  $V$  is the reaction volume (ml)

The sonication amplitude ( $P_A$ ) and acoustic ( $P_a$ ) pressures were calculated according to Eqs. (14) and (15) respectively, [26].

$$P_A = (2 \cdot \rho \cdot c \cdot I)^{1/2} \quad (14)$$

$$P_a = P_A \cdot \sin 2\pi \cdot f \cdot t \quad (15)$$

where  $\rho$  is the bulk density ( $\text{kg m}^{-3}$ ),  $c$  is the speed of sound ( $1500 \text{ m s}^{-1}$ ) and  $f$  is the sonication frequency.

The particle's maximum velocity ( $v_p$ ) and displacement ( $\xi$ ) are given by Eqs. (16) and (17) respectively.

$$v_p = \frac{P_A}{\rho \cdot c} \quad (16)$$

$$\xi = \frac{v_p}{2\pi \cdot f} \quad (17)$$

Particle acceleration ( $a$ ) is given by Eq. (18).

$$A = 4 \cdot \pi^2 \cdot f^2 \cdot \xi \quad (18)$$

The ultrasonic degradation rate  $k$  ( $\text{s}^{-1}$ ) was calculated according to,

$$K = \frac{(M_0 - M_c)}{M_0 \cdot \Delta t} \quad (19)$$

where  $M$  is the initial average molecular weight and at time  $t$ .

### 3. Results and discussion

The lipase catalyzed ring-opening copolymerization of two cyclic lactone monomers was interpreted in terms of the random sequential Bi Bi kinetics shown in Fig. 1. This led to the rate Eq. (3). Concentrations of the monomers and the enzyme influenced the rate of copolymerization.

The basic enzyme catalyzed copolymerization process is the same irrespective of whether sonication is used, but sonication affects the rate of copolymerization. Sonication influences the copolymerization kinetics in multiple ways: 1. by enhancing the rate of mass transfer of the monomers to the active site of the enzyme [1,21]; 2. by directly affecting the catalytic activity of the enzyme and how it interacts with the monomers and the growing copolymer [1,21]; and 3. by affecting the stability of the enzyme [9,21,27]. The characteristics of the product formed and the effects of the various factors on the kinetics of copolymerization are discussed in the following sections.

#### 3.1. Product characterization

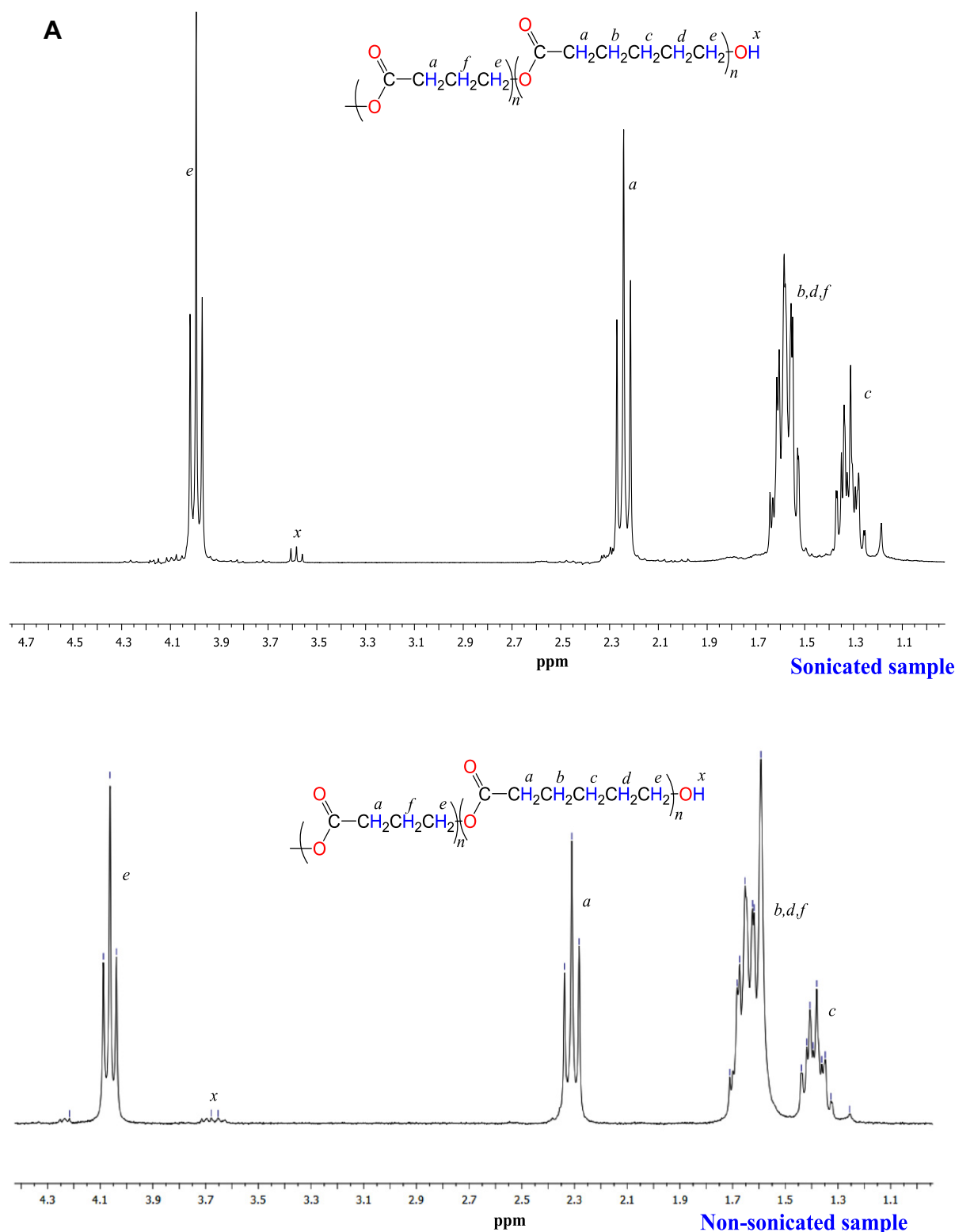
The synthesized copolymer was characterized by  $^1\text{H}$  NMR, FTIR, TGA, GPC and DSC. Fig. 2A shows the comparative  $^1\text{H}$  NMR spectra of the copolymers synthesized in both ultrasonic and non-ultrasonic processes. In general, the chemical shift 'a' at 2.35 ppm is due to the methylene protons located at the  $\alpha$ -position of the ester carbonyl carbons ( $-\text{C}(=\text{O})-\text{C}$ ) in both caprolactone and butyrolactone copolymers, respectively. The broad quartet of chemical shifts 'b, d, f' at 1.67 ppm is due to the  $\beta$ -methylene protons located at  $-\text{OC}(=\text{O})-\text{C}$ , respectively. The broad quartet of shifts 'c' at 1.31 ppm is assigned to the  $\beta$ -methylene proton at the  $-\text{C}$  in caprolactone copolymer. The peak 'e' at 4.05 ppm is associated with the  $\alpha$ -methylene protons at positions of  $-\text{OC}(=\text{O})-\text{C}-$ . The narrow peaks (x) at 3.66 ppm are due to the terminal carbinol protons ( $-\text{O}$ ) adjacent to  $\alpha$ -methylene protons. Both spectra (Fig. 2A) were found to be in consistent with previously reported data for the same copolymer [28]. As expected, the  $^1\text{H}$  NMR spectra were independent of the type of lipase used. However, in comparison to the non-sonicated sample, the signal strength was more pronounced in the sample from ultrasonic processes than that in the conventional shaking process, and this was attributed to the increased concentration of the product in the sonicated sample.

The FTIR spectrum of the synthesized copolymer is shown in Fig. 2B. The absorption bands at  $3499 \text{ cm}^{-1}$  indicate the presence of hydroxyl group confirming the formation of a linear copolymer chain [29]. The absorption bands at  $2995 \text{ cm}^{-1}$  correspond to the expected  $\text{CH}_2$  stretching vibrations. The absorption band at  $1731 \text{ cm}^{-1}$  is linked to the carbonyl ( $\text{C}=\text{O}$ ) stretching vibrations. The absorption band at  $1330 \text{ cm}^{-1}$  is due to the asymmetric stretching vibration of COC. The band at  $1258 \text{ cm}^{-1}$  is due to the C–O stretching vibration in OC–O. The bands from  $1125$  to  $1174 \text{ cm}^{-1}$  are due to symmetric COC stretching vibrations. The series of absorption bands from  $1108$  to  $453 \text{ cm}^{-1}$  correspond to C–O and C–C stretching vibrations, respectively (Fig. 2B). The FTIR spectrum (Fig. 2B) agreed well with the literature data [25,28]. Consistent with expectation, the FTIR spectra were independent of the type of lipase used.

The GPC analysis showed that the copolymer molecular weight ( $M_w$  and  $M_n$ ) depended on the specific type of the lipase biocatalyst used (Table 1). The lipases that had a high value of the maximum reaction rate ( $v_{\text{max}}$ , Table 2) produced a copolymer with a higher molecular weight (Table 1), simply because the high reaction rate with increasing sonication time allowed the copolymer chain to grow longer in a given timeframe. No peaks of low molecular weight were observed in the GPC chromatograms, thus indicating an absence of  $\epsilon$ -caprolactone and  $\gamma$ -butyrolactone monomers. Any residual monomer had been washed away in the preparation of the copolymer sample for the GPC analysis.

The DSC calorimetric analysis showed the copolymer samples to have an average melting temperature ( $T_m$ ) of  $54.1 \pm 0.7^\circ\text{C}$  and an average apparent degree of crystallinity ( $X_p$ ) of 0.5 (Table 1), irrespective of the catalyst used. The average value of the apparent melting enthalpy ( $\Delta H_f$ ) was  $70.4 \pm 5.3 \text{ J g}^{-1}$ . For all products





**Fig. 2.** (A)  $^1\text{H}$  NMR spectrum of the copolymer produced in ultrasonic and conventional shaking process using Lecitase Ultra<sup>TM</sup>. Reaction conditions: ultrasound-assisted process (40 °C, 37 kHz ultrasound at 1.1 W sonication power and  $2.6 \times 10^3 \text{ W m}^{-2}$  power intensity); Shaking process (200 rpm, 40 °C) and (B) FTIR spectrum of the copolymer produced using Novozym 435 lipase in a sonicated process at the same conditions as in (A).

(Table 1), the average entropy of fusion was  $1.3 \pm 0.1 \text{ J g}^{-1} \text{ }^\circ\text{C}^{-1}$ . The thermal gravimetric analysis revealed the copolymer to have an average degradation temperature ( $T_d$ ) of  $205.1 \pm 6.3 \text{ }^\circ\text{C}$  (Table 1). These observed properties of the copolymer were consistent with the earlier reports [28,30].

Depending on the enzyme, the GCMSMS analysis of the residual monomers showed the copolymer to contained about 92% caprolactone and 8% butyrolactone in Lecitase Ultra<sup>TM</sup> catalyzed synthesis. Novozym 435 was observed to polymerize a copolymer of 85% caprolactone and 15% butyrolactone components. *C. rugosa* lipase

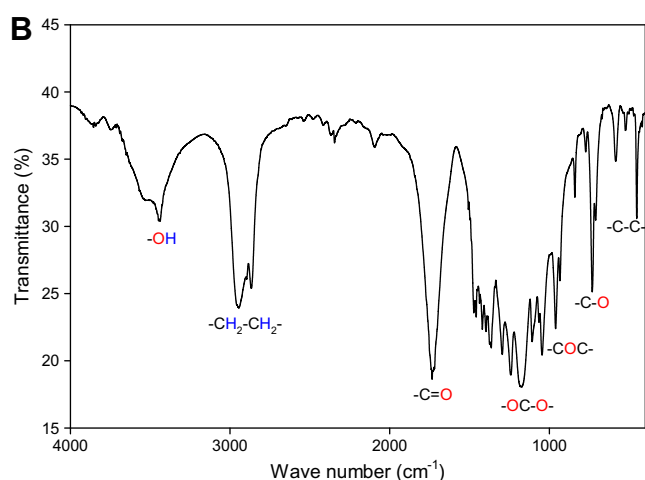


Fig. 2. (continued)

synthesized a copolymer of 96% caprolactone and 4% butyrolactone while *C. antarctica* lipase A synthesized a copolymer of only 2% butyrolactone component. This variation in copolymer component among the enzymes could be due to reported differences in enzymatic selectivity, reactivity, specificity and thermodynamic stability especially in micro-aqueous media [2,9,31]. The observed low butyrolactone content could be due to the reported thermodynamic stability of the butyrolactone monomer which make it difficult to enzymatically be polymerized as a result of low ring strain energy ( $36.6 \pm 0.2 \text{ kJ mol}^{-1}$ ) as compared to caprolactone ( $44.7 \text{ kJ mol}^{-1}$ ) making  $\epsilon$ -caprolactone to be more active in ROP than the butyrolactone [28,32]. Similar observation has been reported in literatures [28,30,32].

### 3.2. Effect of ultrasonic on the enzymes activity

The induction of cavitation bubbles collapse leads to the generation of very high local pressure (up to 1000 atm), temperatures (up to 5000 K) and shear forces that increased the fluid velocity which facilitates mass transfer and enhanced mixing of substrate, enzyme, and products [33]. Ultrasonic irradiation has previously been reported to increase different enzymes activity. In this study, we observed a general increase in enzymatic activity in ultrasonic process (Fig. 3A) as compared to the conventional shaking process

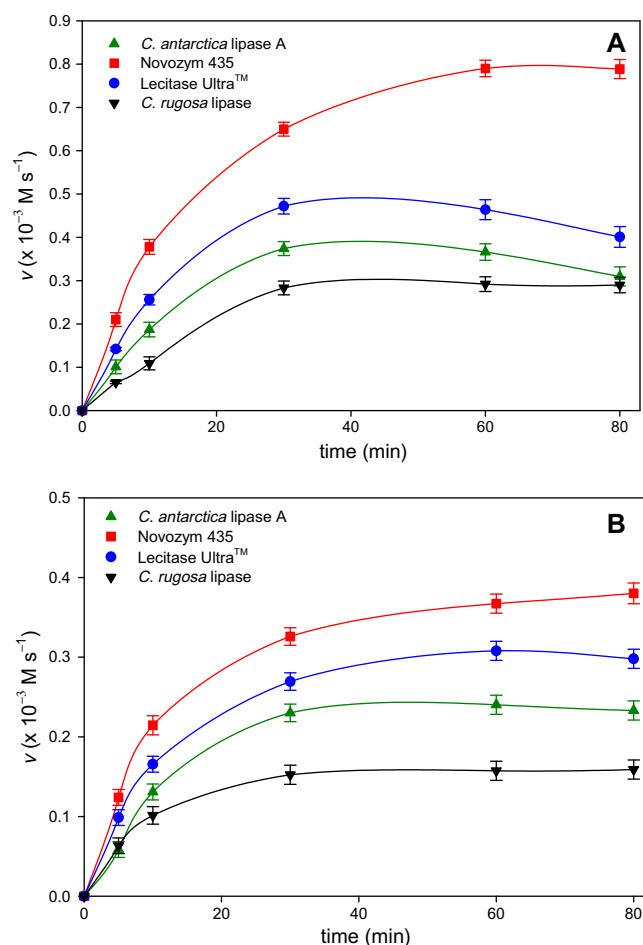


Fig. 3. Enzyme activity as a function of sonication time (A) ultrasonic process at 37 kHz, 30 °C, 1.6 W and 80 min (B) conventional automatic shaking process at 200 rpm, 30 °C and 80 min.

(Fig. 3B). In fact, in comparison to the shaking process about 2.5-fold increase in activity was observed in Novozym 435 under ultrasonic process with highest activity  $7.9 \times 10^{-3} \text{ M s}^{-1}$  been observed at 60 min and continue to increase albeit at lower rate up to 80 min. The increase in activity of the free enzymes (unbound) samples was observed to range between 1.8 and 1.5-fold with

**Table 1**  
Thermal properties of the copolymer made using various lipases.

| Enzyme                             | $T_m (\pm 0.2) ^\circ\text{C}$ | $T_d (\pm 0.2) ^\circ\text{C}$ | $X_p$ | $\Delta H_f (\pm 0.1) \text{ J g}^{-1}$ | $\Delta S_f (\pm 0.1) \text{ J g}^{-1} ^\circ\text{C}^{-1}$ | $M_n \text{ Da}$ | $M_w \text{ Da}$ | PDI |
|------------------------------------|--------------------------------|--------------------------------|-------|---|---|------------------|------------------|-----|
| <i>Candida antarctica</i> lipase A | 53.7                           | 198.7                          | 0.5   | 67.9                                    | 1.3   | 6745             | 8799             | 1.3 |
| Novozym 435                        | 54.5                           | 209.5                          | 0.5   | 75.3                                    | 1.4   | 11,689           | 13,567           | 1.2 |
| Lecitase Ultra™                    | 54.8                           | 211.3                          | 0.5   | 74.2                                    | 1.4   | 10,909           | 12,502           | 1.1 |
| <i>C. rugosa</i> lipase            | 53.2                           | 200.8                          | 0.5   | 64.1                                    | 1.2   | 2729             | 3456             | 1.3 |

**Table 2**  
Kinetics parameters of the various enzymes during synthesis of the copolymer.

| Enzyme                             | $v_{\max} \times 10^{-3} \text{ M s}^{-1}$ | $K_M^{CB} \times 10^{-1} \text{ M}$ | $K_M^{BC} \times 10^{-1} \text{ M}$ | $K_S^C \times 10^{-1} \text{ M}$ | $K_S^B \times 10^{-1} \text{ M}$ | $k_{\text{cat}} \times 10^{-4} \text{ s}^{-1}$ | $\eta \times 10^{-3} \text{ s}^{-1} \text{ M}^{-1}$ | Conversion % (M/M) | $R^2$ | $\sigma \times 10^{-5}$ |
|------------------------------------|--|-------------------------------------|-------------------------------------|----------------------------------|----------------------------------|--|---|--------------------|-------|-------------------------|
| <i>Candida antarctica</i> lipase A | 4.7  | 2.75                                | 1.17                                | 1.29                             | 3.03                             | 2.35   | 2.01  | 11.0               | 0.98  | 5.72                    |
| Novozym 435                        | 9.8  | 2.81                                | 1.18                                | 1.31                             | 3.12                             | 4.90   | 4.15  | 48.5               | 0.98  | 5.77                    |
| Lecitase Ultra™                    | 6.8  | 2.76                                | 1.18                                | 1.30                             | 3.04                             | 3.40   | 2.88  | 28.4               | 0.98  | 5.75                    |
| <i>C. rugosa</i> lipase            | 3.5  | 2.72                                | 1.18                                | 1.27                             | 2.93                             | 1.75   | 1.48  | 8.2                | 0.97  | 6.02                    |



activity varying from  $4.7 \times 10^{-3} \text{ M s}^{-1}$  in Lecitase Ultra™ to  $2.9 \times 10^{-3} \text{ M s}^{-1}$  in *C. rugosa* lipase, while *C. antarctica* lipase A have an activity of  $3.7 \times 10^{-3} \text{ M s}^{-1}$ . Similar observations were previously reported where Lin and Liu [34] observed 83-fold increase in lipase activity under ultrasonication during lipase-catalyzed acylation of a naphthol derivative with vinyl acetate in benzene-ether mixture. Barton et al. [35] reported 37% increase in activity of invertase at 0.9 M sucrose hydrolysis, while 20% and 43% increase in glucoamylase and  $\alpha$ -amylase activities in starch hydrolysis respectively. Vulfson et al. [36] reported an increased in subtilisin activity when pretreated by ultrasound in alcohol. They observed the increment to be influenced by the chain-length of the alcohol with 6–8 times increase in octanol as compared to shorter chains alcohol. They concluded that the increase in enzymatic activity depend largely on the solvents type and chemical structure.

In general, Novozym 435 activity was observed to be unaffected by the ultrasonic condition up to 80 min, probably due to the immobilization which has been reported to enhance the stability of the enzymes. Unlike in Novozym 435, the highest activities in the unbound enzymes were achieved at earlier time (30 min) probably due to the free and constant contact with the substrates (Fig. 3A). Unfortunately, these unbound enzymes are highly exposed and hence susceptible to the physical and chemical effects of cavitation collapse as well as reaction media water activity. Thus, they suffer the effect of ultrasonic irradiation more at a longer reaction time, which could probably led to the lowered activity as compared to the immobilized Novozym 435. On the other hand, Fig. 3B showed that due to the absence of a more efficient mass transfer via ultrasound irradiation, the enzymes activities were relatively lower although gradual increase up to 80 min of reaction time was observed.

### 3.3. Enzyme kinetics

The kinetic parameters of the copolymerization reaction with the different catalysts are shown in Table 2. In this study, all reactions were carried out at 40 °C with a sonication power level of 1.6 W using 37 kHz ultrasound. The initial concentration of  $\epsilon$ -caprolactone and  $\gamma$ -butyrolactone was 5 and 3 mM, respectively. The concentration of the enzyme catalyst was 20 U mL<sup>-1</sup>.

The maximum reaction rate ( $v_{\text{max}}$ ), the turnover number ( $k_{\text{cat}}$ ) and the catalytic efficiency ( $\eta$ ) depended on the enzyme used (Table 2). Novozym 435 was found to be the best in terms all these parameters (Table 2). The *C. rugosa* lipase was the least effective enzyme (Table 2). This may have been due to different amounts of the active enzyme being present in the different preparations.

The steady-state Michaelis constants ( $K_{\text{M}}^{\text{BC}}$ ,  $K_{\text{M}}^{\text{CB}}$ ) and the equilibrium dissociation constants of both monomers ( $K_{\text{S}}^{\text{C}}$ ,  $K_{\text{S}}^{\text{B}}$ ) had comparable values, irrespective of the enzyme used (Table 2). The steady-state Michaelis constant for the formation of the ternary complex ECB (Fig. 1) was higher for caprolactone ( $0.281 \geq K_{\text{M}}^{\text{CB}} \geq 0.275 \text{ M}$ ) when compared to butyrolactone ( $0.117 \geq K_{\text{M}}^{\text{BC}} \geq 0.118 \text{ M}$ ). This may have been due to a high thermodynamic stability of the  $\gamma$ -butyrolactone monomer compared to  $\epsilon$ -caprolactone as reported in literature [28,32]. In contrast, the values of the equilibrium dissociation constants were lower for the EC complex ( $0.131 \leq K_{\text{S}}^{\text{C}} \leq 0.127$ ) compared to for the EB complex ( $0.312 \leq K_{\text{S}}^{\text{B}} \leq 0.293$ ). The different reaction rates for the different enzymes are therefore largely explained by the deferent values of the turnover number ( $k_{\text{cat}}$ , Table 2).

### 3.4. Conversion of monomers

The percentage conversion of the monomers increased as the sonication reaction progressed, but the conversion rate depended

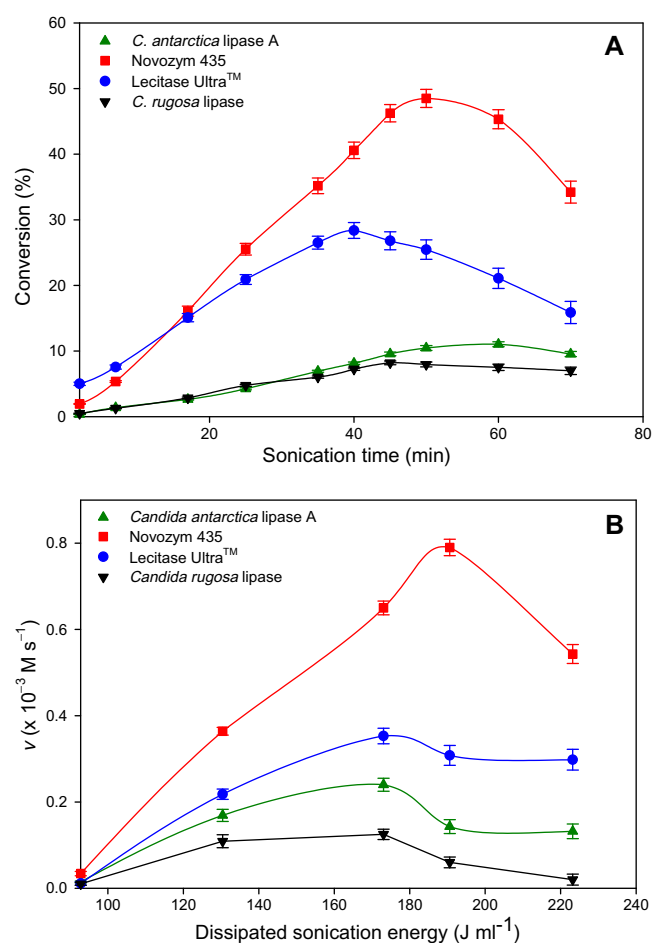


Fig. 4. (A) Monomer conversion versus sonication time during the synthesis of the copolymer using various lipases. The process conditions were 40 °C, 37 kHz ultrasound at 1.1 W sonication power and  $2.6 \times 10^3 \text{ W m}^{-2}$  sonication power intensity. (B) Polymerization rate as a function of dissipated sonication energy during the synthesis of the copolymer using various lipases. The process conditions were 40 °C, 37 kHz ultrasound at 1.1 W sonication power and  $2.6 \times 10^3 \text{ W m}^{-2}$  sonication power intensity.

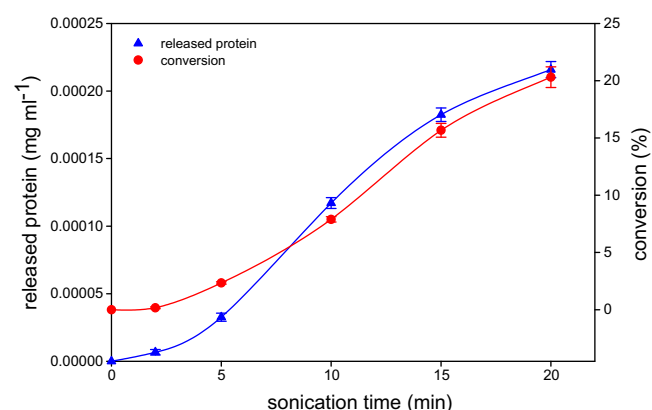


Fig. 5. Effect of sonication time on protein leakage from the immobilized Novozym 435. The process conditions were 40 °C, 37 kHz ultrasound at 0.8 W sonication power and  $1.9 \times 10^3 \text{ W m}^{-2}$  sonication power intensity.

on the enzyme (Fig. 4A) and the sonication dissipating energy (Fig. 4B). The maximum value of the conversion was 48.5% and it was attained after 50 min of reaction using the immobilized Novozym 435. Using Lecitase Ultra™, the peak conversion was lower at 28.4% but the peak was attained by 40 min (Fig. 4A). The cata-

lytic performance of the dissolved lipases, the *C. rugosa* lipase and *C. antarctica* lipase A, were comparable, but much lower than for the immobilized Novozym 435. In Fig. 4B, the enzymatic polymer production rate generally decreases with increasing sonication energy beyond  $173 \text{ J ml}^{-1}$  except in Novozym 435 where the rate continue to increase with the increasing sonic energy value up to  $191 \text{ J ml}^{-1}$ , there after a progressive reduction in the rate was observed. The relatively poor performance of the two dissolved lipases may have been due to the ultrasound cavitation deactivation effect (high cavitation threshold) on them [37]. The immobilized enzymes tend to be generally more stable compared to soluble enzymes and may have better resisted the deactivating effect of ultrasound.

For the immobilized Novozym 435 preparation, there was evidence for enzyme leakage from the support matrix into the liquid medium. Thus, the protein concentration in the reaction medium increased as the reaction progressed (Fig. 5). The protein concentration was measured as previously explained [38].

In general, the conversion declined after reaching the maximum value (Fig. 4). This suggested a hydrolysis of the copolymer. Lipases catalyze both copolymerization and hydrolysis. During copolymerization water is produced and its concentration rises as the reaction progresses. An increasing concentration of water in an initially microaqueous environment, tends to drive the reaction towards hydrolysis [7]. Furthermore, as the reaction progresses, the rate of copolymerization slows because an increased viscosity of the reaction medium progressively hinders the mass transfer of the monomers to the active site of the enzyme. A reduced rate of copolymerization combined with an increased rate of hydrolysis of the copolymer, results in the hydrolysis becoming the dominant reaction beyond a certain point in time.

### 3.5. Effect of sonication temperature on the reaction rate

The anticipated effect in the increase of temperature on the copolymerization system would be the enhancement of rate along with the reduction of medium viscosity as the polymerization progresses. The ultrasonication-assisted (34 kHz, 1.1 W of sonication power) copolymerization was carried out at different constant reaction temperatures (30–60 °C). The rate of copolymerization depended on temperature as shown in Fig. 6. The initial rate of the reaction at various temperatures was measured and found to increase with increasing temperature mostly to 40 °C with the exception of Novozym 435, which showed sustained increase in rate up to 50 °C. The reaction rate was observe to increase from

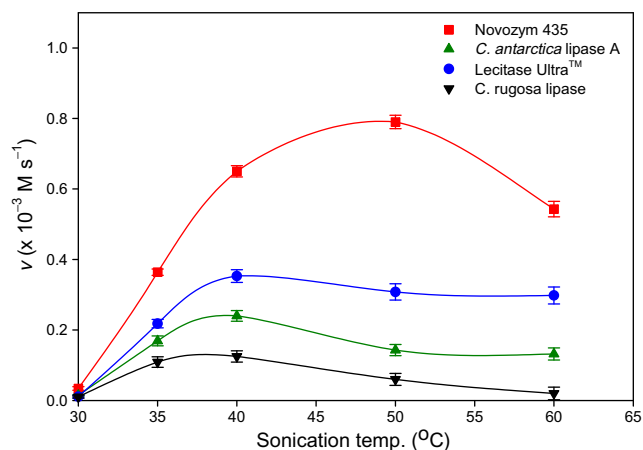


Fig. 6. Effect of sonication temperature on the rate of polymer production ( $v$ ) catalyzed by different lipases. Ultrasound irradiation (37 kHz) at 1.1 W sonication power and  $2.6 \times 10^3 \text{ W m}^{-2}$  sonication power intensity.

$0.01 \times 10^{-3}$  at 30 °C to  $0.35 \times 10^{-3} \text{ M s}^{-1}$  at 40 °C in Lecitase Ultra™, increasing the reaction temperature further caused the observed rate to decrease gradually to  $0.30 \times 10^{-3} \text{ M s}^{-1}$  at 60 °C (Fig. 6). In contrast, the reaction rate was observed to increase in Novozym 435 approximately 26-fold from 30 to 50 °C ( $0.79 \times 10^{-3} \text{ M s}^{-1}$ ). The reaction rate was observed to reach a maximum value of  $0.24 \times 10^{-3} \text{ M s}^{-1}$  in *C. antarctica* lipase A at 40 °C, but in *C. rugosa* lipase the rate was found generally to be lower with maximum value of  $0.13 \times 10^{-3} \text{ M s}^{-1}$ . A temperature of 40 °C was observed to be optimal for most of the enzymes studied except for Novozym 435 where the highest initial reaction rate occurred at 50 °C (Fig. 6), which was attributed to its high thermal stability, diverse substrate selectivity coupled with advantageous immobilization. In short, Novozym 435 was clearly the best catalyst for the reaction being studied (Fig. 6). The general decrease in reaction rates at higher temperatures (Fig. 6) apparently was due to thermal deactivation effects [39], which appeared to be more pronounced in the unbound enzymes (Fig. 6).

Despite the fact that there is short-lived dissipation of intense heat and kinetic energy as a result of cavitation collapse which may have deleterious effects on protein folding and enzyme deactivation in ultrasonic process, the differences in enzymatic reaction rates in this process should not be attributed solely to ultrasonic effects. Several factors e.g. solvent polarity, reaction media water activity, enzymatic specificity, substrate selectivity, solvent compatibility, thermal stability and physical preparation (i.e. immobilized or free enzymes) were among the reported parameters to have an influence on the enzymatic reactivity in micro-aqueous catalysis [31,40].

### 3.6. Effect of the sonication power on the reaction rate

The sonication power is known to be an important factor affecting the rate of reaction in an ultrasound-mediated process [4,41,42]. In previously reported literatures of enzyme catalyzed reactions, sonication has been generally performed at a fixed ultrasound power and therefore the effect of sonication power on the reaction rate is poorly understood. Nevertheless, despite the beneficial effect of sonication waves in assisting micromixing hence improving mass transfer, there must be an optimum value of the sonication power beyond which the deleterious effects on biocatalytic activity and production degradation would be observed. In this study, the effect of sonication power (W) on the initial copolymerization rate was investigated at various sonication power

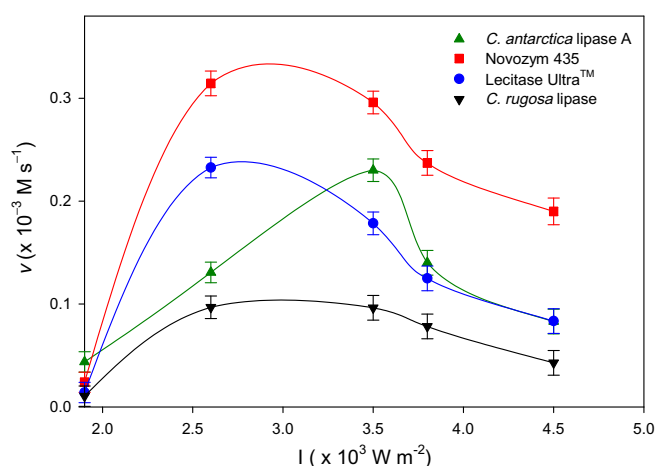


Fig. 7. Sonication power versus the rate of copolymer production ( $v$ ) using various lipases at 37 kHz, 35 °C.

intensities ( $I$ ) from  $1.9 \times 10^3$  to  $4.5 \times 10^3 \text{ W m}^{-2}$  and constant reaction temperature  $35^\circ\text{C}$  (Fig. 7).

The optimum sonication power level was  $\approx 1.1 \text{ W}$  ( $2.6 \times 10^3 \text{ W m}^{-2}$ ) for the Novozym 435 ( $3.1 \times 10^{-4} \text{ M s}^{-1}$ ) and Lecitase Ultra™  $2.3 \times 10^{-4} \text{ M s}^{-1}$  (Fig. 7). For *C. antarctica* lipase A, the optimal power level was  $\approx 1.4 \text{ W}$  ( $3.3 \times 10^3 \text{ W m}^{-2}$ ) (Fig. 7). At this power level, the *C. antarctica* lipase A afforded a reaction rate ( $2.3 \times 10^{-4} \text{ M s}^{-1}$ ) that was comparable to the reaction rate attained with Lecitase Ultra™ at  $\approx 1.1 \text{ W}$  ( $2.6 \times 10^3 \text{ W m}^{-2}$ ) sonication power level (Fig. 7).

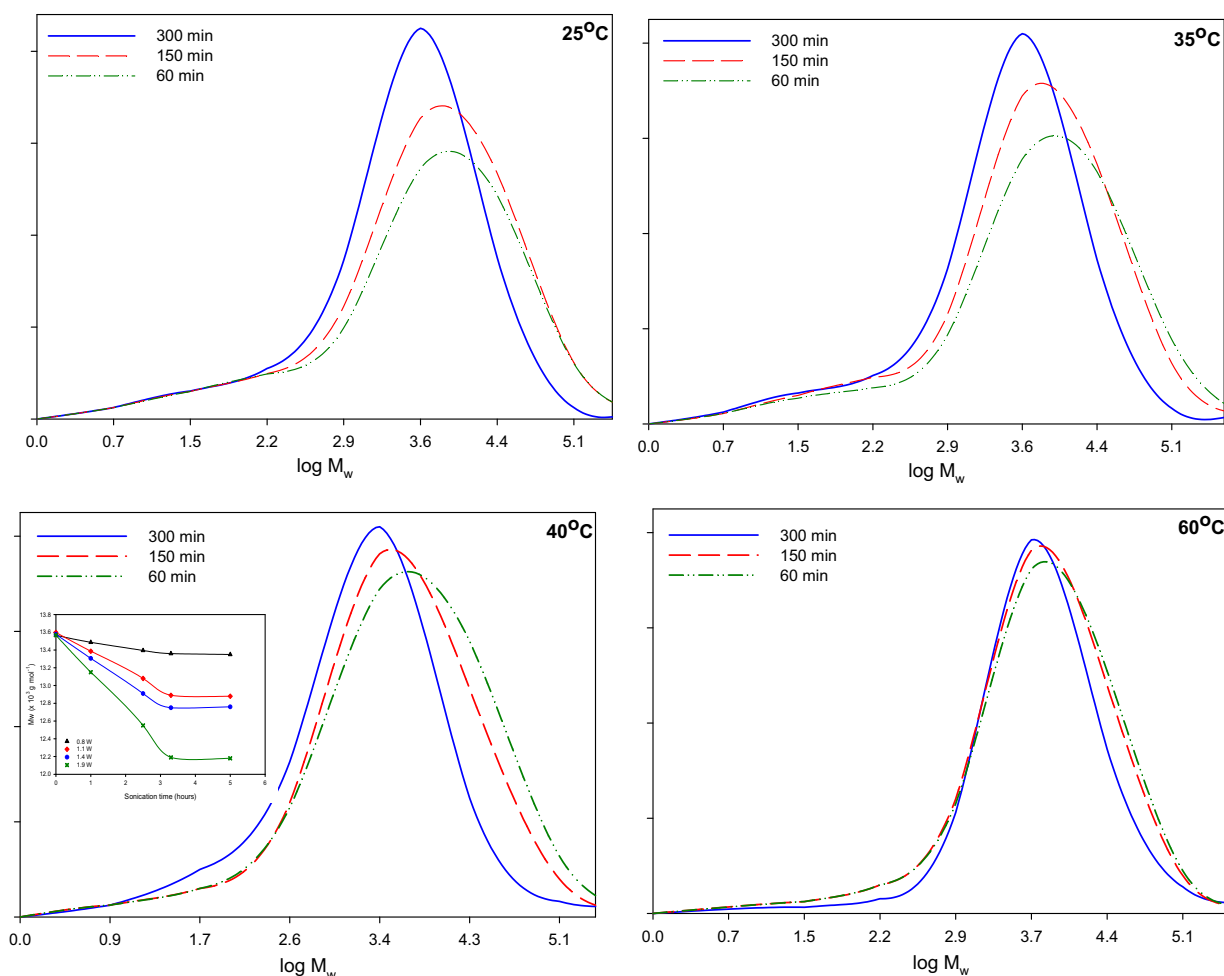
In all the enzymes studied, the reaction rate increased as the power intensity increased from  $1.9 \times 10^3$  to  $3.5 \times 10^3 \text{ W m}^{-2}$  (Fig. 7), with corresponding amplitude pressure of  $9.2 \times 10^4$ – $1.4 \times 10^5 \text{ N m}^{-2}$ . At these power intensities, the acoustic pressure was calculated to range from  $3.7 \times 10^8$  to  $5.0 \times 10^8 \text{ N m}^{-2}$ , approximately 2.4–3.3 times greater than the reported acoustic pressure of  $1.5 \times 10^8 \text{ N m}^{-2}$  required to cause cavitation in water [26]. Furthermore, this pressure level was used to calculate a particle maximum velocity ( $v_p$ ) that span from  $4.1 \times 10^{-2} \text{ m s}^{-1}$  at  $0.8 \text{ W}$  to  $5.6 \times 10^{-2} \text{ m s}^{-1}$  at  $1.4 \text{ W}$  with a varying amplitude particle displacement ( $\xi$ ) ranging from  $1.8 \times 10^{-7}$  to  $2.4 \times 10^{-7} \text{ m}$ . This is translated to an acoustic particle acceleration ( $a$ ) of  $9.6 \times 10^3$ – $1.3 \times 10^3 \text{ m s}^{-2}$ , an acceleration that is  $\approx 984$  to 1335 times greater than under the action of gravity, making the generation of radicals highly likely. A further increase in sonication power beyond the point of the peak reaction rate (Fig. 7) actually decreased the rate

of reaction for all enzymes. For instance, increasing the intensity ( $I$ ) to  $4.5 \times 10^3 \text{ N m}^{-2}$  resulted in an enormous acoustic pressure of  $5.7 \times 10^8 \text{ N m}^{-2}$  with an acoustic particle acceleration of  $1.5 \times 10^4 \text{ m s}^{-2}$  i.e. more than 1500 times greater than under the gravitational influence. This resulted in corresponding decrease in reaction rate ( $v$ ) for example in Novozym 435 from  $2.9 \times 10^{-4} \text{ M s}^{-1}$  at  $3.5 \times 10^3 \text{ W m}^{-2}$  to  $1.9 \times 10^{-4} \text{ M s}^{-1}$  at  $4.5 \times 10^3 \text{ W m}^{-2}$ .

This observed reduction in enzyme reaction rate at high sonic power intensities could likely be due to bubbles with larger radii, which upon collapsing induces high shear forces and high temperature. Therefore continuous increase in sonication power per unit volume creates a large number of bigger cavitation bubbles resulting in high local temperatures and shear stresses, exhibiting enzyme activity deactivating effects by denaturing the enzyme or tempering with its active site [9,21,43].

### 3.7. Effects of ultrasonic temperature, power and time on the synthesized polymer molecular weight

It is believed that in ultrasonic process the polymer chain degradation occurs mostly due to the subjected large forces in the rapid liquid flows near collapsing cavitation bubbles and in the shock waves generated after bubble implosion. Both the kinetics and regiospecificity of ultrasonic degradation were reported to be different from those of thermal processes. Unlike thermal degradation that occurs by random chain scission, in ultrasonic process, the



**Fig. 8.** GPC chromatograms of sonication temperature and time as a function of synthesized copolymer molecular weight at  $2.6 \times 10^3 \text{ W m}^{-2}$  ultrasound irradiation. The inset in plot of  $40^\circ\text{C}$  depicts the profiles of copolymer molecular weight in the degradation reaction as a function of sonication power and time at  $40^\circ\text{C}$ .

degradation was hypothesized to have a preferential occurrence at the middle of the chain [13,42]. Van der Hoff and Gall [44] explained the hypothesis using a quantitative model in their study on the degradation of polystyrene in tetrahydrofuran. They suggested that the degradation could be best modeled when one assumed the probability of chain breakage to be distributed in a Gaussian manner within  $\approx 15\%$  of the chain-center. Using Glyn's model Koda et al. [42] further tested this hypothesis in their study on the ultrasonic degradation of water-soluble polymers. They postulated the degradation to occur with a Gaussian probability.

In our study, the effect of ultrasonic temperature, power and time on the synthesized polymer degradation was studied using 0.5 g of the synthesized polymer ( $M_w$  13.6 kDa, PDI 1.4) in 10 ml chloroform at 37 kHz and 1.2 W when studying temperature effect at ranges of 25–60 and 40 °C in studying the power effect at ranges of 0.8–1.9 W over a period of 5 h. Aliquot samples were withdrawn and subjected to GPC analysis at specified time intervals. In the GPC chromatograms (Fig. 8), at the earlier reaction time (60–150 min) the rate of ultrasonic polymer degradation ( $k$ ) was observed to decrease progressively from  $3.11 \times 10^{-8} \text{ s}^{-1}$  at 25 °C to  $1.14 \times 10^{-9} \text{ s}^{-1}$  at 60 °C. This decrease in degradation with increasing sonication temperature was found to contradict Yen and Yang [45] reports on increase in degradation with increasing ultrasonic temperature in polyacrylamide. It is however found to be in consistent with previously reported literatures [13,46–49]. The reason to this decrease in degradation at higher temperature has previously been attributed to the increased vapor pressure that causes vapor to enter into the bubbles forming a kind of cushioning which reduces the effect of violent collapse [13,46,48,49].

In all the temperatures studied, it is further observed that the degradation rate increases with increasing sonication time up to a specific limiting time ( $t_{lim}$ ) beyond which the degradation rate becomes lower. For example, in observing the sonication effect at 35 °C, the degradation rate was observed to be  $2.58 \times 10^{-8} \text{ s}^{-1}$  at 60 min, the rate increased to  $3.12 \times 10^{-8} \text{ s}^{-1}$  at 150 min. However, as the sonication time reaches 300 min the degradation rate was observed to decrease as low as  $\approx 7.12 \times 10^{-9} \text{ s}^{-1}$ . The accumulation of degradation products, which increases the solution's viscosity thence reduces the shear gradients around the collapsing bubbles were thought to be responsible for the decreased degradation rate [13,43,50].

On the other hand, studying the effect of sonication power as a function of time on the ultrasonic degradation of the product (Fig. 8, inset 40 °C), in all the power levels tested, the degradation was observed to proceed more rapidly at earlier time and approaches a molecular weight limiting value ( $M_{lim}$ ) at time  $t_{lim} = 3 \text{ h}$  below which the polymer seems to be unaffected by ultrasound irradiation effects. Observing the degradation at 1.1 W, the polymer was found to degrade from  $M_w \approx 13.62 \text{ kDa}$  to  $\approx 12.89 \text{ kDa}$  at 3 h; increasing the time to 5 h the  $M_w$  was observed to be  $\approx 12.88 \text{ kDa}$ . In comparison, when the sonication power was increased from 1.1 to 1.9 W, increased degradation was observed with  $M_w$  decreasing to 12.19 kDa at 3 h and 12.18 kDa at 5 h (Fig. 8, inset 40 °C). This observation was found to be in good agreement with previously reported literature [47,48]. Pasupuleti and Madras [48] reported that at the level above the cavitation threshold during ultrasonication, the maximum radius of the bubble is proportional to the square root of the sonication intensity. Hence increasing sonication power intensity creates bubbles with larger radii, which upon collapsing induces high shear forces. Therefore continuous increase in sonication power per unit volume increases the shear field that in turns increases the rate of degradation [43]. As expected in Fig. 8 (40 °C inset), increasing the sonication power resulted in the increased degradation of the product up to 3 h whereby beyond this time the degradation assumed a plateau.

## 4. Conclusions

Ultrasound-assisted lipase-catalyzed ring-opening copolymerization was used to produce a biodegradable polyhydroxyalkanoate copolymer. Four commercial lipases were compared for this copolymerization. The immobilized lipase Novozym 435 proved to be best in every respect for this reaction. This enzyme afforded the highest value of the maximum reaction rate, the turnover number, the monomer conversion and the product molecular weight. Compared to the other enzymes, Novozym 435 was most stable to temperature and ultrasound irradiation. The optimal sonication power level depends on the enzyme preparation.

## Acknowledgement

The University of Malaya is acknowledged for funding this work through research grants RG165/11AFR, PV036/2012A, UM.C/625/1/HIR/MOHE/05 and RP024-2012A.

## References

- [1] A.M. Gumel, M.S.M. Annuar, Y. Chisti, T. Heidelberg, Ultrasound assisted lipase catalyzed synthesis of poly-6-hydroxyhexanoate, *Ultrason. Sonochem.* 19 (2012) 659–667.
- [2] B. Yeniad, H. Naik, A. Heise, Lipases in polymer chemistry biofunctionalization of polymers and their applications, in: G.S. Nyanhongo, W. Steiner, G. Gübitz (Eds.), Springer Berlin, Heidelberg, 2011, pp. 69–95.
- [3] M. Adamczak, S.H. Krishna, Strategies for improving enzymes for efficient biocatalysis, *Food Technol. Biotechnol.* 42 (2004) 251–264.
- [4] K.K. Darani, M. Reza Mozafari, Supercritical fluids technology in bioprocess industries: a review, *J. Biochem. Technol.* 2 (2010) 144–152.
- [5] S. Sinnwell, H. Ritter, Recent advances in microwave-assisted polymer synthesis, *Aust. J. Chem.* 60 (2007) 729–743.
- [6] D.-Z. Wei, J.-H. Zhu, X.-J. Cao, Enzymatic synthesis of cephalixin in aqueous two-phase systems, *Biochem. Eng. J.* 11 (2002) 95–99.
- [7] K.G. Fiametti, M.M. Sychoski, A. De Cesaro, A. Furigo Jr., L.C. Bretanha, C.M.P. Pereira, H. Treichel, D. de Oliveira, J.V. Oliveira, Ultrasound irradiation promoted efficient solvent-free lipase-catalyzed production of mono- and diacylglycerols from olive oil, *Ultrason. Sonochem.* 18 (2011) 981–987.
- [8] T.J. Mason, Ultrasound in synthetic organic chemistry, *Chem. Soc. Rev.* 26 (1997) 443–451.
- [9] S. Shweta, G. Munishwar, The effect of ultrasonic pre-treatment on the catalytic activity of lipases in aqueous and non-aqueous media, *Chem. Cent. J.* 2 (2008) 1–9.
- [10] Y. Liu, Q. Jin, L. Shan, W. Shen, X. Wang, The effect of ultrasound on lipase-catalyzed hydrolysis of soy oil in solvent-free system, *Ultrason. Sonochem.* 15 (2008) 402–407.
- [11] Z. Ming-hua, D.U. Wei, L.I. Hui-ing, L.I.U. Yun, Enhancement of lipase-catalysed esterification in organic solvent by ultrasonic irradiation, *J. S. China Uni. Technol. Nat. Sci.* 3 (2000).
- [12] L.A. Lerin, M.C. Feiten, A. Richetti, G. Toniazio, H. Treichel, M.A. Mazutti, J.V. Oliveira, E.G. Oestreich, D. de Oliveira, Enzymatic synthesis of ascorbyl palmitate in ultrasound-assisted system: process optimization and kinetic evaluation, *Ultrason. Sonochem.* (2011).
- [13] K.S. Suslick, G.J. Price, Applications of ultrasound to materials chemistry, *Annu. Rev. Mater. Sci.* 29 (1999) 295–326.
- [14] K.S. Suslick, Y. Didenko, M.M. Fang, T. Hyeon, K.J. Kolbeck, W.B. McNamara Jr., M.M. Mdleleni, M. Wong, Acoustic cavitation and its chemical consequences, *Philos. Trans. R. Soc. A* 357 (1999) 335–353.
- [15] T.J. Mason, *Advances in Sonochemistry*, Jai Press Inc., England, London, 1996.
- [16] Y. Asakura, T. Nishida, T. Matsuoka, S. Koda, Effects of ultrasonic frequency and liquid height on sonochemical efficiency of large-scale sonochemical reactors, *Ultrason. Sonochem.* 15 (2008) 244–250.
- [17] J.V. Sinisterra, Application of ultrasound to biotechnology: an overview, *Ultrasonics* 30 (1992) 180–185.
- [18] B. Avvaru, A.B. Pandit, Oscillating bubble concentration and its size distribution using acoustic emission spectra, *Ultrason. Sonochem.* 16 (2009) 105–115.
- [19] J. Collis, R. Manasseh, P. Liovic, P. Tho, A. Ooi, K. Petkovic-Duran, Y. Zhu, Cavitation microstreaming and stress fields created by microbubbles, *Ultrasonics* 50 (2010) 273–279.
- [20] P.R. Gogate, V.S. Sutkar, A.B. Pandit, Sonochemical reactors: important design and scale up considerations with a special emphasis on heterogeneous systems, *Chem. Eng. J.* 166 (2011) 1066–1082.
- [21] Y. Chisti, Sonochemical reactors: using ultrasound for enhanced microbial productivity, *Trends Biotechnol.* 21 (2003) 89–93.
- [22] Y. Teng, Y. Xu, A modified para-nitrophenyl palmitate assay for lipase synthetic activity determination in organic solvent, *Anal. Biochem.* 363 (2007) 297–299.

- [23] P. Dubois, O. Coulembier, J.M. Raquez, Handbook of Ring-Opening Polymerization, Wiley-VCH Verlag GmbH, Weinheim, 2009.
- [24] A.G. Marangoni, Enzyme Kinetics: A Modern Approach, John Wiley and Sons, 2003.
- [25] T. Elzein, M. Nasser-Eddine, C. Delaite, S. Bistac, P. Dumas, FTIR study of polycaprolactone chain organization at interfaces, *J. Colloid Interface Sci.* 273 (2004) 381–387.
- [26] T.J. Mason, J.P. Lorimer, Applied Sonochemistry: The Uses of Power Ultrasound in Chemistry and Processing, Wiley-VCH Verlag GmbH, Weinheim, 2002.
- [27] L. Gebicka, J.L. Gekicki, The effect of ultrasound on heme enzymes in aqueous solution, *J. Enzyme Inhib. Med. Chem.* 12 (1997) 133–141.
- [28] F. He, S. Li, H. Garreau, M. Vert, R. Zhuo, Enzyme-catalyzed polymerization and degradation of copolyesters of  $\epsilon$ -caprolactone and  $\gamma$ -butyrolactone, *Polymer* 46 (2005) 12682–12688.
- [29] M.C. Sin, I.K.P. Tan, M.S.M. Annuar, S.N. Gan, Characterization of oligomeric hydroxyalkanoic acids from thermal decomposition of palm kernel oil-based biopolyester, *Int. J. Polym. Anal. Charact.* 16 (2011) 337–347.
- [30] M. Monsalve, J.M. Contreras, E. Laredo, F. López-Carrasquero, Ring-opening copolymerization of (R, S)- $\beta$ -butyrolactone and  $\epsilon$ -caprolactone using sodium hydride as initiator, *EXPRESS Pol. Lett.* 4 (2010) 431–441.
- [31] A.M. Gumel, M.S.M. Annuar, T. Heidelberg, Y. Chisti, Lipase mediated synthesis of sugar fatty acid esters, *Process Biochem.* 46 (2011) 2079–2090.
- [32] K.B. Wiberg, R.F. Waldron, Lactones. 2. Enthalpies of hydrolysis, reduction, and formation of the C4–C13 monocyclic lactones. Strain energies and conformations, *J. Am. Chem. Soc.* 113 (1991) 7697–7705.
- [33] M.N. Gupta, I. Roy, Enzymes in organic media, *Eur. J. Biochem.* 271 (2004) 2575–2583.
- [34] G. Lin, H.-C. Liu, Ultrasound-promoted lipase-catalyzed reactions, *Tetrahedron Lett.* 36 (1995) 6067–6068.
- [35] S. Barton, C. Bullock, D. Weir, The effects of ultrasound on the activities of some glycosidase enzymes of industrial importance, *Enzyme Microb. Technol.* 18 (1996) 190–194.
- [36] E.N. Vulfson, D.B. Sarney, B.A. Law, Enhancement of subtilisin-catalysed interesterification in organic solvents by ultrasound irradiation, *Enzyme Microb. Technol.* 13 (1991) 123–126.
- [37] K.S. Suslick, S.E. Skrabalak, Sonocatalysis, in: G. Ertl, H. Knözinger, F. Schüth, J. Weitkamp (Eds.), Handbook of Heterogeneous Catalysis, vol. 3, Wiley-VCH, Weinheim, 2008.
- [38] M.M. Bradford, A rapid and sensitive method for the quantitation of microgram quantities of protein utilizing the principle of protein-dye binding, *Anal. Biochem.* 72 (1976) 248–254.
- [39] B. Kwiatkowska, J. Bennett, J. Akunna, G.M. Walker, D.H. Bremner, Stimulation of bioprocesses by ultrasound, *Biotechnol. Adv.* 29 (2011) 768–780.
- [40] A.M. Gumel, M.S.M. Annuar, T. Heidelberg, Y. Chisti, Thermo-kinetics of lipase-catalyzed synthesis of 6-O-glucosyldecanoate, *Bioresour. Technol.* 102 (2011) 8727–8732.
- [41] S. Koda, T. Kimura, T. Kondo, H. Mitome, A standard method to calibrate sonochemical efficiency of an individual reaction system, *Ultrason. Sonochem.* 10 (2003) 149–156.
- [42] S. Koda, H. Mori, K. Matsumoto, H. Nomura, Ultrasonic degradation of water-soluble polymers, *Polymer* 35 (1994) 30–33.
- [43] G.J. Price, P.F. Smith, Ultrasonic degradation of polymer solutions-III. The effect of changing solvent and solution concentration, *Eur. Polym. J.* 29 (1993) 419–424.
- [44] B.M.E. Van der hoff, C.E. Gall, A method for following changes in molecular weight distributions of polymers on degradation: development and comparison with ultrasonic degradation experiments, *J. Macromol. Sci. A* 11 (1977) 1739–1758.
- [45] H.Y. Yen, M.H. Yang, The ultrasonic degradation of polyacrylamide solution, *Polym. Test.* 22 (2003) 129–131.
- [46] S. Chattopadhyay, G. Madras, Influence of temperature on the ultrasonic degradation of poly (vinyl acetate) and poly (vinyl chloride), *J. Appl. Polym. Sci.* 88 (2003) 2818–2822.
- [47] J.P. Lorimer, T.J. Mason, T.C. Cuthbert, E.A. Brookfield, Effect of ultrasound on the degradation of aqueous native dextran, *Ultrason. Sonochem.* 2 (1995) S55–S57.
- [48] S. Pasupuleti, G. Madras, Ultrasonic degradation of poly (styrene-co-alkyl methacrylate) copolymers, *Ultrason. Sonochem.* 17 (2010) 819–826.
- [49] S.P. Vijayalakshmi, G. Madras, Effect of temperature on the ultrasonic degradation of polyacrylamide and poly(ethylene oxide), *Polym. Degradation Stab.* 84 (2004) 341–344.
- [50] M.T. Taghizadeh, T. Asadpour, Effect of molecular weight on the ultrasonic degradation of poly(vinyl-pyrrolidone), *Ultrason. Sonochem.* 16 (2009) 280–286.

**Biosynthesis and characterization of polyhydroxyalkanoates  
copolymers produced by *Pseudomonas putida* Bet001 isolated  
from palm oil mill effluent**

<sup>1</sup> Institute of Biological Sciences,    <sup>2</sup> Department of Chemistry  
Faculty of Science, University of Malaya, Kuala Lumpur 50603, Malaysia

(ISI cited publication: tier 1)

Writing and compilation of manuscript, established methodology, data collection, presentation and analyses. Main author of the manuscript

Supervised and assisted with manuscript compilation, editing and co-author of the manuscript.

Supervised and assisted with chemical analyses, structure elucidation and co-author of the manuscript



# Biosynthesis and Characterization of Polyhydroxyalkanoates Copolymers Produced by *Pseudomonas putida* Bet001 Isolated from Palm Oil Mill Effluent

Ahmad Mohammed Gumel<sup>1</sup>, Mohamad Suffian Mohamad Annuar<sup>1\*</sup>, Thorsten Heidelberg<sup>2</sup>

<sup>1</sup> Institute of Biological Sciences, Faculty of Science, University of Malaya, Kuala Lumpur, Malaysia, <sup>2</sup> Department of Chemistry, Faculty of Science, University of Malaya, Kuala Lumpur, Malaysia

## Abstract

The biosynthesis and characterization of medium chain length poly-3-hydroxyalkanoates (mcl-PHA) produced by *Pseudomonas putida* Bet001 isolated from palm oil mill effluent was studied. The biosynthesis of mcl-PHA in this newly isolated microorganism follows a growth-associated trend. Mcl-PHA accumulation ranging from 49.7 to 68.9% on cell dry weight (CDW) basis were observed when fatty acids ranging from octanoic acid (C<sub>8:0</sub>) to oleic acid (C<sub>18:1</sub>) were used as sole carbon and energy source. Molecular weight of the polymer was found to be ranging from 55.7 to 77.7 kDa. Depending on the type of fatty acid used, the <sup>1</sup>H NMR and GCMSMS analyses of the chiral polymer showed a composition of even and odd carbon atom chain with monomer length of C4 to C14 with C8 and C10 as the principal monomers. No unsaturated monomer was detected. Thermo-chemical analyses showed the accumulated PHA to be semi-crystalline polymer with good thermal stability, having a thermal degradation temperature (*T<sub>d</sub>*) of 264.6 to 318.8 (±0.2) °C, melting temperature (*T<sub>m</sub>*) of 43. (±0.2) °C, glass transition temperature (*T<sub>g</sub>*) of −1.0 (±0.2) °C and apparent melting enthalpy of fusion (*ΔH<sub>f</sub>*) of 100.9 (±0.1) J g<sup>−1</sup>.

**Citation:** Gumel AM, Annuar MSM, Heidelberg T (2012) Biosynthesis and Characterization of Polyhydroxyalkanoates Copolymers Produced by *Pseudomonas putida* Bet001 Isolated from Palm Oil Mill Effluent. PLoS ONE 7(9): e45214. doi:10.1371/journal.pone.0045214

**Editor:** Melanie R. Mormile, Missouri University of Science and Technology, United States of America

**Received:** May 8, 2012; **Accepted:** August 13, 2012; **Published:** September 20, 2012

**Copyright:** © 2012 Gumel et al. This is an open-access article distributed under the terms of the Creative Commons Attribution License, which permits unrestricted use, distribution, and reproduction in any medium, provided the original author and source are credited.

**Funding:** This study was funded by University of Malaya research grants RG165-11AFR, PV36/2012A, UM.C/625/1/HIR/MOHE/05 and RP024-2012A. The funders had no role in study design, data collection and analysis, decision to publish, or preparation of the manuscript.

**Competing Interests:** The authors have declared that no competing interests exist.

\* E-mail: suffian\_annuar@um.edu.my

## Introduction

The current increase in the utilization of polyhydroxyalkanoates (PHAs) in various industrial and biomedical applications is due to their biodegradability, compatibility, resorbability and piezoelectricity [1]. Their diverse chemical properties have made them a subject of many research interests. In fact, the diversity of different monomeric components in accumulated PHA that arises from superb biological polymerization system resulted in potentially diversified high-molecular weight polymeric materials. Growing concern over environmental pollution has heightened the interest in these biodegradable polymers over their chemically synthesized counterparts.

The low level of medium-chain-length PHA (mcl-PHA) and limited substrate utilization in different bacterial species, poses limitation to industrial production of these polymers [2]. The increasing demand of highly functionalized PHA for specialty applications, warrant the bio-prospecting of bacterial species capable of accumulating these biodegradable polymers. Several bacterial species known to accumulate PHA have been isolated from different ecological niches [3,4,5,6,7,8]. Among the extensively studied bacterial species are those belonging to genus *Pseudomonas* [9,10,11,12,13], that are known to accumulate intracellular PHA under limited cell growth phase in the presence

of abundant carbon source and minimal nutrient condition [14]. When fatty acid is fed to these bacteria, it passes through beta-oxidation biosynthetic pathway to produce the PHA intermediates thereby losing two (2) carbon atoms per each cycle [15,16].

A number of published works use unsaturated fatty acids such as oleic acid (C<sub>18:1</sub>) to produce mcl-PHA with unsaturated side-chain monomers [17,18,19,20]. In this study, the growth and biosynthesis of mcl-PHA by a strain of *Pseudomonas putida* isolated from palm oil mill effluent are reported, along with characterization of the mcl-PHA copolymer produced when the bacterium is fed with oleic acid (C<sub>18:1</sub>). For comparison, selected fatty acids *viz.* octanoic acid (C<sub>8:0</sub>), dodecanoic acid (C<sub>12:0</sub>) and hexadecanoic acid (C<sub>16:0</sub>) were also tested as substrates.

## Methods

### Bacterial Isolation and Characterization

*Pseudomonas putida* Bet001 was isolated from palm oil mill effluent using isolation agar medium containing (g L<sup>−1</sup>): peptone 20; K<sub>2</sub>SO<sub>4</sub> 10; MgCl<sub>2</sub>·6H<sub>2</sub>O 1.4; irgasan 0.025; glycerol 25.2 and agar 13.6. Preliminary biochemical characterization was done using api<sup>®</sup> 20 NE (bioMérieux<sup>®</sup> USA) biochemical typing kits as stated in manufacturer's guideline. Intracellular PHA accumulation was screened using both Sudan Black B and Nile red staining



techniques according to literatures [21,22]. Intracellular PHA granules accumulation was also observed using transmission electron microscopy (Philips CM12, United Kingdom). The morphology of the bacterial colonies isolated and the Gram staining characteristics were observed under Motic® microscope BA200 equipped with Moticam 2300 camera (Motic®, Japan). GF1 DNA extraction kit (Vivantis Sdn Bhd, Malaysia) was used to extract the bacterial DNA for the 16S rRNA molecular characterization according to manufacturer's guidelines. Post PCR analysis was done by blasting of both forward and reverse sequences against sequences in GeneBank (NCBI) and RDP II (Ribosomal Database Project II) databases to search for homology sequences. The extracted DNA nucleotide sequence has been deposited in European Nucleotide Archive (ENA) with accession number HE573173.

### Culture Conditions and Fermentation Process

Sterile growth medium (100 ml per each 250 ml conical flask) containing (g L<sup>-1</sup>): yeast extract 10.0 (Bacto™ USA), nutrient broth 15.0 (Merck, Germany) and ammonium sulfate 5.0 (Sigma Aldrich, Germany) was used as inoculum cultivation medium for the bacterium. 3% (v/v) of *P. putida* Bet001 stock inoculum was introduced into this medium aseptically and incubated in shaking incubator (Daihan LabTech®, Korea) at 30°C, 250 rpm for 24 hours. The biomass was harvested from 3 ml culture broth *via* centrifugation at 4°C, 9000 ×g for 10 min. The recovered biomass was seeded aseptically into PHA production medium. The medium contains sterile minerals of (g L<sup>-1</sup>) sodium ammonium hydrogen phosphate tetrahydrate [NaNH<sub>4</sub>H-PO<sub>4</sub>·4H<sub>2</sub>O] 3.5, K<sub>2</sub>HPO<sub>4</sub> 5.7, KH<sub>2</sub>PO<sub>4</sub> 3.7, and 10 mM oleic acid (unless otherwise stated) at a pH of 7.0 (±0.1). Separate sterile solutions of 0.1 M MgSO<sub>4</sub>·7H<sub>2</sub>O and trace elements (MT) containing (g L<sup>-1</sup>): CaCl<sub>2</sub>·2H<sub>2</sub>O 1.47, CoCl<sub>2</sub>·6H<sub>2</sub>O 2.38, CuCl<sub>2</sub>·2H<sub>2</sub>O 0.17, FeSO<sub>4</sub>·7H<sub>2</sub>O 2.78, MnCl<sub>2</sub>·4H<sub>2</sub>O 1.98 and ZnSO<sub>4</sub>·7H<sub>2</sub>O 0.29 dissolved in 1 M HCl were aseptically added to the PHA production media prior to inoculation at 1.0% (v/v) and 0.1% (v/v), respectively. 5 g L<sup>-1</sup> of harvested biomass from inoculum growth media was seeded into this medium (100 ml per 250 ml conical flask) aseptically and incubated as described previously for a total period of 48 hours unless otherwise stated. PHA extraction was done according to literature [10]. 5 g of vacuum dried biomass was suspended in 30 ml chloroform and refluxed at 60°C for 4 hours. The refluxed chloroform containing the extracted PHA was filtered out of the residual biomass debris using Buchner filter funnel equipped with sintered glass. The filtrate was then concentrated under vacuum using rotary evaporator at 40°C until about a fifth of the total volume. The polymer was precipitated out of the concentrate by dispersing it into a beaker containing excess cold methanol (at least 1:4 volume ratio). The mcl-PHA obtained underwent a minimum of three-repeated purification process by sequential chloroform dissolution and methanol re-precipitation.

### Biomass Estimation

A known biomass dry weight concentrations were used to prepare a standard calibration, using Jasco V-630 UV/VIS spectrophotometer (Jasco, Japan) at the absorbance of 600 nm. Aliquot samples were withdrawn aseptically at regular intervals and centrifuged at 9000 ×g for 10 min, then washed twice with 0.05 M phosphate buffer. After final centrifugation, the cells were re-suspended in the same buffer prior to absorbance reading against the phosphate buffer blank.

### Residual Fatty Acid Quantification

The residual fatty acid estimation was done according to Marseno et al. [23] modified protocol. Cell free supernatant (1 ml) was mixed with *n*-heptane (3 ml) and centrifuge at 9000 ×g to separate the residual fatty acid. 2 ml of the top layer of *n*-heptane was withdrawn into a test tube, to this solution, 200 µl of 5% (w/v) copper (II) acetate monohydrate solution (5 g copper (II) acetate monohydrate dissolved in 90 ml distilled water; pyridine and distilled water were respectively used to adjust the solution pH to 6 and bring the final volume to 100 ml) was added and vortexed for 60 sec. This mixture was allowed to stand for 20 sec before it was read at 705 nm against distilled water blank using Jasco V-630 UV/VIS spectrophotometer (Jasco, Japan). A standard calibration was performed using a stock of different fatty acid concentrations (0.5 to 1 mM) that were made by dissolving the specified mass of fatty acid in *n*-heptane and treated as mentioned earlier.

### Residual Ammonium Quantification

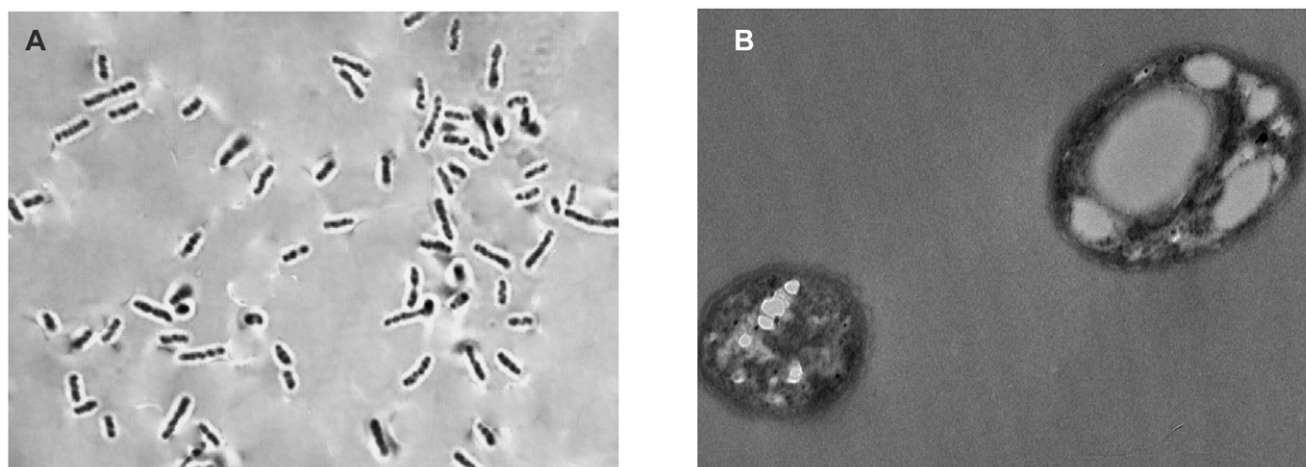
Residual ammonium was quantified using phenol hypochlorite method as described by Solorzano [24]. Cell free supernatant (2 ml) was diluted with distilled water to 5 ml. To this solution 0.2 ml of alcoholic phenol (10 g phenol in 90 ml absolute ethanol) was added followed by the addition of 0.2 ml of sodium nitroprusside solution (0.5 g sodium nitroprusside in 99.5 ml distilled water). Oxidizing solution (0.5 ml) was added to the mixture while agitating to ensure uniform indole-phenol coloration. The oxidizing solution was composed of 4:1 mixture of alkaline solution to oxidizing reagent. The alkaline solution was composed of 100 g trisodium citrate, 5 g sodium hydroxide dissolved in 500 ml of distilled water. The oxidizing reagent was 1.5 N sodium hypochlorite solution. The mixture was then allowed to stand for an hour at room temperature (27°C) resulting in light-blue coloration that was measured as described above at 640 nm against blank distilled water. Residual ammonium concentration was then quantified in reference to standard calibration curve of known ammonium concentrations.

### PHA Authentication

**FTIR spectroscopy.** Attenuated total reflectance (ATR) FTIR was used to record the PHA spectrum on Perkin-Elmer FTIR *spectrum-400* spectrometer (Perkin-Elmer Inc., Wellesley, MA, USA) at room temperature (27°C) and a scan range of 400 to 4000 cm<sup>-1</sup> was applied for 10 scans. A paste of 0.01 g of the sample was prepared in dichloromethane. A liquid film of the mixture was then applied on to NaCl crystal window and the spectrum was read after the solvent has been dried.

**Proton NMR analysis.** JEOL JNM-GSX 270 FT-NMR (JOEL Ltd, Tokyo, Japan) spectrometer was used to record the <sup>1</sup>H NMR spectrum at 250 MHz against tetramethylsilane (TMS) internal reference standard. Approximately 5 mg PHA sample was dissolved in 2 ml deuterated chloroform (CDCl<sub>3</sub>) and filtered into NMR tube using borosilicate glass syringe equipped with 0.22 µm PTFE disposable filter (11807–25, Sartorius Stedim, Germany).

**GC-MSMS analysis.** GC-MSMS was recorded on Agilent triple quadrupole 7000B (Agilent, USA), equipped with GCMSMS triple axis detector carrying Agilent HP-5 ms column (30 m length × 0.25 mm internal diameter × 0.25 µm film). PHA sample in the form of hydroxyalkanoic acids methyl esters were used for the GC-MSMS analysis according to method reported in literatures [25,26]. Methanolized sample (1 µl) was automatically injected into the GC at a split ratio of 1:50. The injection temperature was set at 280°C while the oven and column temperatures were programmed as 40°C for 1 min then increase



**Figure 1. *Pseudomonas putida* Bet001 cells showing PHA inclusion.** (A) phase contrast (X 100 magnification) and (B) T.E.M (X 5000 magnification) when cultivated on palmitic acid ( $C_{16:0}$ ) at 30°C, 200 rpm for 48 h. doi:10.1371/journal.pone.0045214.g001

to 120°C at 15°C min<sup>-1</sup>, hold for 2 min, and increase to 250°C at 10°C min<sup>-1</sup> hold for 15 min. Helium was used as carrier gas at 48.3 ml min<sup>-1</sup> and 0.41 bar pressure. Mass spectra were acquired at 1250 scan speed using electron impact energy of 70 eV at 200°C ion-source and 280°C interface temperatures respectively. Standard monomers of methyl hydroxyalkanoates (Larodan, Sweden) were used as reference for peak retention time and ionization mass determination.

**Gel permeation chromatography (GPC).** Waters 600 (Waters Corp, Milford, MA, USA) equipped with a Waters refractive index detector (model 2414) having the following gel columns (7.8 mm internal diameter 300 mm) in series: HR1, HR2, HR5E and HR5E Waters Styragel HR-THF was used to record the chromatogram relative to calibration curve of standard monodisperse polystyrenes ( $3.72 \times 10^2$ ,  $2.63 \times 10^3$ ,  $9.10 \times 10^3$ ,  $3.79 \times 10^4$ ,  $3.55 \times 10^5$ ,  $7.06 \times 10^5$ ,  $3.84 \times 10^6$  and  $6.77 \times 10^6$  Da). The PHA samples were dissolved in tetrahydrofuran (THF) at a concentration of 2.0 mg mL<sup>-1</sup>, filtered through a 0.22 µm PTFE filter. 100 µL aliquot of the sample was injected at 40°C using THF as a mobile phase at a flow rate of 1.0 mL min<sup>-1</sup>.

### Thermal Analyses

**Differential scanning calorimetry (DSC).** The extracted PHA was subjected to differential thermal analysis using Mettler-Toledo differential scanning calorimeter (DSC 822e; Mettler-Toledo, USA) running STARe DSC ver 8.10 software; equipped with HAAKE EK90/MT digital immersion cooler (Thermo Fischer Scientific, USA). Scans were made at a temperature range of -60°C to 180°C with a heating rate of 10°C min<sup>-1</sup> under a nitrogen flow rate of 0.12 L min<sup>-1</sup> at a head pressure of 1.5 bar. The melting temperature ( $T_m$ ) was taken at the endothermic peak of the DSC thermogram. The endothermic melting enthalpy ( $\Delta H_m$ ) was used to calculate the polymer crystallinity ( $X_p$ ) on the basis of melting enthalpy ( $\Delta H_m^0$ ) of 100% crystalline PHB according to equation 1 as reported somewhere else [27], assuming 142 J g<sup>-1</sup> as the melting enthalpy of 100% crystalline PHB as cited in literature [28].

$$X_p = \frac{\Delta H_m}{\Delta H_m^0} \quad (1)$$

**Thermogravimetric analysis (TGA).** TGA analysis was performed on a Perkin-Elmer TGA 4000 instrument. The sample was heated from 50°C to 900°C at a rate of 10°C min<sup>-1</sup> under a nitrogen flow rate of 20 ml min<sup>-1</sup>.

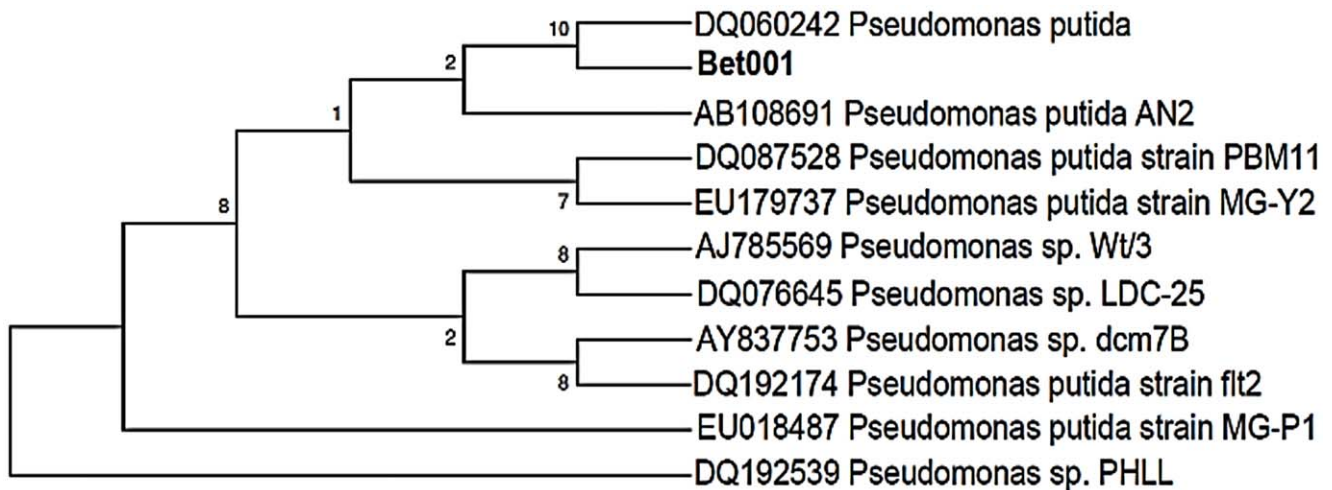
## Results and Discussion

### Strain Characterization and PHA Production

Sudan Black B staining was used in the microscopic observation for a possible accumulation of intracellular PHA by the isolated strain (Fig. 1a). Further confirmation of the presence of accumulated granule was made by transmission electron microscopy (Fig. 1b). The bacterial strain was further characterized using biochemical analyses and 16S rRNA molecular characterization. The biochemical analyses indicated a probability of 99.5% for the isolate to be identified as *Pseudomonas putida*. This result was corroborated by RDP blast neighbor-joining phylogenetic analysis (Fig. 2), where 99% analogy was observed between the isolate and *Pseudomonas putida* strains AJ785569, AN2, BCNU106, DQ060242 and DQ087528. This isolate was designated as *P. putida* Bet001 and subsequently used in the PHA production using shake flask in a two-step batch fermentation process with different fatty acids as a sole carbon and energy source. PHA accumulation was observed to span from 49.7 to 68.9 dry weight % and was composed of varied monomer fractions ranging from 3-hydroxyhexanoate to 3-hydroxytetradecanoate depending on the culture conditions and the type of fatty acids used.

### PHA Authentication

**FTIR spectroscopy.** The extracted PHA sample was subjected to nondestructive attenuated total reflectance FT-IR. Observed infrared absorption at 3420.20 cm<sup>-1</sup> was assigned to the hydroxyl group of the polymer chain [29]. Absorption band at 2955.76 cm<sup>-1</sup> was assigned to asymmetric methyl group. Asymmetric CH<sub>2</sub> of the lateral monomeric chains were assigned to the stretching vibration at 2925.98 cm<sup>-1</sup>. The absorption at 2855.99 cm<sup>-1</sup> has been assigned to symmetrical CH<sub>3</sub> and the intensity of the band has been reported to be due to conformational disorder obtained in the process of crystallization [28]. While the absorption band of 1741.44 cm<sup>-1</sup> has been reported to be a PHA marker band assigned to carbonyl (C=O) ester bond stretching vibration according to Randria-

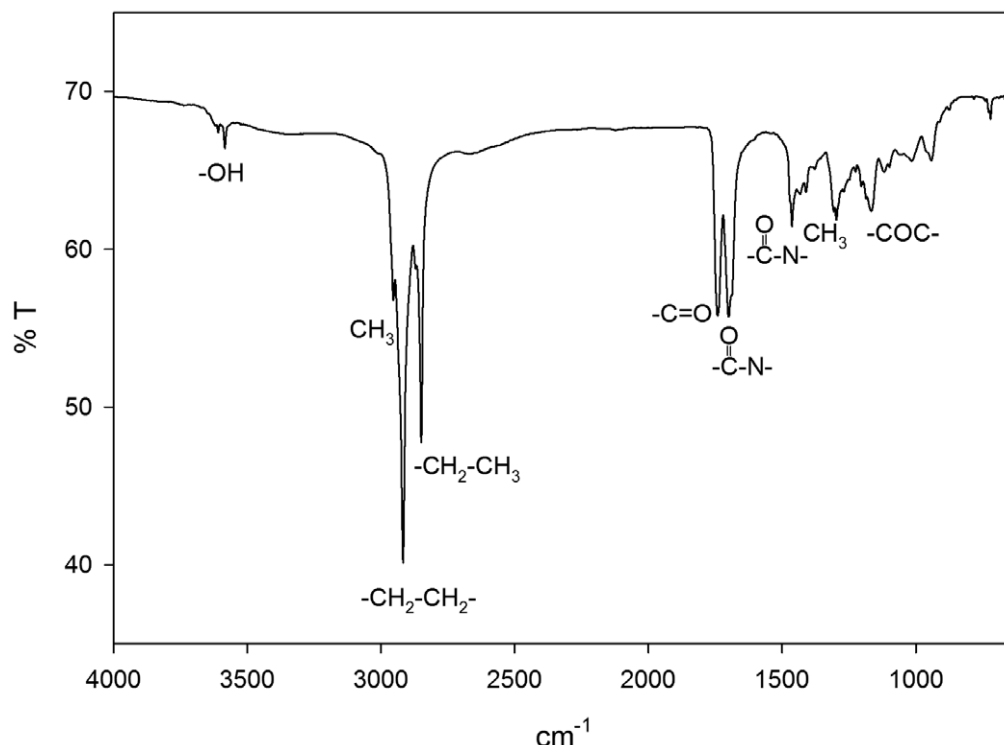


**Figure 2. Neighbor joining phylogenetic tree showing the interrelationship between isolate Bet001 and top 10 Blast hits from RDP database.**

doi:10.1371/journal.pone.0045214.g002

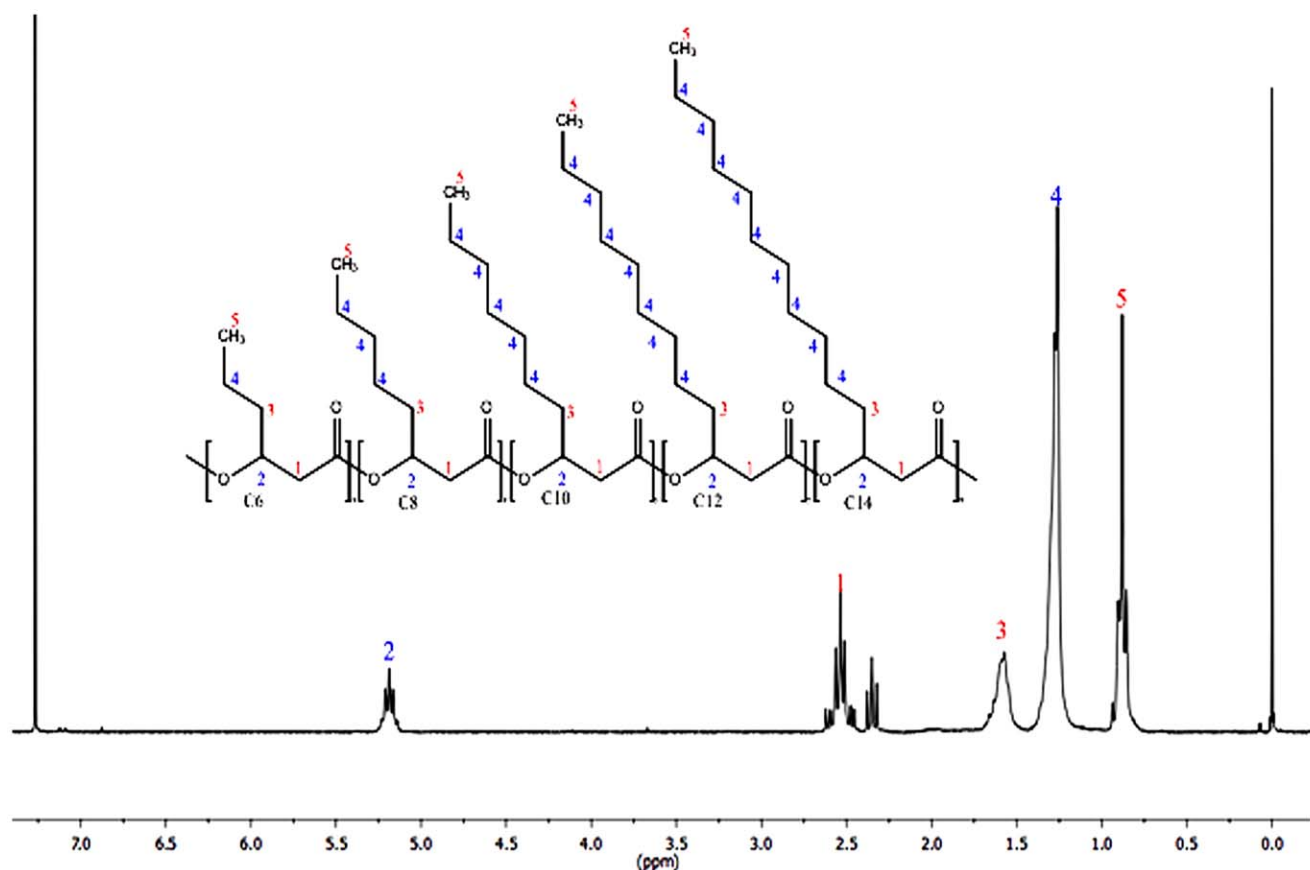
mahefa et al. [30]. The vibrations at  $1659.50$  and  $1460.39\text{ cm}^{-1}$  have been assigned to bacterial intracellular amide ( $-\text{CO}-\text{N}-$ ) I and II respectively (Fig. 3); furthermore, these bands were also reported to be species specific [30]. Absorption at  $1378.83\text{ cm}^{-1}$  is assigned to terminal  $\text{CH}_3$  groups [12], while that at  $1259.89\text{ cm}^{-1}$  is due to asymmetric  $\text{C}-\text{O}-\text{C}$  stretching vibration. Series of absorption bands at  $1166.87\text{ cm}^{-1}$  to  $619.39\text{ cm}^{-1}$  were assigned to  $\text{C}-\text{O}$  and  $\text{C}-\text{C}$  stretching vibration in the amorphous phase.

**PHA proton NMR characterization.** The proton NMR spectrum of the produced PHA was characterized in reference to the internal standard trimethylsilane. The observed multiplet peaks number 1 ( $\delta$  2.5 ppm) and triplet peaks 2 ( $\delta$  5.2 ppm) are assigned to methylene and methine protons of the  $\alpha$  and  $\beta$ -carbon respectively [15,16,18,31]. Contrary to some literatures assigning the observed triplets at chemical shift 2.3 ppm (Fig. 4) to unsaturation of PHA monomers [18,26], upon further analysis using GCMSMS, we proposed the peak to be due to hydrophobic oleate and palmitate from cellular membrane lipids. Peak number



**Figure 3. FTIR-ATR spectrum of the PHA extracted from *P. putida* Bet001 fed on oleic acid ( $\text{C}_{18:1}$ ).**

doi:10.1371/journal.pone.0045214.g003



**Figure 4. NMR ( $^1\text{H}$ ) spectrum of the PHA extracted from *P. putida* Bet001 fed on palmitic acid ( $\text{C}_{16:0}$ ).**  
doi:10.1371/journal.pone.0045214.g004

3 ( $\delta$  1.6 ppm) is assigned to methylene protons adjacent to the  $\beta$ -carbon in the side-chains [15,16,18,31]. Peak number 4 ( $\delta$  1.3) and triplet number 5 ( $\delta$  0.9) are assigned to the methylene protons and terminal methyl proton of the side-chains respectively [15,16,18,31].

### Thermal Analyses

The calorimetric scan of the extracted PHA showed the endothermic melting temperature ( $T_m$ ) of this polymer to be  $43.0 (\pm 0.2)^\circ\text{C}$ , glass transition temperature ( $T_g$ ) of  $-1.0 (\pm 0.2)^\circ\text{C}$  and apparent melting enthalpy of fusion ( $\Delta H_f$ ) of  $100.9 (\pm 0.1) \text{ J g}^{-1}$ . The relatively low melting and glass transition temperatures were attributed to the random composition of 3HA monomers in the polymer (see later discussion). This observation was found to be in good agreement with what has been reported by Matsusaki et al. [32] when observing the PHA biosynthesis in recombinant *Pseudomonas* sp. 6 1–3 strain fed with dodecanoic acid ( $\text{C}_{12:0}$ ). The bacterium produced random copolymer of PHA with endothermic melting temperature of  $42^\circ\text{C}$ . The observed high apparent heat of fusion could be due to the presence of long chain monomer fraction which in turn was reported to favor side-chain crystallization resulting in polymer with high apparent enthalpy of fusion. This observation was found to agree with reported literatures [15,16,33].

PHA thermal stability is an important parameter to be studied during polymer analyses as it reflects the maximum temperature the polymer can withstand before thermal decomposition. Thermal gravimetric analysis of the extracted polymer showed an increase in polymer thermal stability with increasing fatty acid

chain length fed i.e. from  $\text{C}_{8:0}$  to  $\text{C}_{18:1}$  (thermal degradation temperature of  $264.6$  to  $318.8^\circ\text{C} \pm 0.2$ ). This is attributed to the increase in the fractions of longer monomer such as 3HDD and 3HTD that became incorporated into the PHA from the metabolism of the longer fatty acid substrates (Table 1). It has been reported also that this increase in thermal stability could be due to random co-monomer chain-length that resulted in high side chain crystallization conferring thermal stability to the polymer [15,33].

### Effect of Carbon Source on the PHA Composition and Yield

The effect of different carbon source on PHA composition has been studied. The composition of PHA accumulated by *P. putida* Bet001 grown on different carbon sources at  $30^\circ\text{C}$  for 48 hours is presented in Table 1. PHA accumulation in the range of 49.7 to 68.9% (w/w) has been observed when the organism is fed with  $\text{C}_{8:0}$  to  $\text{C}_{18:1}$  fatty acids, with a polymer composition ranging from 3HB (four carbon atom length) to 3HTD (fourteen carbon atom length) except when oleic acid was used as substrate, a small amount of odd chain monomer i.e. 3HHp (seven carbon atom length) was also detected. At first, this was considered as possible contamination of the extracted polymer sample by cellular components. Thus, the purification step was repeated at least three times and the polymer re-extracted for GCMSMS analysis. The persistence of the strong signal detected by mass spectrometry for the presence of 3HHp entails re-consideration of the contamination hypothesis with non-PHA components. From the

**Table 1.** PHA composition as a function of carbon source (max. standard error  $\pm 5\%$ ).

| Carbon source     | %PHA (w/w) | PHA mole fraction (mole %) |                           |                            |                          |                           |                            |                            | $M_n$ | $M_w$ | PDI |
|-------------------|------------|----------------------------|---------------------------|----------------------------|--------------------------|---------------------------|----------------------------|----------------------------|-------|-------|-----|
|                   |            | 3HB <sup>†</sup><br>(C4)   | 3HHx <sup>‡</sup><br>(C6) | 3HHp <sup>  </sup><br>(C7) | 3HO <sup>†</sup><br>(C8) | 3HD <sup>#</sup><br>(C10) | 3HDD <sup>§</sup><br>(C12) | 3HTD <sup>*</sup><br>(C14) |       |       |     |
| C <sub>8:0</sub>  | 49.7       | ND                         | 8.1                       | ND                         | 76.2                     | 11.0                      | 4.7                        | ND                         | 38685 | 77657 | 2.0 |
| C <sub>12:0</sub> | 54.5       | ND                         | 3.5                       | ND                         | 38.2                     | 38.9                      | 19.4                       | ND                         | 31388 | 60056 | 1.9 |
| C <sub>16:0</sub> | 65.3       | ND                         | 4.1                       | ND                         | 36.9                     | 34.8                      | 18.0                       | 6.3                        | 13608 | 55685 | 4.1 |
| C <sub>18:1</sub> | 68.9       | 1.5                        | 5.0                       | 0.7                        | 31.8                     | 24.1                      | 22.9                       | 14.1                       | 35308 | 74958 | 2.1 |

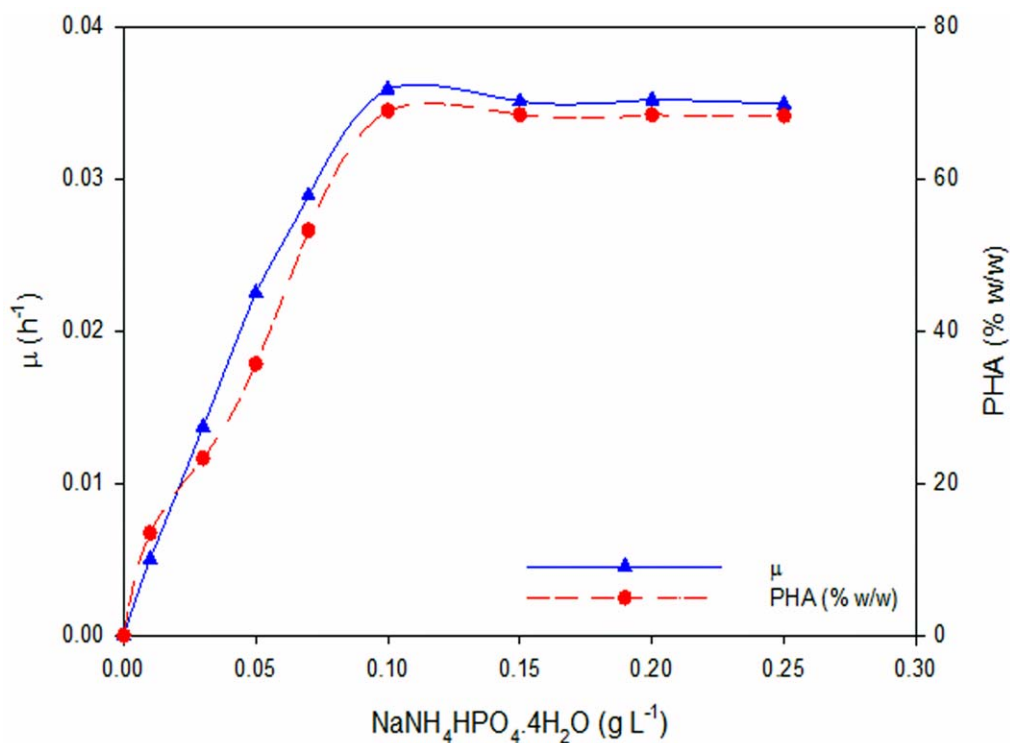
<sup>†</sup>(hydroxybutyrate)<sup>‡</sup>(hydroxyhexanoate)<sup>||</sup>(hydroxyheptanoate)<sup>#</sup>(hydroxyoctanoate)<sup>§</sup>(hydroxydecanoate)<sup>\*</sup>(hydroxydodecanoate)<sup>\*</sup>(hydroxytetradecanoate), ND (not detected).

doi:10.1371/journal.pone.0045214.t001

basic knowledge about  $\beta$ -oxidation of even carbon atom length of fatty acids, it is not clear at this point the exact reason for the incorporation of an odd carbon atom length monomer like 3HHp into the polymer when oleic acid (C<sub>18:1</sub>) was used as a sole carbon and energy source for the bacterial growth and PHA accumulation, and not with other fatty acids tested.

Based on mass spectrometric analyses, feeding dodecanoic acid as sole carbon source resulted in PHA composed of four different monomers (3HHx 3.54 mole%, 3HO 38.19 mole%, 3HD 38.85 mole% and 3HDD 19.42 mole%). Similarly, Chung

et al. [15] reported *P. entomophila* L48 to accumulate PHA having four different monomer units when fed with dodecanoic acid, with monomer fractions of 3HD (38.6%), 3HO (44.5%) as the dominant fractions. Feeding hexadecanoic acid as a carbon and energy source to *P. putida* Bet001 resulted in PHA with five different monomers (3HHx 4.06 mole%, 3HO 36.93 mole%, 3HD 34.78 mole%, 3HDD 17.97 mole% and 3HTD 6.26 mole%). When oleic acid (C<sub>18:1</sub>) was fed under the same conditions, copolymer with up to seven different monomers of 3HB (1.52 mole%), 3HHx (5.01 mole%), 3HO (31.81 mole%),

**Figure 5.** Specific growth rate and PHA content as a function of ammonium ion concentrations in *P. putida* Bet001 fed on oleic acid (C<sub>18:1</sub>).

doi:10.1371/journal.pone.0045214.g005

**Table 2.** Effect of carbon-to-nitrogen molar ratio on PHA content and biomass in batch culture of *P. putida* Bet001 grown on oleic acid (C<sub>18:1</sub>) (max. standard error  $\pm 5\%$ ).

| C:N    | PHA                   | Biomass              | $M_w$ | $X_p$ | PDI |
|--------|-----------------------|----------------------|-------|-------|-----|
| (mole) | (% w/w dried biomass) | (g L <sup>-1</sup> ) | (Da)  |       |     |
| 10     | 16.2                  | 9.60                 | 49147 | 0.76  | 2.1 |
| 15     | 39.3                  | 11.4                 | 52143 | 0.74  | 2.1 |
| 20     | 55.5                  | 15.3                 | 74958 | 0.72  | 2.1 |
| 25     | 68.9                  | 14.5                 | 45678 | 0.75  | 2.1 |
| 30     | 68.4                  | 13.9                 | 37444 | 0.73  | 2.2 |

doi:10.1371/journal.pone.0045214.t002

3HD (24.07 mole%), 3HDD (22.86 mole%), 3HTD (14.05 mole%) and a small amount of odd carbon chain length monomer of 3-hydroxyheptanoate (3HHp) (0.68 mole mole%) were obtained. In contrast to other fatty acids tested, when oleic acid was fed, a short-chain length monomer of 3HB (four carbon atom length) accumulated. The accumulation of 3HB monomer was not detected in the bacterium when fatty acids C<sub>8:0</sub>, C<sub>12:0</sub> and C<sub>16:0</sub> were fed. Again, similar to the accumulation of 3HHp, the exact reason for this observation is not clear at this stage. It was also observed that when oleic acid (C<sub>18:1</sub>) was fed, no unsaturated PHA monomer was detected in the polymer produced. The most abundant monomers were C8 and C10 in all the samples tested, and this is in agreement with the hypothesis that PHA formed by *Pseudomonads* belonging to rRNA homology group I have C8 and C10 monomers as dominant components when grown on C8 to C18 fatty acids substrate [18,34].

From the results presented in Table 1, the relationship between the PHA composition and the structure of the carbon source substrate showed that the PHA biosynthetic precursors in this bacterium are very likely fed by  $\beta$ -oxidation pathway.

### Effect of Nitrogen Source Concentration on Specific Growth Rate ( $\mu$ ) and PHA Yield

The effect of nitrogen source concentration on specific growth rate and PHA yield during PHA biosynthesis in *P. putida* Bet001 is depicted in Fig. 5. It is clear that as the ammonium ion concentration increases from 0.01 to 0.1 g L<sup>-1</sup>, the specific growth ( $\mu$ ) also increases from 0.005 to 0.036 h<sup>-1</sup> with corresponding PHA yield of 13.4 to 68.9% (w/w) respectively. Increasing nitrogen source beyond this point resulted in a gradual plateau in the specific growth rate, probably due to the carbon source concentration began to be limited as in this study where the ammonium ion concentration was varied and the carbon source concentration was kept fixed. In a similar study, Annur et al. [35] observed the increase in specific growth rate of *P. putida* PGA1 from 0 to 0.18 h<sup>-1</sup> by increasing the ammonium ion concentration from 0 to 0.1 g L<sup>-1</sup>; further increase in ammonium ion concentration (0.6 to 0.8 g L<sup>-1</sup>) resulted in a decrease in the

specific growth rate to 0.14 h<sup>-1</sup>. Interestingly, the PHA fraction from the total biomass also increases as the specific growth rate increases, indicating a growth associated PHA biosynthesis in this bacterium. The PHA fraction reached a constant value when specific growth rate became constant at high ammonium ion concentrations. This is in contrast with the recognized PHA accumulation in many *Pseudomonas* species, where the highest accumulation is observed when the specific growth rate of the organism is low under nutrient limitation/starvation [14,18,35]. The observed increase in the specific growth rate at low ammonium ion concentrations ( $\leq 0.1$  g L<sup>-1</sup>) could probably be due to high ammonium uptake by the cells [35].

### Influence of Carbon-nitrogen Molar Ratio on Biomass and Polymer Content

It has been observed that PHA content of the cell can be increased by changing the molar ratio between carbon-to-nitrogen (C:N) source (Table 2). By fixing the ammonium ion concentration at 0.1 g L<sup>-1</sup> while varying the carbon source concentration; it is observed that increase in C:N molar ratio from 10 to 30 was followed by increase in percentage PHA accumulation and biomass from 16 to 69% and from 9.6 to 15.3 g L<sup>-1</sup>, respectively. The proportional increase in biomass with increase of C:N ratio up to 20, could indicate that below 20 carbon is limiting growth. Additional increase in C:N molar ratio after 20 however, did not results in further increase in biomass amount, as it is expected that the ammonium concentration no longer sufficient to sustain extended growth. The results from this experiment offer additional support for the growth-linked PHA accumulation in this bacterium. Maximum PHA accumulation at approximately 70% was found for C:N molar ratios of 25 and 30. The molecular weight of the PHA from the different C:N molar ratios tested fell within a narrow range of 37 to 75 kDa. The crystallinity ( $X_p$ ) and poly dispersity index (PDI) remained constant at all the C:N molar ratio tested.

### Conclusions

A chiral PHA copolymer consisting of monomers ranging from 3-hydroxybutyrate (3HB) to 3-hydroxytetradecanoate (3HTD) were synthesized by a new isolate *P. putida* Bet001 when fed with different fatty acids. The biosynthesis of the PHA by this new isolate is growth-associated. When fed with oleic acid (C<sub>18:1</sub>), the PHA extracted from the isolate showed the presence of a monomer with odd carbon atom length i.e. 3-hydroxyheptanoate (3HHp). However, no unsaturated monomer was detected when oleic acid (C<sub>18:1</sub>) was fed. *P. putida* Bet001 accumulated about 69% PHA on cell dry weight basis with good thermal stability, relatively high molecular weight and crystallinity.

### Author Contributions

Conceived and designed the experiments: AMG MSMA. Performed the experiments: AMG. Analyzed the data: AMG MSMA TH. Contributed reagents/materials/analysis tools: MSMA. Wrote the paper: AMG MSMA.

### References

- Rai R, Keshavarz T, Roether J, Boccaccini A, Roy I (2011) Medium chain length polyhydroxyalkanoates, promising new biomedical materials for the future. *Mat Sci Eng R* 72 29–47.
- Gumel AM, Annur MSM, Heidelberg T (2012) Effects of carbon substrates on biodegradable polymer composition and stability produced by *Delfia tsurhatensis* Bet002 isolated from palm oil mill effluent. *Polym Degradation Stab* 97: 1227–1231.
- Akaraonye E, Keshavarz T, Roy I (2010) Production of polyhydroxyalkanoates: the future green materials of choice. *J Chem Technol Biotechnol* 85: 732–743.
- Bohmert-Tatarev K, Mcavoy S, Peoples OP, Snell KD (2010) Stable, fertile, high polyhydroxyalkanoate producing plants and methods of producing them. US Patent App. 20,100/229,258.



5. Grothe E, Chisti Y (2000) Poly (3-hydroxybutyric acid) thermoplastic production by *Alcaligenes latus*: Behavior of fed-batch cultures. *Bioproc Biosyst Eng* 22: 441–449.
6. Thomson N, Roy I, Summers D, Sivaniah E (2010) *In vitro* production of polyhydroxyalkanoates: achievements and applications. *J Chem Technol Biotechnol* 85: 760–767.
7. Yamane T (1992) Cultivation engineering of microbial bioplastics production. *FEMS Microbiol Lett* 103: 257–264.
8. Dalal J, Sarma PM, Lavania M, Mandal AK, Lal B (2010) Evaluation of bacterial strains isolated from oil-contaminated soil for production of polyhydroxyalkanoic acids (PHA). *Pedobiologia* 54: 25–30.
9. Allen AD, Anderson WA, Ayorinde FO, Eribo BE (2010) Biosynthesis and characterization of copolymer poly (3HB-co-3HV) from saponified *Jatropha curcas* oil by *Pseudomonas oleovorans*. *J Ind Microbiol Biotechnol* 37: 849–856.
10. Annuar MSM, Tan IKP, Ibrahim S, Ramachandran KB (2007) Production of medium-chain-length poly (3-hydroxyalkanoates) from crude fatty acids mixture by *Pseudomonas putida*. *Food and Bioprocess Proc* 85: 104–119.
11. Elbahloul Y, Steinbüchel A (2009) Large-scale production of poly (3-hydroxyoctanoic acid) by *Pseudomonas putida* GPo1 and a simplified downstream process. *Appl Environ Microbiol* 75: 643–651.
12. Sha K, Li D, Li Y, Zhang B, Wang J (2008) The chemoenzymatic synthesis of a novel CBABC-type pentablock copolymer and its self-assembled “crew-cut” aggregation. *Macromolecules* 41: 361–371.
13. Vishnuvardhan Reddy S, Thirumala M, Mahmood S (2009) Production of PHB and P (3HB-co-3HV) biopolymers by *Bacillus megaterium* strain OU303A isolated from municipal sewage sludge. *World J Microbiol Biotechnol* 25: 391–397.
14. Annuar MSM, Tan IKP, Ramachandran KB (2008) Evaluation of nitrogen sources for growth and production of medium-chain-length poly-(3-hydroxyalkanoates) from palm kernel oil by *Pseudomonas putida* PGA1. *Asia-Pac J Mol Biol Biotechnol* 16: 11–15.
15. Chung AL, Jin HL, Huang LJ, Ye HM, Chen JC, et al. (2011) Biosynthesis and characterization of poly (3-hydroxydodecanoate) by  $\beta$ -oxidation inhibited mutant of *Pseudomonas entomophila* L48. *Biomacromolecules* 12: 3559–3566.
16. Liu Q, Luo G, Zhou XR, Chen G-Q (2011) Biosynthesis of poly(3-hydroxydecanoate) and 3-hydroxydodecanoate dominating polyhydroxyalkanoates by  $\beta$ -oxidation pathway inhibited *Pseudomonas putida*. *Metab Eng* 13: 11–17.
17. Albuquerque MGE, Martino V, Pollet E, Averous L, Reis MAM (2011) Mixed culture polyhydroxyalkanoate (PHA) production from volatile fatty acid (VFA)-rich streams: Effect of substrate composition and feeding regime on PHA productivity, composition and properties. *J Biotechnol* 151: 66–76.
18. Haba E, Vidal-Mas J, Bassas M, Espuny MJ, Llorens J, et al. (2007) Poly 3-(hydroxyalkanoates) produced from oily substrates by *Pseudomonas aeruginosa* 47T2 (NCBIM 40044): Effect of nutrients and incubation temperature on polymer composition. *Biochem Eng J* 35: 99–106.
19. Ni Y-Y, Kim DY, Chung MG, Lee SH, Park H-Y, et al. (2010) Biosynthesis of medium-chain-length poly(3-hydroxyalkanoates) by volatile aromatic hydrocarbons-degrading *Pseudomonas fulva* TY16. *Bioresour Technol* 101: 8485–8488.
20. Tan IKP, Kumar KS, Theanmalar M, Gan SN, Gordon Ii B (1997) Saponified palm kernel oil and its major free fatty acids as carbon substrates for the production of polyhydroxyalkanoates in *Pseudomonas putida* PGA1. *Appl Microbiol Biotechnol* 47: 207–211.
21. Burdon KL (1946) Fatty material in bacteria and fungi revealed by staining dried, fixed slide preparations. *J Bacteriol* 52: 665–678.
22. Spiekermann P, Rehm BHA, Kalscheuer R, Baumeister D, Steinbüchel A (1999) A sensitive, viable-colony staining method using Nile red for direct screening of bacteria that accumulate polyhydroxyalkanoic acids and other lipid storage compounds. *Arch Microbiol* 171: 73–80.
23. Marseno DW, Indrati R, Ohta Y (1998) A Simplified Method for Determination of Free Fatty Acids for Soluble and Immobilized Lipase Assay. *Indon Food Nutr Prog* 5: 79–83.
24. Solorzano L (1969) Determination of ammonia in natural waters by the phenylhypochlorite method. *Limnol Oceanogr* 14: 799–801.
25. Lee EY, Choi CY (1997) Structural identification of polyhydroxyalkanoic acid (PHA) containing 4-hydroxyalkanoic acids by gas chromatography-mass spectrometry (GC-MS) and its application to bacteria screening. *Biotechnol Tech* 11: 167–171.
26. Sin MC, Annuar MSM, Tan IKP, Gan SN (2010) Thermodegradation of medium-chain-length poly (3-hydroxyalkanoates) produced by *Pseudomonas putida* from oleic acid. *Polym Degradation Stab* 95: 2334–2342.
27. Dai Y, Lambert L, Yuan Z, Keller J (2008) Characterisation of polyhydroxyalkanoate copolymers with controllable four-monomer composition. *J Biotechnol* 134: 137–145.
28. López-Cuellar M, Alba-Flores J, Rodríguez J, Pérez-Guevara F (2011) Production of polyhydroxyalkanoates (PHAs) with canola oil as carbon source. *Int J Biol Macromol* 48: 74–80.
29. Bonduelle C, Martin-Vaca B, Bourissou D (2009) Lipase-catalyzed ring-opening polymerization of the *O*-carboxylic anhydride derived from lactic acid. *Biomacromolecules* 10: 3069–3073.
30. Randriamahafa S, Renard E, Guérin P, Langlois V (2003) Fourier transform infrared spectroscopy for screening and quantifying production of PHAs by *Pseudomonas* grown on sodium octanoate. *Biomacromolecules* 4: 1092–1097.
31. Huijberts G, Eggink G, de Waard P, Huisman GW, Witholt B (1992) *Pseudomonas putida* KT2442 cultivated on glucose accumulates poly (3-hydroxyalkanoates) consisting of saturated and unsaturated monomers. *Appl Environ Microbiol* 58: 536–544.
32. Matsusaki H, Abe H, Doi Y (2000) Biosynthesis and properties of poly (3-hydroxybutyrate-co-3-hydroxyalkanoates) by recombinant strains of *Pseudomonas sp.* 61–3. *Biomacromolecules* 1: 17–22.
33. Zhang HF, Ma L, Wang ZH, Chen GQ (2009) Biosynthesis and characterization of 3 hydroxyalkanoate terpolyesters with adjustable properties by *Aeromonas hydrophila*. *Biotechnol Bioeng* 104: 582–589.
34. Madison LL, Huisman GW (1999) Metabolic engineering of poly (3-hydroxyalkanoates): from DNA to plastic. *Microbiol Mol Biol Rev* 63: 21–53.
35. Annuar MSM, Tan IKP, Ibrahim S, Ramachandran KB (2006) Ammonium uptake and growth kinetics of *Pseudomonas putida* PGA1. *Asia-Pac J Mol Biol Biotechnol* 14: 1–10.



## CHAPTER 8

# Effects of carbon substrates on biodegradable polymer composition and stability produced by *Delftia tsuruhatensis* Bet002 isolated from palm oil mill effluent

**A. M. Gumel<sup>1</sup>, M. S. M. Annuar<sup>1\*</sup>, T. Heidelberg<sup>2</sup>,**

<sup>1</sup> Institute of Biological Sciences, <sup>2</sup> Department of Chemistry  
Faculty of Science, University of Malaya, Kuala Lumpur 50603, Malaysia

**Published:** *Polymer Degradation and Stability* (2012) **97**(8): 1224-1231

(ISI cited publication: tier 1)

### Statement of contributions of joint Authorship

**Gumel, A.M:** (Candidate)

Writing and compilation of manuscript, established methodology, data collection, presentation and analyses. Main author of the manuscript

**Annur, M.S.M:** (Principal Supervisor)

Supervised and assisted with manuscript compilation, editing and co-author of the manuscript.

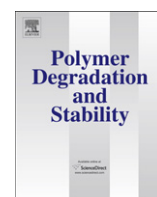
**Heidelberg, T:** (Co-Supervisor)

Supervised and assisted with chemical analyses, structure elucidation and co-author of the manuscript



Contents lists available at SciVerse ScienceDirect

## Polymer Degradation and Stability

journal homepage: [www.elsevier.com/locate/polydegstab](http://www.elsevier.com/locate/polydegstab)Effects of carbon substrates on biodegradable polymer composition and stability produced by *Delftia tsuruhatensis* Bet002 isolated from palm oil mill effluentA.M. Gumel<sup>a</sup>, M.S.M. Annuar<sup>a,\*</sup>, T. Heidelberg<sup>b</sup><sup>a</sup> Institute of Biological Sciences, Faculty of Science, University of Malaya, 50603 Kuala Lumpur, Malaysia<sup>b</sup> Department of Chemistry, Faculty of Science, University of Malaya, 50603 Kuala Lumpur, Malaysia

## ARTICLE INFO

## Article history:

Received 13 April 2012

Received in revised form

20 May 2012

Accepted 31 May 2012

Available online 8 June 2012

## Keywords:

Biodegradable

Biopolymer

Fatty acids

Polyhydroxyalkanoates

Stability

## ABSTRACT

The effects of carbon substrate (C<sub>8:0</sub>–C<sub>18:1</sub>) on the biosynthesis and the properties poly-3-hydroxybutyrate and its copolymer (PHA) produced by *Delftia tsuruhatensis* Bet002 were investigated. Growth-associated accumulation yielded PHA at 76.7% cell dried weight with molecular weight ranging from 131 to 199 kDa. Carbon source type also influences the thermal stability of the PHA. The molar concentration ratio of carbon to nitrogen source has little effect on the PHA composition, but affected the biomass, PHA yield and polymer degradation stability. In general, polymer composition of even and odd carbon atom chain length (C<sub>4</sub>–C<sub>10</sub>) was obtained. The PHA produced is semi-crystalline polymer with good thermal stability with thermal degradation temperature ( $T_d$ ) 269.8 to 391.8 ( $\pm 0.2$ ) °C, melting temperature ( $T_m$ ) 163.6 to 177.4 ( $\pm 0.2$ ) °C, glass transition temperature ( $T_g$ ) –1.0 to 4.4 ( $\pm 0.2$ ) °C and apparent melting enthalpy of fusion ( $\Delta H_f$ ) of 53.2 to 210.9 ( $\pm 0.1$ ) J g<sup>–1</sup>.

© 2012 Elsevier Ltd. All rights reserved.

## 1. Introduction

The growing concern over environmental pollution heightened the research interests in biodegradable polymers such as bacterial polyhydroxyalkanoates (PHAs). The biodegradability, compostability, compatibility, resorbability and piezoelectricity of polyhydroxyalkanoates incurs their current exploitation in industrial applications such as biodegradable polymeric packaging materials, biofuels, fermentation of wastes biomass [1], paper sizing [2], biomaterials and drug delivery devices [3–5]. The current attention on these biodegradable polymers is owed to their diverse physico-chemical properties. Diversity in the monomeric composition of PHA resulted in potentially high-molecular weight polymeric materials with myriads of applications as compared to their chemically synthesized counterparts. In addition, the increasing demand of highly functionalized PHA for specialty applications warrants the bio-prospecting of bacterial species capable of accumulating these biodegradable polymers.

The substrate utilization capability in different bacterial species poses limitation to industrial production of these polymers [6]. The choice of suitable fermentation substrate such as readily available carbon and nitrogen sources is an important parameter in PHA production and optimization. Carbon source alone is reported to

account for about 38% of total PHA production costs [7]. In fact, the nature of carbon source used as substrate not only determines the PHA yield, but also influences the type and monomeric composition of the polymer being accumulated.

PHA is known to be accumulated in several bacterial species that were isolated from different ecological niches [8–13]. A number of literature used different kind of fermentation substrates to produce PHA with different monomeric compositions [10,14–18]. Among the extensively studied bacterial species are those belonging to genus *Aeromonas* [19], *Alcaligenes* [20], *Cupriavidus* [21], *Halomonas* [22], *Pseudomonas* [23], *Wautersia* [18] etc. Literature concerning PHA accumulation in *Delftia* sp. is very limited [24]. In specific, PHA accumulation in *Delftia tsuruhatensis* has never been reported to the best of our knowledge. In this study, we reported for the first time PHA biosynthesis and characterization in *D. tsuruhatensis* Bet002, and the effects of different carbon source feeding on the polymer physico-chemical properties.

## 2. Materials and methods

## 2.1. Bacterial isolation and characterization

*D. tsuruhatensis* Bet002 was isolated from palm oil mill effluent using classical isolation on agar medium containing (g L<sup>–1</sup>): peptone 20; K<sub>2</sub>SO<sub>4</sub> 10; MgCl<sub>2</sub>·6H<sub>2</sub>O 1.4; irgasan 0.025; glycerol 25.2 and agar 13.6. Biochemical characterization was done using api<sup>®</sup> 20

\* Corresponding author. Tel.: +60 379674003; fax: +60 379677182.  
E-mail address: [suffian\\_annuar@um.edu.my](mailto:suffian_annuar@um.edu.my) (M.S.M. Annuar).

NE (bioMérieux® USA) biochemical typing kits as stated in manufacturer's guideline. Intracellular PHA accumulation was screened using both Sudan black B and Nile red staining techniques according to literature [25,26]. Intracellular PHA granules accumulation was also observed using transmission electron microscopy (Philips CM12, United Kingdom). The morphology of the bacterial colonies isolated and the Gram staining characteristics were observed under Motic® microscope BA200 equipped with Moticam 2300 camera (Motic®, Japan). GF1 DNA extraction kit (Vivantis Sdn Bhd, Malaysia) was used to extract the bacterial DNA for the 16S rRNA molecular characterization according to manufacturer's guidelines. Post PCR analysis was done by blasting of both forward and reverse sequences against sequences in GeneBank (NCBI) and RDPPII (Ribosomal Database Project II) databases to search for homology sequences. The extracted DNA nucleotide sequence has been deposited in European Nucleotide Archive (ENA) with accession number HE573174.

## 2.2. Culture conditions and fermentation process

Sterile growth medium containing (g L<sup>-1</sup>): yeast extract 10.0 (Bacto™ USA), nutrient broth 15.0 (Merck, Germany) and ammonium sulfate 5.0 (Sigma Aldrich, Germany) was used as cultivation medium for the bacterium. Stock inoculum 3% (v/v) was introduced into this medium aseptically and incubated in shaking incubator (Daihan LabTech®, Korea) at 30 °C, 250 rpm for 24 h. The biomass was harvested via centrifugation at 4 °C, 9000 × g for 10 min. This was seeded aseptically into PHA production medium. The medium contained sterile minerals (g L<sup>-1</sup>): sodium ammonium hydrogen phosphate tetrahydrate [NaNH<sub>4</sub>HPO<sub>4</sub>·4H<sub>2</sub>O] 3.5 (Sigma Aldrich, Germany), K<sub>2</sub>HPO<sub>4</sub> 5.7, KH<sub>2</sub>PO<sub>4</sub> 3.7, and 10 mM specified fatty acids as a sole carbon and energy source at a pH of 7.0 (±0.1) except otherwise stated. To this mixture, separate sterile 1.0% (v/v) Mg<sub>2</sub>SO<sub>4</sub>·7H<sub>2</sub>O solution and 0.1% (v/v) trace elements (MT) solution containing (g L<sup>-1</sup>): CaCl<sub>2</sub>·2H<sub>2</sub>O 1.47, CoCl<sub>2</sub>·6H<sub>2</sub>O 2.38, CuCl<sub>2</sub>·2H<sub>2</sub>O 0.17, FeSO<sub>4</sub>·7H<sub>2</sub>O 2.78, MnCl<sub>2</sub>·4H<sub>2</sub>O 1.98 and ZnSO<sub>4</sub>·7H<sub>2</sub>O 0.29 dissolved in 1 M HCl were added. These sterile solutions were aseptically added prior to inoculation. 5 g L<sup>-1</sup> of harvested biomass from inoculum growth media was seeded into this medium aseptically and incubated as described previously for a total period of 48 h except otherwise stated. PHA extraction was done according to literature [27]. The mcl-PHA obtained undergone a minimum of three-repeated purification process and dried *in vacuo*. The PHA volumetric productivity of the PHA in g L<sup>-1</sup> h<sup>-1</sup> was calculated as

$$\Phi = \frac{[P]}{t} \quad (1)$$

where [P] is the extracted PHA concentration, and *t* is the fermentation time.

## 2.3. Analyses

### 2.3.1. Biomass estimation

A known biomass dry weight concentrations were used to prepare a standard calibration, using Jasco V-630 UV/VIS spectrophotometer (Jasco, Japan) at the absorbance of 600 nm. Sample aliquotes were withdrawn aseptically at regular intervals and centrifuged at 9000 × g for 10 min, then washed twice with 0.05 M phosphate buffer. After final centrifugation, the cells were resuspended in the same buffer prior to absorbance reading against the phosphate buffer blank.

### 2.3.2. Residual fatty acid quantification

The residual fatty acid estimation was done according to Marseno et al. [28] modified protocol. Cell free suspension (1 ml) was

mixed with *n*-heptane (3 ml) and centrifuge at 9000 × g to separate the residual fatty acid. 2 ml of the top layer of *n*-heptane was withdrawn into a test tube. To this solution, 200 μl of 5% (w/v) copper (II) acetate monohydrate solution (5 g copper (II) acetate monohydrate dissolved in 90 ml distilled water; pyridine and distilled water were used to adjust the solution pH to 6 and bring the final volume to 100 ml) was added and vortexed for 60 s. This mixture was allowed to stand for 20 s before it was read at 705 nm against distilled water blank using Jasco V-630 UV/VIS spectrophotometer (Jasco, Japan). A standard calibration was made using different fatty acid concentrations (0.5–1 mM) that were prepared by dissolving specified mass of a particular fatty acid in *n*-heptane and treated as described earlier.

### 2.3.3. Residual ammonium quantification

Residual ammonium was quantified using phenol hypochlorite method as described by Solorzano [29]. Cell free medium solution (2 ml) was diluted with distilled water to 5 ml. To this solution 0.2 ml of alcoholic phenol (10 g phenol in 90 ml absolute ethanol) was added followed by the addition of 0.2 ml sodium nitroprusside solution (0.5 g sodium nitroprusside in 99.5 ml distilled water). Oxidizing solution (0.5 ml) containing 4:1 (v/v) alkaline solution (100 g trisodium citrate, 5 g sodium hydroxide dissolved in 500 ml distilled water) and sodium hypochlorite solution (1.5 N) were added to the mixture while agitating to ensure uniform indole-phenol coloration. The mixture was then allowed to stand for an hour at room temperature (27 °C) resulting in light-blue coloration that was measured at 640 nm against distilled water as blank. Residual ammonium concentration was then quantified in reference to standard calibration of known ammonium concentrations.

## 2.4. PHA authentication

### 2.4.1. FTIR spectroscopy

Nondestructive attenuated total reflectance (ATR) FTIR was used to record the PHA spectrum on Perkin-Elmer FTIR spectrum-400 spectrometer (Perkin-Elmer Inc., Wellesley, MA, USA) at room temperature (25 °C). A scan range of 400–4000 cm<sup>-1</sup> was applied for 10 scans. A paste of 0.01 g of the sample was prepared in dichloromethane. A liquid film of the mixture was then applied on to NaCl crystal window and the spectrum was read after the solvent has been dried.

### 2.4.2. Proton NMR analysis

JEOL JNM-GSX 270 FT-NMR (JOEL Ltd, Tokyo, Japan) spectrometer was used to record the <sup>1</sup>H NMR spectrum at 250 MHz against trimethylsilane (TMS) internal reference standard. Approximately 5 mg PHA sample was dissolved in 2 ml deuterated chloroform (CDCl<sub>3</sub>) and filtered into NMR tube using borosilicate glass syringe equipped with 0.22 μm PTFE disposable filter (11807-25, Sartorius Stedim, Germany).

### 2.4.3. GC-MSMS analysis

GC-MSMS was recorded on Agilent triple quadrupole 7000B (Agilent, USA), equipped with GC-MSMS triple axis detector carrying Agilent HP-5ms column (30 m length × 0.25 mm internal diameter × 0.25 μm film). PHA sample in the form of hydroxyalkanoic acids methyl esters were used for the GC-MSMS analysis according to method reported in literature [30,31]. Methanolized sample (1 μl) was automatically injected into the GC at a split ratio of 1:50. The injection temperature was set at 280 °C while the oven and column temperatures were programmed at 40 °C for 1 min, and then increased to 120 °C at 15 °C min<sup>-1</sup> before being held constant for 2 min. The temperature was increased to 250 °C at 10 °C min<sup>-1</sup> and then held constant for 10 min. Helium was

used as carrier gas at  $48.3 \text{ ml min}^{-1}$  and 0.41 bar pressure. Mass spectra were acquired at 1250 scan speed using electron impact energy of 70 eV at  $200^\circ\text{C}$  ion-source and  $280^\circ\text{C}$  interface temperatures, respectively. Standard monomers of methyl hydroxyalkanoates (Larodan, Sweden) were used as reference to determine peak retention time and ionization mass determination.

#### 2.4.4. Gel permeation chromatography (GPC)

Waters 600 (Waters Corp, Milford, MA, USA) equipped with a Waters refractive index detector (model 2414) having the following gel columns (7.8 mm internal diameter 300 mm) in series: HR1, HR2, HR5E and HR5E Waters Styrogel HR-THF was used to record the chromatogram relative to calibration curve of standard monodisperse polystyrenes ( $3.72 \times 10^2$ ,  $2.63 \times 10^3$ ,  $9.10 \times 10^3$ ,  $3.79 \times 10^4$ ,  $3.55 \times 10^5$ ,  $7.06 \times 10^5$ ,  $3.84 \times 10^6$  and  $6.77 \times 10^6$  Da). The PHA samples were dissolved in chloroform at a concentration of  $2.0 \text{ mg mL}^{-1}$  before being filtered through a  $0.22 \mu\text{m}$  PTFE filter.  $100 \mu\text{L}$  aliquot of the filtered sample was injected at  $40^\circ\text{C}$  using THF as a mobile phase at a flow rate of  $1.0 \text{ mL min}^{-1}$ .

### 2.5. Thermal analyses

#### 2.5.1. Differential scanning calorimetry (DSC)

Preparatory thermal analysis of the synthesized poly-3-hydroxyalkanoates was carried out using Perkin-Elmer differential scanning calorimeter DSC 6 (Perkin-Elmer Inc., Wellesley, MA, USA) running Pyris series 6 DSC software. Scans were performed under nitrogen flow rate of  $50 \text{ mL min}^{-1}$  at temperature range from  $-60^\circ\text{C}$  to  $185^\circ\text{C}$ , with a heating rate of  $10^\circ\text{C min}^{-1}$ . The melting temperature ( $T_m$ ) was taken at the endothermic peak of the DSC thermogram. The endothermic melting enthalpy ( $\Delta H_m$ ) was used to calculate the polymer crystallinity index ( $X_p$ ) on the basis of melting enthalpy ( $\Delta H_{m0}$ ) of 100% crystalline PHB according to equation (2) as reported elsewhere [32], assuming  $142 \text{ J g}^{-1}$  as the melting enthalpy of 100% crystalline PHB as cited in literature [18].

$$X_p = \frac{\Delta H_m}{\Delta H_{m0}} \quad (2)$$

#### 2.5.2. Thermogravimetric analysis (TGA)

TGA analysis was performed on a Perkin-Elmer TGA 4000 instrument. The sample was heated from  $50^\circ\text{C}$  to  $950^\circ\text{C}$  at a rate of  $10^\circ\text{C min}^{-1}$  under a nitrogen flow rate of  $20 \text{ mL min}^{-1}$ .

## 3. Results and discussion

### 3.1. Strain characterization and PHA production

A strain isolated from palm oil mill effluent (POME) and designated as Bet002 was stained using Sudan Black B to observe possible accumulation of intracellular PHA. Further confirmation of the presence of accumulated granule was done using transmission electron microscopy (Fig. 1). The ribosomal database project II (RDPII) homology search and blasting of the obtained results from 16S rRNA molecular characterization of the isolate Bet002 showed 99% analogy between the isolate and *D. tsuruhatensis* strains AY 684787, AY738262 and AY052781 (Fig. 2). The isolate was henceforth designated as *D. tsuruhatensis* Bet002 with EMBL nucleotide archive accession number HE573174 and subsequently tested for the PHA production in shake flasks using a two-step batch fermentation process with different fatty acids as a sole carbon and energy source.

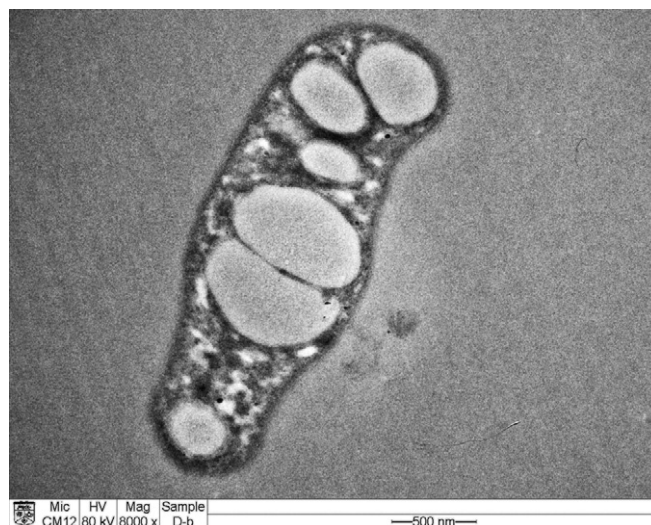


Fig. 1. Transmission electron micrograph of PHA inclusion in *Delftia tsuruhatensis* Bet002 grown on oleic acid.

### 3.2. PHA characterization

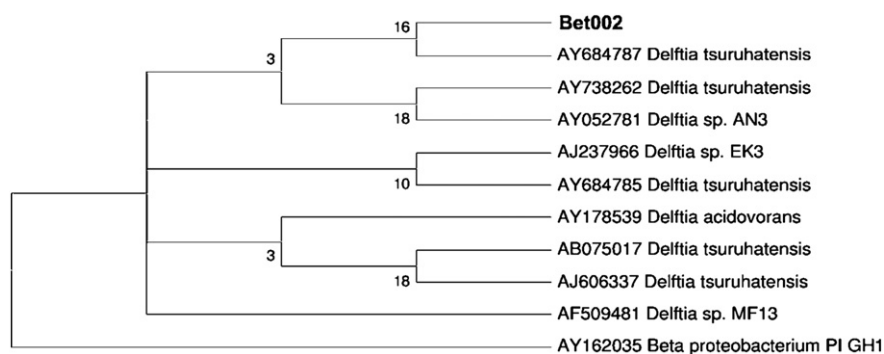
#### 3.2.1. FTIR spectroscopy

The extracted PHA sample was subjected to nondestructive attenuated total reflectance FT-IR (Fig. 3a). Observed infrared absorption at  $3438.27 \text{ cm}^{-1}$  was assigned to the hydroxyl group of the polymer chain [33]. Absorption band at  $2927.28 \text{ cm}^{-1}$  was assigned to asymmetric methylene group of the lateral monomeric chains. The absorption at  $2855.11 \text{ cm}^{-1}$  is assigned to symmetrical  $\text{CH}_3$  and the intensity of the band has been reported to be due to conformational disorder obtained in the process of crystallization [18]. While the absorption band of  $1728.96 \text{ cm}^{-1}$  was assigned to carbonyl ( $\text{C}=\text{O}$ ) ester bond stretching vibration according to literature [34]. The vibrations at  $1457.40 \text{ cm}^{-1}$  have been assigned to bacterial intracellular amide ( $-\text{CO}-\text{N}-$ ) that has been reported to be specie specific [34]. Absorption at  $1380.14 \text{ cm}^{-1}$  is assigned to terminal  $\text{CH}_3$  groups [35]. Series of absorption bands at  $1282.21 \text{ cm}^{-1}$  to  $723.12 \text{ cm}^{-1}$  were assigned to asymmetric  $\text{C}-\text{O}-\text{C}$ ,  $\text{C}-\text{O}$  and  $\text{C}-\text{C}$  stretching vibration in the amorphous phase.

#### 3.2.2. PHA chemical and physical characterization

The extracted polymers were characterized with reference to the internal standard trimethylsilane in  $^1\text{H}$  NMR spectrum (Fig. 3b). The observed multiplet peaks at chemical shift 2.50 ppm and triplet peaks at 5.25 ppm are assigned to methylene and methine protons of the  $\alpha$  and  $\beta$ -carbon in both 3-hydroxybutyrate (3HB) and 3-hydroxyalkanoates copolymers (3-HA) respectively [36,37]. The chemical shift at 1.75 ppm is assigned to methylene protons adjacent to the  $\beta$ -carbon in the side-chains of 3HA copolymer [1,38]. Chemical shift at 1.25 and 0.85 ppm are assigned to the terminal methyl protons of the 3HB and 3HA polymers respectively [36].

The quadrupole GCMSMS analyses showed the extracted PHA to be homopolymer of 3-hydroxybutyrate when  $\text{C}_{14:0}$ ,  $\text{C}_{16:0}$  and  $\text{C}_{18:0}$  were fed as carbon substrate. Interestingly, when oleic acid ( $\text{C}_{18:1}$ ) was fed as sole carbon and energy source, a copolymer with five different monomeric composition was obtained (Table 1) showing 87.7 mol% 3-hydroxybutyrate and traces amount of 3-hydroxyvalerate, 3-hydroxyhexanoate, 3-hydroxyoctanoate and 3-hydroxydecanoate.

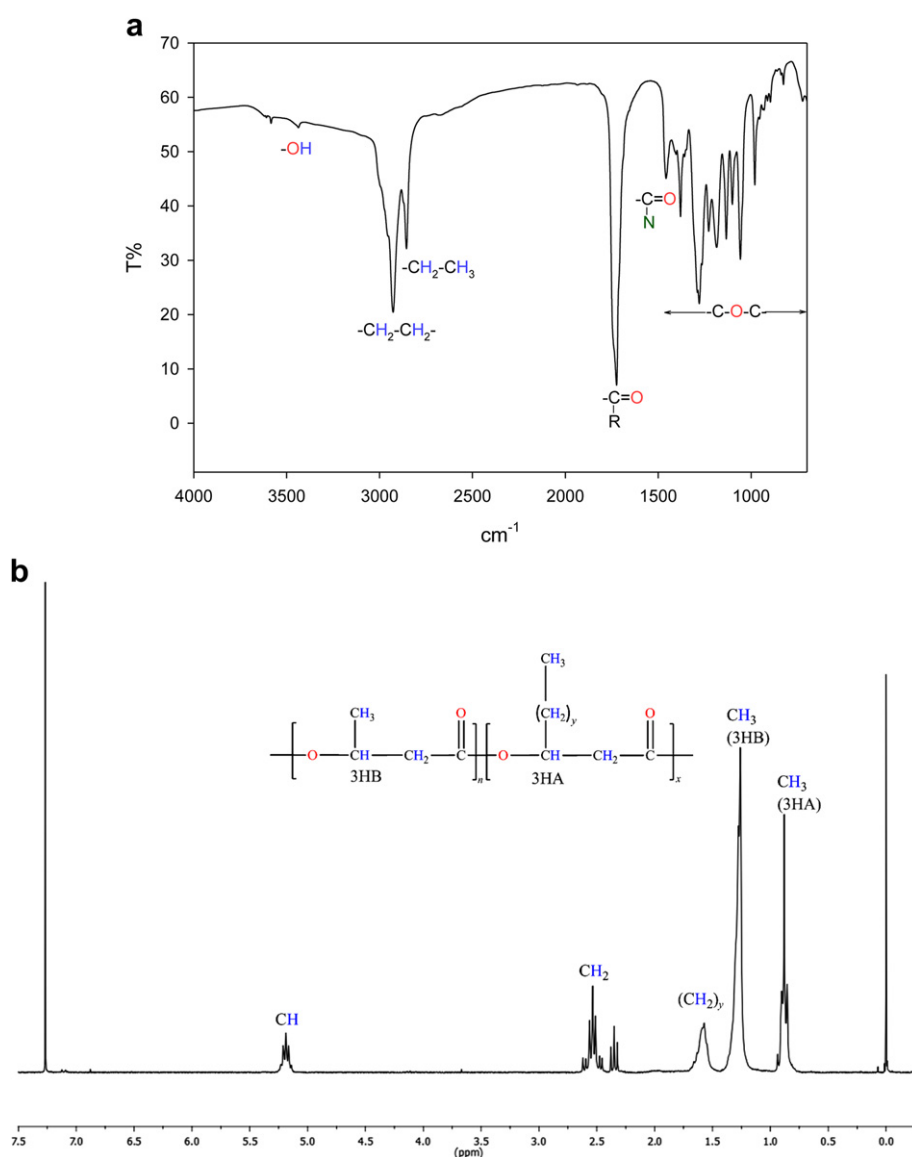


**Fig. 2.** Neighbor joining phylogenetic tree showing the interrelationship between isolate Bet002 and top 10 Blast hits from RDP II database.

### 3.3. Effect of carbon source on polymer thermal stability

PHA thermal stability reflects the maximum temperature the polymer could withstand before decomposition. The calorimetric

scan of the extracted PHA showed the endothermic melting temperature ( $T_m$ ) of this polymer to vary with the type of substrate fed (Table 1). For example using myristic acid ( $C_{14:0}$ ), a polymer with  $T_m$  value of  $173.2 (\pm 0.2) ^\circ\text{C}$  and apparent melting enthalpy of



**Fig. 3.** (a) FTIR spectrum(b)  $^1\text{H}$  NMR spectrum of the PHA synthesized by *Delftia tsuruhatensis* Bet002 using oleic acid as sole carbon source at  $30 ^\circ\text{C}$ , 200 rpm for 48 h.



**Table 1**  
PHA physico-chemical properties as a function of carbon source fed.

| Carbon source     | PHA %w/w (CDW) | $\Phi$ (g L <sup>-1</sup> h <sup>-1</sup> ) | $X_p$ | $T_m$ (°C) | $T_g$ (°C) | $T_d$ (°C) | $\Delta H_f$ (J g <sup>-1</sup> ) | PHA mole fraction (mole %) |                       |                        |                       |                        | $\overline{M}_n$ | $\overline{M}_w$ | PDI |
|-------------------|----------------|---|-------|------------|------------|------------|-----------------------------------|----------------------------|-----------------------|------------------------|-----------------------|------------------------|------------------|------------------|-----|
|                   |                |   |       |            |            |            |                                   | 3HB <sup>a</sup> (C4)      | 3HV <sup>b</sup> (C5) | 3HHx <sup>c</sup> (C6) | 3HO <sup>d</sup> (C8) | 3HD <sup>e</sup> (C10) |                  |                  |     |
| C <sub>14:0</sub> | 76.7           | 0.18  | 1.5   | 173.2      | -1.0       | 289.8      | 210.9                             | 100                        | ND                    | ND                     | ND                    | ND                     | 120,000          | 131,000          | 1.1 |
| C <sub>16:0</sub> | 53.8           | 0.14  | 1.5   | 175.7      | -1.3       | 302.9      | 208.6                             | 100                        | ND                    | ND                     | ND                    | ND                     | 110,000          | 166,000          | 1.5 |
| C <sub>18:0</sub> | 45.0           | 0.11  | 0.8   | 177.4      | -1.5       | 391.8      | 113.5                             | 100                        | ND                    | ND                     | ND                    | ND                     | 102,000          | 188,000          | 1.8 |
| C <sub>18:1</sub> | 62.4           | 0.16  | 0.4   | 163.6      | 4.4        | 272.2      | 53.2                              | 87.7                       | 2.03                  | 0.96                   | 8.35                  | 0.96                   | 101,000          | 199,000          | 2.0 |

ND (not detected).

<sup>a</sup> (3-hydroxybutyrate).

<sup>b</sup> (3-hydroxyvalerate).

<sup>c</sup> (3-hydroxyhexanoate).

<sup>d</sup> (3-hydroxyoctanoate).

<sup>e</sup> (3-hydroxydecanoate).

fusion ( $\Delta H_f$ ) of 210.2 ( $\pm 0.1$ ) J g<sup>-1</sup> was accumulated. In contrast, both palmitic (C<sub>16:0</sub>) and stearic (C<sub>18:0</sub>) acids were found to yield polymers displaying a  $T_m$  value of 175.7 and 177.4 ( $\pm 0.2$ ) °C with  $\Delta H_f$  value of 113.5 and 208.6 ( $\pm 0.1$ ) J g<sup>-1</sup>, respectively. However, the glass transition temperature ( $T_g$ ) of these polymers was almost in the same range -1.0 to -1.5 ( $\pm 0.2$ ) °C. In general, this observation was found to be in agreement with what has been reported on the average melting temperature (174–179 °C) for PHB [39–41].

When oleic acid (C<sub>18:1</sub>) was fed to the bacterium, the extracted polymer was found to have a  $T_m$  of 163.6 ( $\pm 0.2$ ) °C,  $T_g$  of 4.4 ( $\pm 0.2$ ) °C and  $\Delta H_f$  value of 53.2 ( $\pm 0.1$ ) J g<sup>-1</sup>. The decrease in melting temperatures may be due to the amorphous nature of the polymer arising from varied monomeric composition. In one aspect, this has the advantage of ease of processing and relatively less energy consumption during molding or casting. The observed low degree of crystallinity ( $0.8 \leq X_p \leq 3.7$ ) of these polymers lends further evidence of the amorphous nature of the polymer. In general, the thermal stability of these polymers increased with increasing carbon atom length in the fatty acid, with unsaturated fatty acid having the highest thermal stability due to more favorable side chain crystallization by the monomers, which in turn was reported to influence the polymer's high apparent enthalpy of fusion [19,36,37].

Thermal gravimetric analysis of the extracted polymer showed an increase in polymer thermal stability with increasing fatty acid chain length fed i.e. from C<sub>8:0</sub> to C<sub>18:0</sub>, the thermal degradation temperature ( $T_d$ ) of 289.8–391.8 °C ( $\pm 0.2$ ) was observed (Fig. 4). The increase in the carbon atom chain length favors the increase in weight average molecular weight ( $M_w$ ) of the PHB homopolymer (Fig. 4). In contrast, when the bacterium was fed with C<sub>18:1</sub>, the thermal degradation temperature seems to decrease to 272.2 °C ( $\pm 0.2$ ), which could be due to the presence of the different comonomers giving lower crystallinity of the heteropolymer as compared to PHB homopolymer. The thermal degradation temperature of the synthesized polymer was also found to be affected by the varying of carbon and nitrogen (C:N) ratio (data not shown). At C:N ratio 2.5, the  $T_d$  was observed to be 330 °C ( $\pm 0.2$ ), whilst increasing the C:N ratio to 6 increased the  $T_d$  to 470.0 °C ( $\pm 0.2$ ). The observed increase in  $T_d$  was in linear fashion.

#### 3.4. Effects of carbon source on the PHA composition, molecular weight and yield

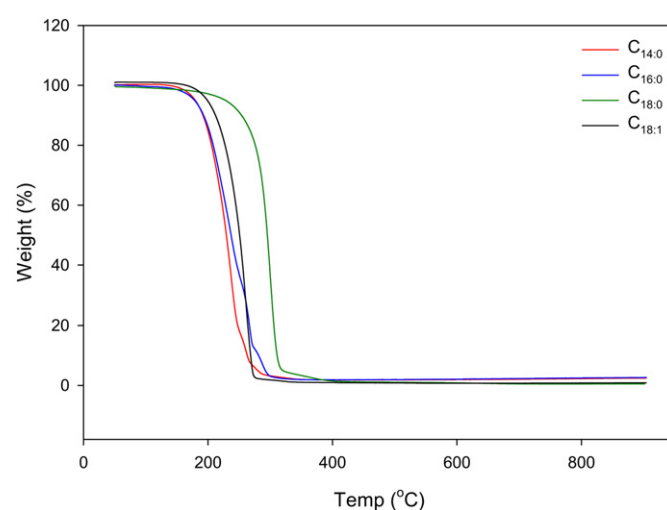
Different carbon sources such as aromatic dicarboxylic acid (phthalic acid), caprylic, myristic, palmitic, stearic and oleic acids were tested on biomass growth, biopolymer accumulation and composition. Among the carbon sources tested, the bacterium was unable to utilize phthalic, caprylic or decanoic acids as growth substrate since negligible growth was observed when these carbon

sources were used as a substrate in 48-h fermentation. For this reason, we only reported data obtained from other mentioned fatty acids (Table 1). It is obvious that the type of carbon source not only affects the accumulated polymer in terms of its thermal stability but also its yield and composition. PHA yield was observed to range from 45.0 to 76.7 % on cell dry weight basis. In fact, both the corresponding volumetric productivity ( $\Phi$ ) and the molecular weight were also found to vary as well (Table 1).

Myristic acid (C<sub>14:0</sub>) was observed to give the highest PHA yield (76.7% cell dry weight) with the highest number averaged molecular weight,  $M_n$  (120 kDa) but lowest  $M_w$  (131 kDa). In comparison, stearic acid (C<sub>18:0</sub>) was observed to have the lowest PHA yield (45.0% cell dry weight) with a relatively low  $M_n$  (102 kDa) albeit higher  $M_w$  (188 kDa). In general, the polymerization seems to be a tightly controlled process with polydispersity index of  $1 \geq PDI \geq 2$ . Depending on the fatty acid fed, the polymer composition was observed to range from a homopolymer of 3-hydroxybutyrate (C<sub>14:0</sub>, C<sub>16:0</sub> and C<sub>18:0</sub> as substrate) to a copolymer (C<sub>18:1</sub> substrate) consisting of five different 3-hydroxyalkanoates monomeric units (Table 1).

#### 3.5. Effect of nitrogen source on the specific growth rate and PHA yield

Changing the type of ammonium (nitrogen) source has no effect on polymer composition but rather on the bacterium's specific



**Fig. 4.** TGA thermogram showing carbon substrate as a function of polymer degradation stability in PHA synthesized by *Delftia tsuruhatensis* Bet002 using ammonium sulphate as sole nitrogen source at 30 °C 200 rpm for 48 h.

**Table 2**

Nitrogen source as a function of biomass, specific growth and PHA yield.

| Nitrogen source                                       | Biomass (g L <sup>-1</sup> ) | PHA (%CDW) | $\mu$ ( $\times 10^{-3}$ h <sup>-1</sup> ) | $M_n$   | $M_w$   | PDI |
|---|------------------------------|------------|--|---------|---------|-----|
| (NH <sub>4</sub> ) <sub>2</sub> SO <sub>4</sub>       | 6.3                          | 58.8       | 3.2  | 103,000 | 114,000 | 1.1 |
| NH <sub>4</sub> NO <sub>3</sub>                       | 0.8                          | 45.0       | 1.4  | 68,000  | 76,000  | 1.1 |
| NaNH <sub>4</sub> HPO <sub>4</sub> ·4H <sub>2</sub> O | 7.2                          | 53.9       | 3.5  | 120,000 | 131,000 | 1.1 |
| Urea  | 2.2                          | 11.1       | 2.3  | 4700    | 5300    | 1.1 |
| Peptone   | 3.8                          | 56.0       | 2.5  | 128,000 | 136,000 | 1.1 |

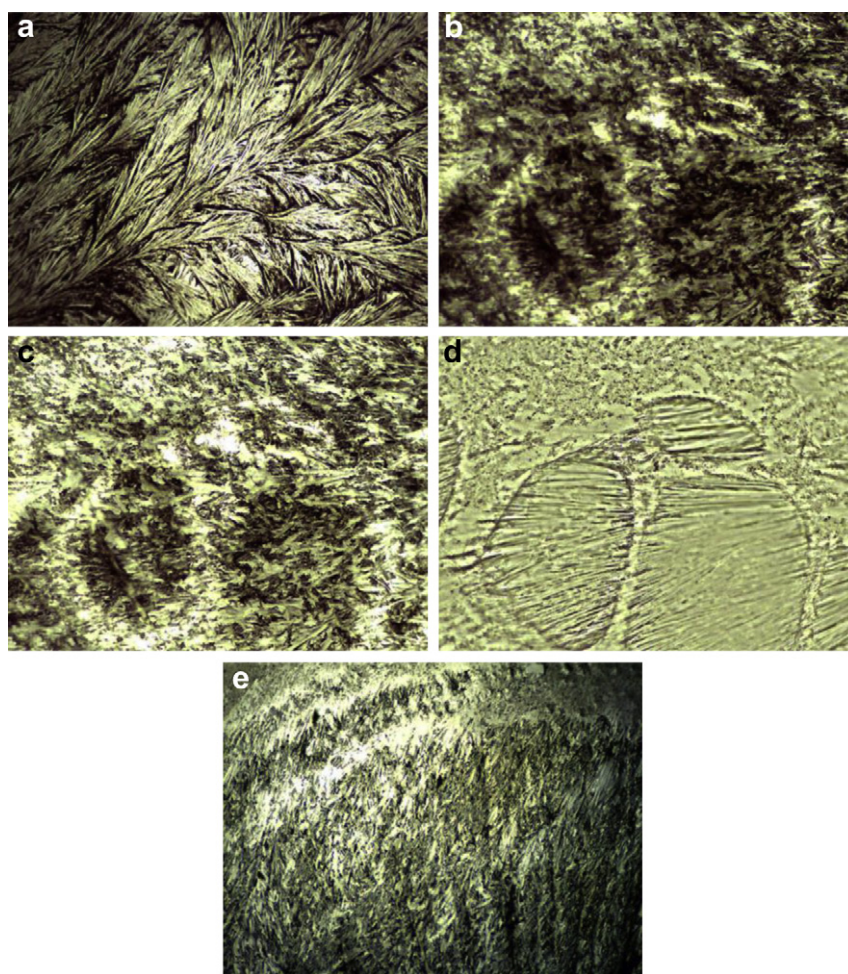
CDW: cell dry weight.

growth rate and the PHA yield. When myristic acid was fed with 0.11% w/w nitrogen content of different ammonium ion sources for 48 h, high PHA and biomass yields were observed on ammonium sulphate or sodium ammonium hydrogen phosphate supplementation with specific growth of  $3.2\text{--}3.5$  ( $\times 10^{-3}$  h<sup>-1</sup>), respectively (Table 2). In contrast to previous observation on nitrogen source evaluation in *Pseudomonas putida* PGA1 [42], both bacteriological peptone and ammonium nitrate were observed to yield low biomass with high PHA yield in *D. tsuruhatensis* Bet002, while urea was found to have the lowest PHA accumulation. The chloroform casted polymer film also showed different morphologies following the bacterium cultivation in different nitrogen sources e.g. when ammonium sulphate was used, an epitaxial crystallized film was formed (Fig. 5(a)) as compared to a more amorphous film when the other nitrogen sources were used in this study (Fig. 5(b–e)). The

exact reason for the observed differences is not immediately clear at this stage although the same protocol was used in the preparation of the films.

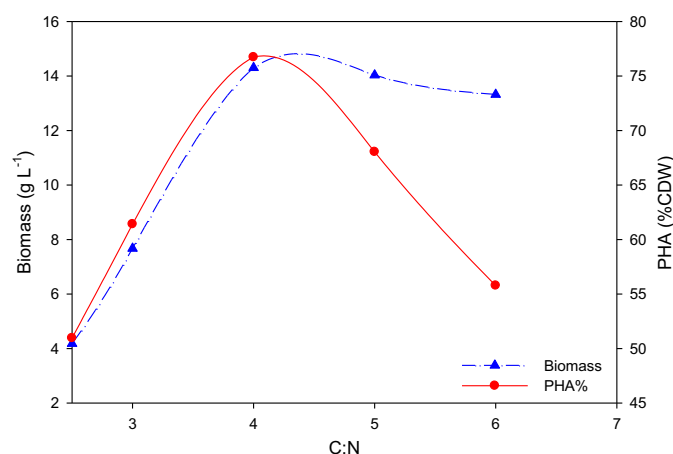
### 3.6. Effect of carbon–nitrogen ratio on the biomass and PHA yield

It was observed that both the PHA content and biomass growth can be increased by changing the molar ratio between carbon-to-nitrogen (C:N) source (Fig. 6). The increase in the C:N molar ratio from 2.5 to 4 exhibited an increase in biomass and PHA accumulation between the range of  $4.2\text{--}14.3$  g L<sup>-1</sup> with a corresponding PHA yield of 51.0–76.7 % w/w cell dry weight, respectively. The increase in biomass as the C:N molar ratio increases until 4 was indicative of the carbon-limited growth condition below the C:N 4. Additional increase in C:N molar ratio after 4 however, did not



**Fig. 5.** Micrograph of PHA film morphology after chloroform solution casting. Myristic acid was used as a sole carbon source and (a) ammonium sulphate (b) ammonium nitrate (c) Urea (d) Sodium ammonium hydrogen phosphate (e) peptone as nitrogen source (X4 magnification).





**Fig. 6.** Carbon-nitrogen ratio as a function of biomass and polymer accumulation in the of PHA by *Delftia tsuruhatensis* Bet002 using myristic acid as sole carbon source at 30 °C 200 rpm for 48 h.

results in further increase in biomass but rather a significant reduction of PHA accumulation was observed. Conversely, the results from this experiment offer additional support for the growth-linked PHA accumulation in this bacterium. Maximum PHA accumulation at approximately 76.7% w/w cell dry weight was attained for C:N molar ratio of 4. The molecular weight of the PHA from the different C:N molar ratios tested fell within a narrow range of 110–167 kDa. The crystallinity index ( $X_p$ ) and poly dispersity index (PDI) remained constant at all the C:N molar ratios tested.

#### 4. Conclusions

Effects of different fatty acids on the composition and stability of biodegradable polymer produced by newly isolated strain *D. tsuruhatensis* Bet002 was studied. The synthesized PHA was found to chemically consist of monomers ranging from 3-hydroxybutyrate (3HB) to 3-hydroxydecanoate (3HTD). Depending on the fatty acid used, a relatively high molecular weight PHA ( $\approx 199$  kDa) and accumulation as high as 76.7% on cell dry weight basis was observed. The fermentation substrate was observed to influence the thermal stability and crystallinity of the synthesized polymer. Varying the ratio of carbon and nitrogen substrates in the fermentation medium a polymer with degradation temperature as high as 470 °C was achieved.

#### Acknowledgement

The authors acknowledged University of Malaya for research grant RG165/11AFR. All authors declared no conflict of interest.

#### References

- [1] Huijberts G, Eggink G, de Waard P, Huisman GW, Witholt B. *Pseudomonas putida* KT2442 cultivated on glucose accumulates poly (3-hydroxyalkanoates) consisting of saturated and unsaturated monomers. *Appl Environ Microbiol* 1992;58:536.
- [2] Bourbonnais R, Marchessault RH. Application of polyhydroxyalkanoate granules for sizing of paper. *Biomacromolecules* 2010;11:989–93.
- [3] Francis L. Biosynthesis of polyhydroxyalkanoates and their medical applications. London, UK: University of Westminster; 2011.
- [4] Kiliçay E, Demirbilek M, Türk M, Güven E, Hazer B, Denkbaz EB. Preparation and characterization of poly(3-hydroxybutyrate-co-3-hydroxyhexanoate) (Phbhx) based nanoparticles for targeted cancer therapy. *Eur J Pharm Sci* 2011;44:310–20.
- [5] Zhou J, Peng S-W, Wang Y-Y, Zheng S-B, Wang Y, Chen G-Q. The use of poly(3-hydroxybutyrate-co-3-hydroxyhexanoate) scaffolds for tarsal repair in eyelid reconstruction in the rat. *Biomaterials* 2010;31:7512–8.
- [6] Palmans ARA, van As BAC, van Buijtenen J, Meijer E. Ring-opening of -substituted lactones by Novozym 435: selectivity issues and application to iterative tandem catalysis. In: *Polymer biocatalysis and biomaterials II*. American Chemical Society Publications; 2008. 230–244.
- [7] Choi J, Lee SY. Factors affecting the economics of polyhydroxyalkanoate production by bacterial fermentation. *Appl Microbiol Biotechnol* 1999;51:13–21.
- [8] Akaraonye E, Keshavarz T, Roy I. Production of polyhydroxyalkanoates: the future green materials of choice. *J Chem Technol Biotechnol* 2010;85:732–43.
- [9] Bohmert-Tatarev K, Mcavoy S, Peoples OP, Snell KD. Stable, fertile, high polyhydroxyalkanoate producing plants and methods of producing them. US Patent App. 20,100/229,258; 2010.
- [10] Grothe E, Chisti Y. Poly ( $\beta$ -hydroxybutyric acid) thermoplastic production by *Alcaligenes latus*: behavior of fed-batch cultures. *Bioprocess Biosyst Eng* 2000;22:441–9.
- [11] Thomson N, Roy I, Summers D, Sivaniah E. In vitro production of polyhydroxyalkanoates: achievements and applications. *J Chem Technol Biotechnol* 2010;85:760–7.
- [12] Yamane T. Cultivation engineering of microbial bioplastics production. *FEMS Microbiol Lett* 1992;103:257–64.
- [13] Dalal J, Sarma PM, Lavania M, Mandal AK, Lal B. Evaluation of bacterial strains isolated from oil-contaminated soil for production of polyhydroxyalkanoic acids (PHA). *Pedobiologia* 2010;54:25–30.
- [14] Albuquerque MGE, Martino V, Pollet E, Avérous L, Reis MAM. Mixed culture polyhydroxyalkanoate (PHA) production from volatile fatty acid (VFA)-rich streams: effect of substrate composition and feeding regime on PHA productivity, composition and properties. *J Biotechnol* 2011;151:66–76.
- [15] Gaucher G, Marchessault RH, Leroux JC. Polyester-based micelles and nanoparticles for the parenteral delivery of taxanes. *J Control Release* 2010;143:2–12.
- [16] Butcher JT, Mahler GJ, Hockaday LA. Aortic valve disease and treatment: the need for naturally engineered solutions. *Adv Drug Del Rev* 2011;63:242–68.
- [17] Renard E, Vergnol G, Langlois V. Adhesion and proliferation of human bladder RT112 cells on functionalized polyesters. *IRBM* 2011;32:214–20.
- [18] López-Cuellar M, Alba-Flores J, Rodríguez J, Pérez-Guevara F. Production of polyhydroxyalkanoates (PHAs) with canola oil as carbon source. *Int J Biol Macromol* 2011;48:74–80.
- [19] Zhang HF, Ma L, Wang ZH, Chen GQ. Biosynthesis and characterization of 3 hydroxyalkanoate terpolyesters with adjustable properties by *Aeromonas hydrophila*. *Biotechnol Bioeng* 2009;104:582–9.
- [20] Penloglou G, Chatzidoukas C, Kiparissides C. Microbial production of polyhydroxybutyrate with tailor-made properties: an integrated modelling approach and experimental validation. *Biotechnol Adv* 2011. <http://dx.doi.org/10.1016/j.biotechadv.2011.06.021>.
- [21] Chanprateep S, Buasri K, Muangwong A, Utiswannakul P. Biosynthesis and biocompatibility of biodegradable poly(3-hydroxybutyrate-co-4-hydroxybutyrate). *Polym Degrad Stab* 2010;95:2003–12.
- [22] Kulkarni SO, Kanekar PP, Jog JP, Patil PA, Nilegaonkar SS, Sarnaik SS, et al. Characterisation of copolymer, poly (hydroxybutyrate-co-hydroxyvalerate) (PHB-co-PHV) produced by *Halomonas campisalis* (MCM B-1027), its biodegradability and potential application. *Bioresour Technol* 2011;102:6625–8.
- [23] Vishnuvardhan Reddy S, Thirumala M, Mahmood S. Production of PHB and P (3HB-co-3HV) biopolymers by *Bacillus megaterium* strain OU303A isolated from municipal sewage sludge. *World J Microbiol Biotechnol* 2009;25:391–7.
- [24] Chen WM, Lin YS, Sheu DS, Sheu SY. *Delftia lipopenaei* sp. nov., a poly- $\beta$ -hydroxybutyrate-accumulating bacterium isolated from a freshwater shrimp culture pond. *Int J Syst Evol Microbiol* 2011. <http://dx.doi.org/10.1099/ijs.0.037507-0>.
- [25] Burdon KL. Fatty material in bacteria and fungi revealed by staining dried, fixed slide preparations. *J Bacteriol* 1946;52:665.
- [26] Spiekermann P, Rehm BHA, Kalscheuer R, Baumeister D, Steinbüchel A. A sensitive, viable-colony staining method using Nile red for direct screening of bacteria that accumulate polyhydroxyalkanoic acids and other lipid storage compounds. *Arch Microbiol* 1999;171:73–80.
- [27] Annur MSM, Tan IKP, Ibrahim S, Ramachandran KB. Production of medium-chain-length poly (3-hydroxyalkanoates) from crude fatty acids mixture by *Pseudomonas putida*. *Food Bioprod Process* 2007;85:104–19.
- [28] Marseno DW, Indrati R, Ohta Y. A simplified method for determination of free fatty acids for soluble and immobilized lipase assay. *Indonesian Food Nutr Prog* 1998;5.
- [29] Solorzano L. Determination of ammonia in natural waters by the phenylhypochlorite method. *Limnol Oceanogr* 1969;14:799–801.
- [30] Lee EY, Choi CY. Structural identification of polyhydroxyalkanoic acid (PHA) containing 4-hydroxyalkanoic acids by gas chromatography–mass spectrometry (GC–MS) and its application to bacteria screening. *Biotechnol Tech* 1997;11:167–71.
- [31] Sin MC, Annur MSM, Tan IKP, Gan SN. Thermodegradation of medium-chain-length poly (3-hydroxyalkanoates) produced by *Pseudomonas putida* from oleic acid. *Polym Degrad Stab* 2010;95:2334–42.
- [32] Dai Y, Lambert L, Yuan Z, Keller J. Characterisation of polyhydroxyalkanoate copolymers with controllable four-monomer composition. *J Biotechnol* 2008;134:137–45.

- [33] Bonduelle C, Martin-Vaca B, Bourissou D. Lipase-catalyzed ring-opening polymerization of the O-carboxylic anhydride derived from lactic acid. *Biomacromolecules* 2009;10:3069–73.
- [34] Randriamahefa S, Renard E, Guérin P, Langlois V. Fourier transform infrared spectroscopy for screening and quantifying production of PHAs by *Pseudomonas* grown on sodium octanoate. *Biomacromolecules* 2003;4:1092–7.
- [35] Sha K, Li D, Li Y, Zhang B, Wang J. The chemoenzymatic synthesis of a novel CBABC-type pentablock copolymer and its self-assembled “crew-cut” aggregation. *Macromolecules* 2008;41:361–71.
- [36] Chung AL, Jin HL, Huang LJ, Ye HM, Chen JC, Wu Q, et al. Biosynthesis and characterization of poly (3-hydroxydodecanoate) by  $\beta$ -oxidation inhibited mutant of *Pseudomonas entomophila* L48. *Biomacromolecules* 2011;12: 3559–66.
- [37] Liu Q, Luo G, Zhou XR, Chen G-Q. Biosynthesis of poly(3-hydroxydecanoate) and 3-hydroxydodecanoate dominating polyhydroxyalkanoates by  $\beta$ -oxidation pathway inhibited *Pseudomonas putida*. *Metab Eng* 2011;13:11–7.
- [38] Haba E, Vidal-Mas J, Bassas M, Espuny MJ, Llorens J, Manresa A. Poly 3-(hydroxyalkanoates) produced from oily substrates by *Pseudomonas aeruginosa* 47T2 (NCBIM 40044): effect of nutrients and incubation temperature on polymer composition. *Biochem Eng J* 2007;35:99–106.
- [39] Allen AD, Anderson WA, Ayorinde FO, Eribo BE. Biosynthesis and characterization of copolymer poly (3HB-co-3HV) from saponified *Jatropha curcas* oil by *Pseudomonas oleovorans*. *J Ind Microbiol Biotechnol* 2010;37:849–56.
- [40] Khanna S, Srivastava AK. Recent advances in microbial polyhydroxyalkanoates. *Process Biochem* 2005;40:607–19.
- [41] Pereira SMF, Rodriguez RS, Gomes JGC. Biosynthesis and characterization of biodegradable Poly (3-hydroxybutyrate) from renewable sources. *Matéria (Rio de Janeiro)* 2008;13:1–11.
- [42] Annur MSM, Tan IKP, Ramachandran KB. Evaluation of nitrogen sources for growth and production of medium-chain-length poly-(3-hydroxyalkanoates) from palm kernel oil by *Pseudomonas putida* PGA 1. *Asia Pac J Mol Biol Biotechnol* 2008;16.

# Single-step lipase-catalyzed functionalization of medium-chain-length polyhydroxyalkanoates

<sup>1</sup> Institute of Biological Sciences,    <sup>2</sup> Department of Chemistry  
Faculty of Science, University of Malaya, Kuala Lumpur 50603, Malaysia

## Statement of contributions of joint Authorship

Supervised and assisted with chemical analyses, structure elucidation and co-author of the manuscript

# Single-step lipase-catalyzed functionalization of medium-chain-length polyhydroxyalkanoates

Ahmad M Gumel,<sup>a</sup> Suffian M Annuar<sup>a\*</sup> and Thorsten Heidelberg<sup>b</sup>

## Abstract

**BACKGROUND:** Functionalization of aliphatic biopolymers such as bacterial polyhydroxyalkanoates (PHA) using biologically active hydrophilic moieties like sugars helps to improve the hydrophilicity and biodegradability of the biomaterial.

**RESULTS:** The effects of reaction variables reaction time, temperature, enzyme concentration and substrate ratio on reaction rate and yield in the synthesis of poly(1'-O-3-hydroxyacyl-sucrose) using *Candida antarctica* lipase B (EC 3.1.1.3) were studied. Using H<sub>2</sub>O<sub>2</sub> as micro-initiator, enzyme-mediated synthesis yielded reaction rate,  $v^{app}$  of  $0.076 \times 10^{-5} \text{ mol L}^{-1} \text{ s}^{-1}$ . The biodegradability of the functionalized polymer was observed to increase by 1.5 fold compared with the non-functionalized material apart from showing better compostability. Increasing the reaction temperature ( $> 50^\circ \text{C}$ ), enzyme concentration ( $> 15 \text{ g L}^{-1}$ ) and reactant ratio (w/w) of sucrose:PHA ( $> 2$ ) did not increase further the rate or yield. The sucrose-functionalized mcl-PHA was characterized with respect to the non-functionalized material.

**CONCLUSIONS:** Novozym<sup>®</sup> 435 can be used effectively to synthesize poly(1'-O-3-hydroxyacyl sucrose) in micro-aqueous medium bypassing the need for chemo-synthetic steps. The synthesized biomaterials have potential applications in biomedical and industrial niches.

© 2012 Society of Chemical Industry

**Keywords:** biopolymer; *Candida antarctica*; lipase; polyhydroxyalkanoates; sugar-ester; sucrose

## INTRODUCTION

Polyhydroxyalkanoates (PHA) are known to have important industrial and biomedical applications as a result of their biodegradability, biocompatibility, compostability and versatile structural composition. In fact, the current concerns over environmental pollution and degradation, favor the application of these biodegradable polymers over their petrochemical counterparts. Despite their applications in the biomedical field spanning from surgical sutures, drug delivery devices to tissue engineering scaffolds,<sup>1–4</sup> the biopolymers may exhibit slow degradability and resorbability especially within the extracellular matrixes.<sup>3</sup> For instance, the *in vivo* degradability of poly-2-oxepanone was reported to take about 3–4 years in tissue in addition to lack of total elimination of the degraded monomers out of the body.<sup>5</sup> Among the reported strategies employed to address this issue is the functionalization of the polymer.<sup>3</sup> One such approach is functionalization by transesterification *via* sugar-acylation, which not only improve the hydrophilicity of these carbohydrate esters but also impart novel properties for specialty applications such as antimicrobial activity,<sup>6,7</sup> lectins interaction,<sup>8</sup> galactosyl transferase inhibition,<sup>9</sup> specific ligands to the ASGPR receptor that is overexpressed in hepatocellular carcinoma,<sup>10</sup> water repelling and oil absorption.<sup>11</sup>

The use of conventional chemical catalysis in polymer functionalization and modification processes is viewed as unfavorable due to byproduct(s) formation that are complicated to control particularly when the main products are intended for use in biomedical and environmental applications. Alternatively,

enzymatic catalysis offers excellent enantiomeric selectivity, specificity and catalytic activity under mild reaction conditions, making the enzyme catalyzed functionalization process highly desirable. Lipases (EC 3.1.1.3) were among the most commonly used triacylglycerol hydrolases that catalyze the synthesis of ester bonds in micro-aqueous media.<sup>6,12</sup> A wide range of biodegradable functionalized polymers has been produced using enzymatic catalysis.<sup>11,13–16</sup> Most reported polymer functionalization was based on polyvinyl,<sup>17–19</sup> polyacrylate<sup>20</sup> and polycaprolactone<sup>11,21</sup> esters. In addition, most of the synthetic process is not solely enzymatic but a hybrid system (chemo-enzymatic)<sup>13,18,22,23</sup> where enzymatic transesterification of the vinyl or acrylic ester with the sugar moiety is followed by chemical radical polymerization. In most cases, the functionalized polymer obtained through this approach has toxic chemical impurities, which make it less attractive for biomedical applications. Secondly, the pendant carbohydrate moiety is attached to the main polymeric chain

\* Correspondence to: Suffian M Annuar, Institute of Biological Sciences, Faculty of Science, University of Malaya, 50603 Kuala Lumpur, Malaysia.  
E-mail: suffian\_annuar@um.edu.my

<sup>a</sup> Institute of Biological Sciences,

<sup>b</sup> Department of Chemistry, Faculty of Science, University of Malaya, 50603, Kuala Lumpur, Malaysia

by a di-carboxylic acid spacer arm,<sup>19,22,24</sup> which could probably increase the hydrophobicity of the polymer rather than the hydrophilicity. Literature reporting bacterial PHA functionalization is very scarce,<sup>25</sup> particularly reports on the single-step enzymatic functionalization of medium chain length PHA (mcl-PHA).

This study reported *Candida antarctica* lipase B catalyzed functionalization of bacterial mcl-PHA with sucrose in the absence of the spacer arm to yield poly(1'-O-3-hydroxyacyl-sucrose). Effects of reaction variables such as temperature, enzyme loading, reactant ratio and reaction time in relation to enzymatic reaction rate,  $v^{app}$  and reactant conversion were studied. In addition to characterization of the functionalized mcl-PHA, biodegradability and compostability of the biomaterial were also studied.

## MATERIALS AND METHODS

### Materials

*Candida antarctica* lipase B (Novozym 435) immobilized on acrylic resin beads (Sigma-Aldrich; L4777), *p*-nitrophenyl palmitate (Sigma-Aldrich; N2752), dimethyl sulfoxide (Sigma-Aldrich; D8418), molecular sieve 4 Å (Sigma-Aldrich; 334308), NaCl crystal window (Sigma-Aldrich; Z267724). Sucrose (Merck; 107651), hydrogen peroxide (Merck; 822287), methanol (Merck; 106012), chloroform (Merck; 102395), dichloromethane (Merck; 106051), acetone (Merck; 100299), *N*-(trimethylsilyl) imidazole (Merck; 818204). All chemicals were of analytical grade.

Biodegradable mcl-PHA with co-monomeric compositions of C<sub>6:0</sub> to C<sub>14:0</sub> was obtained based on reported fermentation culture conditions<sup>26</sup> using *Pseudomonas putida* Bet001 as producer microorganism and fatty acids as sole carbon and energy source.

### Methods

#### Enzyme activity

The enzymatic activity was measured as reported by Teng and Xu.<sup>27</sup> Novozym 435 (150 mg) was added to a vial containing 10 mL of a 10 mmol L<sup>-1</sup> 4-nitrophenyl palmitate solution in *n*-hexane. To this mixture 60 µL of 1 mol L<sup>-1</sup> absolute ethanol was added. The resulting slurry was incubated at 40°C, 200 rpm for a period of 20 min. Aliquots (30 µL each) of the reaction mixture were withdrawn at intervals and quenched by mixing with 1 mL of 0.1 mol L<sup>-1</sup> NaOH in a quartz cuvette. The 4-nitrophenol liberated by the reaction was measured at 412 nm (UV-Vis spectrophotometer V-630; Jasco, Japan) against distilled water as blank. The enzyme activity was calculated as the slope of a plot of 4-nitrophenol released versus time.

#### Enzymatic transesterification

All reactions were performed in triplicate. A solution of sucrose (0.16 g) dissolved in 2 mL DMSO under mild warming (40°C, 3 min) was mixed into 20 mL capped reaction vials containing 0.08 g mcl-PHA dissolved in 8 mL chloroform. To this mixture, 150 mg lipase, 30 mg molecular sieve 4Å and 10 µL H<sub>2</sub>O<sub>2</sub> (micro-initiator) were added. The initial water activity ( $a_w$ ) of the mixture was then recorded using Rotronic hygropalm water activity meter (HP23-AW; www.rotronic.co.uk). The reaction was then allowed to progress for a total period of 24 h at 50°C, 200 rpm. All reactions were carried out according to the aforementioned procedure except if stated otherwise.

#### Residual sugar quantification

At specific intervals the residual carbohydrate moiety was quantified by withdrawing aliquot samples (20 µL) of the reaction

mixture and mixed with 5 µL absolute ethanol to stop the reaction. This mixture was then diluted with 1.0 mL chloroform and thereafter derivatized by adding 5 µL *N*-(trimethylsilyl) imidazole (TMSI) followed by sonication at 37 kHz, 1.9 W and 30°C for 2 min and immediately filtered into GC vials. The residual sugar was then measured on Agilent triple quadrupole 7000B instrument (Agilent, USA) equipped with GCMSMS triple axis detector carrying Agilent HP-5ms column (30 m long × 0.25 mm internal diameter × 0.25 µm film thickness). A sample (2 µL) was automatically injected into the GCMSMS at a split ratio of 1:10. The injection temperature was 280°C. The column oven temperature ramping was as follows: 110°C for 1 min then increased to 200°C at 20°C min<sup>-1</sup>; held at 200°C for 2 min then increased to 280°C at 20°C min<sup>-1</sup>; then held at 280°C for 5 min. Helium at 0.76 bar and 14 mL min<sup>-1</sup> was used as the carrier gas. Mass spectra were acquired at 1250 scan speed using electron impact energy of 70 eV at 230°C ion-source and 250°C interface temperatures. The data obtained per each reaction time was used to quantify the residual sucrose by comparing with the calibration plot prepared by analyzing different concentrations of sucrose standard solutions in DMSO. The enzymatic reaction rate (mol L<sup>-1</sup> s<sup>-1</sup>) was calculated as the slope of a plot of converted sucrose concentration versus time.

#### Product extraction

At the end of the reaction, the functionalized polymer (poly(1'-O-3-hydroxyacyl-sucrose)) was extracted by diluting the reaction mixture with 20 mL of dichloromethane, followed by filtration using glass fritted Buchner filter funnel to separate the immobilized enzyme and molecular sieves. The filtrate was then concentrated under reduced pressure to about 3 mL at 40°C. The functionalized polymer was precipitated out from the filtrate by adding the concentrate into 10 mL of cold acetone (4°C). The solvent was then decanted and the precipitate was re-purified by subjecting it to three-cycle precipitation. At each stage, the functionalized polymer was dissolved in dichloromethane (3 mL) then added to cold acetone (10 mL, 4°C) and the white precipitate was recovered. The final extracted product was dried to a constant weight at 30°C under vacuum. A portion of the dried sample was subsequently subjected to further authentication analyses.

#### Product authentication

Perkin-Elmer FTIR RX 1 spectrometer (Perkin-Elmer Inc., Wellesley, MA, USA) was used to record FTIR-ATR spectra of the poly(1'-O-3-hydroxyacyl-sucrose) as previously reported.<sup>25</sup> Proton NMR spectra were recorded on a JEOL JNM-GSX 270 FT-NMR (JEOL Ltd, Tokyo, Japan) machine at 250 MHz according to reported literature.<sup>26</sup>

Gel permeation chromatography of the poly(1'-O-3-hydroxyacyl-sucrose) was recorded on Waters 600 (Waters Corp, Milford, MA, USA) equipped with a Waters refractive index detector (model 2414) and the following gel columns (7.8 mm internal diameter × 300 mm each) in series: HR1, HR2, HR5E and HR5E Waters Styrogel HR-THF. Monodisperse polystyrene of different molecular weights (3.72 × 10<sup>2</sup>, 2.63 × 10<sup>3</sup>, 9.10 × 10<sup>3</sup>, 3.79 × 10<sup>4</sup>, 3.55 × 10<sup>5</sup>, 7.06 × 10<sup>5</sup>, 3.84 × 10<sup>6</sup> and 6.77 × 10<sup>6</sup> Da) were used as standards to produce the calibration curve. The polymer samples (2.0 mg mL<sup>-1</sup>) were dissolved in dichloromethane (DCM), filtered through a 0.22 µm PTFE filter and then injected into the GPC (100 µL) at 40°C. DCM was used as mobile phase at a flow rate of 1.0 mL min<sup>-1</sup>.

Differential scanning calorimetric (DSC) analysis of the poly(1'-O-3-hydroxyacyl-sucrose) was performed on a Perkin-Elmer Diamond



DSC instrument using HyperDSC<sup>®</sup> technique (Perkin-Elmer Inc., Wellesley, MA, USA). Scans over the temperature range  $-50^{\circ}\text{C}$  to  $180^{\circ}\text{C}$  at a heating and cooling rate  $10^{\circ}\text{C min}^{-1}$  in nitrogen at flow rate  $50\text{ mL min}^{-1}$ .

Thermal gravimetric analyses were performed on a Perkin-Elmer TGA4000 instrument (Perkin-Elmer Inc., Wellesley, MA, USA). The samples were heated from  $50^{\circ}\text{C}$  to  $800^{\circ}\text{C}$  at a rate of  $10^{\circ}\text{C min}^{-1}$  in nitrogen at flow rate  $20\text{ mL min}^{-1}$ .

#### Biodegradability and compostability test

The biodegradability of both the functionalized and control (non-functionalized) mcl-PHA was performed quantitatively according to reported literature.<sup>28</sup> This was tested by culturing *Candida rugosa* (ATCC 10571) in two sets with three replicates each in a batch fermentation process (100 mL in 250 mL conical flask) using previously reported media composition.<sup>29</sup> First, the yeast was cultured on agar plate growth medium ( $30^{\circ}\text{C}$ , 200 rpm, 48 h) composed of ( $\text{L}^{-1}$ ): 3.5 g peptone, 30 g yeast extract, 20 g glucose, 2 g  $\text{KH}_2\text{PO}_4$ , 1 g  $\text{MgSO}_4 \cdot 7\text{H}_2\text{O}$  and 20 g agar in distilled water. The harvested biomass (1% w/v) was aseptically suspended in sterile 2% NaCl solution (15 mL). The suspended cells solution (5 mL) was aseptically inoculated into sterile basal liquid medium ( $30^{\circ}\text{C}$ , 200 rpm) that contained ( $\text{L}^{-1}$ ): 15 g  $\text{KH}_2\text{PO}_4$ , 6 g  $\text{Na}_2\text{HPO}_4$ , 6 g  $(\text{NH}_4)_2\text{SO}_4$ , 1 g  $\text{MgSO}_4 \cdot 7\text{H}_2\text{O}$  and 0.2% (v/v) filter (0.22  $\mu\text{m}$ ) sterilized micronutrients (0.01 g  $\text{FeCl}_3 \cdot 6\text{H}_2\text{O}$ , 0.004 mg inositol, 0.006 mg biotin, 0.2 mg thiamine hydrochloride). Carbon source (PHA sample) was added at a final concentration of  $5\text{ g L}^{-1}$ . The pH value of the media was adjusted to 7.0 ( $\pm 0.2$ ) with NaOH. The oxygen consumption of each sample over time was determined using CyberScan dissolve oxygen meter DO300 (Eutech Instruments; The Netherlands). The percentage biodegradation rate was calculated by expressing the ratio of experimental biochemical oxygen demand (BOD) to that of theoretical oxygen demand as a percentage.

The qualitative biodegradability test was observed by compostability of both polymer samples based on the microbial degradation of polymer surface in a laboratory simulated environment using about 300 g of 70% ( $\pm 3\%$ ) humid garden soil in a 50 mL sample bottle. A solvent-cast film (0.5 cm  $\times$  1 cm) of both poly(1'-O-3-hydroxyacyl-sucrose) and the control were buried 4 cm deep each in separate sample bottles and incubated at  $30^{\circ}\text{C}$  ( $\pm 2^{\circ}\text{C}$ ) for a period of 8 weeks. At regular intervals, the surface topological analyses of both polymers before and after composting were obtained at 360 to 450  $\mu\text{m}$  view using 3D Alicona InfiniteFocus<sup>®</sup> optical surface texture analyzer (Alicona; Austria).

#### Calculations

Enzymatic apparent catalytic reaction rate ( $v^{\text{app}}$ ;  $\text{M s}^{-1}$ ) was calculated using Equation (1):

$$v^{\text{app}} = \frac{\Delta[S]}{\Delta t} \quad (1)$$

where  $[S]$  is the converted sucrose molar concentration at time  $t$ .

The polymeric apparent degree of crystallinity ( $X_c^{\text{ap}}$ ) is given by Equation (2):

$$X_c^{\text{ap}} = \frac{\Delta H}{\Delta H^*} \quad (2)$$

where  $\Delta H$  is the DSC endothermic melting enthalpy of the poly(1'-O-3-hydroxyacyl-sucrose), assuming  $142\text{ J g}^{-1}$  as the endothermic melting enthalpy ( $\Delta H^*$ ) of standard PHB as cited in the literature.<sup>30</sup>

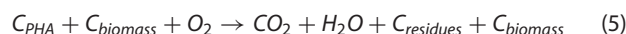
The biochemical oxygen demand (BOD) and percentage BOD biodegradability were determined according to Equations (3) and (4), respectively:<sup>28</sup>

$$\text{BOD} = \frac{DO_0 - DO_t}{\varphi} \quad (3)$$

where  $DO_0$  and  $DO_t$  is the dissolved oxygen (DO) initially and at time  $t$ , respectively;  $\varphi$  is the fractional oxygen volume defined as the ratio of the experimental DO volume to that of theoretical DO volume calculated from the ideal gas equation and according to stoichiometry in Equation (5).

$$\text{BOD degradability \%} = \frac{\left(\frac{DO_0 - DO_t}{\varphi}\right)}{\text{BOD}_0} \times 100 \quad (4)$$

where  $\text{BOD}_0$  is the theoretical BOD which equals  $DO_0$  in a batch process.



Polydispersity index (PDI) of the polymer was calculated using Equation (6):

$$\text{PDI} = M_w/M_n \quad (6)$$

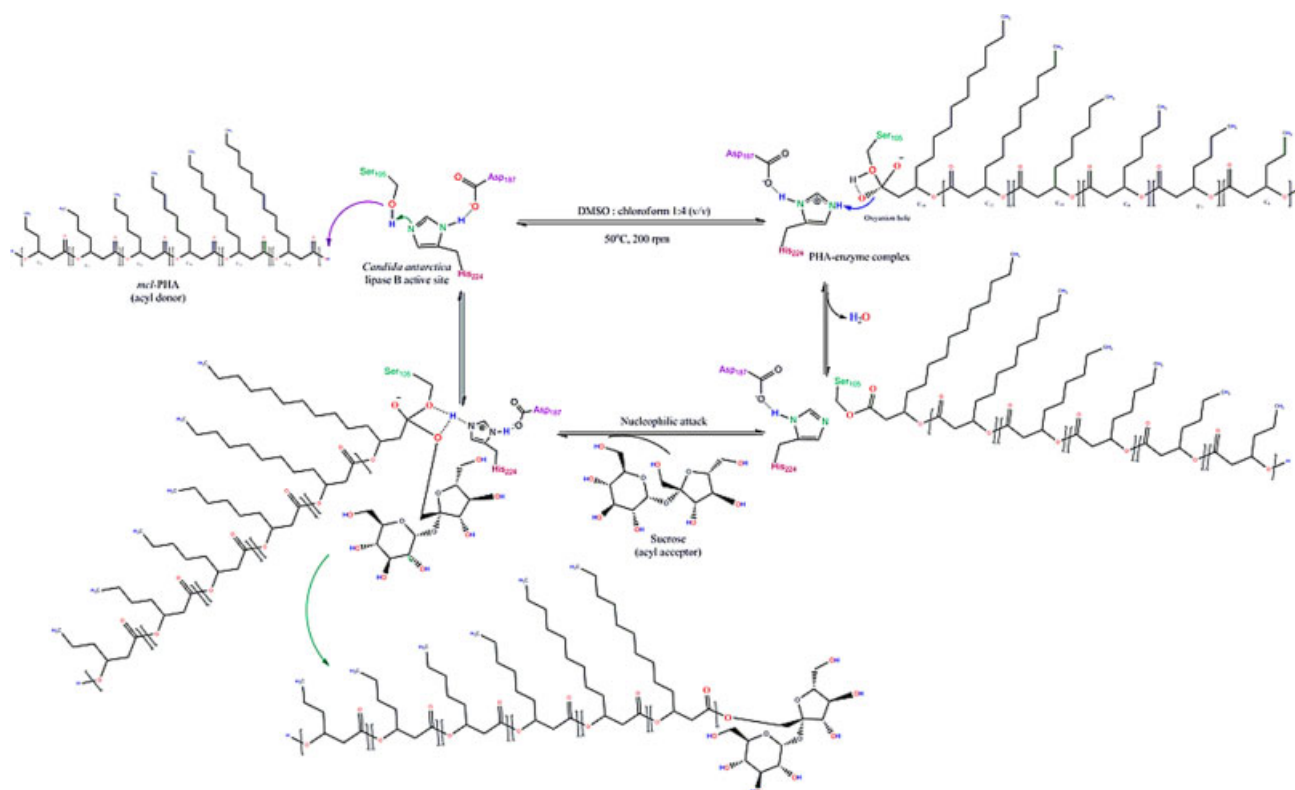
where  $M_w$  is weight-averaged molecular weight and  $M_n$  is number averaged molecular weight.

## RESULTS AND DISCUSSION

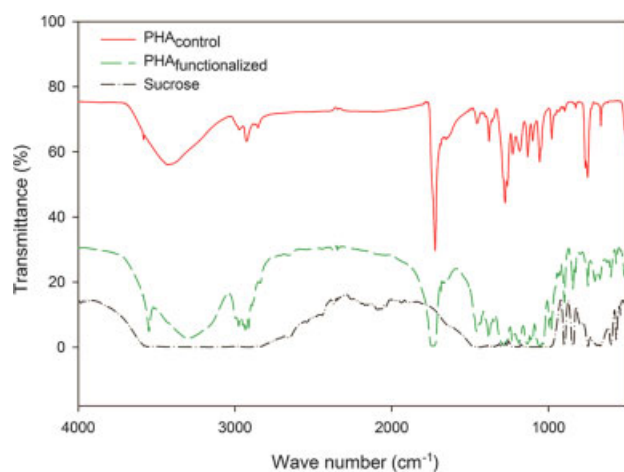
### Characterization of sucrose-based functionalized mcl-PHA

The synthesis of sucrose-based functionalized mcl-PHA (poly(1'-O-3-hydroxyacyl-sucrose)) was achieved using Novozym 435 from *Candida antarctica* as a catalyst in a co-solvent system (Fig. 1). In this process, a sucrose conversion yield of 34.1% ( $\pm 1\%$ ) was observed within 24 h. The solvent-cast film of the extracted polymeric product (white amorphous film) was subjected to analytical authentication. FTIR-ATR (Fig. 2): wave number 3389 ( $\nu$  -O-H), 2979 ( $\nu$  -CH<sub>2</sub>-CH<sub>2</sub>-), 2891 ( $\nu$  -CH<sub>2</sub>-CH<sub>3</sub>), 1734 ( $\nu$  C=O), 1295 ( $\nu$  -C-O-C-). <sup>1</sup>H NMR (Fig. 3) relative to trimethylsilane (TMS):  $\delta$  5.30 (1H, 1 $\alpha$ -H of glucose), 4.72 (1H,  $J_{4'\beta\text{-H}}$ , 4'  $\beta$ -H of sucrose), 4.50 (1H,  $J_{1'\beta\text{-Ha'}}$ , 1'  $\beta$ -H<sub>a'</sub> of sucrose), 4.33 (1H, 5'  $\beta$ -H of sucrose), 4.19 (1H,  $J_{1'\beta\text{-Hb'}}$ , 1'  $\beta$ -H<sub>b'</sub> of sucrose), 3.83 - 3.20 (1H-3' $\beta$ ; 2H-6' $\beta$   $J_{6'a',b'\beta\text{-H}}$ ; 2H-6 $\alpha$   $J_{6a,b\alpha\text{-H}}$ ; 1H-2 $\alpha$ ; 1H-3 $\alpha$ ; 1H-4 $\alpha$ ; 1H-5 $\alpha$ ; OH of 3', 4', 6', 2,3,4,6 of sucrose, 1H-PHA $\beta$ -carbon -CH= and 1H of PHA<sub>OH-terminal</sub>), 2.56, 2.32 (2H-PHA $\alpha$ -carbon -CH<sub>2</sub>-), 1.75-1.40 (2H of -CH<sub>2</sub>- PHA<sub>side-chain</sub>) and 0.86 (3H PHA<sub>side-chain</sub> -CH<sub>3</sub>).

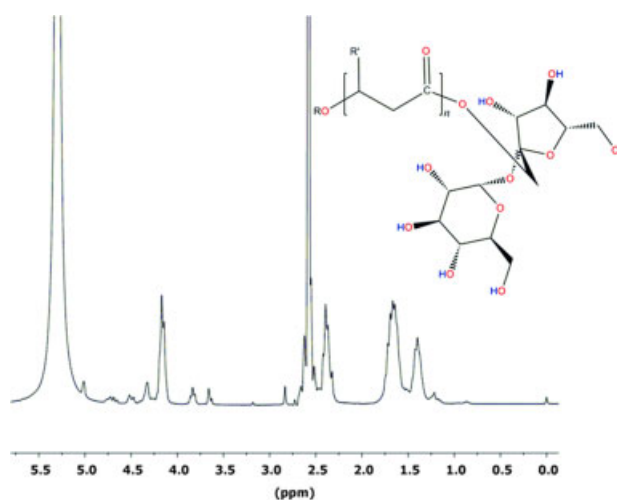
*Candida antarctica* lipase B (CALB) is reported to be composed of 317 different amino acid residues and have a total molecular weight of about 33 kDa.<sup>31,32</sup> Like other hydrolases, the catalytic site of this enzyme is composed of a catalytic triad of three polar amino acid residues i.e. serine-histidine-aspartic acid (Ser<sub>105</sub>, His<sub>224</sub> and Asp<sub>187</sub>) as depicted in Fig. 1. These amino acids are responsible for the enzyme catalytic activity.<sup>31</sup> In Fig. 1, the overall reaction mechanism is proposed to follow a two-step mechanism with an initial acylation step where the PHA polymer interact with the Ser<sub>105</sub> residue resulting in a covalent acyl-enzyme intermediate.<sup>1,33</sup> In this step, the primary hydroxyl group on Ser<sub>105</sub> serves as a nucleophile, which attack the terminal acyl-carbonyl-carbon of the PHA forming a transition state which leads to the formation of covalently bonded tetrahedral intermediate. This intermediate is then stabilized by the proton-accepting His<sub>224</sub> residue due to the formation of two important hydrogen bonds between itself (His<sub>224</sub>)



**Figure 1.** Proposed reaction mechanism of *C. antarctica* lipase B catalyzed PHA functionalization using sucrose as acyl acceptor in biphasic solvent.



**Figure 2.** FTIR spectra of the control PHA (non-functionalized), standard sucrose and sucrose-based functionalized PHA.



**Figure 3.**  $^1\text{H}$  NMR spectrum of sucrose based functionalized PHA.

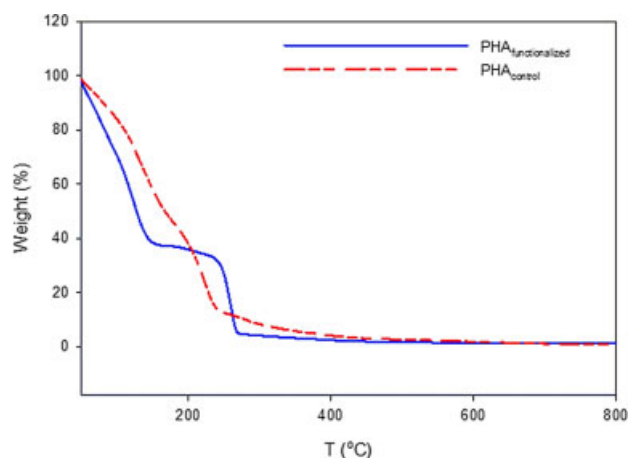
and the other two amino acids (Ser<sub>105</sub> and Asp<sub>187</sub>). This is followed by deacylation as a result of interaction between the Ser<sub>105</sub> primary amide nitrogen and the ester bond hydroxyl group resulting in the release of water molecule and Ser<sub>105</sub> activated complex. Further nucleophilic attack by alcohol (sucrose) results in the glycosylation of the sugar moiety onto the polymer chain (Fig. 1).

In Fig. 2, the FTIR spectrum of the poly(1'-O-3-hydroxyacyl-sucrose) shows an increased absorption at wave number ( $\nu$ ) 3389  $\text{cm}^{-1}$  corresponding to increased -OH group and the persistence of ester absorption at 1734  $\text{cm}^{-1}$  reveals a successful functionalization of the PHA with the sugar moiety compared with the spectra of non-functionalized PHA that has been used as control (Fig. 2).

This observation was found to be in accord with the proton NMR spectrum of the product (Fig. 3), which reveals a series of chemical shifts at  $\delta$  5.30 to 3.20 ppm, signifying the presence of sugar in the product. These observations were found to be in good agreement with reported literature on sucrose polyesters characterization.<sup>19,22</sup>

In contrast to control mcl-PHA ( $T_m$  42°C;  $T_d$  264.4°C,  $X_c^{ap}$  0.7), the thermal analyses of the poly(1'-O-3-hydroxyacyl-sucrose) was observed to have low degree of crystallinity ( $X_c^{ap}$  = 0.3), two peak endothermic melting temperature ( $T_m$ ) of 123.3 and 131.8°C ( $\pm 0.2^\circ\text{C}$ ) corresponding to the distinct melting of the sucrose moiety and PHA, respectively. The thermogravimetric analysis revealed a two-step degradation temperature  $T_d$  (Fig. 4) at 186.2





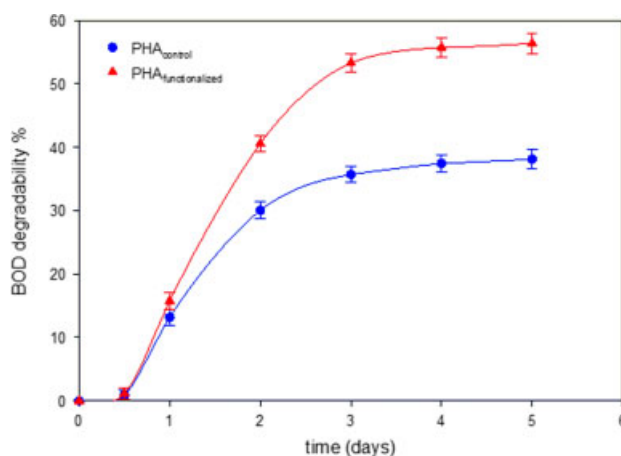
**Figure 4.** TGA thermogram of functionalized PHA and non-functionalized PHA.

and  $275.5^{\circ}\text{C}$  ( $\pm 0.2^{\circ}\text{C}$ ), signifying the decomposition of both the hydrophilic sugar moiety and the hydrophobic mcl-PHA backbone, respectively. Furthermore, the GPC analysis of the poly(1'-O-3-hydroxyacyl-sucrose) revealed a general decrease in weight average molecular weight ( $M_w$  35.4 kDa) with increasing number average molecular weight ( $M_n$  48.7 kDa) and 0.7 PDI compared with the non-functionalized PHA ( $M_w$  41.2 kDa,  $M_n$  21.3 kDa, PDI 1.9). This reduction in  $M_w$  and the increase in the  $M_n$  of the poly(1'-O-3-hydroxyacyl-sucrose) were attributed to the possible enzymatic hydrolysis of the polymeric backbone by random chain scission, which explains the increase in  $M_n$ . The observed increase in  $T_m$  could be attributed to the increased hydrophilicity of the polymer as a result of sugar moiety hydrogen bonding causing strong intermolecular attraction, thus at the same time increasing the amount of thermal energy required to break the bond. This observation is further supported by the differences in the  $T_d$  between  $264.4^{\circ}\text{C}$  for non-functionalized mcl-PHA and  $275.5^{\circ}\text{C}$  for functionalized mcl-PHA.

#### Biodegradability and compostability of the poly(1'-O-3-hydroxyacyl-sucrose)

The biodegradability of polymeric materials has been documented to rely substantially on their basic physical and chemical structure properties.<sup>28</sup> These are not only restricted to the polymeric molecular structures but also the length of the polymeric chain and crystallinity of the polymer since it is more difficult to degrade the crystalline part compared with the amorphous parts. Reaction conditions (vessel's volume and shape, temperature, pH, aerobic or anaerobic, mixing and duration) and polymeric polarity were also reported to affect the rate of degradation process.<sup>28</sup> Indeed, the hydrophilicity of the sugar moiety on the polymer will also influence the absorption of water favoring high microbial growth and attract more microbial cells to the sample.<sup>24</sup>

As expected the biodegradability of the poly(1'-O-3-hydroxyacyl-sucrose) was observed to surpass that of non-functionalized polymer by about 1.5 fold (Fig. 5). In fact, poly(1'-O-3-hydroxyacyl-sucrose) was observed to be degraded by 56.4% after 5 days compared with 38.1% of non-functionalized mcl-PHA. In Fig. 5, a short lag period between incubation times of 0 to 12 h was observed, which could be attributed to the microbial adaptation in the culture medium and the substrate. After that time a progressive increase in degradation was observed up to day 3 indicating successful use of the polymer



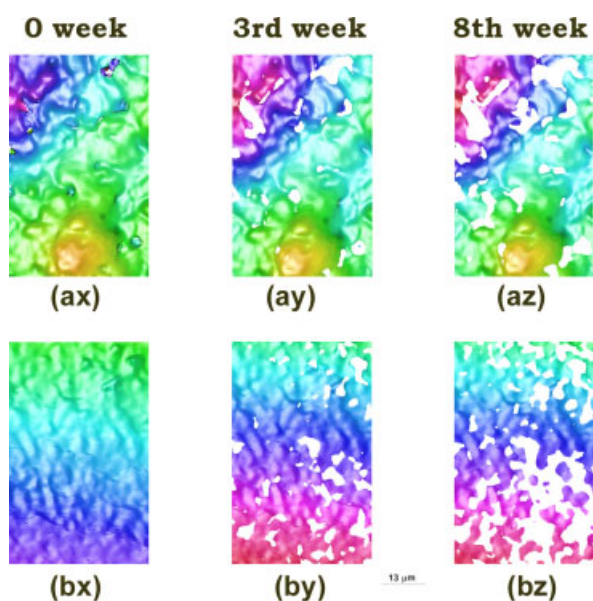
**Figure 5.** BOD degradability % as a function of incubation time at  $3\text{ g L}^{-1}$  PHA,  $30^{\circ}\text{C}$ , 200 rpm for 5 days.

as a carbon and energy source by the yeast. A plateau was observed after day 3, thus, indicating a probable end of the degradation under the mentioned incubation conditions. In contrast to the control polymer this difference in percentage degradation could be due to the increase hydrophilicity and microbial growth in the sucrose-based polymer sample. These results are in agreement with the reported increase in biodegradation of sugar-based polymers. For instance, Barros *et al.*<sup>34</sup> investigated the biodegradation of poly(6-O-methacryloyl sucrose-co-styrene) and poly(6-O-crotonyl sucrose-co-styrene) using *Aspergillus niger*, the authors reported a very good biodegradability after 90 days of incubation. Lu *et al.*<sup>22</sup> reported a decrease in  $M_n$  from 33 kDa to 1080 Da in their studies on the biodegradation of poly(1'-O-vinyladipoyl-sucrose) using *Bacillus subtilis* alkaline protease (EC 3.4.21.62) at  $37^{\circ}\text{C}$  in a shake flask process.

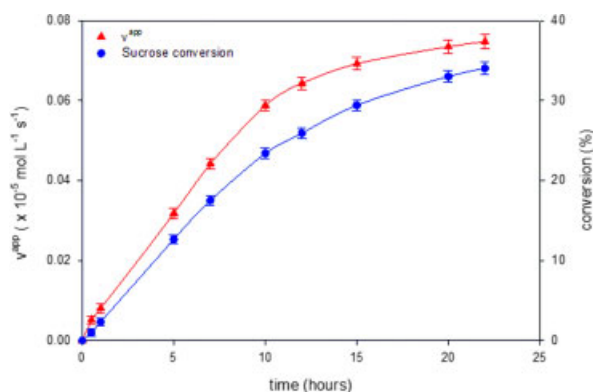
The observations in this study were supported by the results of the solid-phase surface texture analysis. The functionalized mcl-PHA seems to be well degraded under the simulated composting conditions. In Fig. 6, relative to the initial PHA film in both samples (Fig. 6 ax, bx), the non-functionalized PHA (Fig. 6 ay) was observed to have less surface degradation after 3 weeks of composting compared with poly(1'-O-3-hydroxyacyl-sucrose), which showed more degraded surface (Fig. 6 by). In both samples maximum surface degradation was observed after 8 weeks of composting; as expected poly(1'-O-3-hydroxyacyl-sucrose) (Fig. 6 bz) degraded more than the non-functionalized PHA (Fig. 6 az). This could be due to the presence of sucrose moiety improving the hydrophilicity of the functionalized mcl-PHA. In general, the degradation in both samples was localized to specific areas. This could be the amorphous phase of the film, which is more readily degraded by the composting microorganisms in relation to the more organized crystalline phase.<sup>28</sup>

#### Effects of reaction time on reactant (sucrose) conversion in the lipase-catalyzed functionalization of mcl-PHA

The effect of reaction time on the enzymatic reaction rate and acyl acceptor conversion was observed at w/w ratio of 0.5 PHA to sucrose (Fig. 7). Strong increase in both the apparent reaction rate  $v^{app} = 0.073 \times 10^{-5} \text{ mol L}^{-1} \text{ s}^{-1}$  and corresponding sucrose conversion (23.4%) were observed during the early hours of the reaction ( $\sim 10$  h). Both the reaction rate and the conversion increased gradually up to 20 h; thereafter the reaction rate and



**Figure 6.** Optical 3D Aicona InfiniteFocus® micrograph comparing the surface degradation in the simulated composting of control mcl-PHA (ax, ay and az) and the functionalized mcl-PHA (bx, by and bz) recorded at 25°C, 360 to 450 µm view.



**Figure 7.** Enzymatic reaction rate  $v^{app}$  and sucrose conversion as a function of reaction time at 50°C, 200 rpm, 24 h.

the conversion tapered off to a maximum  $v^{app}$  of  $0.075 \times 10^{-5} \text{ mol L}^{-1} \text{ s}^{-1}$  with corresponding conversion of 34.1% (Fig. 7). The gradual decrease in the apparent reaction rate could be due to the observed increased water activity ( $a_w = 0.06$  at  $t = 10 \text{ h}$ ;  $a_w = 0.17$  at  $t = 24 \text{ h}$ ) in the media, which may eventually cause polymer hydrolysis instead of synthesis. This observation is in good agreement with previous reports<sup>35–37</sup> on the observed reduction of lipase reaction rate and conversion in sugar ester synthesis due to water accumulation in the reaction media. Furthermore, the results were found to be in accord with data reported by Chamouleau *et al.*<sup>38</sup> These authors studied the influence of water activity and content on the *C. antarctica* lipase catalyzed synthesis of sugar esters in organic media. They reported a reaction rate of  $4.9 \text{ g L}^{-1} \text{ h}^{-1}$  and corresponding sugar conversion of 28.5% at  $a_w$  lower than 0.07 within 8 h reaction time. They further reported that increase in water activity (from  $a_w = 0.1$  to 0.75) in the media coincided with the decrease in reaction rate (from  $v \geq 8$  to  $< 0.5 \text{ g L}^{-1} \text{ h}^{-1}$ ) and product yield (from  $Y_{p/s} \geq 18$  to  $< 1 \text{ g L}^{-1}$ ).

**Table 1.** Reaction temperature as a function of apparent reaction rate,  $v^{app}$  and sucrose conversion (%) (maximum standard deviation  $\pm 5\%$ )

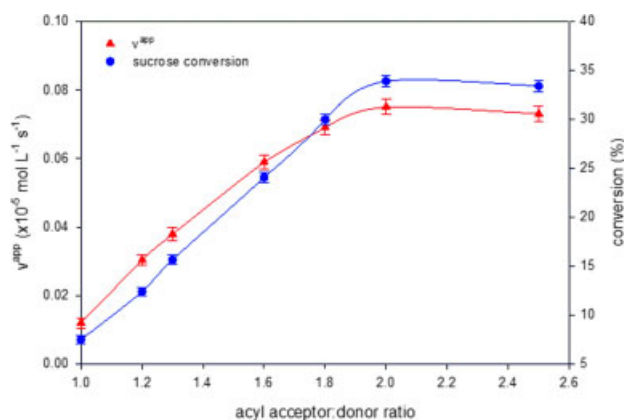
| Temp | $v^{app}$  | Conversion | $\bar{M}_n$ | $\bar{M}_w$ | PDI |
|------|--|------------|-------------|-------------|-----|
| (°C) | ( $\times 10^{-5} \text{ mol L}^{-1} \text{ s}^{-1}$ ) | (%)        | (kDa)       | (kDa)       |     |
| 25   | 0.012  | 7.51       | 17.2        | 15.5        | 0.9 |
| 30   | 0.031  | 12.4       | 24.1        | 18.2        | 0.8 |
| 40   | 0.059  | 24.1       | 32.2        | 29.1        | 0.9 |
| 50   | 0.075  | 34.1       | 48.7        | 35.4        | 0.7 |
| 55   | 0.076  | 34.2       | 32.4        | 38.3        | 1.2 |

### Effects of reaction temperature on $v^{app}$ and molecular weight

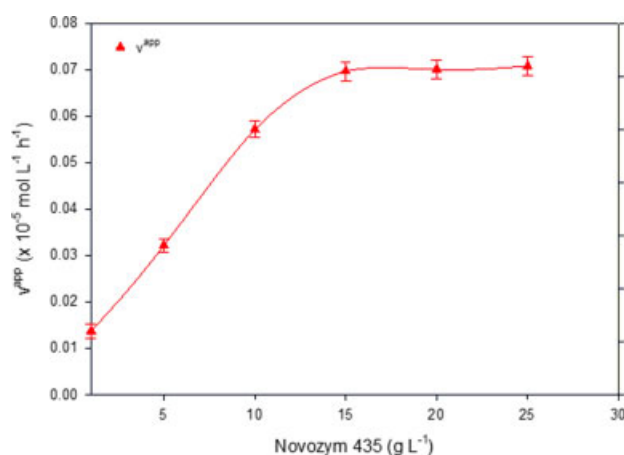
The effect of reaction temperature on the  $v^{app}$  and molecular weight in the Novozym 435 catalyzed synthesis of poly(1'-O-3-hydroxyacyl-sucrose) in chloroform-DMSO ratio 4:1 (v/v) was observed (Table 1). It has been previously stated that in micro-aqueous sugar ester synthesis, the solubility and rate of sugar dissolution play an important role in product yield.<sup>37,39</sup> In fact, in such reaction, the solubility of sugar moiety has been reported to largely rely on the reaction temperature and solvent polarity.<sup>37,39,40</sup> It is observed that the change in temperature from 25 to 50°C causes a progressive increase in both the  $v^{app}$  from  $0.012 \times 10^{-5}$  to  $0.075 \times 10^{-5} \text{ mol L}^{-1} \text{ s}^{-1}$  and a conversion from 7.51 to 34.1% (Table 1). Although the solubility of the sucrose can be improved at high temperature, increasing the reaction temperature beyond 50°C resulted in a negligible increase in  $v^{app}$  ( $0.076 \times 10^{-5} \text{ mol L}^{-1} \text{ s}^{-1}$ ) and conversion (34.2%). This could be attributed largely to the reported low enzyme stability at higher temperature.<sup>37,39,40</sup> Mat Radzi *et al.*<sup>40</sup> observed a similar trend in their study on Novozym 435 catalyzed synthesis of oleyl oleate (Cis-9-octadecenyl octadecanoate). The authors reported an observed increased in ester conversion (0–95%) with increasing temperature from 0 to 40°C; between 40 and 60°C the conversion remained constant (95.1–95.9%). These findings were in agreement with previously reported literature,<sup>39–41</sup> which cited the optimal temperature for lipase in micro-aqueous sugar ester synthesis to be between 40 and 60°C.

### Effects of reactant ratio on $v^{app}$ and reactant conversion

The relative amount and proportion of reactants in a reaction system is said to influence the kinetic behavior of the process.<sup>6,37,40</sup> This is because in this kind of heterogeneous catalysis, the solubility of the carboxylic group is affected by the concentration of dissoluble alcohol, which increases the polarity of the medium. The effect of reactant ratio (w/w sucrose to PHA) in the lipase catalyzed synthesis of poly(1'-O-3-hydroxyacyl-sucrose) was studied using  $8 \text{ g L}^{-1}$  PHA and  $15 \text{ g L}^{-1}$  Novozym 435 incubated at 50°C, 200 rpm for 24 h. It is observed that changing the sugar concentration from a weight ratio of 1.0 to 2.0 (Fig. 8), progressively influenced both the  $v^{app}$  and the corresponding conversion. At a sucrose weight ratio of 2, highest  $v^{app}$  of  $0.075 \times 10^{-5} \text{ mol L}^{-1} \text{ s}^{-1}$  and conversion of 34.1% was achieved. In our experimental condition (10 mL reaction solvent), increasing the ratio beyond 2, resulted in no further improvement in the  $v^{app}$  ( $0.073 \times 10^{-5} \text{ mol L}^{-1} \text{ s}^{-1}$ ) and the conversion (33.4%). A probable explanation for high  $v^{app}$  at ratio of 2 could be increased availability of soluble sugar for the transesterification. Since the solubility of sucrose in micro-aqueous media is known to be poor, increasing the concentration will increase the availability of the soluble sugar. However, the



**Figure 8.** Enzymatic reaction rate  $v^{app}$  and sucrose conversion as a function of reaction temperature at 200 rpm, 24 h.



**Figure 9.** Enzymatic reaction rate  $v^{app}$  as a function of enzyme loading at 50 °C, 200 rpm, 24 h.

low solubility of the sugar moiety in this kind of micro-aqueous media restricts the possible mass increment to a certain limit per reaction volume. Therefore, continuous loading of the low solubility sugar moiety resulted in altered media viscosity<sup>6,37,39,40</sup> causing complication in mass transfer of the reactants to the active site of the enzyme resulting in the decrease in  $v^{app}$ . Moreover, the increased solvation of the sugar moiety within the constant media volume increases the polarity of the media, which in turn drives the reaction equilibrium towards ester-bond hydrolysis instead of synthesis culminating in decreased conversion. Mat Radzi *et al.*<sup>40</sup> reported a similar observation in attempting to achieve highest conversion (97.1%) of oleyl alcohol to oleyl oate ester at alcohol:carboxylic acid ratio of 2. Contrary to this observation, Ha *et al.*<sup>39</sup> reported achieving highest conversion of glucose to glucosyl laurate in ionic liquid at molar ratio of 1. However, these authors reported low solubility of the lauric acid in their ionic liquids, which could probably explain the high conversion at equimolar ratio.<sup>39</sup>

#### Effects of enzyme loading on $v^{app}$

The influence of enzyme concentration on the  $v^{app}$  is shown in Fig. 9. Increase in enzyme loading from 1 to 15  $\text{g L}^{-1}$  resulted in increased  $v^{app}$  ( $0.014$ – $0.069 \times 10^{-5} \text{ mol L}^{-1} \text{ s}^{-1}$ ). The increase in excess enzyme concentration beyond 15  $\text{g L}^{-1}$  was not positively contributing to further increase in the  $v^{app}$ . For example,

increasing enzyme loading from 20–25  $\text{g L}^{-1}$  resulted in almost constant  $v^{app}$  of  $0.070$ – $0.071 \times 10^{-5} \text{ mol L}^{-1} \text{ s}^{-1}$ , most likely due to the altered and uncondusive mixing dynamics in the batch reaction system used. This observation was found to agree well with earlier reports.<sup>1,39,40</sup> Previously, Kitagawa and Tokiwa<sup>13</sup> reported an increase in reaction rate with increasing *Alcaligenes sp.* lipase loading achieving a maximum reaction rate of  $3.05 \times 10^{-3} \text{ mol L}^{-1} \text{ s}^{-1}$  at enzyme loading of 10  $\text{g L}^{-1}$  during sugar based polyvinylsebacate ester synthesis. The researchers observed that increasing the concentration beyond this value resulted in an almost constant reaction rate.<sup>13</sup>

## CONCLUSIONS

The industrial applications of bacterial mcl-PHA could be further broadened by functionalizing the biopolymers for specific characteristics like increased hydrophilicity and degradability. While most of the previously reported functionalization processes relied on hybrid chemo-enzymatic syntheses, this study demonstrated that *C. antarctica* lipase B can be used to synthesize poly(1'-O-3-hydroxyacyl sucrose) in a single-step within a micro-aqueous medium. The biodegradability of the functionalized polymer was observed to increase 1.5-fold compared with the non-functionalized material. The effects of different variables such as reaction time, temperature, enzyme concentrations and reactant ratio were studied: time 20 h, temperature 50 °C, enzyme loading 15  $\text{g L}^{-1}$  and reactant ratio 2 improved the reaction rate and yield. Indeed, these values could serve as initial points for further optimization.

## ACKNOWLEDGEMENT

The authors thank the University of Malaya for research grants PV036/2012A, RG165/11AFR and RP024-2012A.

## REFERENCES

- Gumel AM, Annuar MSM, Chisti Y and Heidelberg T, Ultrasound assisted lipase catalyzed synthesis of poly-6-hydroxyhexanoate. *Ultrason Sonochem* **19**:659–667 (2012).
- Seyednejad H, Ghassemi AH, van Nostrum CF, Vermonden T and Hennink WE, Functional aliphatic polyesters for biomedical and pharmaceutical applications. *J Controlled Release* **152**:168–176 (2011).
- Tian H, Tang Z, Zhuang X, Chen X and Jing X, Biodegradable synthetic polymers: preparation, functionalization and biomedical application. *Prog Polym Sci* **37**:237–280 (2012).
- Rai R, Yunos DM, Boccaccini AR, Knowles JC, Barker IA, Howdle SM, Tredwell GD, Keshavarz T and Roy I, Poly-3-hydroxyoctanoate P (3HO), a medium chain length polyhydroxyalkanoate homopolymer from *Pseudomonas mendocina*. *Biomacromolecules* **12**:2126–2136 (2011).
- Woodruff MA and Hutmacher DW, The return of a forgotten polymer Polycaprolactone in the 21st century. *Prog Polym Sci* **35**:1217–1256 (2010).
- Gumel AM, Annuar MSM, Heidelberg T and Chisti Y, Lipase mediated synthesis of sugar fatty acid esters. *Process Biochem* **46**:2079–2090 (2011).
- Shi Y, Li J and Chu YH, Enzyme-catalyzed regioselective synthesis of sucrose-based esters. *J Chem Technol Biotechnol* **86**:1457–1468 (2011).
- Kobayashi K, Tsuchida A, Usui T and Akaike T, A new type of artificial glycoconjugate polymer: a convenient synthesis and its interaction with lectins. *Macromolecules* **30**:2016–2020 (1997).
- Hatanaka K, Takeshige H, Kanno KI, Maruyama A, Oishi J, Kajihara Y and Hashimoto H, New polymeric inhibitor of galactosyl transferase 1. *J Carbohydr Chem* **16**:667–672 (1997).



- 10 Ross JF, Chaudhuri PK and Ratnam M, Differential regulation of folate receptor isoforms in normal and malignant tissues in vivo and in established cell lines. Physiologic and clinical implications. *Cancer* **73**:2432–2443 (1994).
- 11 Li J, Xie W, Cheng HN, Nickol RG and Wang PG, Polycaprolactone-modified hydroxyethylcellulose films prepared by lipase-catalyzed ring-opening polymerization. *Macromolecules* **32**:2789–2792 (1999).
- 12 Veld M and Palmans A, *Hydrolases Part I: Enzyme Mechanism, Selectivity and Control in the Synthesis of Well-Defined Polymers, in Enzymatic Polymerisation*, ed by Palmans ARA and Heise A. Springer Berlin/Heidelberg, 55–78 (2011).
- 13 Kitagawa M and Tokiwa Y, Synthesis of polymerizable sugar ester possessing long spacer catalyzed by lipase from *Alcaligenes sp.* and its chemical polymerization. *Biotechnol Lett* **20**:627–630 (1998).
- 14 Uyama H, Takeya K and Kobayashi S, Synthesis of polyesters by enzymatic ring-opening copolymerization using lipase catalyst. *Proc Japan Acad Ser B: Physical Biological Sci* **69**:203–207 (1993).
- 15 Varma AJ, Kennedy JF and Galgali P, Synthetic polymers functionalized by carbohydrates: a review. *Carbohydr Polym* **56**:429–445 (2004).
- 16 Yeniad B, Naik H and Heise A, *Lipases in Polymer Chemistry Biofunctionalization of Polymers and their Applications*, ed by Nyanhongo GS, Steiner W and Gübitz G. Springer Berlin/Heidelberg, 69–95 (2011).
- 17 Kitagawa M, Fan H, Raku T, Shibatani S, Maekawa Y, Hiraguri Y, Kurane R and Tokiwa Y, Selective enzymatic preparation of vinyl sugar esters using DMSO as a denaturing co-solvent. *Biotechnol Lett* **21**:355–359 (1999).
- 18 Tokiwa Y, Raku T, Kitagawa M and Kurane R, Preparation of polymeric biosurfactant containing sugar and fatty acid esters. *Clean Technol Environ Policy* **2**:108–111 (2000).
- 19 Wang X, Wu Q, Wang N and Lin XF, Chemo-enzymatic synthesis of disaccharide-branched copolymers with high molecular weight. *Carbohydr Polym* **60**:357–362 (2005).
- 20 Martin BD, Ampofo SA, Linhardt RJ and Dordick JS, Biocatalytic synthesis of sugar-containing polyacrylate-based hydrogels. *Macromolecules* **25**:7081–7085 (1992).
- 21 Córdova A, Synthesis of amphiphilic poly (epsilon-caprolactone) macromonomers by lipase catalysis. *Biomacromolecules* **2**:1347 (2001).
- 22 Lu D, Wu Q and Lin X, Chemoenzymatic synthesis of biodegradable poly (1'-O-vinyladipoyl-sucrose). *Chin J Polym Sci* **20**:579–584 (2002).
- 23 Wang Y-W, Wu Q, Chen J and Chen G-Q, Evaluation of three-dimensional scaffolds made of blends of hydroxyapatite and poly(3-hydroxybutyrate-co-3-hydroxyhexanoate) for bone reconstruction. *Biomaterials* **26**:899–904 (2005).
- 24 Tokiwa Y, Fan H, Hiraguri Y, Kurane R, Kitagawa M, Shibatani S and Maekawa Y, Biodegradation of a sugar branched polymer consisting of sugar, fatty acid, and poly (vinyl alcohol). *Macromolecules* **33**:1636–1639 (2000).
- 25 Gross RA, Kumar A and Kalra B, *Enzyme-catalyzed polycondensations*. *USA* **6972315** B2 (2005).
- 26 Gumel AM, Annuar MSM and Heidelberg T, Biosynthesis and characterization of polyhydroxyalkanoates copolymers produced by *Pseudomonas putida* Bet001 isolated from palm oil mill effluent. *PLoS One* **7**:e45214 (2012).
- 27 Teng Y and Xu Y, A modified para-nitrophenyl palmitate assay for lipase synthetic activity determination in organic solvent. *Anal Biochem* **363**:297–299 (2007).
- 28 Massardier-Nageotte V, Pestre C, Cruard-Pradet T and Bayard R, Aerobic and anaerobic biodegradability of polymer films and physico-chemical characterization. *Polym Degradation Stab* **91**:620–627 (2006).
- 29 Wei D, Zhang L-y and Song Q, Studies on a novel carbon source and cosolvent for lipase production by *Candida rugosa*. *J Ind Microbiol Biotechnol* **31**:133–136 (2004).
- 30 Gumel AM, Annuar MSM and Heidelberg T, Effects of carbon substrates on biodegradable polymer composition and stability produced by *Delftia tsuruhatensis* Bet002 isolated from palm oil mill effluent. *Polym Degradation Stab* **97**:1227–1231 (2012).
- 31 Li C, Tan T, Zhang H and Feng W, Analysis of the conformational stability and activity of *Candida antarctica* Lipase B in organic solvents. *J Biol Chem* **285**:28434 (2010).
- 32 Uppenberg J, Hansen MT, Patkar S and Jones TA, The sequence, crystal structure determination and refinement of two crystal forms of lipase B from *Candida antarctica*. *Structure* **2**:293–308 (1994).
- 33 Ottosson J, *Enthalpy and Entropy in Enzyme-catalysis: A Study of Lipase Enantioselectivity*. Royal Institute of Technology, Stockholm, Sweden (2001).
- 34 Barros MT, Petrova KT and Singh RP, Synthesis and biodegradation studies of new copolymers based on sucrose derivatives and styrene. *Eur Polym J* **46**:1151–1157 (2010).
- 35 Antczak T, Patura J, Szczesna-Antczak M, Hiler D and Bielecki S, Sugar ester synthesis by a mycelium-bound *Mucor circinelloides* lipase in a micro-reactor equipped with water activity sensor. *J Mol Catal B: Enzym* **29**:155–161 (2004).
- 36 Cheng Y-C and Tsai S-W, Effects of water activity and alcohol concentration on the kinetic resolution of lipase-catalyzed acyl transfer in organic solvents. *Enzyme Microbiol Technol* **32**:362–368 (2003).
- 37 Gumel AM, Annuar MSM, Heidelberg T and Chisti Y, Thermo-kinetics of lipase-catalyzed synthesis of 6-O-glucosyldecanoate. *Bioresource Technol* **102**:8727–8732 (2011).
- 38 Chamouleau F, Coulon D, Girardin M and Ghouil M, Influence of water activity and water content on sugar esters lipase-catalyzed synthesis in organic media. *J Mol Catal B: Enzym* **11**:949–954 (2001).
- 39 Ha SH, Hiep NM, Lee SH and Koo YM, Optimization of lipase-catalyzed glucose ester synthesis in ionic liquids. *Bioproc Biosyst Eng* **33**:63–70 (2010).
- 40 Mat Radzi S, Basri M, Bakar Salleh A, Ariff A, Mohammad R, Abdul Rahman MB and Abdul Rahman RNZR, High performance enzymatic synthesis of oleyl oleate using immobilised lipase from *Candida antarctica*. *Electron J Biotechnol* **8**:291–298 (2005).
- 41 Lozano P, Villora G, Gomez D, Gayo AB, Sánchez-Conesa JA, Rubio M and Iborra JL, Membrane reactor with immobilized *Candida antarctica* lipase B for ester synthesis in supercritical carbon dioxide. *J Supercrit Fluid* **29**:121–128 (2004).

## CHAPTER 10

# Enzymatic synthesis of 6-*O*-glucosyl-poly(3-hydroxyalkanoate) in organic solvents and their binary mixture

**Gumel A.M.,<sup>1</sup> Annuar M.S.M,<sup>1\*</sup> Heidelberg T.<sup>2</sup>**

<sup>1</sup> Institute of Biological Sciences, <sup>2</sup> Department of Chemistry  
Faculty of Science, University of Malaya, Kuala Lumpur 50603, Malaysia

**Published:** *International Journal of Biological Macromolecules* (2013) **55**: 127– 136

(ISI cited publication: tier 3)

### Statement of contributions of joint Authorship

**Gumel, A.M:** (Candidate)

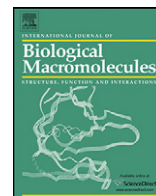
Writing and compilation of manuscript, established methodology, data collection, presentation and analyses. Main author of the manuscript

**Annuar, M.S.M:** (Principal Supervisor)

Supervised and assisted with manuscript compilation, editing and co-author of the manuscript.

**Heidelberg, T:** (Co-Supervisor)

Supervised and assisted with chemical analyses, structure elucidation and co-author of the manuscript



# Enzymatic synthesis of 6-O-glucosyl-poly(3-hydroxyalkanoate) in organic solvents and their binary mixture

A.M. Gumel<sup>a</sup>, M.S.M. Annuar<sup>a,\*</sup>, T. Heidelberg<sup>b</sup>

<sup>a</sup> Institute of Biological Sciences, Faculty of Science, University of Malaya, 50603 Kuala Lumpur, Malaysia

<sup>b</sup> Department of Chemistry, Faculty of Science, University of Malaya, 50603 Kuala Lumpur, Malaysia

## ARTICLE INFO

### Article history:

Received 17 October 2012

Received in revised form

28 November 2012

Accepted 16 December 2012

Available online xxx

### Keywords:

Biopolymer

*Thermomyces lanuginosus*

Lipase

Polyhydroxyalkanoates

Phospholipase

Sugar-ester

## ABSTRACT

The effects of organic solvents and their binary mixture in the glucose functionalization of bacterial poly-3-hydroxyalkanoates catalyzed by Lecitase<sup>TM</sup> Ultra were studied. Equal volume binary mixture of DMSO and chloroform with moderate polarity was more effective for the enzyme catalyzed synthesis of the carbohydrate polymer at  $\approx 38.2 (\pm 0.8)\%$  reactant conversion as compared to the mono-phasic and other binary solvents studied. The apparent reaction rate constant as a function of medium water activity ( $a_w$ ) was observed to increase with increasing solvent polarity, with optimum  $a_w$  of 0.2, 0.4 and 0.7 ( $\pm 0.1$ ) observed in hydrophilic DMSO, binary mixture DMSO:isooctane and hydrophobic isooctane, respectively. Molecular sieve loading between 13 to 15 g L<sup>-1</sup> ( $\pm 0.2$ ) and reaction temperature between 40 to 50 °C were found optimal. Functionalized PHA polymer showed potential characteristics and biodegradability.

© 2012 Elsevier B.V. All rights reserved.

## 1. Introduction

Biodegradable polymers such as polyhydroxyalkanoates (PHA) are an important class of polymeric biomaterials with diverse industrial and biomedical applications as a result of their biodegradability, compatibility, compostability and versatile structures. However, despite widely used in biomedical fields, their slow degradability and resorbability within the extra cellular matrixes restrict their applications as short-time drug delivery devices and nano-DNA carriers [1]. Enzymatic catalyzed esterification using glycosylation to functionalize the polymer is one of the strategies to address this issue [1]. Following the functionalization, not only the hydrophilicity of the glyco-polymer ester is improved but it also impart specific properties for niche applications such as antimicrobial activities [2–4], lectin interaction [5], galactosyl transferase inhibition [6], anti-carcinogenic activities [7], water repelling and oil absorption [8] traits.

Since aqueous solution is a natural reaction milieu for almost all enzymes, there is a tendency for enzyme hydration layer that serves as structure lubricant to be stripped out when organic solvents are used as reaction medium, thus leaving a rigid protein behind with lowered catalytic activity [9]. On the other hand, the use of such solvents as reaction medium could also be beneficial.

Some of the reported advantages are: (i) an increase in solubility of substrates that are poorly soluble or unstable in water; (ii) minimized water dependent side-reactions (iii) improved enzymatic stability as a result of low water activity and (iv) thermodynamic stability of ester bond synthesis over hydrolysis [2,10]. There are instances where the hydrophobic organic solvents even afforded higher enzymatic activity than their hydrophilic counterparts [11]. Hence, in the attempt to balance these contradictions, the use of micro-aqueous medium for enzyme catalysis is adopted in synthetic biotechnology. In fact, it is possible to influence the product formation, substrate specificity, the regio- and enantio-selectivity of a given enzyme by manipulating the solvent(s) used as reaction media [12,13]. In PHA functionalization with carbohydrate moiety, a solvent applied as reaction medium must be able to dissolve sufficient amount of reactants for the reaction to be feasible i.e. the hydrophilic sugar moiety and the hydrophobic polymer compound. However, both the sugar and the polymer exhibit markedly different solubilities in micro-aqueous solvents, which in turn made the esterification reaction complicated. In view of all the reported effects above and the solvation requirement for the current study, it is postulated that the compromise between reactants solvation, enzymatic activity and stability could be made via rational reaction medium manipulation.

Most commercial lipase (EC 3.1.1.3) preparation, which is a triacylglycerol hydrolase have been used to catalyze the synthesis of ester bonds in micro-aqueous media [14,15]. Among these lipases are the commercially available phospholipase preparations that are

\* Corresponding author. Tel.: +60 379674003; fax: +60 379677182.

E-mail address: [suffian.annuar@um.edu.my](mailto:suffian.annuar@um.edu.my) (M.S.M. Annuar).

known to exhibit hydrolytic activities [16]. On the other hand, the potential of these enzymes are yet to be explored in the esterification of carbohydrate polymers in micro-aqueous catalysis; in particular Lecitase™ Ultra (EC 3.1.1.32), a protein-engineered phospholipase A<sub>1</sub> having both engineered phosphatase stability and lipase activity produced by *Thermomyces lanuginosus*.

The chemo-enzymatic functionalization of polymers such as polyvinyl [17,18], polyacrylate [19] and polycaprolactone [20,21] using sugars has been reported. However, these polymers were synthesized bearing di-carboxylic acid spacer arms, which may contributed to the increase in hydrophobicity of the polymer instead of its hydrophilicity. In most cases, the functionalized polymer obtained through this approach has toxic chemical impurities, which makes it less attractive for biomedical applications.

Literatures reporting on functionalization of bacterial PHA with carbohydrates solely via enzymatic route are very scarce [22] particularly on the solvent effects toward single-step enzymatic functionalization of medium-chain-length PHA (mcl-PHA). In this work, we reported the effects of different organic solvents viz. chloroform, dichloromethane, DMSO and isooctane along with their binary mixtures and solvent's water activity influence on the Lecitase™ Ultra catalyzed functionalization of medium-chain-length PHA with glucose. In addition, the need for chemo-synthetic steps was bypassed by using H<sub>2</sub>O<sub>2</sub> as micro-initiator to effectively synthesize the carbohydrate polymer using the enzyme. The characterization of the functionalized mcl-PHA and its biodegradability studies were also carried out.

## 2. Materials and methods

### 2.1. Materials

Lecitase™ Ultra from *Thermomyces lanuginosus* (Sigma–Aldrich; L3295), *p*-nitrophenyl palmitate (Sigma–Aldrich; N2752), dimethyl sulfoxide (Sigma–Aldrich; D8418), molecular sieve 4 Å (Sigma–Aldrich; 334308), NaCl crystal window (Sigma–Aldrich; Z267724), D-glucose (Merck; 137048), hydrogen peroxide (Merck; 822287), methanol (Merck; 106012), chloroform (Merck; 102395), dichloromethane (DCM) (Merck; 106051), dimethylsulfoxide (DMSO) (Merck; 102931), acetone (Merck; 100299), isooctane (Merck; 104715), *N*-(trimethylsilyl) imidazole (Merck; 818204). All chemicals used were of analytical grade.

mcl-PHA with monomeric composition of C<sub>6:0</sub> to C<sub>14:0</sub> was extracted from *Pseudomonas putida* Bet001 as producer microorganism grown in hexadecanoic acid as sole carbon and energy source [23].

### 2.2. Methods

#### 2.2.1. Enzyme assay

The enzyme activity was measured according to procedure described earlier [24]. Lecitase™ Ultra (200 mg) was added to a vial containing 10 mL of a 10 mM *p*-nitrophenyl palmitate solution in *n*-hexane. To this mixture, 60 µL of 1 M absolute ethanol was added. The resulting slurry was incubated at 30 °C, 200 rpm for a period of 20 min. Aliquots (30 µL each) of the reaction mixture were withdrawn at intervals and quenched by mixing with 1 mL of 0.1 M NaOH in a quartz cuvette. The 4-nitrophenol liberated by the reaction was measured at 412 nm (UV–Vis spectrophotometer V-630; Jasco, Japan) against distilled water as blank. The enzyme activity was calculated as the slope of a plot of 4-nitrophenol released versus time.

**2.2.1.1. Enzymatic esterification.** All reactions were performed in triplicate. A batch of 10 mL solution of different organic solvents (chloroform; dichloromethane; DMSO; isooctane) and their binary

mixtures (DMSO:chloroform and isooctane:chloroform) containing glucose (89 mM) and 0.08 mg mcl-PHA were mixed into 20 mL capped reaction vials. DMSO:isooctane mixture resulted in an immiscible solution as compared to the other mixtures tested (isooctane is the most hydrophobic solvent followed sequentially by chloroform and DMSO). To this mixture, 200 mg enzyme, 30 mg molecular sieve 4 Å and 10 µL H<sub>2</sub>O<sub>2</sub> (micro-initiator) was added. The initial water activity (*a<sub>w</sub>*) of the mixture was recorded using Rotronic hygroPalm water activity meter (HP23-AW; [www.rottronic.co.uk](http://www.rottronic.co.uk)). The reaction was then allowed to proceed for a total period of 24 h at 30 °C, 200 rpm, while assessing the water activity at specified intervals. All reactions were carried out according to aforementioned procedure except stated otherwise.

#### 2.2.2. Residual sugar quantification

At specific interval, the residual carbohydrate moiety was quantified by withdrawing aliquot samples (20 µL) of the reaction mixture and mixed with 5 µL absolute ethanol to stop the reaction. This mixture was then diluted with 1.0 mL chloroform and thereafter derivatized by adding 5 µL *N*-(trimethylsilyl) imidazole (TMSI) followed by sonication at 37 kHz, 1.9 W and 30 °C for 2 min and immediately filtered into GC vials. The residual glucose was then measured on Agilent triple quadrupole 7000B instrument (Agilent, USA) equipped with GCMSMS triple axis detector carrying Agilent HP-5 ms column (30 m long × 0.25 mm internal diameter × 0.25 µm film thickness). A sample (2 µL) was automatically injected into the GCMSMS at a split ratio of 1:10. The injection temperature was 280 °C. The column oven temperature ramping was as follows: 110 °C for 1 min then increased to 200 °C at 20 °C min<sup>-1</sup>; held at 200 °C for 2 min then increased to 280 °C at 20 °C min<sup>-1</sup>; then held at 280 °C for 5 min. Helium at 0.76 bar and 14 mL min<sup>-1</sup> was used as the carrier gas. Mass spectra were acquired at 1250 scan speed using electron impact energy of 70 eV at 230 °C ion-source and 250 °C interface temperatures. The data obtained per each reaction time was used in the determination of the residual glucose quantity by comparing with the calibration plot prepared by analyzing different concentrations of glucose standard solutions in DMSO (Supplementary Fig. S1 and Table S1). The enzymatic reaction rate (M s<sup>-1</sup>) was calculated as the slope of converted glucose concentration plot versus time.

#### 2.2.3. Product extraction

At the end of the reaction, the sugar functionalized polymer i.e. 6-*O*-glucosyl-poly(3-hydroxyalkanoates) was extracted by diluting the reaction mixture with 20 mL of dichloromethane, followed by filtration using glass-fritted Buchner filter funnel to separate the immobilized enzyme and molecular sieves. The filtrate was then concentrated under reduced pressure to about 3 mL at 40 °C. The functionalized polymer was precipitated out from the filtrate by adding the concentrate into 10 mL of cold acetone (4 °C). The solvent was then decanted and the precipitate was re-purified by subjecting it to three-cycle precipitation consecutively. At each stage, the functionalized polymer was dissolved in dichloromethane (3 mL) then added to cold acetone (10 mL, 4 °C) and the white precipitate was recovered. The final extracted product was dried to a constant weight at 30 °C under vacuum. A portion of the dried sample was subsequently subjected to further authentication analyses.

#### 2.2.4. Product authentication

Perkin-Elmer FTIR RX 1 spectrometer (Perkin-Elmer Inc., Wellesley, MA, USA) was used to record FTIR-ATR spectra of the 6-*O*-glucosyl-poly(3-hydroxyalkanoates) as previously reported [25]. Proton NMR spectra were recorded on a JEOL JNM-GSX 270 FT-NMR



(JOEL Ltd, Tokyo, Japan) machine at 250 MHz according to reported literature [25].

Differential scanning calorimetric (DSC) analysis of the functionalized polymer was performed on Perkin-Elmer Diamond DSC instrument using HyperDSC® technique (Perkin-Elmer Inc., Wellesley, MA, USA). Scans over the temperature range of  $-50^{\circ}\text{C}$  to  $180^{\circ}\text{C}$  at heating and cooling rate of  $10^{\circ}\text{C min}^{-1}$  in nitrogen flow rate of  $50\text{ mL min}^{-1}$  was carried out.

Thermal gravimetric analyses were performed on a Perkin-Elmer TGA4000 instrument (Perkin-Elmer Inc., Wellesley, MA, USA). The samples were heated from  $50^{\circ}\text{C}$  to  $800^{\circ}\text{C}$  at a rate of  $10^{\circ}\text{C min}^{-1}$  in nitrogen flow rate of  $20\text{ mL min}^{-1}$ .

### 2.2.5. Gel permeation chromatography (GPC)

For non-functionalized PHA, gel permeation chromatography was carried out using Waters 600 (Waters Corp, Milford, MA, USA) GPC system equipped with Waters refractive index detector (model 2414) having the following gel columns (7.8 mm internal diameter; 300 mm) in series: HR1, HR2, HR5E and HR5E Waters Styrogel HR-THF. Monodisperse polystyrene standards of different molecular weights ( $3.72 \times 10^2$ ,  $2.63 \times 10^3$ ,  $9.10 \times 10^3$ ,  $3.79 \times 10^4$ ,  $3.55 \times 10^5$ ,  $7.06 \times 10^5$ ,  $3.84 \times 10^6$  and  $6.77 \times 10^6$  Da) were used for the calibration curve. The PHA samples were dissolved in tetrahydrofuran (THF) at a concentration of  $2.0\text{ mg mL}^{-1}$ , and then filtered through a  $0.22\text{ }\mu\text{m}$  PTFE filter.  $100\text{ }\mu\text{L}$  aliquot sample was injected at  $40^{\circ}\text{C}$ . THF was used as a mobile phase at a flow rate of  $1.0\text{ mL min}^{-1}$ .

On the other hand, the  $M_n$  of the 6-O-glucosyl-poly(3-hydroxyalkanoates) sample was calculated based on the integral of the observed proton NMR spectra.

### 2.2.6. Biodegradability test

The qualitative biodegradability test based on compostability was observed using 3D Alicona InfiniteFocus® optical surface texture analyzer (Alicona; Austria), after the samples were composted in simulated environment using about 300 g of 70% ( $\pm 3\%$ ) humid garden soil in 50 ml sample bottle. Replicated solvent-casted films ( $0.5\text{ cm} \times 1\text{ cm}$ ) of both the 6-O-glucosyl-poly(3-hydroxyalkanoates) and the control (poly-3-hydroxyalkanoates) were buried 4 cm deep in separate sample bottles and incubated at  $30 (\pm 2)^{\circ}\text{C}$  for a period of 8 weeks. At regular intervals, the surface topological analyses of both polymers were performed at 360 to  $450\text{ }\mu\text{m}$  view using 3D Alicona InfiniteFocus® optical microscope.

### 2.3. Calculations

Enzymatic apparent catalytic reaction rate ( $\nu^{\text{app}}$ ;  $\text{M s}^{-1}$ ) was calculated using Eq. (1)

$$\nu^{\text{app}} = \frac{\Delta[S]}{\Delta t} \quad (1)$$

where  $[S]$  is the converted glucose molar concentration at time  $t$ .

The apparent rate constant ( $k_1^{\text{app}}$ ;  $\text{s}^{-1}$ ) is given by Eq. (2)

$$k_1^{\text{app}} = \frac{-\ln(1 - (S_t - S_0))}{t} \quad (2)$$

where  $S_0$  and  $S_t$  are initial and converted reactant concentrations, respectively.

The apparent diffusion rate constant ( $k_d^{\text{app}}$ ;  $\text{L mol}^{-1} \text{s}^{-1}$ ) is given by Eq. (3) and it provides a measure of whether the reaction is likely to be diffusion limited ( $k_1^{\text{app}} \ll k_d^{\text{app}}$ ) or otherwise.

$$k_d^{\text{app}} = \frac{8RT}{3\eta_s} \quad (3)$$

where  $R$  is molar gas constant ( $8.314\text{ J mol}^{-1} \text{K}^{-1}$ ),  $T$  is temperature (K) and  $\eta_s$  ( $\text{kg m}^{-1} \text{s}^{-1}$ ) is the viscosity of the

reaction solvent that was measured at  $25 (\pm 1)^{\circ}\text{C}$  using Cannon–Fenske Opaque (Reverse-Flow) viscometer No. 400 D283 ([www.canoninstrument.com](http://www.canoninstrument.com)) and calculated using Eq. (4) as reported in literature [12].

$$\eta_s = \frac{\rho_s t_s}{\rho_w t_w} \cdot \eta_w \quad (4)$$

where  $\rho_s$  and  $\rho_w$  are the respective densities of the solvent and water that were measured at  $25 (\pm 1)^{\circ}\text{C}$  using Anton–Paar DMA 35 Density Meter ([www.anton-paar.com](http://www.anton-paar.com));  $t_s$  and  $t_w$  are the time taken by the solvent and water to drop under the influence of gravity to a specified level in the viscometer; and  $\eta_w$  is the viscosity of water at  $25 (\pm 1)^{\circ}\text{C}$ .

The binary solvent mixture viscosity ( $\eta_{\text{mix}}$ ) was also calculated using Jouyban–Acree model [26] as shown in Eq (5)

$$\ln \eta_{\text{mix}} = x_s \ln \eta_{s,T} + x_i \ln \eta_{i,T} + A_0 \left[ \frac{(x_s x_i)}{T} \right] + A_1 \left[ \frac{(x_s x_i (x_s - x_i))}{T} \right] + A_2 \left[ \frac{(x_s x_i (x_s - x_i)^2)}{T} \right] \quad (5)$$

where  $s$  and  $i$  stand for solvent and co-solvent, respectively,  $x$  denotes their respective mole fractions and  $T$  stands for temperature.  $A_0$ ,  $A_1$  and  $A_2$  are model constants.

The polymeric apparent degree of crystallinity ( $X_c^{\text{ap}}$ ) is given by Eq. (6)

$$X_c^{\text{ap}} = \frac{\Delta H}{\Delta H^*} \quad (6)$$

where  $\Delta H$  is the DSC endothermic melting enthalpy of the poly(glucosyl-3-hydroxyalkanoates), assuming  $142\text{ J g}^{-1}$  as the endothermic melting enthalpy ( $\Delta H^*$ ) of standard PHB as cited in literature [25].

Polydispersity index (PDI) of the polymer was calculated using Eq. (7):

$$\text{PDI} = \frac{M_w}{M_n} \quad (7)$$

where  $M_w$  is weight-averaged molecular weight and  $M_n$  is number-averaged molecular weight.

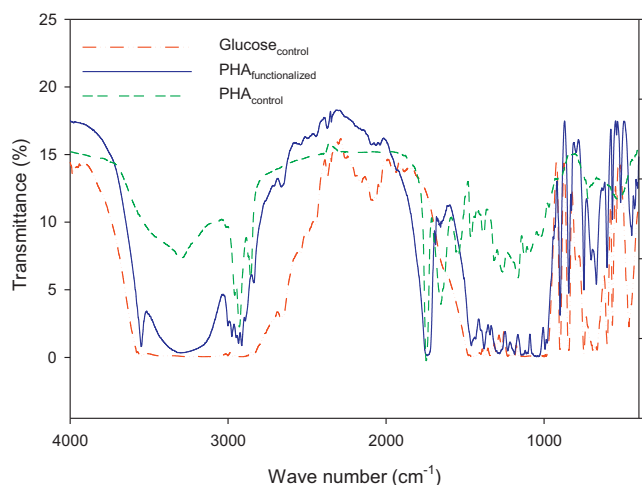
The solvent mixture  $\log P_{\text{mix}}$  was calculated according to reported literature [27] as shown by Eq. (8)

$$\log P_{\text{mix}} = (x_s \cdot \log P_s) + (x_i \cdot \log P_i) \quad (8)$$

## 3. Results and discussion

### 3.1. Characterization of glucose-based functionalized mcl-PHA

The effects of the reaction media in the synthesis of glucose-based functionalized mcl-PHA was studied using Lecitase™ Ultra as a catalyst in a micro-aqueous system. In this process, a glucose conversion yield as high as 38.2% ( $\pm 0.8\%$ ) was observed in DMSO:chloroform (1:1, v/v) within 24 h. The solvent-casted film of the extracted polymeric product (white amorphous film) was subjected to analytical authentication. FTIR–ATR (Fig. 1): wave number 3339 ( $\nu_{\text{O-H}}$ ), 2948 ( $\nu_{\text{CH}_2\text{-CH}_2\text{-}}$ ), 2830 ( $\nu_{\text{CH}_2\text{-CH}_3}$ ), 1735 ( $\nu_{\text{C=O}}$ ), 1292 ( $\nu_{\text{C-O-C}}$ ).  $^1\text{H}$  NMR (Fig. 2) relative to tetramethylsilane (TMS):  $\delta$  5.55 (1H,  $\text{C}_{1\text{-H}}$  of glucose), 4.29 (1H,  $\text{C}_{2\text{-H}}$  of glucose), 4.29, 4.10 (2H,  $J_{\text{C6-H}\alpha,\beta}$  of glucose), 4.26 (1H,  $\text{C}_{5\text{-H}}$  of glucose), 3.88 (1H,  $\text{C}_{\beta\text{-H}}$  of PHA), 3.81 (1H,  $\text{C}_{1\text{-OH}}$  of glucose), 3.78 (multiple H,  $\text{C}_2$ ,  $\text{C}_{3\text{-OH}}$ ,  $\text{C}_{4\text{-OH}}$  of glucose and terminal PHA-OH), 3.68 (1H,  $\text{C}_{2\text{-H}}$ ,  $\text{C}_{3\text{-H}}$  of glucose), 3.63 (1H,  $\text{C}_{4\text{-H}}$  of glucose), 2.21, 2.02 (2H,  $J_{\text{C}\alpha\text{-H}\alpha,\beta}$  of PHA), 1.45–1.29 ( $\text{CH}_2$  of PHA side chain), 0.86, 0.52 (terminal  $\text{CH}_3$  of PHA side chain).



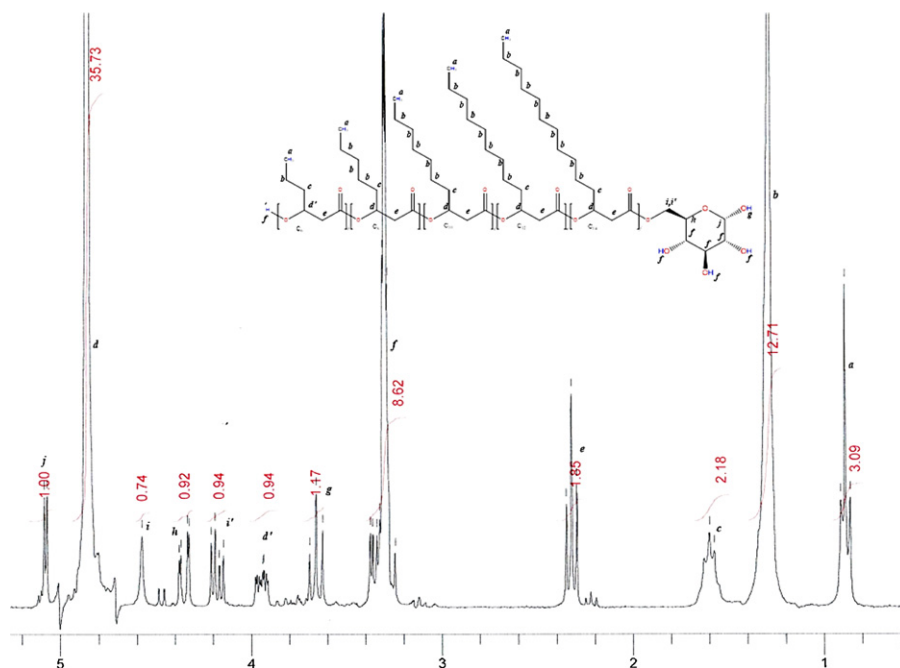
**Fig. 1.** Samples FTIR spectrum of the control PHA (non-functionalized), glucose standard and glucose-based functionalized PHA.

FTIR spectra of the control PHA and the glucose functionalized PHA were compared (Fig. 1). The spectrum of the 6-O-glucosyl-poly(3-hydroxyalkanoates) showed a very broad absorption at wave number ( $\nu$ )  $3339\text{ cm}^{-1}$  corresponding to the increase in  $-\text{OH}$  groups contributed by those present in glucose and the functionalized polymer. The persistence of ester-bond absorption at  $1735\text{ cm}^{-1}$  can only be observed in control PHA and the functionalized PHA spectra, while totally absent in the glucose FTIR spectrum. This revealed a successful functionalization of the PHA with the glucose moiety. This observation was found to be consistent with the  $^1\text{H}$  NMR spectrum of the product (Fig. 2), which revealed a series of chemical shifts at  $\delta$  5.55–3.63 ppm, signifying the presence of sugar in the product. These observations were found to be in good agreement with reported literature on carbohydrate polymers characterization ([8,28]. Based on the previously determined chemical structure of medium-chain-length poly(3-hydroxyalkanoates) obtained from *P. putida* Bet011 [23], the functionalized polymer is proposed to possess chemical structure as shown in Fig. 3.

In contrast to control mcl-PHA ( $T_m$   $43^\circ\text{C}$ ;  $T_d$   $298.9^\circ\text{C}$ ,  $X_c^{\text{ap}}$  0.78), the thermal analyses of the 6-O-glucosyl-poly(3-hydroxyalkanoates) was observed to have low degree of crystallinity ( $X_c^{\text{ap}}$  0.32), two peak endothermic melting temperature ( $T_m$ ) of  $59.2$  and  $151^\circ\text{C}$  ( $\pm 0.2^\circ\text{C}$ ) corresponding to the distinct melting of the PHA and the glucose moiety respectively. The thermogravimetric analysis revealed a two-step degradation temperature  $T_d$  (Fig. 4) at  $240.7$  and  $306.4^\circ\text{C}$  ( $\pm 0.2^\circ\text{C}$ ), signifying the decomposition of both the hydrophilic glucose moiety and the hydrophobic mcl-PHA backbone, respectively. Furthermore, the molecular weight analysis of the functionalized polymer revealed a general decrease in average molecular weight ( $M_w$   $15.2 \pm 0.3\text{ kDa}$ ) with increasing number-averaged molecular weight ( $M_n$   $10.0 \pm 0.5\text{ kDa}$ ) and PDI 1.5 as compared to the non-functionalized PHA ( $M_w$   $55.7\text{ kDa}$ ,  $M_n$   $13.6\text{ kDa}$ , PDI 4.1). This reduction in  $M_w$  and the increase in the  $M_n$  of the 6-O-glucosyl-poly(3-hydroxyalkanoate) could be attributed to the possible enzymatic hydrolysis of the polymeric backbone by random chain scission, which explains the increase in  $M_n$ . The observed increase in  $T_m$  could be due to the increased polarity of the polymer as a result of sugar moiety hydrogen bonding causing strong intermolecular attraction, thus at the same time increasing the amount of thermal energy required to break the bond. This observation is further supported by the differences in the  $T_d$   $298.9^\circ\text{C}$  for non-functionalized mcl-PHA and  $306.4^\circ\text{C}$  for functionalized mcl-PHA.

### 3.2. Biodegradability of the 6-O-glucosyl-poly(3-hydroxyalkanoates)

The biodegradability of polymeric materials is reported to rely on several polymeric properties including physical, chemical, molecular structural organization and crystallinity of the polymer [29]. Reaction conditions like reactor-vessel's volume and shape, temperature, pH, aerobic or anaerobic, mixing, polymeric polarity and duration were among the reported parameters to affect the rate of degradation process [29]. Undoubtedly, the presence of sugar moiety in the polymer is considered to attract and favor microbial growth on the sample due to increase water absorption [18].



**Fig. 2.**  $^1\text{H}$  NMR spectrum of glucose based functionalized PHA.

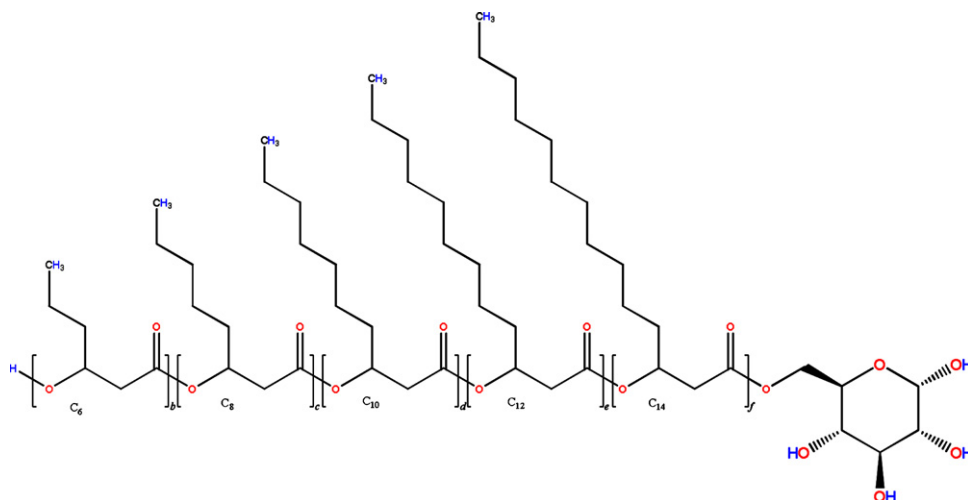


Fig. 3. Structure of 6-O-glucosyl-poly(3-hydroxyalkanoates).

Hence, it is not surprising to observe an increase in surface degradation of the 6-O-glucosyl-poly(3-hydroxyalkanoates) when solid-phase surface texture analysis was performed following simulated composting conditions in the laboratory (Fig. 5). Relative to the initial PHA film in both samples (Fig. 5 ax, bx), the non-functionalized PHA (Fig. 5 ay) was observed to have less surface degradation after three weeks of composting as compared to the functionalized ones which showed more degraded surface (Fig. 5 by). In both samples, maximum surface degradation was observed after eight weeks of composting with 6-O-glucosyl-poly(3-hydroxyalkanoates) (Fig. 5 bz) showing relatively more surface degradation than the non-functionalized PHA (Fig. 5 az). This could probably be due to the presence of glucose moiety that influences the hydrophilicity of the functionalized mcl-PHA. In general, the degradation in both samples was localized to specific areas. This could be the amorphous phase of the film, which is more readily degraded by the composting microorganisms in relation to the more organized crystalline phase [29].

### 3.3. Effect of solvents and co-solvents Log *P* on reaction parameters

The influence of organic solvents in enzyme catalyzed esterification and esterification has been studied extensively and interpreted in various ways [12,30–32]. Several research has attempted to

correlate different solvent parameters such as hydrophobicity (log *P*), polarity (dielectric constant;  $\epsilon$ ), electron acceptance index and solubility (Hildebrand parameter;  $\delta$ ), with the corresponding enzyme catalytic activity and product yield [33,34]. However, most researchers reported no significant correlation between solvent's Hildebrand parameter, dielectric constant and the enzymatic activity; as such the use of these parameters to correlate the enzymatic activity is deemed to be less informative [2,33,35]. Nevertheless, the differences in solvent log *P* have been used by some researchers to help explain the solvent's effect toward the catalytic activity and specificity of enzymes [34]. In lipase mediated synthesis, high enzymatic activity is observed in low polarity solvents (log *P*  $\geq 4$ ) [35]. These types of solvents were proposed to influence the enzymatic activity by modifying the enzyme active site polarity, which may contribute to the stabilization of the charge transition state during the reaction [36]. However, other researchers proposed that the possible reason for the solvent effect in non-aqueous media arise as a result of differences in solvent solvation energy, which causes variations in the total free energy [37].

In this study, we observed that the solvent log *P* value appears to be generally correlated to the observed lipase activity (Table 1), but this could also be attributed to the substrate solvation as well as enzymatic stability. Strongly hydrophobic solvent is not always a good choice for lipase mediated syntheses of sugar based polymers because the hydrophilic glucose tend to be poorly soluble in them, and this adversely affect the product yield of the reaction [38]. This is also evident from Table 1, where in isoctane despite the observed higher apparent reaction rate ( $2.83 \times 10^{-4} \text{ M s}^{-1}$ ) and polymer molecular weight propagation ( $M_n$  10.2 kDa) that could be due to the reported enzymatic stability in the highly hydrophobic solvent [38], a low reactant conversion (15.4%) was observed, which was attributed to the low glucose solvation in this solvent. This is also supported by the low apparent reaction rate constant ( $1.24 \times 10^{-6} \text{ s}^{-1}$ ) determined. In contrast, chloroform and DCM with their moderate polarity, were observed to yield apparent reaction rates of  $1.69 \times 10^{-4}$  and  $1.29 \times 10^{-4} \text{ M s}^{-1}$  with moderate molecular weight propagation (5.2–8.9 kDa). The reactant conversion in these solvents (Table 1) was no higher than observed in DMSO (19.1%) and with the corresponding high apparent reaction rate constant ( $2.88 \times 10^{-6} \text{ s}^{-1}$ ). Despite being highly polar, DMSO expressed lowest apparent reaction rate ( $0.19 \times 10^{-4} \text{ M s}^{-1}$ ) and poor molecular weight propagation (1.7 kDa). The observed high conversion in DMSO could be due to the increase in glucose solvation making it more available to the enzyme active site. On the other hand, the observed low reaction rate could be due to the

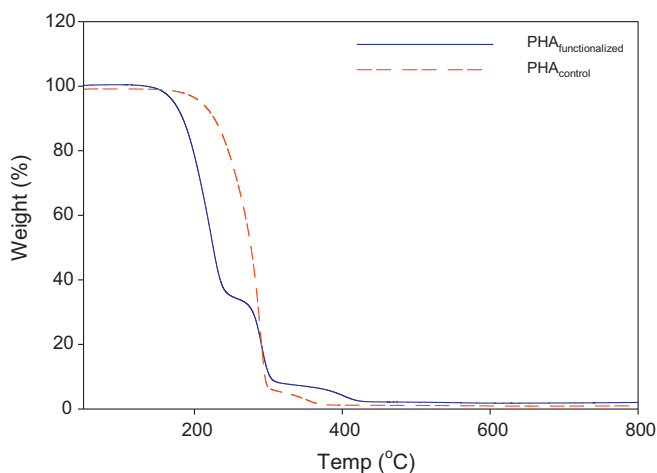
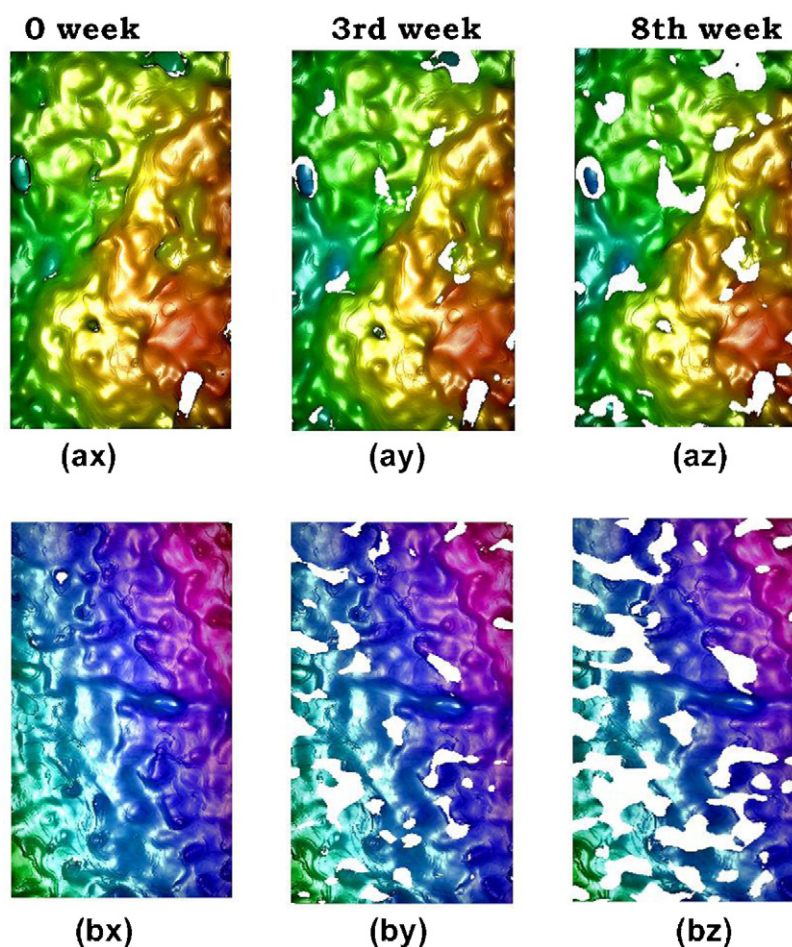


Fig. 4. TGA thermogram of the functionalized PHA and the control PHA.



**Fig. 5.** Optical 3D Alicona InfiniteFocus® micrograph comparing the surface degradation in the simulated composting of control mcl-PHA (ax, ay and az) and the functionalized mcl-PHA (bx, by and bz) recorded at 25 °C, 360 to 450  $\mu\text{m}$  view.

hydrophilic solvents tend to strip some of the enzyme hydration layer that serves as protein structure lubricant inducing possible destruction of hydrogen bond network, which in turn influencing the solvent interaction with protein surface and subsequently affected protein folding which lowers the catalytic activity [9,38]. In contrast to the single solvent system, it was further observed that changing the solvent polarity through blending with other solvent influenced the reaction rate. For a highly hydrophobic isooctane, blending it with moderately polar chloroform changed the log  $P$

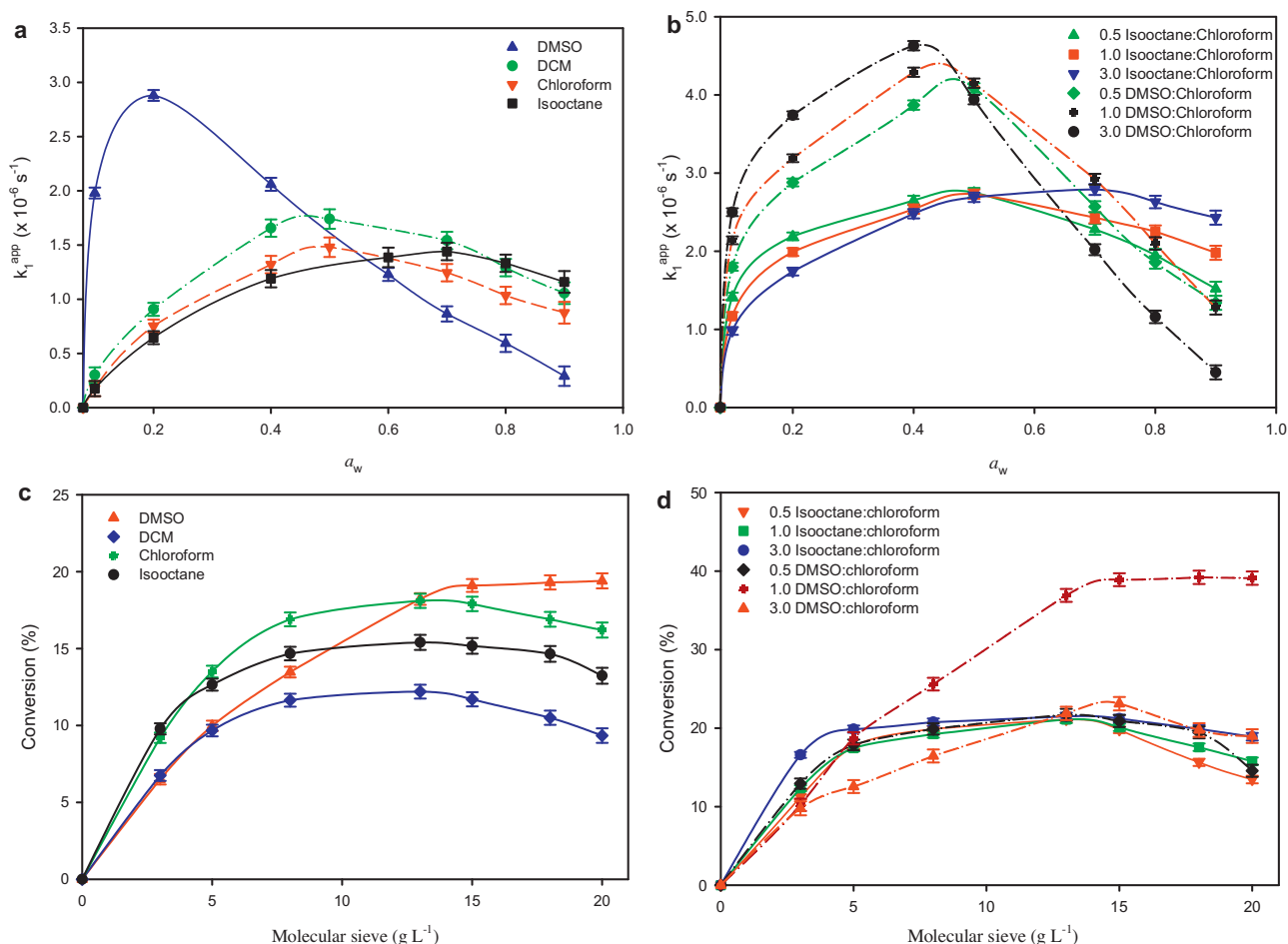
value from 1.99 to 2.05 (isooctane:chloroform v/v ratio of 0.5–3.0) corresponding to apparent reaction rate  $1.72 \times 10^{-4}$ – $1.81 \times 10^{-4} \text{ M s}^{-1}$ . This was observed to cause an increased in both the conversion (about 21%) and the apparent reaction rate constant ( $\approx 2.7 \times 10^{-6} \text{ s}^{-1}$ ) as compared to the pure solvents themselves. Furthermore, the molecular weight propagation was also observed to increase with increasing solvent hydrophobicity. In the binary mixture of highly hydrophilic DMSO and moderately polar chloroform, both hydrophobic polymer and the hydrophilic glucose

**Table 1**

Solvents and co-solvents log  $P$  as a function of reaction parameters (max. standard error  $\pm 5\%$ ).

| Solvents                   | Log $P$ | $\nu^{\text{app}} (\times 10^{-4} \text{ M s}^{-1})$ | $k_1^{\text{app}} (\times 10^{-6} \text{ s}^{-1})$ | $k_d^{\text{app}} (\text{L mol}^{-1} \text{ s}^{-1})$ | $\eta_s (\times 10^3 \text{ N m s}^{-2})$   |                        | Conversion (%) | $M_n$ (kDa) | PDI |
|----------------------------|---------|--|--|---|---|------------------------|----------------|-------------|-----|
|                            |         |  |  |   | Viscometer<br>( $25 \pm 1^\circ \text{C}$ ) | Jouyban–Acree<br>model |                |             |     |
| DMSO                       | −1.41   | 0.19   | 2.88   | 3.67  | 1.83  | –                      | 19.1           | 1.7         | 1.1 |
| DCM                        | 1.41    | 1.29   | 1.74   | 17.0  | 0.39  | –                      | 12.2           | 8.9         | 1.2 |
| Chloroform                 | 1.94    | 1.69   | 1.48   | 12.8  | 0.52  | –                      | 18.1           | 5.2         | 1.1 |
| Isooctane                  | 4.37    | 2.83   | 1.24   | 14.1  | 0.47  | –                      | 15.4           | 10.2        | 1.1 |
| Isooctane:chloroform ratio |         |  |  |   |   |                        |                |             |     |
| 0.5                        | 1.99    | 1.72   | 2.73   | 13.0  | 0.51  | 0.50                   | 21.1           | 12.1        | 1.2 |
| 1.0                        | 1.95    | 1.71   | 2.75   | 13.2  | 0.51  | 0.48                   | 21.1           | 11.3        | 1.1 |
| 2.0                        | 2.04    | 1.81   | 2.79   | 13.4  | 0.50  | 0.50                   | 21.4           | 15.6        | 1.2 |
| 3.0                        | 2.05    | 1.81   | 2.79   | 13.6  | 0.49  | 0.46                   | 21.5           | 16.8        | 1.2 |
| DMSO:chloroform ratio      |         |  |  |   |   |                        |                |             |     |
| 0.5                        | 1.79    | 1.46   | 4.29   | 8.11  | 0.83  | 0.78                   | 21.7           | 9.2         | 1.1 |
| 1.0                        | 2.89    | 1.56   | 4.29   | 6.55  | 1.02  | 0.98                   | 38.2           | 11.6        | 1.3 |
| 2.0                        | 2.53    | 1.38   | 4.63   | 5.35  | 1.25  | 1.10                   | 33.3           | 10.7        | 1.2 |
| 3.0                        | 1.58    | 1.32   | 4.63   | 4.85  | 1.38  | 1.21                   | 23.1           | 9.9         | 1.1 |





**Fig. 6.** Water activity ( $a_w$ ) as a function of reaction rate constant in (a) mono-phasic solvent; (b) binary solvent mixture and molecular sieve loading as a function of glucose conversion in (c) monophasic solvent; (d) binary solvent mixture. Synthesis at 45 °C and 200 rpm using Lecitase™ Ultra 200 mg for 24 h.

would be expected to have appreciable solvation in this blended system concomitantly resulted in increased conversion and apparent reaction rate constant, which supported this proposition. With highest conversion (38.2%) been observed at DMSO:chloroform of 1 (v/v), increasing the DMSO ratio beyond this value increases the systems polarity which resulted in the corresponding decrease in the apparent reaction rate, reactant conversion as well as molecular weight propagation. On the other hand, the apparent reaction rate constant value was not significantly affected. In general, under the tested experimental conditions in all the solvent systems,  $k_1^{app}$  values were observed to be far lower than  $k_d^{app}$  (Table 1), thus showing that the reaction systems studied were not diffusion limited.

It is noted that in terms decreasing order of viscosity DMSO > chloroform > isooctane > DCM (Table 1). For the binary mixture of isooctane and chloroform, the viscosity at 25 ( $\pm 1$ ) °C were observed to be relatively constant for all the blend ratios tested. On the other hand, for DMSO: chloroform binary mixture, there was a steady increase in viscosity value of the blend at 25 ( $\pm 1$ ) °C with the increase in blending ratio (Table 1). Interestingly, the Jouyban-Acree model (Eq. (5)) was able to predict satisfactorily the viscosities of all the binary mixtures studied here (Table 1), with the provision that the model constants ( $A_0$ ,  $A_1$  and  $A_2$ ) were set to 1.

### 3.4. Effect of water activity ( $a_w$ ) on substrate conversion and reaction rate in solvents and co-solvents mixtures

In lipase-catalyzed synthesis of carbohydrate polymers, the activity of water ( $a_w$ ) in the micro-aqueous reaction medium is

an important consideration [39]. In this kind of reaction where polyesters and sugar (or alcohol) are involved, water is one of the reaction byproducts. As a nucleophile for the hydrolysis reaction, water is also a competitive inhibitor of the lipase-catalyzed synthesis of sugar polyesters in organic media [12,40]. Hence, accumulation of water in the reaction media drives the reaction equilibrium toward undesired enzyme-catalyzed side reactions such as hydrolysis. Notwithstanding this, a certain amount of critical water content normally referred to as the “essential water” that serves as protein lubricant to maintain the three-dimensional configuration is also needed to maintain the enzyme catalytic activity [41,42].

The influence of water activity on the apparent reaction rate and conversion was studied using different solvents and their binary mixtures that were initially pre-equilibrated to constant  $a_w$  (0.08) using aqueous solution of KOH as shown in Fig. 6(a) and (b). In the mono-phasic solvent systems (Fig. 6a), a clear distinction was observed between the highly hydrophilic solvent i.e. DMSO and the hydrophobic solvents. Despite the initial steep increase in apparent reaction rate constant in DMSO, the highest  $k_1^{app}$  value ( $2.88 \times 10^{-6} \text{ s}^{-1}$ ) was achieved at lower water activity value ( $a_w \approx 0.2$ ) and the reaction rate constant was observed to decline progressively with increasing  $a_w$ . Similar observations were reported previously in the pre-equilibrated lipase-catalyzed synthesis of ascorbyl palmitate in 2-methyl-2-butanol [43] and in pre-equilibrated papain-catalyzed reaction [44]. In comparison to moderately polar solvents like DCM and chloroform that yield their highest rate constant at  $a_w \approx 0.5$ , the

highly hydrophobic isooctane was observed to have its high-est reaction rate constant ( $1.44 \times 10^{-6} \text{ s}^{-1}$ ) at much higher water activity value ( $a_w \approx 0.7$ ). In general, the accumulation of reaction water content was more tolerable in more hydrophobic medium as compared to the hydrophilic ones. This is because an increase in water content in the hydrophilic solvents increases its polarity, and although allowing more glucose solvation thus resulting in high reaction rate constant, it also affects the enzyme stability due to increased polarity. Generally, the hydrophobic solvents experienced poor glucose solvation, the reaction rate constants were observed to be lower but an increased in enzymatic stability was observed as the reaction progresses even at higher  $a_w$  values (Fig. 6a). This observation is further supported by the observed increase in apparent reaction rate at highly hydrophobic solvents (Table 1) e.g. isooctane ( $\nu^{\text{app}} = 2.83 \times 10^{-4} \text{ M s}^{-1}$ ) as compared to DMSO ( $\nu^{\text{app}} = 0.19 \times 10^{-4} \text{ M s}^{-1}$ ). The improvement of enzymatic stability in hydrophobic solvent environment was previously proposed [38].

On the other hand, blending the solvents into binary mixtures seems to influence both the apparent reaction rate constant and the reaction stability as a function of water content (Fig. 6b). At lower water activity value ( $a_w \leq 0.5$ ), mixing the highly hydrophobic isooctane in lower volume fraction with bulk polar chloroform resulted in a progressive increase in apparent reaction rate constant (Fig. 6b). When the water activity was increased beyond  $a_w = 0.5$ , the apparent reaction rate constant seems to increase with increasing isooctane volume fraction (Fig. 6b). This could probably be due to the effect of increased enzymatic stability as the mixture becomes more hydrophobic [35,36]. In contrast, reverse trends were observed when mixing highly hydrophilic DMSO with moderately polar chloroform (Fig. 6b). Initially, parallel increase in apparent reaction rate constant up to  $a_w \approx 0.4$  were observed at both lower (0.5) and higher (3.0) DMSO volume ratio. When the water activity was increased to 0.5 and above, the  $k_1^{\text{app}}$  was consistently reduced for all the volume fraction of DMSO to chloroform (Fig. 6b) indicating an adverse effect of water activity toward enzymatic esterification capability when it is accumulated within the reaction system.

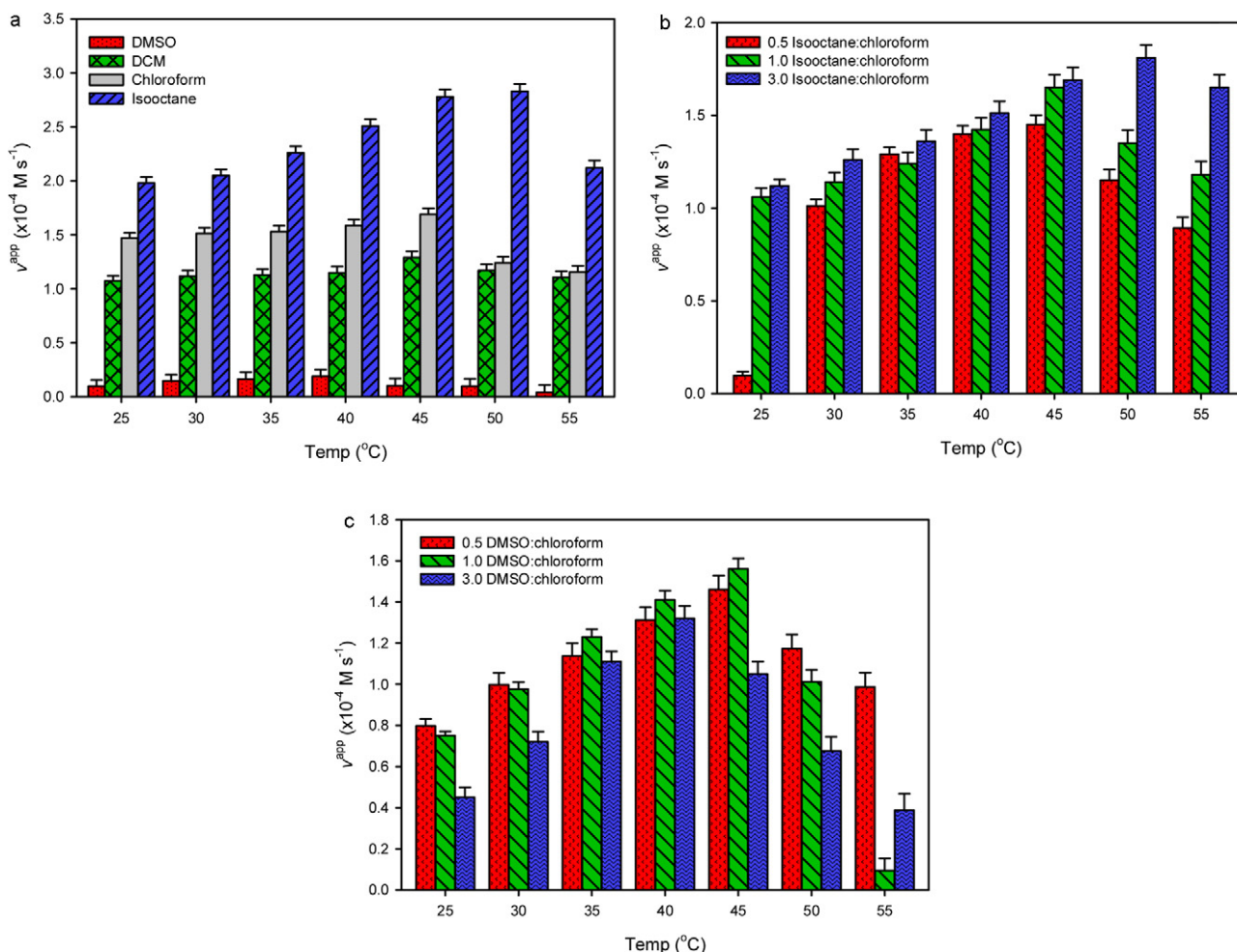
In addition, the esterification reaction produces water molecule that is a nucleophile for the hydrolysis reaction, any strategy to favor synthesis over hydrolysis must incorporate a design for continuous removal of water molecules from the reaction system [45]. One of the methods to achieve this is by using molecular sieves [46,47]. Molecular sieves of 4 Å pore size have been reported to have a superior water removal capability as compared to other water adsorbing agents such as zeolite and molecular sieve of 3 Å pore size [48]. The influence of molecular sieve 4 Å loading on glucose conversion was observed in both the monophasic and binary mixtures (Fig. 6c and d). In the monophasic solvent systems, high molecular sieve loading ( $15 \text{ g L}^{-1}$ ) is required in a more hydrophilic solvent (DMSO) to achieve higher conversion, further increase in molecular sieve loading resulted only in marginal increase in conversion. In comparison to other solvents, it seems that both the highly hydrophobic and moderate hydrophobic solvents were able to achieve highest conversion at molecular sieve loading of  $13 \text{ g L}^{-1}$ . However, not only does the molecular sieve influence conversion but also the solvent substrates solvation and enzymatic stability. In Fig. 6c, the conversion was observed to be higher in chloroform as compared to isooctane, this could be due to either better glucose solvation as compared to isooctane, or enzyme solvent compatibility due to the reported enzymatic molecular recognition effect, which may probably influence the conversion [49]. While comparing more hydrophobic isooctane to moderately hydrophobic DCM, the conversion was observed to be higher in isooctane under the same molecular sieve loading. This could also be attributed to be either due to enzyme stability in more hydrophobic solvent or in

other words, the enzyme is more compatible in the isooctane over the DCM. Observing the effect of molecular sieve loading as a function of glucose conversion in the binary solvent mixtures (Fig. 6d), highest conversion was observed at molecular sieve loading of approximately  $13 \text{ g L}^{-1}$  in all binary mixtures tested. However, a maximum conversion can only be achieved with higher molecular sieve loading at elevated solvent polarity. For instance, a maximum conversion of 38.2% was achieved at molecular sieve loading of  $15 \text{ g L}^{-1}$  at DMSO-chloroform ratio of 1. Increasing the ratio to 3.0 at the same molecular sieve loading resulted in a decreased conversion (23.1%), probably due to the increased solvent polarity effect on the enzyme. In general, from the results presented so far, it can be deduced that at given water activity value, the apparent reaction rate constant and conversion in highly hydrophilic solvent are strongly dependent on the polarity of the solvent. While in hydrophobic solvents, the dependence of a reaction rate constant and conversion could be attributed to the proposed effect of enzymatic stability rather than the solvent's polarity.

### 3.5. Effect of temperature on enzymatic reaction in mono-phasic and binary solvent system

The thermal stability of the reaction with respect to apparent reaction rate in different mono-phasic and binary solvent systems were studied over a temperature range of 25–55 °C (Fig. 7a and c). There is a general increase in reaction rate with increasing temperature for all the solvent systems tested. However, in a more hydrophilic solvent (DMSO), the enzymatic reaction rate was observed to decrease beyond 40 °C (Fig. 7a), probably due to the reported action of hydrophilic solvents on the enzyme hydration layer, causing the enzyme protein to be more prone to thermal deactivation. This is in agreement with the results of Mishra, *et al.* [16], whom assayed Lecitase™ Ultra activity in 0.05 M Tris-HCL buffer and observed a gradual decrease in residual enzyme activity after 40 °C with almost complete thermal deactivation after 60 °C. Wang, *et al.* [50] recently affirmed this observation, reporting an optimum temperature of 40 °C in Lecitase™ Ultra-catalyzed esterification of diacylglycerol-enriched oil from free fatty acids during partial hydrolysis of soybean oil. It has been reported that in polar milieu, Lecitase™ Ultra is said to exhibit a predominant lipase activity at temperature  $\leq 40$  °C, beyond this value the phospholipase activity predominates the reaction [51]. This observation could probably add to the explanation of the observed decrease in the apparent reaction rate in this study at a temperature beyond 40 °C in the polar DMSO.

In contrast to this observation, in the hydrophobic solvents, the enzyme seems to exhibit more thermal stability as the reaction rate continue to increase well beyond 45 °C, with maximum reaction rate ( $2.83 \times 10^{-4} \text{ M s}^{-1}$ ) observed for isooctane at 50 °C (Fig. 7a). Observing the effect of temperature in the binary solvent systems revealed the general trend as in mono-phasic solvent systems (Fig. 7b and c). However, the apparent reaction rate was observed to increase with increasing temperature and hydrophobic solvent volume ratio; achieving the highest reaction rate at  $1.81 \times 10^{-4} \text{ M s}^{-1}$  at 3.0 volume ratio of isooctane-chloroform at 50 °C (Fig. 7b). In comparison, mixing a more hydrophilic DMSO with chloroform improved the hydrophobicity of the media (Fig. 7c), this in turn increases the reaction stability with increasing temperature to 45 °C. However, the reaction stability was observed to rely on the increasing chloroform volume fraction. It is worth noting that in Figure 7c at 45 °C, the highest reaction rate ( $1.56 \times 10^{-4} \text{ M s}^{-1}$ ) was observed for 1.0 volume ratio of DMSO–chloroform instead of 3.0 volume ratio. Probable explanation to this observation could be due to enhanced glucose and polymer solvation at that specific binary mixture polarity. In contrast, despite improved glucose solvation at DMSO volume ratio of 3.0, the increase in the medium



**Fig. 7.** Reaction temperature as a function of apparent reaction rate in (a) mono-phasic, (b) isooctane binary solvents and (c) DMSO binary solvent systems. Synthesis at 200 rpm using Lecitase™ Ultra 200 mg for 24 h.

polarity resulted in the detrimental effects on the enzyme [9,38] resulting in the observed lower reaction rate at  $1.06 \times 10^{-4} \text{ M s}^{-1}$  (Fig. 7c).

#### 4. Conclusions

In this study, Lecitase™ Ultra was used for the first time to catalyze the synthesis of 6-O-glucosyl-poly(3-hydroxyalkanoates) in different solvent systems, affording a polymer with an average molecular weight ( $M_w$ ) of 1.7–16.8 ( $\pm 0.2$ ) kDa with good polydispersity. The average molecular weight of the synthesized polymer was observed to depend on solvent polarity, with highly hydrophobic solvent yielding higher molecular weight polymers. The thermometric analyses revealed the functionalized polymer to exhibit an improved thermal stability with highest melting and thermal degradation temperatures of 151.1( $\pm 0.2$ ) °C and 306.4 ( $\pm 0.2$ ) °C respectively. The presence of glucose moieties in the synthesized polymer influenced its biodegradability as compared to the non-functionalized PHA. Depending on solvent system used, the optimum molecular sieve loading range between 13.0 and 15.0 ( $\pm 0.2$ ) g L<sup>-1</sup>, with optimum reaction temperature 40 to 50 °C. Furthermore, the reaction rate to the medium's water activity ( $a_w$ ) was observed to increase with increasing medium polarity, with optimum water activities of 0.2, 0.5 and 0.7 ( $\pm 0.1$ ) been observed in hydrophilic DMSO, binary mixtures and hydrophobic isooctane, respectively. Solvent hydrophobicity improves the

enzymatic stability toward the reaction, however, poor solvation of polar substrate (glucose) in these media, resulted in lower product yield. On the other hand, the use of polar solvents though improves the glucose solvation, increased the polarity of the solvents and together with increasing water activity affects the enzymatic esterification activities resulting in both lower apparent reaction rate and product yield. Using controlled binary solvent mixtures, equal volume binary mixture of DMSO and chloroform with moderate polarity proved to be the most effective medium for the Lecitase™ Ultra catalyzed synthesis of this carbohydrate polymer as compared to the mono-phasic and other binary solvents tested with  $\approx 38.2 (\pm 0.8)\%$  conversion of glucose to the product.

#### 5. Conflict of Interests

All the authors of the submission declare and clarify that we do not have a direct financial relation with the commercial identities mentioned in the paper that might lead to a conflict of interest for any of the authors.

#### Acknowledgements

The authors acknowledged University of Malaya for research grants PV036/2012A, RG165/11AFR, UM.C/625/1/HIR/MOHE/05 and RP024-2012A.



## Appendix A. Supplementary data

Supplementary data associated with this article can be found, in the online version, at <http://dx.doi.org/10.1016/j.ijbiomac.2012.12.028>.

## References

- [1] H. Tian, Z. Tang, X. Zhuang, X. Chen, X. Jing, *Progress in Polymer Science* 37 (2012) 237–280.
- [2] A.M. Gumel, M.S.M. Annuar, T. Heidelberg, Y. Chisti, *Process Biochemistry* 46 (2011) 2079–2090.
- [3] G. Pauly, G. Philippe, In: U. States (Ed.), *US patents*, Cognis Corporation USA, U.S.A, 2005.
- [4] Y. Shi, J. Li, Y.H. Chu, *Journal of Chemical Technology and Biotechnology* 86 (2011) 1457–1468.
- [5] K. Kobayashi, A. Tsuchida, T. Usui, T. Akaike, *Macromolecules* 30 (1997) 2016–2020.
- [6] K. Hatanaka, H. Takeshige, K.I. Kanno, A. Maruyama, J. Oishi, Y. Kajihara, H. Hashimoto, *Journal of Carbohydrate Chemistry* 16 (1997) 667–672.
- [7] J.F. Ross, P.K. Chaudhuri, M. Ratnam, *Cancer* 73 (1994) 2432–2443.
- [8] J. Li, W. Xie, H.N. Cheng, R.G. Nickol, P.G. Wang, *Macromolecules* 32 (1999) 2789–2792.
- [9] R.M. Daniel, R.V. Dunn, J.L. Finney, J.C. Smith, *Annual Review of Biophysics and Biomolecular Structure* 32 (2003) 69–92.
- [10] F. Secundo, G. Carrea, *Journal of Molecular Catalysis B: Enzymatic* 19–20 (2002) 93–102.
- [11] M. Adamczak, S.H. Krishna, *Food Technology and Biotechnology* 42 (2004) 251–264.
- [12] A.M. Gumel, M.S.M. Annuar, T. Heidelberg, Y. Chisti, *Bioresource Technology* 102 (2011) 8727–8732.
- [13] R. Li, H. Zhang, Q. Qi, *Bioresource Technology* 98 (2007) 2313–2320.
- [14] A.M. Gumel, M.S.M. Annuar, Y. Chisti, T. Heidelberg, *Ultrasonics Sonochemistry* 19 (2012) 659–667.
- [15] M. Veld, A. Palmans, in: A.R.A. Palmans, A. Heise (Eds.), *Enzymatic Polymerisation*, Springer, Berlin/Heidelberg, 2011, pp. 55–78.
- [16] M.K. Mishra, T. Kumaraguru, G. Sheelu, N.W. Fadnavis, *Tetrahedron: Asymmetry* 20 (2009) 2854–2860.
- [17] D. Lu, Q. Wu, X. Lin, *Chinese Journal of Polymer Science* 20 (2002) 579–584.
- [18] Y. Tokiwa, H. Fan, Y. Hiraguri, R. Kurane, M. Kitagawa, S. Shibata, Y. Maekawa, *Macromolecules* 33 (2000) 1636–1639.
- [19] B.D. Martin, S.A. Ampofo, R.J. Linhardt, J.S. Dordick, *Macromolecules* 25 (1992) 7081–7085.
- [20] H. Hatakeyama, Y. Izuta, T. Yoshida, S. Hirose, T. Hatakeyama, in: J.F. Kennedy, G.O. Phillips, P.A. Williams (Eds.), *Recent Advances in Environmentally Compatible Polymers: Cellucon'99 Proceedings*, Woodhead publishing limited, UK, 2001, p. 33.
- [21] X. Chen, B.D. Martin, T.K. Neubauer, R.J. Linhardt, J.S. Dordick, D.G. Rethwisch, *Carbohydrate Polymers* 28 (1995) 15–21.
- [22] R.A. Gross, A. Kumar, B. Kalra, in: *US patents*, Technoprop Colton LLC, USA, 2005.
- [23] A.M. Gumel, M.S.M. Annuar, T. Heidelberg, *PLoS ONE* 7 (2012) e45214.
- [24] Y. Teng, Y. Xu, *Analytical Biochemistry* 363 (2007) 297–299.
- [25] A.M. Gumel, M.S.M. Annuar, T. Heidelberg, *Polymer Degradation and Stability* 97 (2012) 1227–1231.
- [26] A. Jouyban, M. Khoubnasabjafari, Z. Vaez-Gharamaleki, Z. Fekari, W.E.J. Acree, *Chemical and Pharmaceutical Bulletin* 53 (2005) 519–523.
- [27] B. Fu, P.T. Vasudevan, *Energy and Fuels* 24 (2010) 4646–4651.
- [28] C. Wu, J. Quan, J. Xie, C. Branford-White, L. Zhu, Y. Yu, Y. Wang, *Polymer Bulletin* 67 (2011) 593–608.
- [29] V. Massardier-Nageotte, C. Pestre, T. Cruard-Pradet, R. Bayard, *Polymer Degradation and Stability* 91 (2006) 620–627.
- [30] J.F. Kennedy, H. Kumar, P.S. Panesar, S.S. Marwaha, R. Goyal, A. Parmar, S. Kaur, *Journal of Chemical Technology and Biotechnology* 81 (2006) 866–876.
- [31] W. Liu, B. Chen, F. Wang, T. Tan, L. Deng, *Process Biochemistry* 46 (2011) 1993–2000.
- [32] W.S. He, J.J. Li, X.X. Pan, Y. Zhou, C.S. Jia, X.M. Zhang, B. Feng, *Bioresource Technology* 114 (2012) 1–5.
- [33] B. Fu, P.T. Vasudevan, *Energy and Fuels* 23 (2009) 4105–4111.
- [34] M.D. Gagnon, P.T. Vasudevan, *Energy and Fuels* 25 (2011) 4669–4674.
- [35] C. Laane, S. Boeren, K. Vos, C. Veeger, *Biotechnology and Bioengineering* 30 (1987) 81–87.
- [36] Z.F. Xu, R. Affleck, P. Wangikar, V. Suzawa, J.S. Dordick, D.S. Clark, *Biotechnology Bioengineering* 43 (1994) 515–520.
- [37] K. Ryu, J.S. Dordick, *Journal of the American Chemical Society* 111 (1989) 8026–8027.
- [38] A.M. Klibanov, *Nature* 409 (2001) 241–246.
- [39] S.B. Lee, K.J. Kim, *Journal of Fermentation and Bioengineering* 79 (1995) 473–478.
- [40] G.V. Chowdary, S.G. Prapulla, *Process Biochemistry* 38 (2002) 393–397.
- [41] I.-H. Kim, H.S. Garcia, C.G. Hill Jr., *Enzyme and Microbial Technology* 40 (2007) 1130–1135.
- [42] J.H. Salem, C. Humeau, I. Chevalot, C. Harscoat-Schiavo, R. Vanderesse, F. Blanchard, M. Fick, *Process Biochemistry* 45 (2010) 382–389.
- [43] C. Humeau, M. Girardin, B. Rovel, A. Miclo, *Journal of Biotechnology* 63 (1998) 1–8.
- [44] P.J. Halling, *Philosophical Transactions of the Royal Society of London. Series B, Biological Sciences* 359 (2004) 1287–1296.
- [45] N.G. Neena, S.P. Nitin, B.S. Sudhirprakash, B.J. Jyeshtharaj, P.W. Pramod, D. Mukesh, *Catalysis Reviews* 42 (2000) 439–480.
- [46] W.-L. Gao, H. Liu, N. Li, M.-H. Zong, *Bioresource Technology* 118 (2012) 82–88.
- [47] Y. Duan, Z. Du, Y. Yao, R. Li, D. Wu, *Journal of Agricultural and Food Chemistry* 54 (2006) 6219–6225.
- [48] F. Cauglia, P. Canepa, *Bioresource Technology* 99 (2008) 4065–4072.
- [49] V. Léonard-Nevers, Z. Marton, S. Lamare, K. Hult, M. Graber, *Journal of Molecular Catalysis B: Enzymatic* 59 (2009) 90–95.
- [50] F. Wang, H. Tsuno, T. Hidaka, J. Tsubota, *Bioresource Technology* 102 (2011) 9933–9941.
- [51] J.G. Yang, Y.H. Wang, B. Yang, G. Mainda, Y. Guo, *Food Technology and Biotechnology* 44 (2006) 101–104.

# CHAPTER 11

## Conclusions

---

### 11.1 Principal findings

The main research objectives were achieved for (A) Biopolymer synthesis and (B) Enzymatic functionalization of the biopolymer. The key findings from the research are:

#### A. Biopolymer synthesis

##### *(i) in vitro enzymatic catalysis*

- Ultrasonic assistance increases the polymerization from 46% to approximately 75%;
- The ultrasound irradiation helped to enhance rate of polymer propagation by more than two fold, while the enzymatic turnover number increases by more than factor three;
- The catalytic efficiency depends on the enzyme source and ranged from  $4.15 \times 10^{-3} \text{ s}^{-1} \cdot \text{M}^{-1}$  for Novozym 435 to  $1.48 \times 10^{-3} \text{ s}^{-1} \cdot \text{M}^{-1}$  for *C. rugosa* lipase;
- Besides, the sonication power, time and temperature were found to influence the rate of polymerization.

##### *(ii) in vivo microbial fermentation*

- In both bacterial strains used i.e *P. putida* BET001 and *D. tsuruhatensis* BET002, PHA accumulation is growth associated;
- High growth associated PHA accumulation were achieved with both bacteria;

- In *P. putida* Bet001, PHA with medium-chain-length monomers were produced from C<sub>8:0</sub> to C<sub>18:1</sub> fatty acids;
- *D. tsuruhatensis* Bet002 failed to use medium-chain-length fatty acids i.e. C<sub>8</sub> to C<sub>10</sub>, but able to utilize C<sub>14:0</sub> to C<sub>18:0</sub> to accumulate PHB homopolymer;
- With C<sub>18:1</sub>, *D. tsuruhatensis* Bet002 produces PHA containing short 3-hydroxybutyrate and odd 3-hydroxyheptanoate among the monomers;
- In contrast to other reports, no unsaturated monomers were detected in PHA obtained from both bacterial strains;
- Incorporation of longer chained monomers increase the PHA thermal stability;
- The molar concentration ratio of carbon to nitrogen source has little effect on the PHA composition, but affected the biomass, thence the PHA yield.

## **B. Enzymatic functionalization of the biopolymer**

- Functionalization with carbohydrates improves the PHA biodegradability by 50% beside showing better compostability;
- Lecitase™ Ultra was able to functionalize bacterial polyhydroxyalkanoates (PHA) with carbohydrate;
- Binary mixture of organics solvent as reaction medium improve the reaction rate and yield;
- The solvent polarity strongly influenced the average molecular weight of the synthesized polymer;
- Controlling water activity is important for esterification of PHA with carbohydrate.

## References

- Albuquerque, M. G. E., Concas, S., Bengtsson, S., & Reis, M. A. M. (2010). Mixed culture polyhydroxyalkanoates production from sugar molasses: The use of a 2-stage CSTR system for culture selection. *Bioresource Technology*, 101(18), 7112-7122. doi: 10.1016/j.biortech.2010.04.019
- Albuquerque, M. G. E., Martino, V., Pollet, E., Avérous, L., & Reis, M. A. M. (2011). Mixed culture polyhydroxyalkanoate (PHA) production from volatile fatty acid (VFA)-rich streams: Effect of substrate composition and feeding regime on PHA productivity, composition and properties. *Journal of Biotechnology*, 151(1), 66-76. doi: 10.1016/j.jbiotec.2010.10.070
- Annuar, M. S. M., Tan, I. K. P., Ibrahim, S., & Ramachandran, K. B. (2008). A kinetic model for growth and biosynthesis of medium-chain-length poly-(3-hydroxyalkanoates) in *Pseudomonas putida*. *Brazilian J Chem Eng*, 25, 217-228.
- Ariffin, N., Abdullah, R., Rashdan Muad, M., Lourdes, J., & Emran, N. A. (2011). Constructions of Expression Vectors of Polyhydroxybutyrate-Co-Hydroxyvalerate (PHBV) and Transient Expression of Transgenes in Immature oil Palm Embryos. *Plasmid*, doi:10.1016/j.plasmid.2011.1007.1002
- Arumugasamy, S. K., & Ahmad, Z. (2011). *Candida antarctica* as catalyst for polycaprolactone synthesis: effect of temperature and solvents. *Asia-Pacific Journal of Chemical Engineering*, 6, 398-405. doi: 10.1002/apj.583
- Bansal, S. S., Goel, M., Aqil, F., Vadhanam, M. V., & Gupta, R. C. (2011). Advanced Drug-Delivery Systems of Curcumin for Cancer Chemoprevention. *Cancer Prevention Research*, 4, 1158.
- Barinov, V., Dabrowski, R., & Levon, K. (2006). Methods and apparatus for modifying gel adhesion strength: WO Patent WO/2006/050,340.
- Bauwens, T. (2011). First estimates suggest around 4% increase in plastics global production from 2010. Retrieved 18th July 2012, from <http://www.plasticseurope.org/information-centre/press-room-1351/press-releases-2012/first-estimates-suggest-around-4-increase-in-plastics-global-production-from-2010.aspx>
- Bawa, P., Pillay, V., Choonara, Y. E., & du Toit, L. C. (2009). Stimuli-responsive polymers and their applications in drug delivery. *Biomedical Materials*, 4, 022001.
- Bohmert-Tatarev, K., McAvoy, S., Daughtry, S., Peoples, O. P., & Snell, K. D. (2011a). Focus Issue on Plastid Biology: High Levels of Bioplastic Are Produced in Fertile

- Transplastomic Tobacco Plants Engineered with a Synthetic Operon for the Production of Polyhydroxybutyrate. *Plant Physiology*, 155(4), 1690.
- Bohmert-Tatarev, K., McAvoy, S., Daughtry, S., Peoples, O. P., & Snell, K. D. (2011b). High Levels of Bioplastic Are Produced in Fertile Transplastomic Tobacco Plants Engineered with a Synthetic Operon for the Production of Polyhydroxybutyrate. *Plant Physiology*, 155(4), 1690.
- Börnke, F., & Broer, I. (2010). Tailoring plant metabolism for the production of novel polymers and platform chemicals. *Current Opinion in Plant Biology*, 13(3), 353-361.
- Costa, R. R., Custódio, C. A., Arias, F. J., Rodríguez-Cabello, J. C., & Mano, J. F. (2011). Layer-by-Layer Assembly of Chitosan and Recombinant Biopolymers into Biomimetic Coatings with Multiple Stimuli-Responsive Properties. *Small*.
- Cui, W., Qi, M., Li, X., Huang, S., Zhou, S., & Weng, J. (2008). Electrospun fibers of acid-labile biodegradable polymers with acetal groups as potential drug carriers. *International Journal of Pharmaceutics*, 361(1-2), 47-55.
- Francis, L. (2011). Biosynthesis of polyhydroxyalkanoates and their medical applications. PhD thesis, Westminster, UK: University of Westminster; 2011.
- Gaucher, G., Marchessault, R. H., & Leroux, J. C. (2010). Polyester-based micelles and nanoparticles for the parenteral delivery of taxanes. *Journal of Controlled Release*, 143(1), 2-12.
- Gorke, J., Srienc, F., Kazlauskas, R., & Flickinger, M. C. (2010). Enzyme-Catalyzed Reactions in Ionic Liquids *Encyclopedia of Industrial Biotechnology: Bioprocess, Bioseparation and Cell Technology*. John Wiley & Sons, Inc.
- Gumel, A. M., Annuar, M. S. M., & Chisti, Y. (2012a). Recent Advances in the Production, Recovery and Applications of Polyhydroxyalkanoates. *Journal of Polymers and the Environment*, 1-26. doi: 10.1007/s10924-012-0527-1
- Gumel, A. M., Annuar, M. S. M., Chisti, Y., & Heidelberg, T. (2012b). Ultrasound assisted lipase catalyzed synthesis of poly-6-hydroxyhexanoate. *Ultrasonics Sonochemistry*, 19(3), 659-667.
- Gumel, A. M., Annuar, M. S. M., & Heidelberg, T. (2012c). Effects of carbon substrates on biodegradable polymer composition and stability produced by *Delftia tsuruhatensis* Bet002 isolated from palm oil mill effluent. *Polymer Degradation*

- He, F., Li, S., Garreau, H., Vert, M., & Zhuo, R. (2005). Enzyme-catalyzed polymerization and degradation of copolyesters of  $\epsilon$ -caprolactone and  $\gamma$ -butyrolactone. *Polymer*, 46(26), 12682-12688.
- Henderson, L. A., Svirkin, Y. Y., Gross, R. A., Kaplan, D. L., & Swift, G. (1996). Enzyme-catalyzed polymerizations of  $\epsilon$ -caprolactone: Effects of initiator on product structure, propagation kinetics, and mechanism. *Macromolecules*, 29, 7759-7766.
- Hori, K., Ichinohe, R., Unno, H., & Marsudi, S. (2011). Simultaneous syntheses of polyhydroxyalkanoates and rhamnolipids by *Pseudomonas aeruginosa* IFO3924 at various temperatures and from various fatty acids. *Biochemical Engineering Journal*, 53, 196-202.
- Hunsen, M., Azim, A., Mang, H., Wallner, S. R., Ronkvist, A., WENCHUN, X., et al. (2008). Cutinase: A Powerful Biocatalyst for Polyester Synthesis by Polycondensation of Diols and Diacids and ROP of Lactones *Polymer Biocatalysis and Biomaterials II* (Vol. 999, pp. 263-274): Ameircan Chemical Society.
- Jiang, C., Wang, X., Sun, P., & Yang, C. (2011). Synthesis and solution behavior of poly( $\epsilon$ -caprolactone) grafted hydroxyethyl cellulose copolymers. *International Journal of Biological Macromolecules*, 48(1), 210-214.
- Jocić, D., Tourrette, A., & Lavrić, P. K. (2010). Biopolymer-Based Stimuli-Responsive Polymeric Systems for Functional Finishing of Textiles. In M. M. Elnashar (Ed.), *Biopolymers* (pp. 37-40). Croatia: Sciyo.
- Kadokawa, J., & Kobayashi, S. (2010). Polymer synthesis by enzymatic catalysis. *Current Opinion in Chemical Biology*, 14(2), 145-153.
- Kiliçay, E., Demirbilek, M., Türk, M., Güven, E., Hazer, B., & Denkbaz, E. B. (2011). Preparation and characterization of poly(3-hydroxybutyrate-co-3-hydroxyhexanoate) (Phbhxx) based nanoparticles for targeted cancer therapy. *European Journal of Pharmaceutical Sciences*, 44(3), 310-320. doi: 10.1016/j.ejps.2011.08.013
- Kobayashi, S. (2010). Lipase-catalyzed polyester synthesis—A green polymer chemistry. *Proceedings of the Japan Academy, Series B*, 86(4), 338-365.



- Kourtz, L., Peoples, O. P., & Snell, K. D. (2010). Chemically Inducible Expression of Biosynthetic Pathways: US Patent App. 20,100/196,974.
- Kumar, A., & Gross, R. A. (2000). *Candida antarctica* lipase B catalyzed polycaprolactone synthesis: effects of organic media and temperature. *Biomacromolecules*, 1(1), 133-138.
- Lee, J., Jung, S.-G., Park, C.-S., Kim, H.-Y., Batt, C. A., & Kim, Y.-R. (2011). Tumor-specific hybrid polyhydroxybutyrate nanoparticle: Surface modification of nanoparticle by enzymatically synthesized functional block copolymer. *Bioorganic & Medicinal Chemistry Letters*, 21(10), 2941-2944. doi: 10.1016/j.bmcl.2011.03.058
- Li, Q., Li, G., Yu, S., Zhang, Z., Ma, F., & Feng, Y. (2010). Ring-opening polymerization of ε-caprolactone catalyzed by a novel thermophilic lipase from *Fervidobacterium nodosum*. *Process Biochemistry*, 46(1), 253-257.
- Loh, X. J., Cheong, W. C. D., Li, J., & Ito, Y. (2009). Novel poly (N-isopropylacrylamide)-poly [(R)-3-hydroxybutyrate]-poly (N-isopropylacrylamide) triblock copolymer surface as a culture substrate for human mesenchymal stem cells. *Soft Matter*, 5(15), 2937-2946.
- Lu, D., Wu, Q., & Lin, X. (2002). Chemoenzymatic synthesis of biodegradable poly (1'-O-vinyladipoyl-sucrose). *Chinese Journal of Polymer Science*, 20(6), 579-584.
- Meng, F., Zhong, Z., & Feijen, J. (2009). Stimuli-responsive polymersomes for programmed drug delivery. *Biomacromolecules*, 10(2), 197-209.
- Motornov, M., Roiter, Y., Tokarev, I., & Minko, S. (2010). Stimuli-responsive nanoparticles, nanogels and capsules for integrated multifunctional intelligent systems. *Progress in Polymer Science*, 35(1-2), 174-211.
- Nair, L. S., & Laurencin, C. T. (2007). Biodegradable polymers as biomaterials. *Progress in Polymer Science*, 32(8-9), 762-798.
- Nobes, G. A. R., Kazlauskas, R. J., & Marchessault, R. H. (1996). Lipase-catalyzed ring-opening polymerization of lactones: a novel route to poly (hydroxyalkanoate)s. *Macromolecules*, 29(14), 4829-4833.
- Okada, M. (2002). Chemical syntheses of biodegradable polymers. *Progress in Polymer Science*, 27(1), 87-133. doi: 10.1016/s0079-6700(01)00039-9

- Piet, L. P. J. (2010). World-wide production of crude steel and plastics 1950-2010. Netherlands: Eindhoven University of Technology.
- Poirier, Y., & Brumbley, S. (2010). Metabolic engineering of plants for the synthesis of polyhydroxyalkanoates. *Plastics from Bacteria*, 187-211.
- Puppi, D., Chiellini, F., Piras, A. M., & Chiellini, E. (2010). Polymeric materials for bone and cartilage repair. *Progress in Polymer Science*, 35(4), 403-440. doi: 10.1016/j.progpolymsci.2010.01.006
- Rai, R., Keshavarz, T., Roether, J., Boccaccini, A., & Roy, I. (2011a). Medium chain length polyhydroxyalkanoates, promising new biomedical materials for the future. *Mat Sci Eng R*, 72 (3), 29-47.
- Rai, R., Yunos, D. M., Boccaccini, A. R., Knowles, J. C., Barker, I. A., Howdle, S. M., et al. (2011b). Poly-3-hydroxyoctanoate P (3HO), a medium chain length polyhydroxyalkanoate homopolymer from *Pseudomonas mendocina*. *Biomacromolecules*, 12(6), 2126-2136.
- Reemmer, J. (2009). Advances in the synthesis and extraction of biodegradable polyhydroxyalkanoates in plant systems—A review. *MMG 445 Basic Biotechnology eJournal*, 5(1), 44-49.
- Ross, J. F., Chaudhuri, P. K., & Ratnam, M. (1994). Differential regulation of folate receptor isoforms in normal and malignant tissues in vivo and in established cell lines. Physiologic and clinical implications. *Cancer*, 73(9), 2432-2443.
- Sato, S., Minato, M., Kikkawa, Y., Abe, H., & Tsuge, T. (2010). In vitro synthesis of polyhydroxyalkanoate catalyzed by class II and III PHA synthases: a useful technique for surface coatings of a hydrophobic support with PHA. *Journal of Chemical Technology and Biotechnology*, 85(6), 779-782.
- Sharma, R., Chisti, Y., & Banerjee, U. C. (2001). Production, purification, characterization, and applications of lipases. *Biotechnology Advances*, 19(8), 627-662.
- Shrivastav, A., Mishra, S. K., & Mishra, S. (2010). Polyhydroxyalkanoate (PHA) synthesis by *Spirulina subsalsa* from Gujarat coast of India. *International Journal of Biological Macromolecules*, 46(2), 255-260.
- Snell, K. D. (2010). Multi-gene expression constructs containing modified inteins: EP Patent 1,255,846.

- Stuart, M. A. C., Huck, W. T. S., Genzer, J., Müller, M., Ober, C., Stamm, M., et al. (2010). Emerging applications of stimuli-responsive polymer materials. *Nature Materials*, 9(2), 101-113.
- Suriyamongkol, P., Weselake, R., Narine, S., Moloney, M., & Shah, S. (2007). Biotechnological approaches for the production of polyhydroxyalkanoates in microorganisms and plants--A review. *Biotechnology Advances*, 25(2), 148-175.
- Tian, H., Tang, Z., Zhuang, X., Chen, X., & Jing, X. (2012). Biodegradable synthetic polymers: Preparation, functionalization and biomedical application. *Progress in Polymer Science*, 37(2), 237-280. doi: 10.1016/j.progpolymsci.2011.06.004
- Tian, P., Shang, L., Ren, H., Mi, Y., Fan, D., & Jiang, M. (2010). Biosynthesis of polyhydroxyalkanoates: Current research and development. *African Journal of Biotechnology*, 8(5).
- Tilbrook, K., Gebbie, L., Schenk, P. M., Poirier, Y., & Brumbley, S. M. (2011). Peroxisomal polyhydroxyalkanoate biosynthesis is a promising strategy for bioplastic production in high biomass crops. *Plant Biotechnology Journal*, 9(9), 958-969.
- Woodruff, M. A., & Hutmacher, D. W. (2010). The return of a forgotten polymer Polycaprolactone in the 21st century. *Progress in Polymer Science*, 35(10), 1217-1256.
- Xu, F., Yan, T. T., & Luo, Y. L. (2011). Synthesis and micellization of thermosensitive PNIPAAm-b-PLA amphiphilic block copolymers based on a bifunctional initiator. *Macromolecular Research*, 19(12), 1287-1295.
- Zakaria, M. R., Abd-Aziz, S., Ariffin, H., Rahman, N. A., Yee, P. L., & Hassan, M. A. (2010). Comamonas sp. EB172 isolated from digester treating palm oil mill effluent as potential polyhydroxyalkanoate (PHA) producer. *African Journal of Biotechnology*, 7(22).
- Zawidlak-Wegrzynska, B., Kawalec, M., Bosek, I., Luczyk-Juzwa, M., Adamus, G., Rusin, A., et al. (2010). Synthesis and antiproliferative properties of ibuprofen-oligo (3-hydroxybutyrate) conjugates. *European Journal of Medicinal Chemistry*, 45(5), 1833-1842.
- Zhu, J. L., Zhang, X. Z., Cheng, H., Li, Y. Y., Cheng, S. X., & Zhuo, R. X. (2007). Synthesis and characterization of well-defined, amphiphilic poly (N-isopropylacrylamide)-b-[2-hydroxyethyl methacrylate-poly ( $\epsilon$ -caprolactone)] n graft copolymers by RAFT polymerization and macromonomer method. *Journal of Polymer Science Part A: Polymer Chemistry*, 45(22), 5354-5364.

- Zinck, P. (2009). One-step synthesis of polyesters specialties for biomedical applications. *Reviews in Environmental Science and Biotechnology*, 8(3), 231-234.
- Zúñiga, C., Morales, M., Le Borgne, S., & Revah, S. (2011). Production of poly-[beta]-hydroxybutyrate (PHB) by *Methylobacterium organophilum* isolated from a methanotrophic consortium in a two-phase partition bioreactor. *Journal of Hazardous Materials*, 190(1-3), 876-882.